The Interaction of Crude Oil With Arctic Sea Ice

NORCOR Engineering & Research Ltd.

Technical Report No. 27

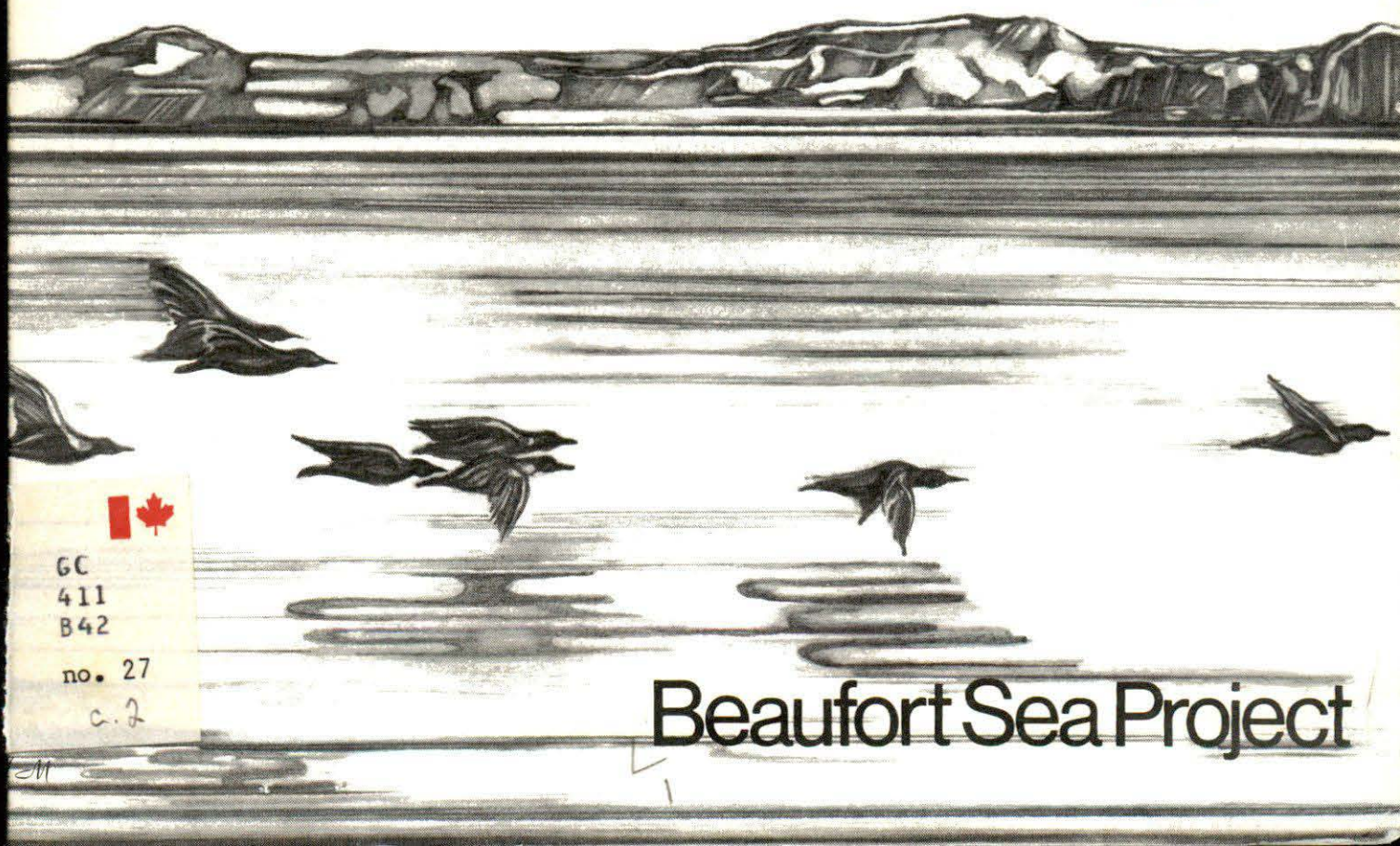

Beaufort Sea Project

THE INTERACTION OF CRUDE OIL WITH ARCTIC SEA ICE

NORCOR Engineering and Research Limited
Yellowknife, N.W.T.

Beaufort Sea Technical Report #27

Beaufort Sea Project
Dept. of the Environment
512 Federal Building
1230 Government St.
Victoria, B.C. V8W 1Y4

December, 1975

ACKNOWLEDGEMENTS

Mr. A. R. Milne, as Scientific Authority for the Department of the Environment, was responsible for the initial design and general administration of this study. Major contributions were also made by Dr. E. L. Lewis and Dr. E. R. Walker with the Frozen Sea Research Group.

As Resident Engineer, Mr. D. F. Dickins was responsible for implementing the field program and much of the analysis. Mr. J. C. Overall co-ordinated physical and chemical analyses at the site and the preparation of related sections of the report. The detailed laboratory studies were carried out at the University of Toronto, under the direction of Dr. D. MacKay. Dr. J. Hellebust, with the University of Toronto was responsible for the design and implementation of the biological program. Dr. Seelye Martin, with the University of Washington, served as a consultant on thermal aspects of oil and ice interaction. The study was directed by Mr. R. F. Brown.

Advice and assistance was provided by numerous people, including Mr. John Hnatiuk, Industry Co-ordinator for the Beaufort Sea Project, Mr. Jerry Gainer, Gulf Oil Canada, and Mr. John Remple, Imperial Oil Limited.

Special recognition is due members of the field crew, who performed a difficult assignment under very demanding conditions. The crew included Messrs. M. Albery, G. Comfort, D. Gardner, L. Kikoak, D. Lapp, T. Kitchen, O. Mullerbeck, and P. Sidey.

1.0 SUMMARY

The principal objectives of the study were to assess the impact of an offshore oil well blowout on the thermal regime of the Beaufort Sea, and to evaluate potential countermeasure techniques.

The main program, which consisted of nine controlled discharges involving 54 m^3 (11,900 gallons) of crude oil, was undertaken in a small bay 20 km to the south west of Cape Parry (70°02' N, 124°53' W). Two types of crude were injected under the ice at various stages of growth, between October 1974 and May 1975. The initial spreading and entrainment was documented by means of divers and a remote video system. An array of eleven point thermistor chains was logged hourly to assess the rate of migration and the effect of the oil on the thermal regime of the sheet. Oil, water and ice samples were recovered at regular intervals to determine the degree of weathering and dissolution of the oil. Detailed radiation studies were undertaken in the spring to assess the impact of surface oil on ice depletion. As well, two small discharges were conducted 30 km north of Cape Parry in April 1975, to determine the importance of currents on the transport of oil under solid ice cover. The oil was injected under the ice in the presence of a 10 cm sec^{-1} current, and the movement documented by means of divers.

When oil is released in the water column, it rises towards the surface in a conical shaped plume. The oil tends to be unstable, and breaks into small spherical particles of about 1 cm in diameter or less. On striking the underside of the ice, the oil radiates outward, progressively filling depressions in the sheet. Since most crudes naturally form sessile drops at an ice-water interface, the minimum oil film thickness is about 0.8 cm. Spherical drops of a lesser diameter can exist, but this normally only occurs near the periphery of the contaminated area, where the probability of collision with other drops is small. The maximum film thickness is controlled by the depth of depressions, or variation in ice thickness, which is typically about 20 percent of the average ice thickness. Within a matter of hours of the oil coming in contact with the ice, a lip of ice forms around the lens, preventing horizontal movement. During the depth of winter, a new layer of ice forms beneath the oil within several days. Once entrapped, the oil is stabilized until spring. The properties of the oil remain unchanged and there is little evidence of weathering or degradation.

Throughout the winter, the oil only penetrates between 5 and 10 cm into the loose skeletal layer. As the sheet begins to warm in the spring, activity intensifies in the brine channels and the oil begins to migrate upward. Initially the movement is slow; typically in the range of 15 to 20 cm during the months of February and March. The rate of migration increases with the level of solar radiation and the ambient air temperature. Oil released in late April under 150 cm of ice, was detected on the surface within one hour.

On reaching the surface of the ice, the oil saturates the snow cover, and substantially reduces the albedo. This causes an increase in the level of absorbed solar radiation, which accelerates the process. Oiled

melt pools quickly develop. The albedo of an oil film on water is about one quarter that of oiled snow, and consequently the melt is further accelerated. Oil is splashed on the surrounding snow by wind and wave action, and the pools gradually enlarge until interconnected. New oil is continually being released until the melt reaches the initial level of the oil lens. Once melt holes develop and surface drainage patterns are established, the sheet rapidly deteriorates. Depending on the nature and location of the sheet, oiled areas are likely to be free of ice between one and three weeks earlier.

A variety of clean-up techniques were investigated and in situ burning was found to be both the most efficient and effective. A minimum film thickness of about 0.5 cm was required to sustain combustion. Even when heavily weathered, most films could be ignited by sprinkling gasoline on a piece of paper towel. Between June 7 and July 17, 1975, four burns were conducted in the study area. On the first burn approximately 20 m^3 or 90 per cent of the oil on the surface was removed. The effectiveness of successive burns decreased, due to the reduction in film thickness. Of the 54 m^3 of oil discharged, approximately 15 m^3 evaporated naturally, and 33 m^3 was removed by burning. About 5 m^3 of residue was manually recovered from the ice. This proved to be a very costly and labour intensive operation. Less than three per cent of the oil reached the shore, of which one third was recovered.

In an effort to determine the impact of the tests, detailed physical and biological studies were conducted prior to the first discharge, and after the clean-up. With the exception of a very light oiling of the shingles in the tidal zone over about 900 m of shoreline, there was no evidence of oil in the water column, or deleterious effects on the marine ecosystem.

2.0 INTRODUCTION AND OBJECTIVES

In response to the increasing demand for hydrocarbons, offshore drilling and production platforms, submarine pipelines and tankers are all being proposed for the Beaufort Sea. Even with improving technology, oil spills are inevitable. There has been considerable speculation as to the likely effects of an oil spill in ice covered and ice infested waters, and the suitability of existing countermeasure techniques. A number of theories have been advanced on the probable interaction of oil and ice, the mechanics of transport, areal extent of contamination, albedo modification and changes in the global energy balance. However, in the absence of detailed field studies, it is impossible to realistically assess the probable impact of a major oil spill in the Beaufort Sea.

The following study was conducted as part of the Beaufort Sea Project. In April 1974, NORCOR Engineering and Research Limited was awarded a contract to undertake the work on behalf of the Marine Sciences Directorate, Department of the Environment, under the Department of Supply and Services contract serial number OSV4-0043.

The program was designed to generate fundamental data on the interaction of crude oil with Arctic sea ice. No attempt was made to simulate a full scale blowout. Since the processes are considerably more complicated in the moving pack, and it would be impossible to maintain control of the oil, the tests were confined to the fast ice zone. After the investigation of a number of potential sites, a permanent camp was established at Balaena Bay in August 1974. Between October and May, eleven controlled discharges involving 56 m^3 (12,300 gallons) of oil were conducted at various stages in the ice growth and depletion cycle. Two types of crude were injected under the ice, inside large 'Fabrene' containment skirts. The test areas were continuously monitored, and oil, water and ice samples were recovered for laboratory analysis. The clean-up operations commenced in June 1975, and the final documentation was completed in August.

The principal objectives of the study were to determine:

- The areal extent of contamination and the disposition of oil released beneath solid ice cover;

- The role of advection currents in the transport of oil along the underside of an ice sheet;

- The effects of relief at the ice-water interface on the transport and pooling of oil;

- The factors controlling the entrainment and migration of crude oil in first year sea ice at various stages of growth;

- Mechanism by which free oil is transported to the surface of an ice sheet;

- Effects of entrained and free oil on the surface heat exchange and

the energy balance of the sheet, with particular emphasis on modifications to freeze-up and break-up;

- The importance of the physical and chemical properties of the oil, ice and water to the various processes;

- The rate and nature of aging of oil in, on and under the ice;

- The suitability of existing methods and techniques for the clean-up of an oil spill in ice covered and ice infested waters; and

- The biological impact of the tests and the possible relevance to other areas.

3.0 RELATED RESEARCH

The potential impact of a number of blowouts in the Beaufort Sea was detailed in a paper by Campbell and Martin (1973) entitled Oil and Ice in the Arctic Ocean: Possible Large Scale Interactions. Although now considered somewhat extreme, the paper emphasized the need for further research. Similar scenarios were developed by Ayers (1973) and Ramseier (1973). The only related studies at the time were two small field tests undertaken by the United States Coast Guard off the coast of Alaska. The first in July 1970 (Glaeser) investigated the rate of spreading of oil on snow, ice and water, the ponding of oil under ice, and the effectiveness of various clean-up techniques. The second conducted during January and February 1972 (McMinn) focused on the spreading and absorption of oil on various snow and ice surfaces. In both cases less than 0.5 m^3 of oil was discharged, which introduced severe scale effects, and precluded the general application of the results. However, these studies did serve to delineate specific problems, and demonstrate the need for large scale, long term studies.

Documentation of the Deception Bay oil spill (Ramseier, 1973), the Arrow disaster (McTaggart Cowan and Lewis) and the Riviere St. Paul spill (NORCOR, 1974) provided some indication of the likely behavior of the oil under specific conditions. As well, a small test at Resolute Bay in the spring of 1974 (Bell) confirmed that the rate of migration of the oil is accelerated in the spring.

A number of laboratory studies have been conducted on oil spreading and evaporation under freezing conditions (Chen 1974, Scott 1975, MacKay 1975, Ramseier 1975). Work by Hoult, Wolfe and associates (1975) under the title Oil in the Arctic contains some of the more recent results of theoretical and laboratory studies of the interaction of oil with sea ice. Included are sections on evaporation, spreading both on and under the ice, and an evaluation of heat transfer relationships for an oil-ice composite. The principal limitations with the theoretical and laboratory studies is the difficulty in simulating the natural conditions.

Papers by Eide and Martin (1974), Lake and Lewis (1970) and Weeks (1966) on the physical and chemical properties of sea ice are useful references. As well, work by Burns (1974), Weller (1975 and 1967) and Fertuck and associates (1971) provide general data on the climate of the Beaufort Sea area, and the relative significance of the various terms in the energy balance.

A number of related studies were also undertaken as part of the Beaufort Sea Project. These include; Oil in Sea Ice (Lewis, 1975), Oil, Ice and Climate in the Beaufort Sea (Walker, 1976), Hydrodynamics of an Oil Well Blowout (Topham, 1976) and Movement of Oil Under Ice (Rosenegger, 1976).

A variety of additional references are included in the bibliography. In most cases they are secondary, and relate to a specific phenomenon, rather than the general problem of oil in sea ice.

4.0 SITE SELECTION AND DESCRIPTION

The following general factors were considered in selecting the oil test sites:

- that the marine environment be similar to that of the near shore zone in Mackenzie Bay;
- that there be sufficient data on the characteristics and movements of the ice for the design of necessary controls, and for the prediction with reasonable certainty, of the ultimate disposition of the oil;
- that there be a minimal effect of the tests on both people and wildlife;
- that the water be sufficiently clear that optical instruments and divers could be employed;
- that there be long term meteorological observations relatively nearby, both for extrapolation of findings and for operational purposes; and
- that the site be accessible year-round by air, and by barge during the summer.

Ideally, the tests should have been undertaken in the Mackenzie Bay area. However, at the time of designing the program, there was insufficient data on the probable performance of the oil to ensure that control could be maintained at all times. The area is on one of the principal routes taken by migratory birds and sea mammals, and oil on the surface or in leads could have resulted in very large kills. As well, the water tends to be very turbid, which would minimize the effectiveness of divers and optical detection systems.

A number of potential sites, ranging from Herschel Island to Sachs Harbour, were considered (Figure 4-1). After discussions with various regulatory authorities, the Cape Parry area was found to be best suited. There are numerous small sheltered bays within about 30 km of the Cape (Figure 4-2). The area tends to be relatively unproductive in comparison with Mackenzie Bay, and is well off the flight path for most migratory waterfowl. The land surface consists primarily of weathered limestone and dolomite. The thin veneer of soil and gravel can support only sparse vegetation. Topographic relief is limited, with elevations over 70 m ASL being common. In general, the shoreline is stable. Small salt marshes and sand beaches can be found, but vertical rock faces and shingle beaches are more typical. For most of the year the water is extremely clear, and it is possible to observe depths of over 10 m from the surface.

The DEW line station PIN MAIN and a meteorological station operated by the Atmospheric Environment Service are located at Cape Parry. There is a 5000 foot all-weather airstrip, scheduled barge service, and

Figure 4 - 1 LOCATION PLAN - BEAUFORT SEA

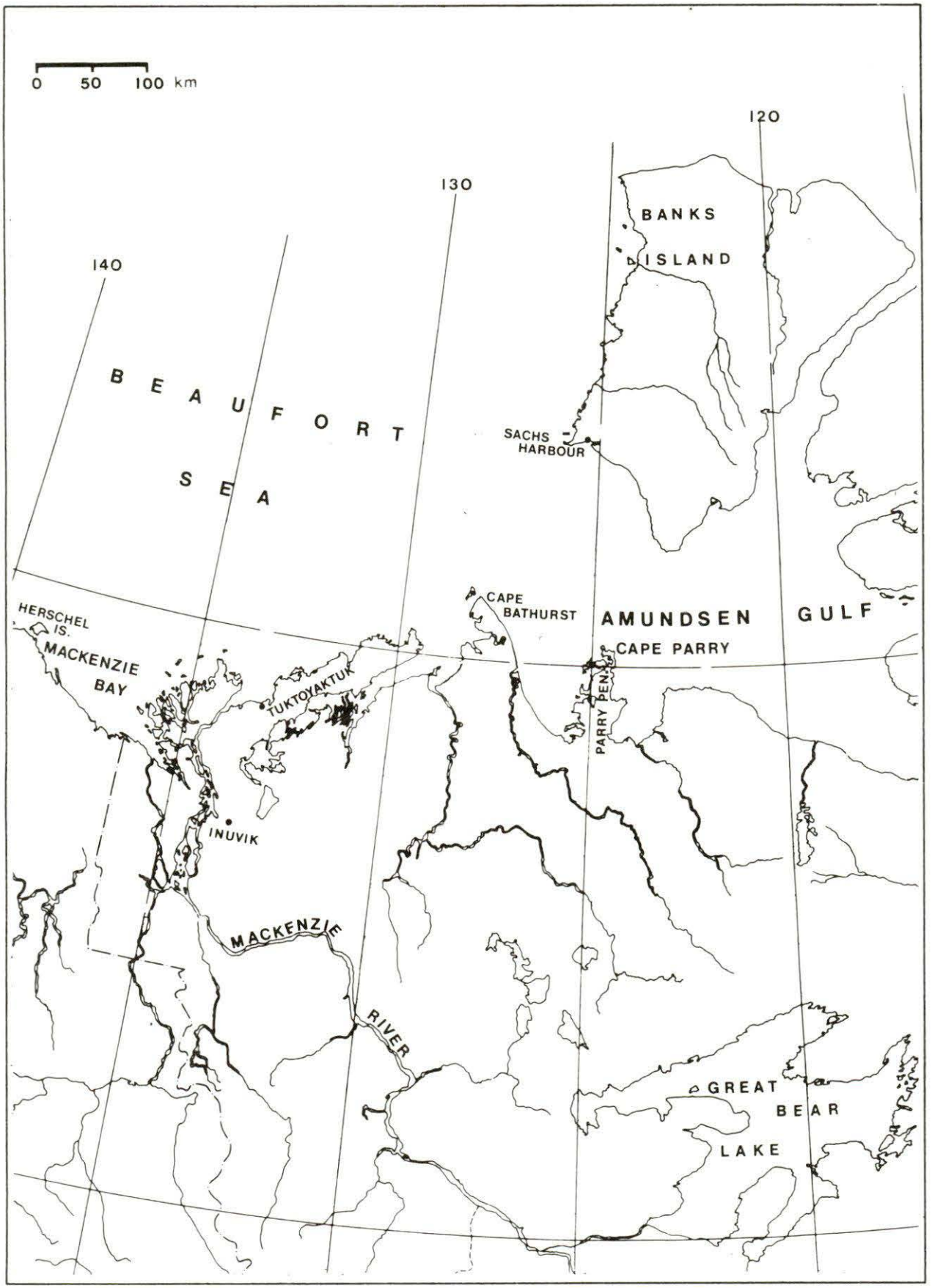

established communications. Meteorological observations have been maintained since 1957, and ice measurements have been made in a small cove to the south of the station for the past 12 years. The nearest permanent community, Paulatuk, is approximately 100 km southeast of Cape Parry, at the base of Darnley Bay. With the exception of several trappers and the occasional social visit, the Cape Parry area is not frequented by the people of Paulatuk.

The climate of the Parry Peninsula is not truly representative of the Beaufort Sea. In general, the Amundsen Gulf tends to be in a transition zone between the pure marine climate, which is detectable as far east as the Nicholson Peninsula, and the more typical continental climate at Cambridge Bay and points to the south. The mean annual temperature at Cape Parry is -12.3°C as compared with -10.5°C and -14.7°C at Shingle Point and Cambridge Bay respectively. A similar pattern exists in the standard deviation of the mean temperature, with the marine stations tending to be more stable. August is the warmest month with an average temperature of 5.8°C, while February is the coldest with an average of -29.6°C. The extreme temperatures observed range from 23.3°C to -43.9°C. The average annual precipitation is 20.4 cm, of which approximately one-half is in the form of rain. Over 46 percent of all precipitation falls between August and October. The prevailing wind direction is from the east and the average annual wind speed is 21.1 km hr^{-1}. The sun is below the horizon from approximately December 1 to January 12, but even at winter solstice there is about 1.5 hours of twilight. The climatic conditions and day light regime for Cape Parry are detailed in Appendix 4.

Four potential sites were selected from low-level aerial photography. In June, 1974, a field investigation was undertaken to determine which of the locations was best suited for the tests, and to document ice break-up in the area. Several of the sites were quite close to the DEW line facility at Cape Parry, which would have simplified logistics. However, the east arm of Balaena Bay was selected on the basis of its unique shape (Figure 4-2). The east arm is about 1.2 km wide by 4.4 km long, but the entrance is less than 100 m wide, with a depth of 2.3 m at the narrowest point. As a result, the ice normally rots in place. Consequently, in the event of loss of control of the oil, contamination would be confined to the bay. Due to the narrow width at the entrance, it would be possible to close off the bay with an oil boom if necessary.

In early August, prior to establishing a permanent camp, or undertaking any tests with oil, the site was documented in detail. Hydrographic, salinity and temperature measurements were taken at selected locations, and conditions along the shoreline documented. As a result of this work, a small cove on the north side of the bay was selected for the tests (Figure 4-3). A similar survey was done on the completion of the clean-up to assess the impact of the tests (Section 11). Following is a summary of conditions in the cove:

Size	400 m by 500 m
Water depth	6 to 10+ m in centre
Salinity	29°/$_{\infty}$ - 0.6%

Figure 4 - 2 LOCATION PLAN - PARRY PENINSULA

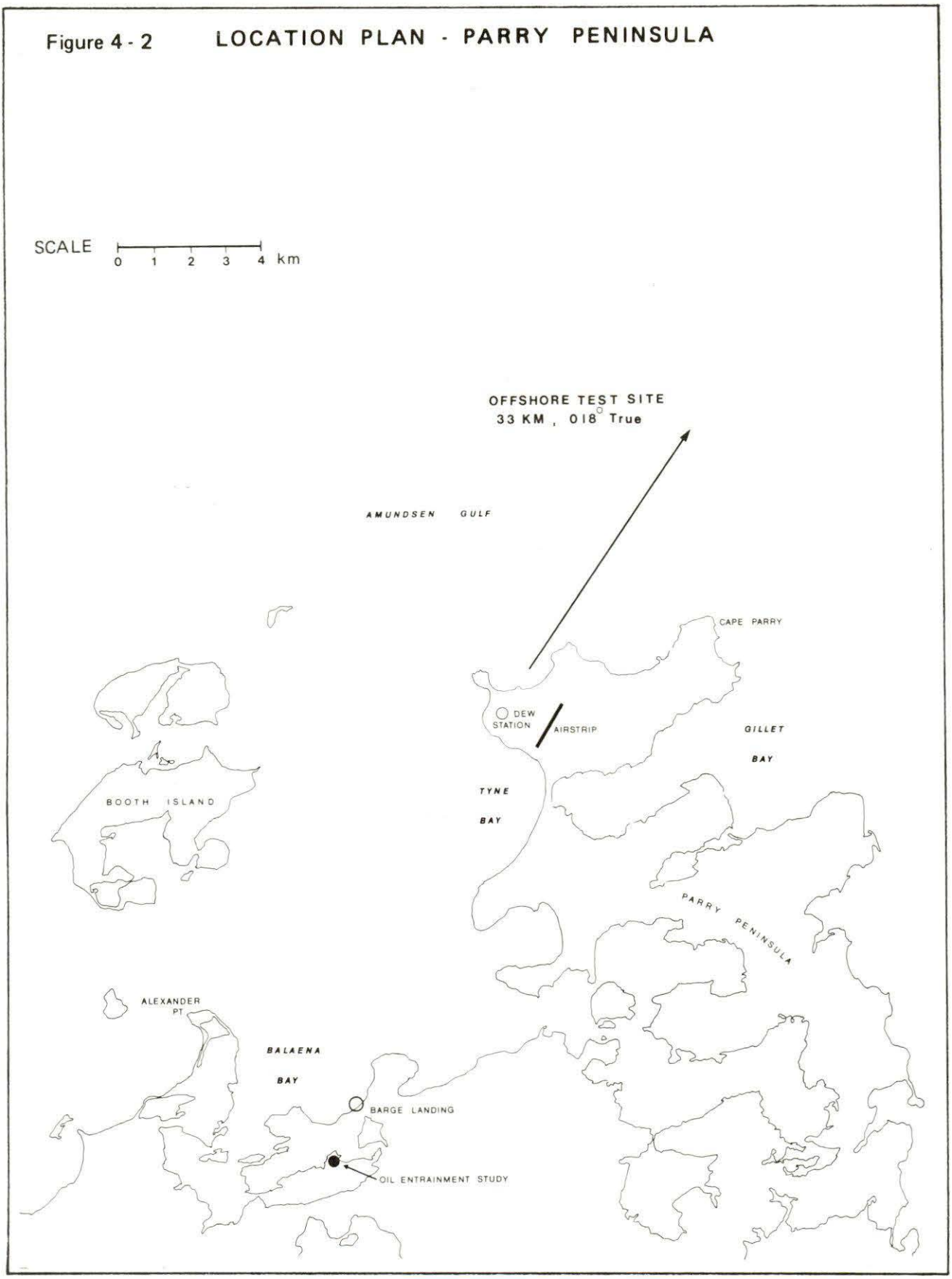

Figure 4 - 3 LOCATION PLAN - TEST SITE, BALAENA BAY

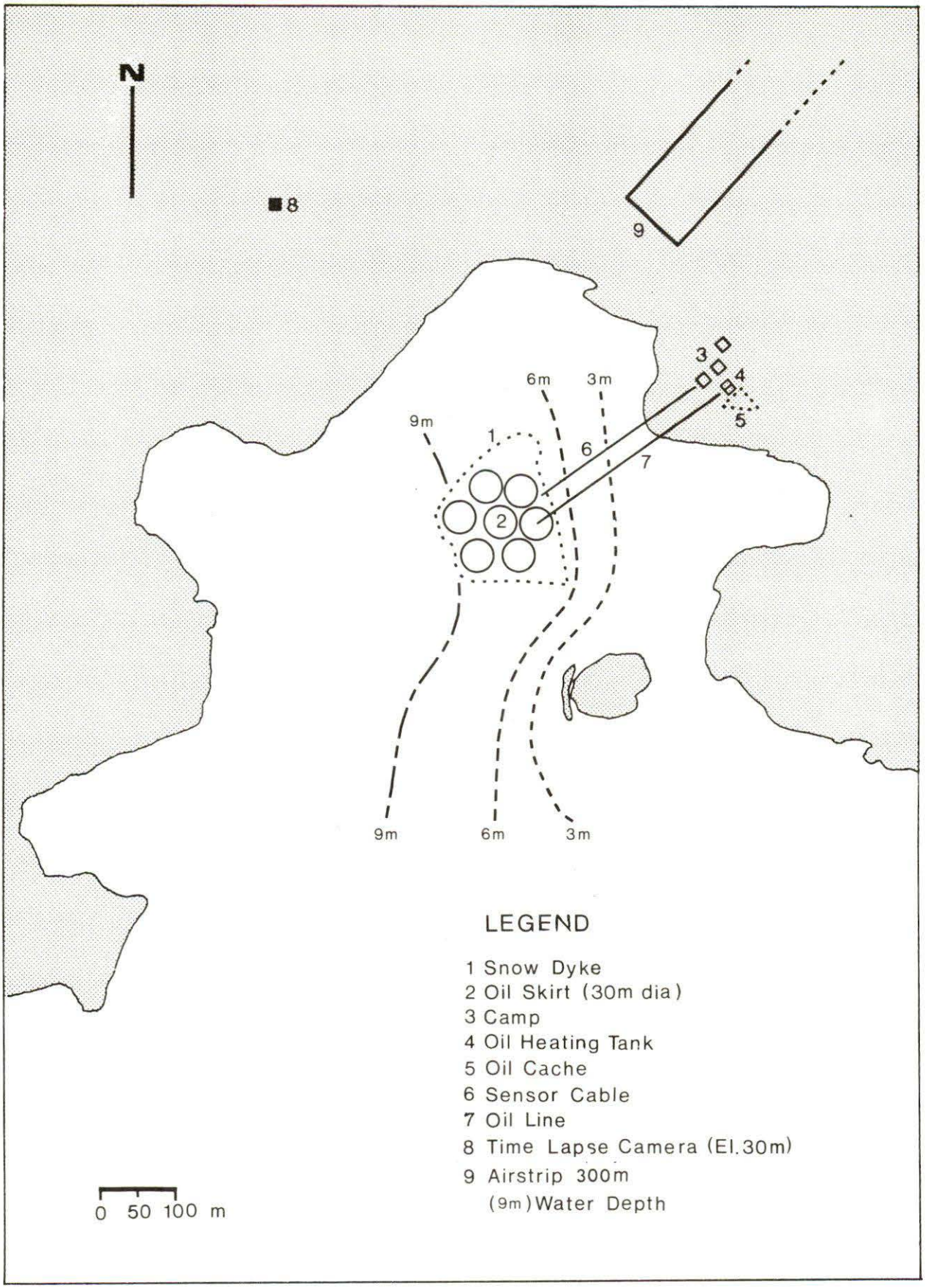

Water temperature	approx. -1.6°C (Winter +2°C (Summer)
Tide	0.3 m, semi diurnal
Current	feeble
Shoreline	principally shingle beach with short sections of salt marsh and low cliffs (Figure 11-2).
Biological (See Section 11)	26 species birds and mammals identified, 53 species terrestrial plants, 76 species marine organisms

Due to exceptionally heavy ice, the barge did not arrive until August 28, approximately six weeks later than normal. It was impossible to gain entrance to the east arm of Balaena Bay, and the freight was landed in the outer bay. Thirteen thousand kilograms of essential goods were shifted to the site by helicopter, and the remaining 120,000 kilograms, of crude oil and support fuels, was hauled by snowmobile throughout the winter. The camp consisted of two Parcol units, a mechanical building, workshop, and storage building. A single-sideband radio was used for communications with Yellowknife, Tuktoyaktuk and Inuvik. A small lake served as a landing strip during the winter.

A second site was required to assess the effect of currents on the transport of oil along the underside of an ice sheet. Work undertaken by the Frozen Sea Research Group, D.O.E., indicated a minimum current of 12 to 15 cm s^{-1} was required. Initially, a site near Babbage Bight on the west side of Mackenzie Bay was selected, but as a result of concern over the possible impact of surface oil on migration waterfowl, the tests were moved to the Cape Parry area. After a survey of currents in Franklin Bay, Darnley Bay and Amundsen Gulf, a maximum current of about 10 cm s^{-1} was located approximately 33 km due north of Cape Parry (Figure 4-2). In April 1975, a temporary camp was established at the site. The site conditions and offshore program are detailed in Section 9.0.

5.0 EXPERIMENTAL TECHNIQUES

5.1 Schedule and Size of Discharges

The principal factor in determining the number and timing of controlled discharges for the entrainment study was thermal fluctuations within the ice sheet. In general, the effects of changes in ambient air temperature, absorbed solar radiation and snow cover are far more pronounced in the upper levels of the sheet. Conditions tend to stabilize with depth, due to the thermal inertia of the ice and the enormous heat sink provided by the sea water. During the depth of winter, which typically extends from early December to late March, the ice structure is relatively constant. With the exception of the immediate vicinity of the skeletal layer, the brine channels tend to be blocked, thereby limiting the movement of oil upward through the ice. The sheet is cooling from initial formation until about mid February, and warming thereafter. Although diurnal variations and other short period disturbances can be detected near the surface, in general the thermal gradient tends to be linear during the fall and winter. During the melt phase, there is a reversal in the gradient, with the coldest temperatures being located near the centre of the sheet.

The timing of discharges was designed to encompass the dominant stages in the ice growth and depletion cycle. Because conditions tend to be stable during the depth of winter, emphasis was placed on the freeze-up and break-up periods. The initial program called for the first discharge in open water, immediately prior to freeze-up, and the second at an ice thickness of 15 cm. However, due to delays in obtaining the necessary approvals to discharge oil, the tests had to be rescheduled. The open water test was simulated by clearing an area of ice approximately 36 m^2. The average ice thickness at the time was 43 cm. Although the results are not truly representative of conditions at freeze-up, they provided some indication of the behavior of oil on water in the presence of growing ice. The final discharge was to be conducted immediately prior to break-up. As a result of other related studies being undertaken at Balaena Bay at the same time, it was felt that a full discharge posed too great a threat, and two small tests were conducted instead. Because there was very little information on the properties of the crude likely to be found in the Beaufort Sea, two types of crude, which spanned the probable range of properties, were used in the tests. Norman Wells (NW) crude, which has a pour point of about -45°C was used on all but two of the tests, due to its availability and ease of handling at low temperatures. Swan Hills (SH) crude, which has a pour point of about -4°C was used for tests in December and April. These discharges were conducted simultaneously with discharges of Norman Wells crude, for the purposes of comparison. The date of each test, the type and quantity of crude, and average ice thickness is shown in Table 5-1.

The size and volume of the test spills depended largely on environmental and physical constraints. The concept of a free flowing spill was environmentally unacceptable. A containment area of 30 m in diameter was selected for each test. This size was considered large enough to avoid scale effects from the containment boundary itself, and to encompass a

TABLE 5-1

SCHEDULE OF DISCHARGES

DATE	TEST	QUANTITY	ICE THICKNESS
Oct 24	NW#2	7.3 m^3	38 cm
Nov 1	NW#1	0.4 m^3	Open Water (43 cm)
Nov 14	NW#3	8.3 m^3	53 cm
Dec 7	SH#1	7.3 m^3	64 cm
Dec 9	NW#4	8.2 m^3	64 cm
Feb 15	NW#6	7.7 m^3	118 cm
Apr 8	NW - Offshore	1.5 m^3	122 cm
Apr 12	SH#2	6.4 m^3	154 cm
Apr 15	NW#7	8.2 m^3	154 cm
May 15	NW#8	0.4 m^3	195 cm
May 21	NW#8	0.2 m^3	195 cm

NOTE: Ice thickness tabled here are representative values. A deviation of approximately 20 percent can be expected depending on sampling location and date (Figure 7-4a).

---

meaningful cross section of natural ice thickness variations within a single test. Approximately 7.3 m^3 (1,620 gal) oil, or enough to cover the total test area to an average thickness of 1 cm, was used on each test.

The specific day of each test was governed by a number of factors. Primarily, the thermistor chain spacing set close limits (± 2 cm) on the ideal ice thickness and hence the day for the test. Figure 5-1 shows the probe spacings selected for each test. As the chains required a minimum of 10 days to freeze in properly, these spacings had to be fixed at the time of chain assembly, 2 to 3 weeks prior to the test. The spacing was designed so that the ice-water interface on the day of the test would fall on a dense array of 5 probes (Plate 6-4). On the basis of ice growth trends to that point, a prediction was made of ice thickness on the test day and the chains designed accordingly. By monitoring the chains for 2 to 5 days prior to the test, the probes reading water temperature would indicate when the interface was in the ideal position for a discharge. Snow cover variations made accurate chain placement difficult. However, attempts were made to install the probes in areas of equal snow cover, and after the first few tests, experience dictated ice variations to be corresponding to different snow covers. Some natural variation in ice thickness between the chains was always present, and some probes were closer to the ideal position than others. Most of the chains were within

Figure 5 - 1 THERMISTOR SPACING

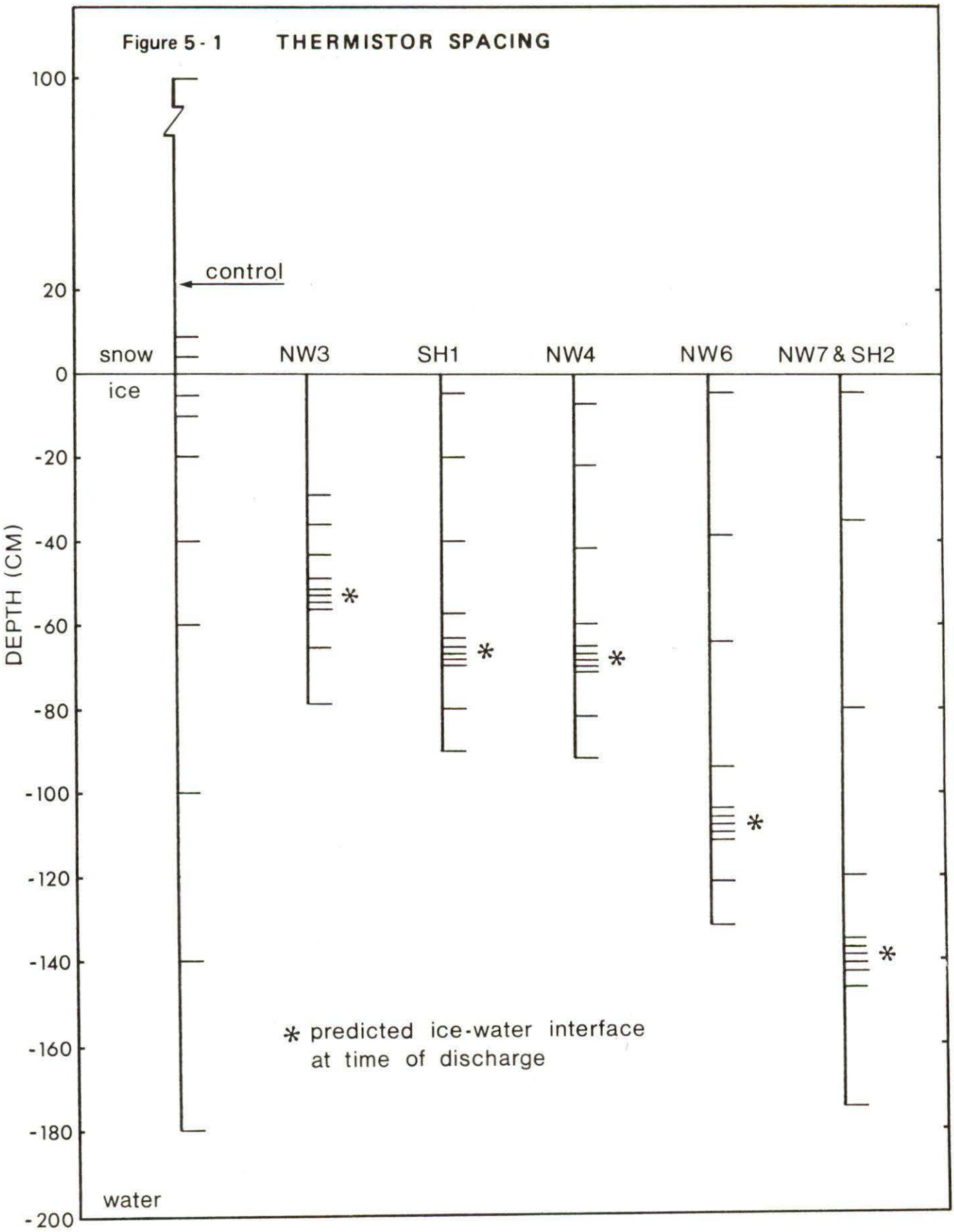

2 cm of the selected depth on the test day.

5.2 Oil Containment and Handling

5.2.1 Containment - Skirts

In selecting the oil booms, the following factors were considered: design, durability, cost, transportability, and ease of installation. In terms of performance, the most critical factor was that the skirt be intact at the ice-water interface for the duration of the test.

All existing techniques had major limitations for this application. A simple skirt embedded in the ice sheet was considered best suited for the Balaena Bay site. The design consists of three components, A Dupont 'Fabrene' membrane, a flotation collar, and cable ballast. Depending on what spill they were designed for, the skirts had lengths varying from 60 cm to 274 cm. The minimum skirt length available below the ice for any discharge was 22 cm.

Assembly was undertaken at the site using prepared lengths of 'Fabrene', sized according to the projected ice thickness at the time of discharge. The collar was constructed of 5 cm diameter PVC tubing, which was inserted into a pre-stitched sleeve along one edge of the 'Fabrene' strip. Sections of tubing were joined with sealed insert couplings and clamps. Similarly, the 1.0 cm diameter cable used as a ballast, was inserted into a smaller sleeve on the bottom edge of the skirt. A two man crew assembled eight 30 m diameter booms in this manner at the rate of 3 per day. Once assembled, the completed strip was dragged out on to the ice sheet by skidoo and laid out in a circular shape. With standard chain saws, a 10 cm wide slot was cut 97.5 m in circumference. The ice in the slot was pushed underneath, and the skirt was inserted through the slot (Plate 5-1).

After joining the ends, the boom was left to freeze in. A two man crew was capable of installing 3 such skirts through 28 cm of ice in a six hour shift. This rate dropped to one per day as the ice thickness reached 44 cm.

A total of 8 skirts were installed through the ice in this manner. The booms were packed tightly together to locate the test area between the 6 and 9 m water depth contours (Figures 4-3, 5-2), and to avoid running long branch-cables from the main data cable to each test area (Sections 5.3, 4). The range of water depths was originally selected to provide enough water under 1.8 m of ice for a realistic test, and to allow operation of a camera scissor boom mast.

The 10 m diameter skirt for the open water test was installed from a small boat while the ice was less than 5 cm thick. The unit froze in place within 24 hours.

The boom scheduled for the NW8 test, incorporated a different collar

Figure 5 - 2 TEST LAYOUT

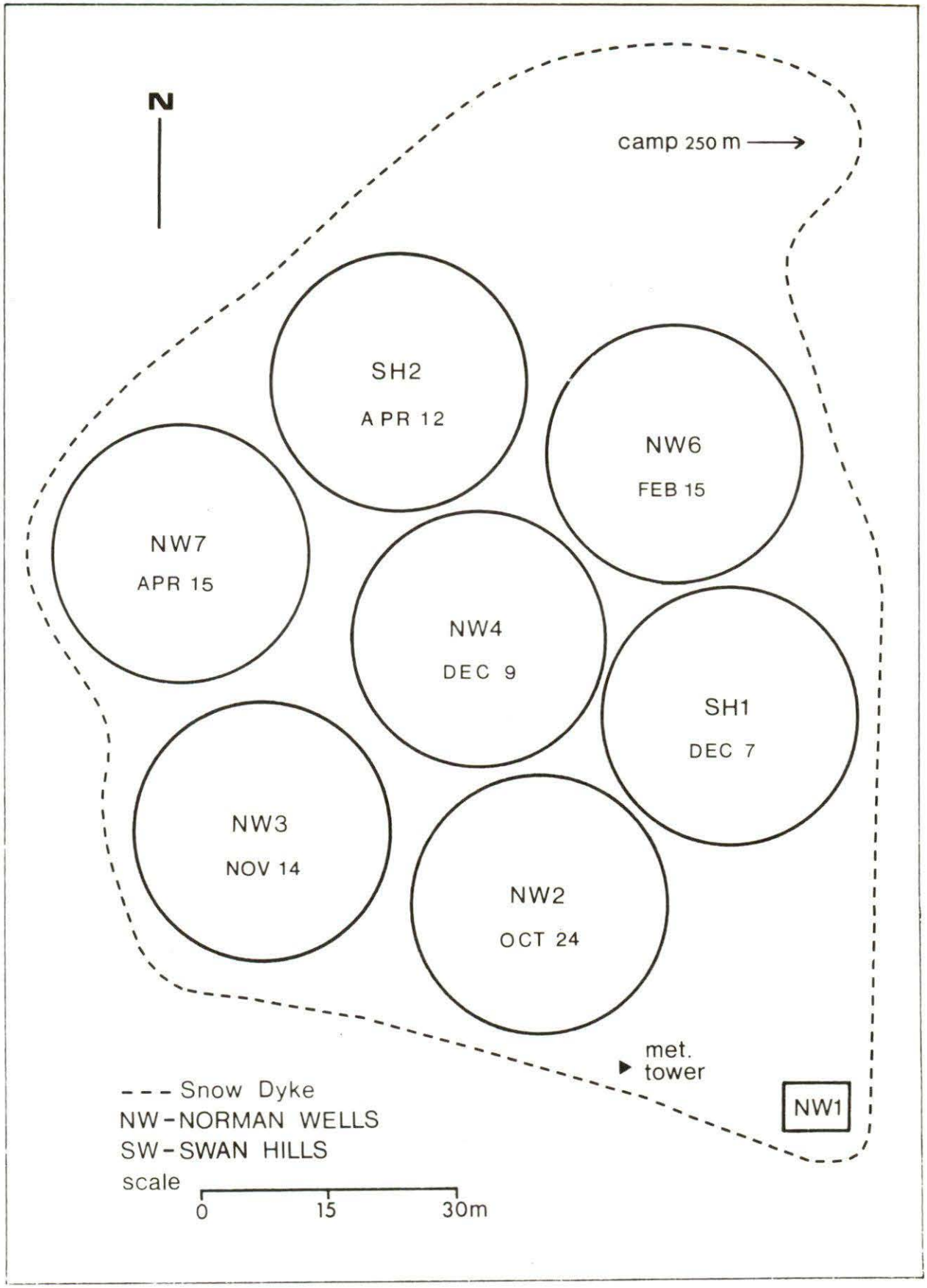

Plate 5 - 1

design to enable installation by a diver from under the ice. In place of the PVC pipe, solid styrofoam strips were used to eliminate the problems with sealed joints and brittle fracture at low temperatures. Also, the foam was extremely flexible, facilitating installation through a 2 by 3 m dive hole.

This skirt had a 'Fabrene' flap designed to float up against the ice and provide a better seal while freezing in. After the skirt was pushed through the dive hole, the diver was used to swim four lines attached to the skirt over to the quarter points of the circle. There, the lines were passed through a drill hole to the surface and used to drag the skirt into a rough circular shape. The diver completed the installation in about 45 minutes by hooking the flotation collar around wood stakes frozen into the ice.

The 'Fabrene' membranes served as an effective barrier throughout the winter. Although the predominant thickness of the oil lenses was 2 to 5 cm in most locations, the skirt held lenses up to 20 cm thick. However, the ice did not adhere well to the 'Fabrene' and in some locations small quantities of oil migrated up the joint between the ice and the skirt. This problem would likely be encountered with any barrier extending through the ice sheet. In June, as surface melt increased, the collar pipes formed partial barriers to surface movement of oil on melt pools.

In addition to the 'Fabrene' skirts, 100 m of 1 m, and 70 m of 0.3 m inshore-offshore boom were stored at the site for the duration of the project, to be used at the mouth of the bay in the spring if

required, or to contain any free oil which might develop in the test area at the time of clean-up.

5.2.2 Containment - Snow Dyke

A snow dyke, approximately 400 m in circumference, was constructed around the entire test area, to restrict the movement of free oil on melt pools in the spring. A number of techniques employing cut snow blocks were attempted, but due to the limited snow cover generally proved ineffective. Finally, empty oil barrels were used to create a wind break, and the snow naturally drifted to form a barrier about 1 m high and 3 m wide. On the average, it took between one and two days for the drift to stabilize. Attempts were made to flood sections of the dyke, but this proved to be time consuming and of little value.

The snow dyke was very effective in containing surface oil, and remained intact until late June. As a rule, the oil did not penetrate more than 15 to 20 cm into the snow. The dyke was breached on several occasions during major burns, but was quickly shored up with fresh snow.

5.2.3 Containment - Sorbents

Large quantities of sorbent in the form of pads, booms and rolls were stockpiled at the camp during April in preparation for the clean-up phase. A wringer designed for use with the sorbents was available.

5.2.4 Discharge Operations

The crude oil and support fuels, contained in palletized drums arrived by barge on August 28, 1974. Unusually heavy ice conditions at the mouth of Balaena Bay prevented the shipment from reaching the test cove as was originally planned, and the 136 metric tons of supplies were cached on the shore 0.7 km NE of the test site. Enough oil for the first three tests was slung by helicopter coincident with the camp move, and the remainder was transferred by skidoo to the test site during the winter.

At the camp, a 9 m^3 (2,000 gal) capacity insulated wooden holding tank was constructed 50 m from shore. Several days before each test, the oil was transferred from 45 gallon drums to the tank. This transfer was accomplished in 2 to 8 hours using a centrifugal pump, with a standpipe transferred manually between drums. Even Swan Hills crude was successfully pumped at temperatures as low as -35°C. Approximately 0.7 m^3 (155 gal) was pumped in excess of the quantity required for the tests, to allow for line losses and residue at the bottom of the tank.

The oil was heated to within approximately 1°C of the ambient water temperature, by means of a single immersed hot water radiator. The 8.6 m^3 of oil could be raised from the ambient air temperature to

about 0°C in less than 24 hours, even in February. Once heated to the required temperature, the oil was pumped through a 5 cm diameter neoprene line approximately 250 m to the test area. A 7 m length of 5 cm diameter steel pipe was used to inject the oil under the ice. On the average, the discharge was completed in 50 minutes, yielding a flow rate of 0.15 m^3 min^{-1} (32 gal min^{-1}).

Divers were employed on all the fully instrumented discharges. Initially, their main function was to document conditions and inspect the containment skirt prior to each discharge. Due to the possible effects of released air, the divers were prohibited from entering the test area within 48 hours of a discharge. A remotely controlled scissor boom, which could be extended up to 15 m, was employed to move the underwater video system and transducer for the first three tests. However, for full coverage the boom had to be inserted in the centre of the test area, and a variety of techniques were attempted to prevent oil from seeping into the well without success. For the discharge in February, the video system was mounted on a rigid boom, which was inserted through the ice from outside the test area. This unit permitted full rotation of the camera, but due to the low light levels, visibility was limited to about 10 m. A diver equipped with a closed circuit breathing system was employed on subsequent discharges. The entire operation was monitored from the surface, and the movements of the diver controlled by means of a surface communications system. This approach also permitted still and 16 mm photography. Since the diver had a range of approximately 40 m, it was possible to locate the dive hole outside the test area.

Two procedures were used to introduce the oil under the ice. For the first tests, the discharge pipe was inserted in a SIPRE hole angled into the test area from a point about 1 m outside the skirt. The pipe end then projected 3 m into the test area at a depth of about 2.5 m below the ice sheet. Commencing with the NW3 test, an effort was made to provide more opportunity for plume spreading, by inserting the pipe section vertically through the ice sheet near the centre of the test area. The oil was then discharged from a depth of about 6 m. This procedure was used for tests NW3 to NW6. A small quantity of oil sometimes rose through the auger hole used to place the discharge pipe. Packing with snow and sorbent usually halted the flow of oil in a matter of minutes. Following the NW6 test, a decision was made to eliminate further surface contamination of the test area, by reverting to the original side insertion of the discharge pipe near the skirt edge. This technique was used for NW7 and SH2, accompanied by a dive hole outside the spill area. Figure 5-3 shows a schematic section through a typical test area.

5.3 Instrumentation

Note: All instrument specifications are contained in Appendix 27A. Figure 5-4 displays graphically the data acquisition systems used at Balaena Bay.

Figure 5 - 3 SCHEMATIC SECTION THROUGH TYPICAL TEST AREA

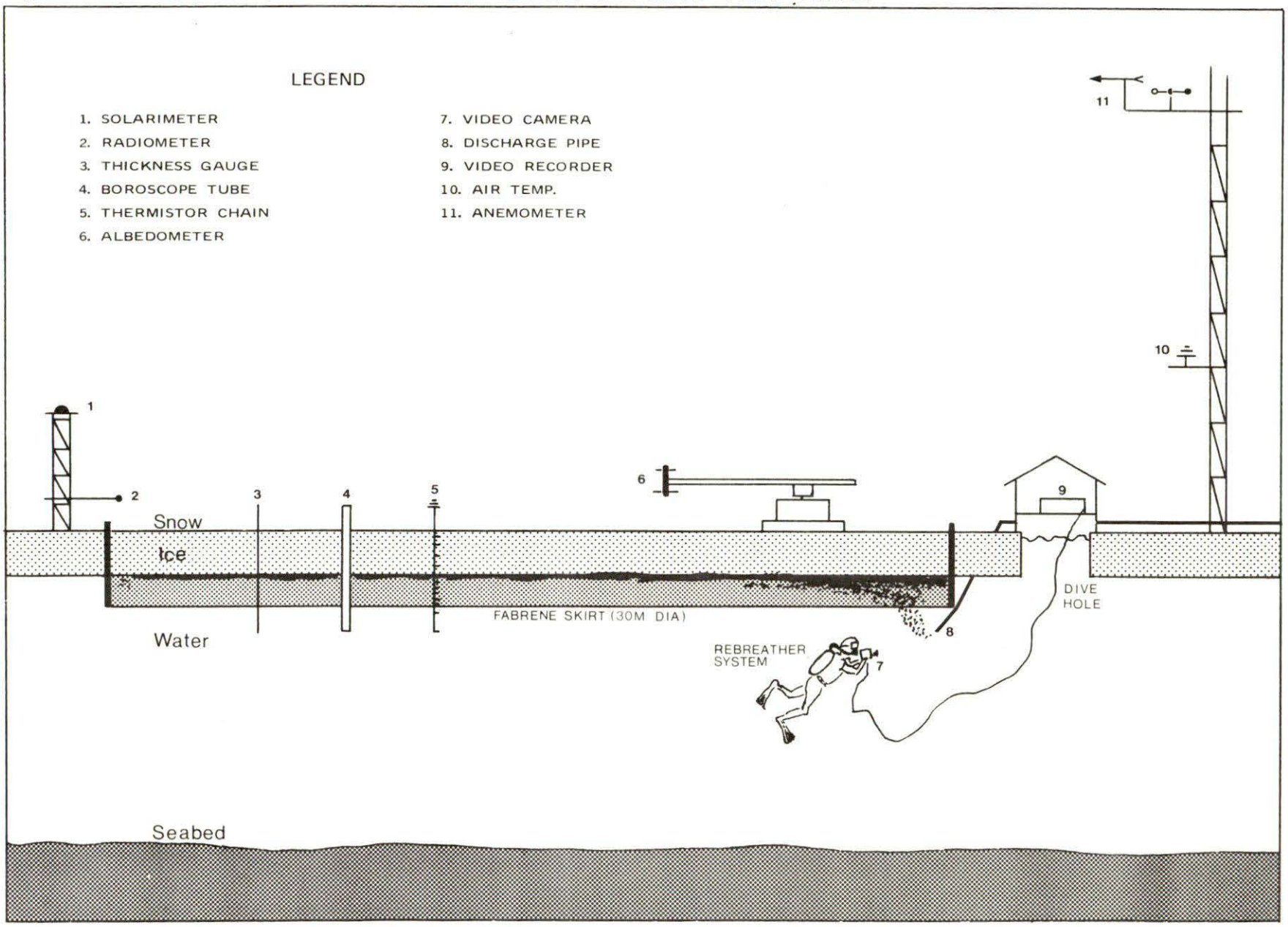

Figure 5-4 DATA ACQUISITION SYSTEMS

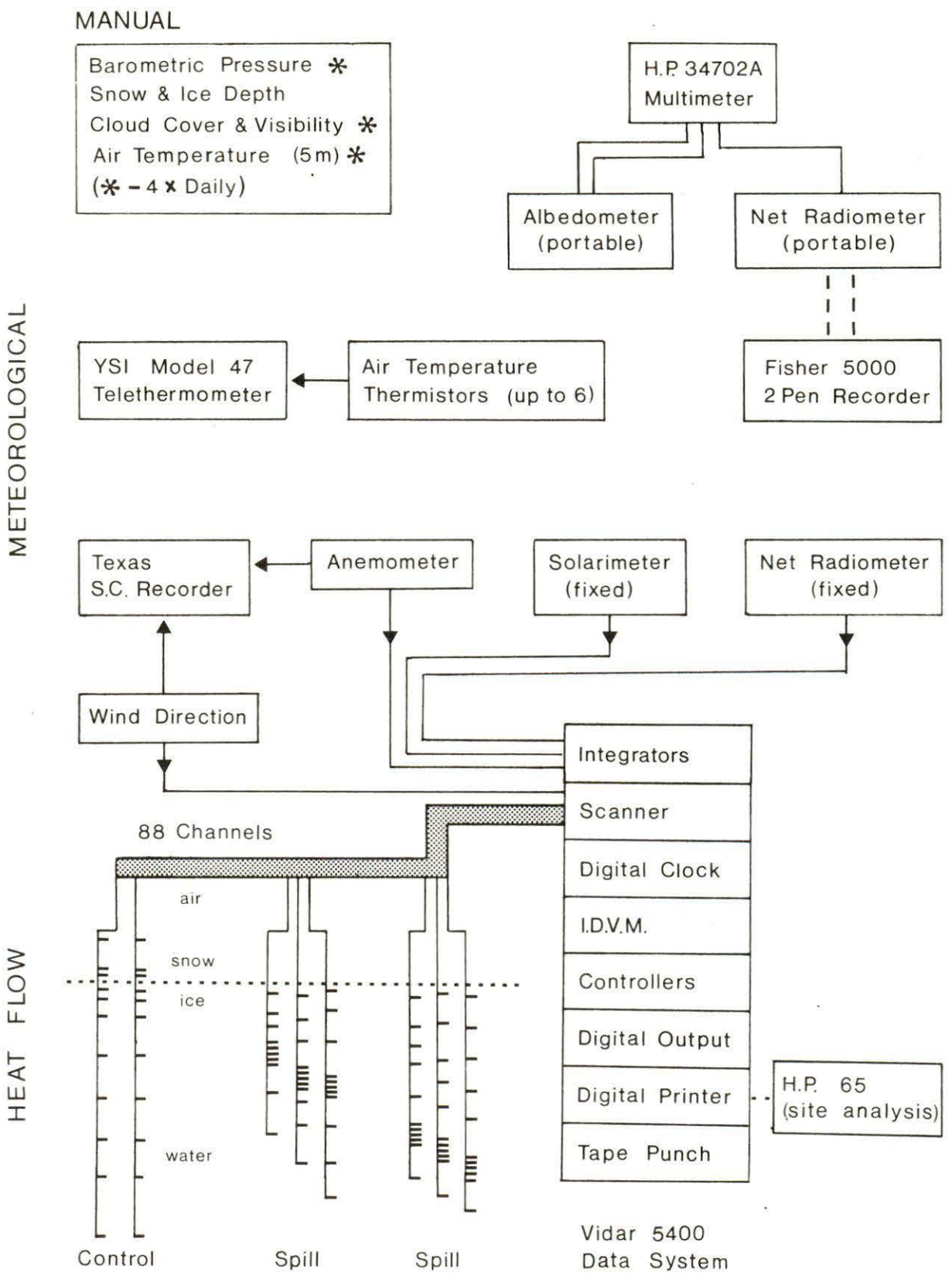

5.3.1 Surface Weather

Detailed observations of surface weather were made four times daily commencing on September 30, 1974 and continuing for the duration of the project, until July 22, 1975. All observations were taken at the following approximate times: 0900 hours, 1300 hours, 1800 hours and 2300 hours. Visual estimates were made of the cloud cover, the height of the cloud ceiling and the visibility. Barometric pressure was recorded. The windspeed and direction were measured and recorded with a Texas Instruments Model 446 system. Basically, this system consisted of a cup anemometer and wind direction indicator mounted on a tower free of obstructions at a height of 8 m above ground level. For the period March 6 to June 7, the wind speed and direction signals were fed into the data logging system integrator package to obtain average hourly values for wind speed (Section 3.3 .4). It was considered adequate to take an hourly spot reading of wind direction.

Air temperature was measured using a YSI Model Telethermometer with the thermistor mounted in a radiation shield at a height of 5 m. A similarly shielded thermistor on each control chain measured air temperature at a height of 1 m. From November 13 to June 7, these temperatures were recorded hourly on the main data logging system.

5.3.2 Radiation

Measurements relating to the radiation balance of the test area were undertaken from February 12 to June 6. To measure the total short wave radiation that was incident on the test area, a Kipp and Zonen CM-6 Solarimeter was mounted on a 3 m tower near the NW2 test area (Figures 3-2 and 3-3). A Fritschen type net radiometer at a height of 1 m was cantilevered 1 m out from the solarimeter tower. Both the solarimeter and net radiometer were connected to the data logging system. Hourly averages are available for the period March 6 to June 6. The albedo of the test site was measured for the period May 9 to June 4 (Section 4.4.2), using a Kipp and Zonen Model CM-7 Albedometer mounted on a mobile cantilever beam, 1 m above the ice surface. The DC voltage output signals were hand-logged every second day at 12 specific locations in the test area and 2 control sites using an H.P. 34702A Multimeter. Errors introduced by instrument limitations are outlined in Appendix 27A.

5.3.3 Ice-Water Temperatures

All ice and water temperatures were measured using precision thermistors, Model #44005X manufactured by Yellow Springs Instruments. Over 450 thermistors were supplied for use in this project. Each thermistor bead was calibrated at -40°C, -20°C and 0°C, the range most likely to be encountered between air and water temperatures over the 9 month period. At 0°C, the average thermistor resistance was 9796 ohms. At this temperature, the line resistance of 29 ohms was 0.23% of the reading. This error was substantially less for lower temperatures. The manufacturer considers that the worst case

error of a single thermistor calibrated at the three points mentioned above is ± 0.05°C over the range -40°C to 0°C. Using a probe spacing of 5 cm and a temperature gradient of 0.2°C cm^{-1}, the error in establishing the gradient would be ± 8%. A total of thirty-three chains with 11 thermistors on each chain were constructed for six tests and three controls, which were installed on November 12. The thermistor chain consisted of a 2.4 m length of hardwood drilled to receive 11 clear acrylic tubes (0.635 cm OD), arranged in a ladder network. The beads were embedded in the tip of each tube which projected about 5 cm out from the wood stem. The leads were run up a slot in the back of the hardwood to a 12 pair connector on top, and the whole assembly potted with silicone rubber. Figure A-1, shows assembly details and Appendix 27A contains specifications for the thermistors.

The rationale behind the spacing of probes is discussed under Section 5.1. Basically, the probe spacings were tailored to suit each spill (Figure 5-1). The control chain spacing was designed to have 3 probes 4 cm, 8 cm, and 100 cm above the ice surface to continuously monitor snow and air temperatures. Also, on the controls, probes projected 180 cm below the snow-ice interface so that even in May at least one probe remained to measure water temperatures.

5.3.4. Data Logging

A Vidar 5400 Data Acquisition System (Figure 3-4) was used to log all ice-air-water thermistors and meteorological instruments, as outlined above. The Vidar system consisted of a 100 channel reed scanner interrogated hourly by a precision DVM. Scan rate and sequence were variable, and controlled by a crystal clock. Data in the forms of ohms for thermistor readings and DC volts for meteorological instruments were recorded on printer paper and IBM compatible paper punch tape. Total scan time for the 92 active channels took less than 1 minute. The normal configuration consisted of 8 thermistor chains, each with 11 beads, and four channels for net radiation, shortwave solar radiation, wind speed and wind direction. Integrator capability was added to one 10 channel batch on March 6, 1975. This enabled hourly average readings for appropriate instruments. The signals were fed through a 22 conductor branch cable to a 200 conductor trunk cable, which ran from the centre of the test area to the Vidar data acquisition system, located in the office parcol. The branch cables were 60 m in length, while the trunk cable was 220 m long. All cables were vinyl wrapped with solid shields, while the conductors were 20 AWG, solid and braided. Twenty-four pin connectors were installed on all cables to permit rapid switching and manual scanning.

Although the operating conditions were less than ideal, the DAS functioned reliably for the eight-month period it was on line. Over 600,000 pieces of data were recorded in total. Initially, some problems were encountered due to unstable power, but these were corrected by inserting a crystal clock. The Vidar was shut down prior to the first burn on June 6, 1975, and the surviving thermistor

chains hand logged until June 23. All data has been converted to engineering units and is available on magnetic tape.

5.4 Sampling and Analytical Procedures

5.4.1 Oil Sampling and Analysis

The purpose of the oil sampling program was to identify and quantify any changes in the oil's physical and chemical properties occurring from the time of the oil discharge to the end of the clean-up operation. The sampling program was arranged so that oil from each spill would be collected at regular intervals. Ultimately, the oil was sampled in four different situations: (1) immediately prior to each discharge; (2) while entrained in the ice; (3) on the ice surface during the melt period; and (4) upon completion of the clean-up.

The sampling program outlined in the original proposal underwent extensive revision during the testing period. Original proposals suggested a sampling program requiring a sample size of one litre. Sampling performed very early in the program indicated that a size of ten ml was more realistic. A sample of about ten ml permitted more extensive coring without destroying the test area.

The approach adopted in the new schedule was to place more emphasis on deriving as much information as possible from the small oil samples that could be collected. This led to increasing the number of gas chromatograms (GC's) done per test from two to about seven for the earlier spills and three or four for the later ones. For a selected number of these samples, the density and viscosity of the oil were measured at the site. These measurements served as a standard for the work done in the laboratory in Toronto. There, tests were done to relate the viscosity, density, pour point, and solubility to the GC profile from the oil sample. This meant that oil samples as small as 20 ml could be collected and the oil properties derived from the GC done on the sample. In all, 57 GC's were done on oil samples. In total, there were about 70 oil samples taken, however, some were used exclusively for site tests and some were damaged in transit.

Two composite oil samples were taken from Swan Hills and Norman Wells crude oil barrels at the start of the program. Each sample contained oil drawn from several stirred oil barrels and served as a baseline to compare later samples. A pole was used to mix the contents of each barrel thoroughly to ensure that when the oil was withdrawn, it would be of uniform composition. Two litres of each oil type were used for baseline GC's, and ASTM distillation, metal and sulphur content tests, refractive index, and pour point tests.

While the oil was beneath or within the ice sheet, three possible oil-ice configurations could occur. Immediately after a discharge, the oil formed pools or lenses at the ice-water interface. As the ice sheet grew, the oil became entrained within the sheet (Section 6.2). As the ice deteriorated prior to breakup, the oil migrated

upwards into the brine channels.

The bulk of the oil samples were recovered during the second phase, while the oil was entrained in the ice sheet. Sampling was avoided during the first phase, when coring operations could drain large areas of oil. Samples taken from oiled brine channels indicated oil properties to be the same as those of oil from lenses, reducing the requirement for sampling of this phase. The results are discussed in Section 8.1.

For all three situations, the following procedure was used, where applicable. The actual sampling schedule shown in Appendix 27B was keyed to other ongoing tests, principally the ice coring. An area within a particular spill was selected according to past experience and the probability of finding oil at that particular location. A standard 8 cm diameter SIPRE corer was used to obtain the ice cores.

After the core was withdrawn, any oil present in the vicinity of the hole would float to the surface of the water in the hole. A one litre glass bottle would then be lowered into the hole until the bottle lip was just below the surface. When withdrawn, the full bottle would contain from 2 to 500 ml of oil, depending upon the thickness of the oil layer. The oil was then transferred into smaller containers. Information as to the thickness of the oil lenses, and their location in the ice sheet was then obtained using an L-shaped probe and this data added to the coring reports. In the third situation, that of oil within the brine channels, the above procedure was followed up to the extraction of the ice core. After the core had been logged, the oil bearing ice section was cut out and put in a glass jar to melt.

Surface sampling of the oil during the melt period took several forms, depending on the condition and location of the oil. In general, the oil could be found: (1) in open pools, usually on top of melt water; (2) beneath the snow cover but on the ice surface, as a layer; and (3) as a discolouration of the snow cover. The second condition usually preceded the first condition, and occurred just after the oil began surfacing in that particular area. The third condition usually occurred concurrently with the second, as oil spread through the snow column in a capillary action.

For collecting oil from open pools, the sample bottle was submerged in the melt pool and the oil allowed to flow into the bottle. For more viscous material, such as remained after the burning operation, a 12 cm diameter jar was used and a piece of the material was scooped up with a spoon, or by hand, and placed in the jar. The same type of jar was used to collect the oiled snow.

After breakup, oil that had been left on the ice drifted into shore on ice chunks and was then washed up onto the beach. Samples of this residue were collected just before the shore clean-up began on July 7.

Since the degree of weathering of the oil was of particular interest, the handling and storage of samples posed special problems. Oil samples were placed in glass bottles of appropriate size, leaving only sufficient air space for thermal expansion. The snow and ice samples were stored in 200 ml jars. A considerable air space was left when the sample melted, which likely introduced some error. All containers were sealed with silicone rubber and polypropolyene tape, then sealed in plastic bags.

Camp Analysis

The viscosity measurements were made with Standard Ostwald viscometers, calibrated with water at the site at +15°C and 0°C. Benzene was used for calibration at temperatures below 0°C. Five to eight tests in the viscometer were made for each sample measured, and the result analyzed. For density measurements, two 50 ml volumetric flasks were used per sample, where possible, and the measured volume of oil weighed on a two-pan balance. For oil volumes less than 50 ml, the oil was transferred to the flask with a graduated pipette. The measurement of water in oil was done according to the ASTM D95 standard, using 200 ml oil samples.

Oil Evaporation Studies

To assess the effect of evaporation on oil at the surface during the winter, 300 ml samples of both Norman Wells and Swan Hills crudes were placed in evaporation pans December 24. The pans, which measured 20 cm in diameter with a 1 cm lip, were located at an elevation of 1 m to avoid ground effects. One ml samples were recovered on January 4 and 20, and February 26.

5.4.2 Ice and Snow Sampling

To fully understand the effect of included oil on the ice sheet, it was necessary to monitor the condition of both contaminated and uncontaminated ice throughout the winter. Since excessive coring would tend to alter conditions, a number of in situ monitoring techniques were tried.

Clear plexiglass tubes which were 2.5 m long with an inside diameter of 5 cm, were installed vertically through the ice early in the season. The lower end of the tubes were sealed, while the tops extended about 0.5 m above the ice. A specially designed borescope, or inverted periscope, was inserted in the tubes periodically to examine conditions adjacent to the wall. The unit was equipped with a variable intensity light source, and a splitter at the surface to permit photography simultaneously with viewing. Despite various attempts at insulating and sealing the tubes, frost build-up on the inside generally reduced visibility to an unacceptable level. In places where the tube was frost free, lack of contrast in the ice, as seen through the borescope made inspection difficult. Although this approach has potential, several major refinements are necessary for general field application.

Weighted hot or resistance wires were installed at a number of locations throughout the test area, for measuring ice thickness. These units worked well in undisturbed ice. However, in contaminated areas, the small melt channel around the wire provided a drainage path for the oil. To avoid disturbing the oil lenses, this method was discontinued.

Full emphasis was then placed on the SIPRE coring program. Although coring is the most disruptive technique, it provides the maximum level of information. Early in November the sampling program was redesigned to ensure all necessary information was generated without unduly disturbing the test areas. As well, a SIPRE corer was used to cut all holes, regardless of the ultimate purpose. The location, snow cover, ice thickness, depth of oil lens, extent of migration and ice structure were logged (Appendix 27C), and the cores immediately photographed. Small sections of core, generally from the region of the oil lens were retained for detailed study.

At regular intervals during the winter, and intensively during the melt phase, salinity profiles were made on representative cores. Each core was cut into 4 cm long slices, as soon after removal from the sheet as possible. The slices were then placed into labelled plastic bags that were sealed until the ice melted. Sorbent was used to remove oil from contaminated samples. The salinometer was routinely calibrated with prepared solutions, and a series of tests were conducted to ascertain the effect of oil in the sample on the sensor.

5.4.3 Water Sampling

The non-biological water sampling program comprised measurements of salinity and temperature profiles, and dissolved hydrocarbon content, at various locations throughout the year.

During the initial site selection survey in August, 1974, salinity and temperature profiling of the water column confirmed the similarity of the test bay to other areas along the coast. Measurements were repeated throughout the winter. Once ice cover was present, the profiling was done via SIPRE core holes through the ice. Most of the profiling was performed in unoiled locations so that reliable measurements could be taken. When measurements were done in oiled areas, care was taken to ensure that the probes did not come in contact with the oil.

Measurement of the dissolved hydrocarbon (HC) content proved difficult in the depth of winter period. Of three proposed sampling methods, only the simplest one proved feasible. As contamination of a sample by trace amounts of undissolved oil would invalidate the results, sampling locations were located just outside of oiled areas. Samples were recovered by lowering a one litre glass bottle through a SIPRE core hole. The bottle then filled with water from just beneath the ice sheet, and was immediately withdrawn and rushed back to the camp before freezing occurred. Glass bottles were

necessary to prevent the possible evaporation of the highly volatile components during the extraction phase after adding five millilitres of n-pentane to the water sample. The bottle was capped, shaken, and left for twenty-four hours. After occasional shaking during that period, the pentane was drawn off and placed in a tightly sealed glass vial for shipment south for analysis by gas chromatography. The sampling schedule is presented in Table 8-3.

5.4.4 Biological Sampling

The biological sampling program was intended to achieve the following basic objectives:

1. to assess the effect of an oil spill under ice at Balaena Bay on rates of primary production;
2. to assess invertebrate species occurrence in the area of the bay and to determine effects of the oil spills;
3. to record basic environmental parameters controlling phytoplankton populations at Cape Parry, eg. water temperatures, light intensities beneath the ice, salinity, oxygen concentration both under the ice and in open waters in the summer;
4. to determine effects of released oil from winter spill sites on the vegetation above and below the tideline when the oil reached it in the summer time;
5. to determine species compositions and productivity of the small salt marsh at the head of the bay near to the spill sites; and
6. to determine the effect of oil washed onto this salt marsh following release of weathered oil from the below ice spills.

The following methods and techniques were employed on the biological sampling programme.

Physical and Chemical Parameters

Salinities were determined with a calibrated Americal Optical Refractometer. Water samples were taken at different depths with a Van Dorn water sampler. Temperatures were read immediately upon removal of water samples from the sampling bottle. Sub-samples were injected into 25 ml glass ampoules and sealed with a torch for laboratory determination of pH and CO_2 (total) content using an infrared gas-analyzer (Beckman Model 915 Total Carbon Analyzer). Light measurements were made with a Montedoro-Whitney Portable Solar Illuminance underwater meter and a matching deck-cell.

Phytoplankton and Zooplankton

Phytoplankton samples of 500 ml, obtained with Van Dorn sampling bottles, were added to volumetric cylinders. Three millilitres of Logol's iodine solution were added, and allowed to settle for 2 days. The supernatant was then removed by siphoning to leave only about

20 ml containing the algae, which were transferred to plastic vials and kept in the dark at 5°C for identification and quantitative analysis using sediment chambers and an inverted Wild microscope.

Zooplankton collections were made by vertical and horizontal tows using a No. 6 mesh (240 µm mesh sizes; 50 cm diameter) and No. 20 mesh (60 µm; 25 cm diameter) nylon nets. The plankton samples were preserved in 8% neutralized formalin, and counted quantitatively in Sedgwick-Rafter counting chambers.

Benthic Algae and Invertebrates

Benthic algae and invertebrates were obtained by the use of Wildco Model 175 biological dredge. For quantitative sampling, a Ponar grab dredge (Wildco Model 1725; 23 cm x 23 cm sampling area) was used. Samples were preserved in plastic jars with 8% neutralized formalin for later identification and counting.

Chlorophyll

Chlorophyll of salt marsh plants and attached algae was determined by extraction with 80% acetone in a mortar and pestle, and with the addition of a small amount of acid-washed silica. The acetone extracts, following centrifugation to remove suspended material, were analyzed for chlorophyll by the method of Arnon (1949).

Primary Productivity

Water samples were taken from different depths with a Van Dorn water sampler. Fifty ml aliquots were transferred to 60 ml transparent plastic bottles. Ten µCi of $NaH^{14}CO_3$ were injected into duplicate light and dark bottles, after which the bottles were suspended at the same depths from which the samples were originally taken. The bottles were incubated in situ for 24 hours (approximately noon to noon). Five hundred µl of 0.1 N HCL were then added to remove inorganic ^{14}C-bicarbonate by aeration. One ml aliquots were later added to 15 ml Aquasol, and the radioactivity in the vials determined in a Packard Tri-Carb Liquid Scintillation Counter. Similar techniques were used for determining photosynthetic rates of phytoplankton used for oil toxicity studies (6 hr incubation only), and for micro-algae from oil contaminated marsh and shingle areas near the oil spill site at Balaena Bay.

Laboratory Oil-Toxicity Studies with Phytoplankton

Aqueous extracts of Norman Wells and Atkinson Point crude oils were prepared by stirring one litre of nutrient seawater medium, and 50 ml crude oil in a 1 litre glass-stoppered bottle. Air was almost completely excluded to minimize losses due to volatilization. The mixture was stirred for 16 hr at a speed producing a 3 cm oil vortex. A siphon was used to remove the aqueous oil extract. This 100% aqueous crude oil extract was tested before and after dilution to 30%, for ability to support algae growth and photosynthesis.

5.5 Photographic Techniques

5.5.1 Underwater

A Hydro Products TC-125 underwater TV camera was used to document all controlled discharges, and to continuously monitor conditions both at the ice-water interface and in the water column. Since the camera measured less than 9 cm in diameter, it could be inserted through a SIPRE core hole. The unit maintains a nearly constant video output level over a dynamic range of illumination of 10,000 to one. Focusing was controlled from the surface. The signal was fed simultaneously to a Sony AV8400 video recorder and a Conrac monitor to permit selective recording. Positional data and information on the discharge were recorded on the sound track. Through the use of a constant current source, the entire system could be operated effectively from one 300 W portable generator.

During the depth of winter, lighting proved very difficult. Although the contrast between the oil and ice permitted high resolution around the edges of lenses or drops, the general lack of relief and the automatic compensation of the camera made the examination of fine details almost impossible, if the entire field of view was either all oil or all ice. A variety of lighting systems were tried, including tungsten, quartz halogen and quartz iodide. It was found that the spectral density was not as critical as the angle. In general, the more oblique the angle, the better the resolution. This was difficult to achieve, since in many cases it meant that the lighting system had to move independently from the camera. The problem was naturally resolved in the spring. Even with up to 2 m of ice and 40 cm of snow, there was sufficient diffused light to permit viewing through 15 to 20 m of water.

For the initial tests the camera and a narrow beam transducer were mounted on a telescopic scissor boom. The unit could be raised and lowered on an aluminum mast, rotated through 360 degrees and extended up to 15 m. However, to obtain full coverage, it was necessary to install the boom in the centre of the test area. A number of different barriers were tried in an effort to prevent oil from flowing into the well constructed for the boom. The only effective method was to thicken the ice around the well, which was equally disruptive to the test. For the NW6 test in February, the camera was mounted on a rigid boom, which was inserted through the ice from outside the test area. The extended distances limited the effectiveness of the system, and on all subsequent tests the camera was hand held by a diver wearing a closed circuit breathing system. The entire operation was monitored on the surface, and the movements of the diver controlled by means of a surface communications system. This approach provided the maximum recovery of data, and the greatest flexibility.

A Nikonos 35 mm camera with a 21 mm corrected lens was used for underwater still photography, and a 16 mm Bolex in an underwater housing for moving photography. Even with the use of flash and flood

systems, lighting proved difficult. As a rule, all critical details were shot at a minimum of five exposures. The best results were obtained by pushing High Speed Ektachrome to 1000 ASA. The resulting grainy finish was not a great disadvantage in that the subject matter was largely high contrast in nature.

5.5.2 Time Lapse - Surface

From May to July 1975, two 8 mm time lapse movie cameras were used to document site conditions. One camera was mounted in a weather-proof housing and positioned on the top of a hill to the north of the test area, at an elevation of approximately 30 m. This unit exposed a frame every 60 seconds. The second camera was mounted at the 15 m level on the anemometer tower and exposed a frame every 22.5 minutes.

5.5.3 Stills - Surface

Over 450 35 mm still pictures were taken throughout the project, covering surface conditions of the test sites, experimental techniques and ice cores. To ensure consistent quality and to accent internal features, all cores were photographed in specially designed light box, which had controlled back lighting.

5.5.4 Movies - Surface

The discharge operation, ice and surface conditions, the initial burn on June 7, and subsequent phases of the clean-up were documented on 16 mm movie film. Altogether, some 5000 feet of film are available through NORCOR Engineering and Research Limited, the A.P.O.A., and the Department of the Environment.

6.0 OIL AND ICE INTERACTION

Since all crude oils are less dense than sea water, they will rise towards the surface in a plume if released at depth. Enroute, the oil generally breaks into small droplets. If the area is ice-covered, the oil will collect on the bottom of the ice. The bulk of the oil will coalesce into pools or lenses, the size of which is controlled by the physical properties of the oil and irregularities along the bottom of the ice. Even with "smooth" first year ice, the variation can be considerable. The oil only penetrates several centimetres up into the skeletal layer and soft ice at the bottom. If the ice is still growing, new ice will begin to form beneath the oil, and the oil will be completely encapsulated or entrained in a matter of days. Once the oil is locked in the ice, further movement is limited until the ice begins to warm in the spring.

As sea ice freezes, approximately 80 percent of the salt or brine is rejected downward through the ice, while the remainder is trapped in small pockets in the ice. In response to increased solar radiation and a higher ambient air temperature in the spring, these isolated pockets of brine begin to etch their way through the ice. As they intersect voids left by the rejected brine, they form a continuous channel referred to as a brine channel. The oil migrates or moves towards the surface by means of these channels. Once oil reaches the surface, it greatly reduces the albedo and an increased quantity of solar radiation is absorbed. This causes an increase in activity in the brine channels and the process becomes self-accelerating. The various processes associated with spreading, entrainment, migration and surface effects of oil are detailed in subsequent sections.

6.1 Oil Plume and Spreading

The disposition of oil under solid ice cover is controlled primarily by three factors; the nature of the discharge, the condition of the ice, and the physical variables associated with the discharge of oil during a blowout. For example, well head temperature, pressure, the quantity of gas and oil, water depth and currents will all influence the plume and ultimately the disposition of the oil. Due to the limited value of conducting a test under one particular set of conditions, and the probable difficulty in controlling a large volume of oil, no attempt was made to simulate a blowout. Instead, the oil was heated to close to the ambient water temperature and injected under the ice in a manner designed to permit the best documentation.

Depending on atmospheric conditions and operational constraints, the oil was heated to between -4°C and 1°C in a holding tank on shore. It was then pumped approximately 250 m out to the test area and injected under the ice. The discharge operation is detailed in Section 5.2.2. Although the minor variation in temperature had little effect on the physical properties of the oil (Table 6-1), on the several occasions when the oil was below approximately -1.8°C, crystallization occurred in the water column. The oil quickly assumed the water temperature, and maximum variation recorded by a thermistor was about 1.0°C. The discharge rate

Plate 6 - 1 Oil plume showing radiating waves of oil.
Note skirt hanging with ballast cable (upper left)
Pipe end is about 2.5m below the ice bottom.

varied from 0.13 to 0.19 $m^3\ min^{-1}$ (28.6 to 41.8 Imp. gal min^{-1}), yielding an exit velocity of 1.1 to 1.6 m s^{-1}. The projected discharge rate for a blowout in the Beaufort Sea is 0.27 $m^3\ min^{-1}$, decreasing to 0.11 $m^3\ min^{-1}$ after one month.

TABLE 6-1

VARIATIONS IN PHYSICAL PROPERTIES OF TEST CRUDES WITH TEMPERATURE

	TEMP.	NORMAN WELLS CRUDE	SWAN HILLS CRUDE
Viscosity (g $cm^{-1}\ s^{-1}$)	0°C	0.12	0.34
	-15°C	0.18	0.45
Density (g cm^{-3})	0°C	0.845	0.837
	-10°C	0.855	0.845
Thermal Conductivity (cal $cm^{-1}\ °C^{-1}\ s^{-1} \times 10^{-4}$)		$\simeq$ 3.0	$\simeq$ 3.0

A number of discharges were recorded on video tape and 16 mm film. In general, the oil rose in a conical plume, which had a half-angle of about 25 to 30 degrees. Flow tended to be unstable, and the oil broke into small particles within 0.3 m of the standpipe (Plate 6-1). The particles, which varied in diameter from about 0.2 to 1.0 cm, were close to spherical. Smaller particles were subsequently located in the ice, but these could not be detected in the plume. The movement of a number of particles was documented by means of the stop-action facility on the video system. The average upward velocity of five representative particles was 27 cm s^{-1} ± 6 cm s^{-1}. On the basis of the behavior of the oil on contacting the bottom of the sheet, it was apparent that a considerable quantity of water was entrained in the plume. The upward movement of jelly fish near the periphery of the plume confirmed this observation. In general, the plumes closely resembled the deep water gas plumes documented by the Frozen Sea Research Group (Topham, 1976).

The behavior of the oil on striking the bottom of the sheet depended very much on ice topography. If there was a depression (or thin ice section) in the ice immediately above the standpipe, the oil would initially be confined to a single pool. Clear, uncontaminated ice could be observed in the splash zone created by the ascending particles. There was no appreciable movement of the oil outside of the splash zone. As additional oil was added, the pool or lens would slowly grow in size and depth until it reached the level of a channel which would permit flow into an adjacent depression. If the standpipe happened to be below a dome, or thicker section of ice, the droplets would radiate out from the centre after striking the ice. As the droplets decelerated, they tended to coalesce into concentric waves of oil, which radiated outward, but at a reduced velocity. There was a distinct surging action, and clear bands of ice

could be observed between rings of oil. Within several metres the wave would break down and the oil would flow outward in a dense array of small streams or rivulets (Plate 6-2). The width of rivulets varied from about 2 to 10 cm.

Plate 6 - 2 Oil rivulets (photographed during offshore Discharge # 2)

In general, flow was unstable, and tended to pulsate in response to the wave action. There were periodic breaks in the oil, but the rivulets repeatedly followed the same course, suggesting that a path had been cut through the skeletal layer. Ice crystals were observed floating immediately below the oil. Occasionally, a surge of oil would flush over the entire area. On passing, the rivulet pattern would quickly re-establish while the ice in between showed no signs of contamination other than the occasional drop of oil. This would indicate that either time or pressure exerted by a new layer of ice below a lens is required for the oil to penetrate up into the skeletal layer.

The areal extent of spreading along the underside of the ice sheet is controlled by a number of factors. Most crude oils will naturally coalesce at an ice-water interface to form a sessile drop, which is similar in shape to mercury on glass. The process has been documented recently by a number of investigators (Lewis 1975, Mackay 1975), and therefore will not be detailed herein. The minimum stable drop thickness is dependent on the properties of the oil, and is typically about 0.8 cm. A very small quantity of oil was deposited on the ice in the form of small spherical particles, which had a diameter less than the minimum film thickness. These normally occurred near the periphery of the contaminated ice, in areas where the currents were feeble, and the chance of collision with other oil particles was small. A typical example of small oil particles is shown in Plate 6-3.

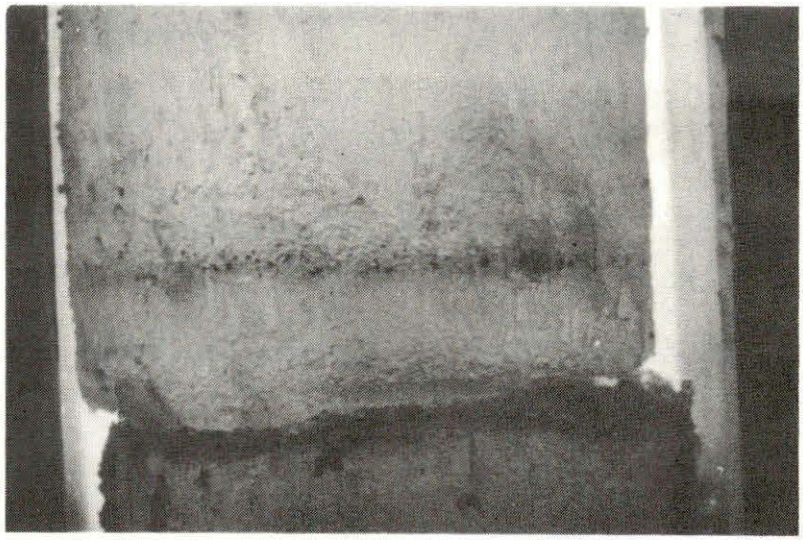

Plate 6 - 3 Included oil droplets.
NW4 core taken Dec. 30/74.

The maximum film thickness is determined by variations in ice thickness, which take two basic forms. Due to differential growth at the skeletal layer, there is a small scale variation which is randomly oriented, and produces pockets about 5 to 10 cm wide and up to several centimetres deep late in the season. It is this pattern which likely accounts for the meandering in the oil rivulets. Consequently, although lenses as thin as 0.8 cm are possible, the minimum thickness tends to be in the range of one to two centimetres. The second form of irregularity is of much larger scale and is caused by variations in snow cover. Due to the insulating effect of the snow, the ice thickness varies inversely with snow depth. As a result, depressions tend to be created under drifts, and domes under more exposed areas. The size, orientation and stability of drifts is influenced by local climate and topography. In Balaena Bay, the drifts tended to be stable throughout most of the growth season. Plots of ice depth vs snow thickness made in November and January confirmed a well defined relationship between heavy snow cover and thin ice. Once the sheet exceeded about 50 cm, the maximum variation in thickness was approximately 20 percent of the average ice thickness. This yielded a maximum variation at the end of the season of 35 cm. For an analysis of variations in ice thickness, see Figure 7-4a.

These large scale variations effectively contained the oil and controlled the maximum lens thickness. With the exception of the early tests, 7.3 m^3 (1620 gals) was insufficient to fill even a single depression. On NW4, when the ice was about 64 cm thick, the oil covered approximately 400 m^2 for an average lens thickness of 2.0 cm. With NW7, when the ice was 154 cm thick, 180 m^2 was covered, yielding an average lens thickness of 4.5 cm. The maximum oil thickness measured was 20 cm, while the average oil thickness for all tests was 2.1 cm.

6.2 Oil Inclusion

The disposition of oil along the underside of the ice sheet has considerable bearing on the nature and rate of inclusion. As described in Section 6.1, the oil can be deposited in various configurations, ranging from very small drops to large pools or lenses, depending on the characteristics of the plume and the roughness of the ice sheet. Although drops and small pools can be scattered over an appreciable area, they tend to contain an insignificant quantity of oil. In the tests at Balaena Bay, over 95 percent of the oil was contained in pools larger than one metre. The average depth of all pools was 2.1 cm, while the maximum observed depth was 20 cm. Because oil forms sessile drops at an ice-water interface, the minimum possible thickness of oil is about 0.8 cm.

If the temperature of the oil is close to the ambient water temperature, which was the case for the tests and would likely be the case for most blowouts, the various processes associated with inclusion come into play shortly after the oil stabilizes on the bottom of the ice. The thermal conductivity of most crudes is about one fifteenth that of natural sea ice, and the insulating effect is detectable within hours. Although free convection could be significant in very thick oil lenses (Section 7.2.3), the required conditions are rarely encountered in the natural environment. For the more typical lens thicknesses encountered in Balaena Bay, the added thermal resistance of the oil caused a depression in the thermal gradient through the ice. Temperature drops of over 1.0°C were observed immediately above the oil within 24 hours. The horizontal transition from a normal temperature gradient through the uncontaminated ice to a depressed gradient above the oil, caused sub-freezing temperatures at the edge of pools, which resulted in the formation of an ice lip. Figure 6-1, shows schematically the depressed thermal gradient and the realignment of isotherms.

Figure 6-1 INITIAL EFFECT OF OIL LENS

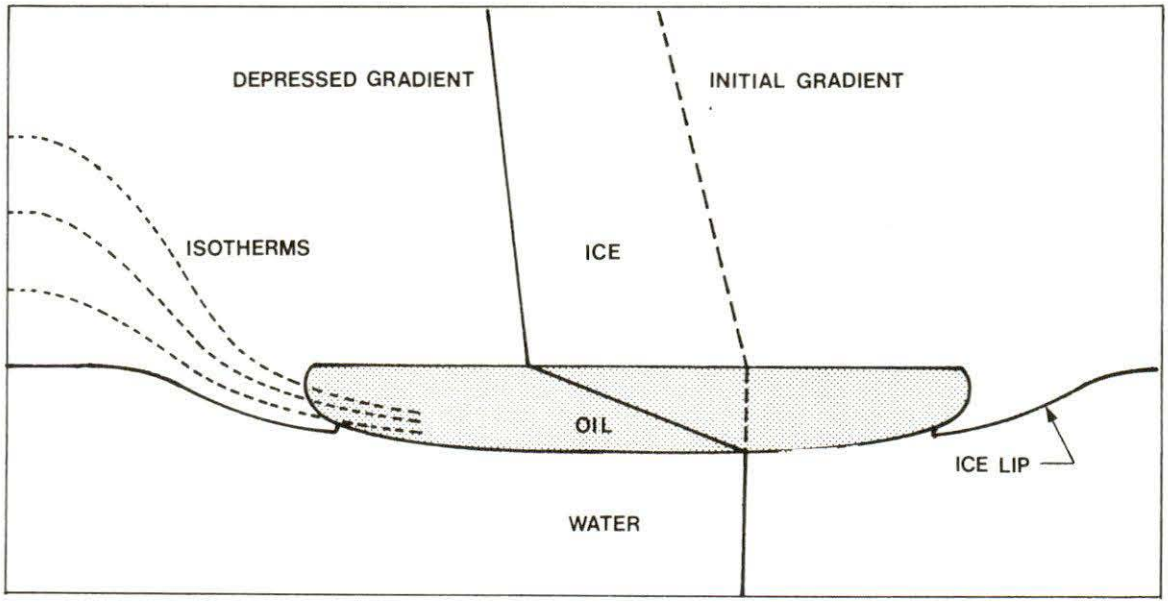

The ice lip is a major feature of the inclusion process. Once it was formed, there is no possibility of further horizontal movement. This could be particularly important in areas with high currents or if there were a continuous flow of oil. During the depth of winter, several ice lips were detected within hours after the oil was released, and in all cases a lip could be observed within 24 hours. A typical ice lip is shown in Plate 6-4. The dark band around the edge of the pool, is an air bubble, which was injected to accent the lip.

The time required for a new sheet of ice to form beneath an oil pool is primarily a function of the thermal gradient and the thickness of the oil. Due to the discrete spacing between thermistors, and gradual change from water to loose crystals then solid ice, it was difficult to ascertain the precise time at which a new sheet was formed. However, by continuously monitoring chains and extrapolating between beads near the water-oil interface, a reasonable approximation was possible. During the late fall, when the ice and oil lenses tended to be relatively thin, the oil appeared to be incorporated within about five days. This period increased to about seven days for a typical lens during the depth of winter and over ten days in the spring. As well as altering the thermal gradient, the oil also altered the system of brine drainage within the ice. In the normal brine rejection process, the freezing skeletal layer at the ice-water interface produces platelets of ice that are of lower salinity than the water. The brine that is rejected from the platelets during freezing flows downward through the forming ice. The rate of ice growth controls the amount of brine that is trapped in the ice sheet. When ice growth is slow, less brine is trapped within the ice.

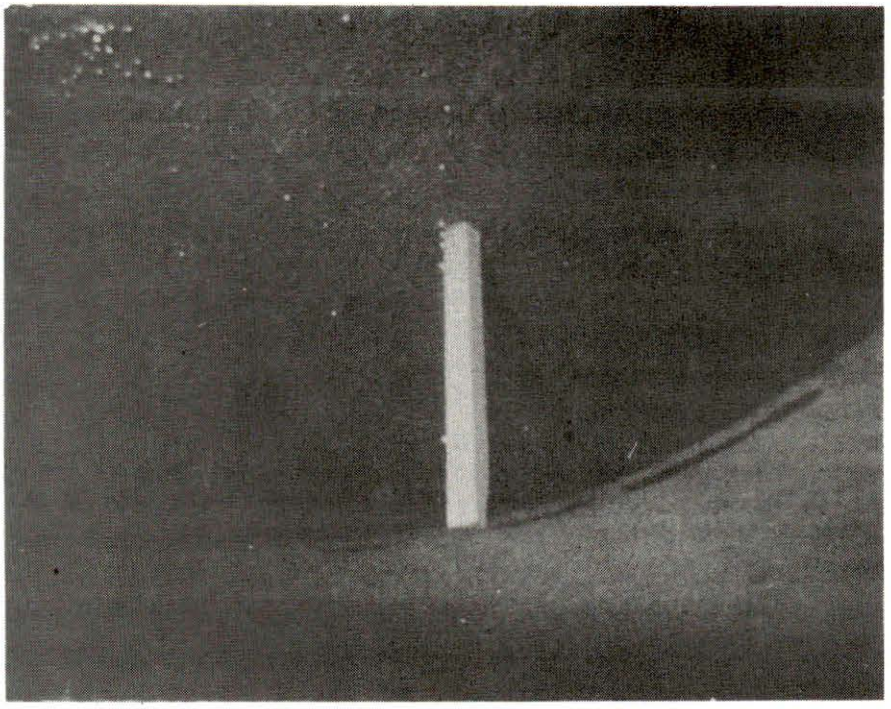

Plate 6 - 4 Stabilized oil pool immediately following SH2 discharge.
Note the close spacing of thermistor probes at the oil-water interface (centre).
An ice lip has started to form at the pool boundary.

Coincident with the drop in temperature, there is an increase in salinity in the ice immediately above an oil lens. This could be due to two factors. Firstly, the oil serves as a barrier to brine rejection, and the brine draining through the ice accumulates above the oil. Since the brine is denser than oil, other physical characteristics must come into play. Secondly, the depressed temperature would naturally cause a somewhat higher concentration of brine. However equally high salinity peaks could not be detected at other locations within the sheet, suggesting that drop in temperature alone did not account for the entire accumulation of brine. The salinity in the new ice immediately below the oil tended to be lower than normal. This was likely due to the slow rate of growth and the barrier to brine drainage from ice above, imposed by the oil. In many respects, the ice which formed beneath an oil lens resembled a sheet grown at the surface under controlled temperatures. Representative salinity profiles through contaminated ice are shown in Figures 6-4 to 6-7. The discharges which were conducted early in the year, when the sheet was growing rapidly, exhibit a far more pronounced jump in salinity above the oil, than do the later discharges. The similar salinity profiles both above and below the oil on the NW4 core (Figure 6-4) should be noted. The temperature at which the brine channels will begin to open in the spring is dependent on brine concentration. The high salinity immediately above the oil will likely cause the brine channels to open somewhat earlier than normal, and thereby permit the upward migration of oil.

In most cases, a distinct band of clear relatively fresh ice could be detected immediately below the oil (Plates 6-5, 6-6). The band was typically two to three centimetres thick, and consisted of small, randomly oriented crystals. The band was likely caused in part by the reduced salinity below the oil and the slow growth rate. Similar, but less pronounced bands were located at several levels in uncontaminated ice. These bands were also of lower salinity than the rest of the core. An attempt was made to correlate these features with temperature fluctuations, but due to variations in snow cover, and thermal lag in the sheet, no firm relationship could be established. There is also the distinct possibility of a periodic influx of fresh water with the tidal flush, but this would not explain the repeated reoccurrance of the band below oil pools.

Frequently, the new ice interface was very smooth, conforming with the underside of the oil lens. A typical example is shown in Plate 6-6. The surface appeared to be polished and did not contain large brine channels or crystals, common to uncontaminated ice at that depth. Occasionally flecks and small patches of oil were observed at the lower interface (Plate 6-11), but they did not penetrate more than a few millimetres into the ice. The effect of the oil at the upper interface was far more pronounced. Within a matter of days, the oil had penetrated several centimetres into the loose skeletal layer (Plates 6-9, 6-13). The surface was very rough and irregular, and individual crystals and brine channels could be easily identified. The ice immediately above a lens tended to be saturated with oil, and plugs of oil could be seen in the brine channels (Plate 6-8).

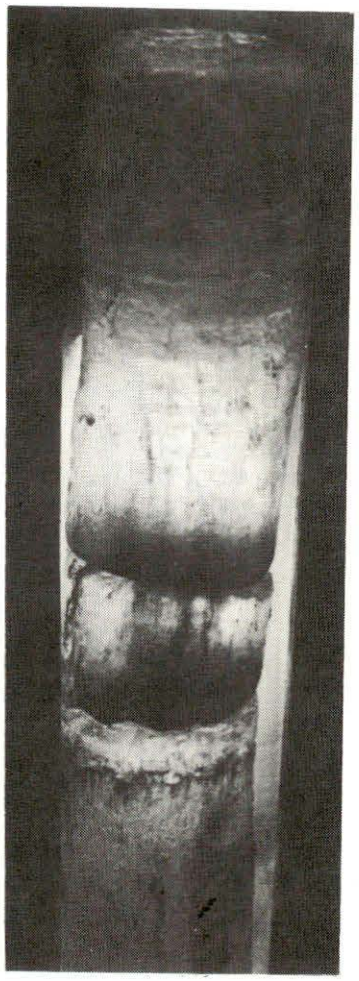

Plate 6-5

NW2 core taken Nov 20/74. Oil lens was at bottom break in.core.
Oil visible below the lens was due to contamination on removal.

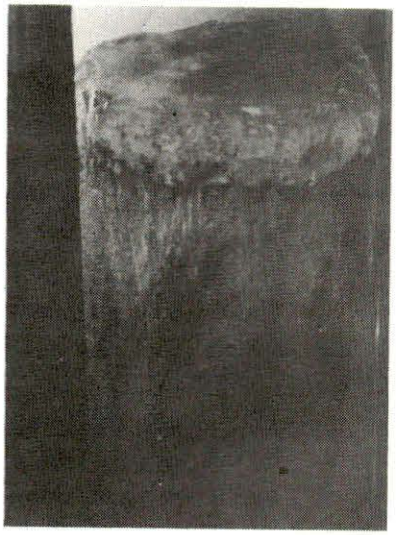

Plate 6 - 6

Above core showing smooth ice interface and distinct band $\approx$ 2cm thick, below the oil lens.

6.3 Oil Migration

The migration, or upward movement of oil through the ice is controlled primarily by the condition of the ice, and to a lesser extent, the physical properties of the oil. The process can be reasonably correlated with the dominant periods in the growth and depletion of the ice sheet. During the depth of winter when the sheet is cooling and growing rapidly, the ice is relatively solid, with the exception of the skeletal layer. Although the oil is less dense than water or sea ice, there are very few passages for it to penetrate, and movement tends to be limited. As the sheet starts to warm in the spring, brine channels begin to open, and the oil slowly moves upward, filling the voids. As the oil approaches the surface, increased solar radiation is absorbed and the process is accelerated. Late in the spring, when the ice is very porous, the oil flows freely through the sheet.

Simultaneous tests were conducted with Norman Wells and Swan Hills crudes primarily to determine the importance of the physical properties of the oil in the incorporation and migration processes. Swan Hills crude is a relatively heavy oil (Table 6-1), while Norman Wells crude is light, and about the same consistency as Number 2 heating oil. It was felt the crude to be found in the Beaufort Sea would likely fall between these two. Although minor variations were observed, no significant differences, which could be attributed solely to the type of oil, were detected. However, the pour point of both crudes was well below the freezing point of the ice, and generally below the temperature of the ice when migration occurred. The effects of viscosity and density would likely be far more pronounced with a very heavy oil such as Bunker C.

Coring was found to be the best method of documenting the migration of oil through the ice sheet. A number of representative core logs and supporting plates are presented at the end of this section. During the coring operation, oil would flow up inside the SIPRE barrel, and surface contamination was unavoidable. Prior to photographing a core, the surface was cleaned with sorbent and then polished. During the winter, when the ice was solid, this proved effective, however, once the ice became porous, it was difficult to determine the source of the oil.

Cores recovered from the open water test area (NW2) showed no signs of the oil having penetrated downward into the ice. The sheet, which grew completely beneath the oil, closely resembled the natural ice sheet. The first 15 to 20 cm of snow above the initial level of the slick was saturated with oil, and had recrystalized (Plate 6-7). The snow above this appeared to be uncontaminated. The oiled snow-ice remained stable throughout the winter, and was not subjected to drifting.

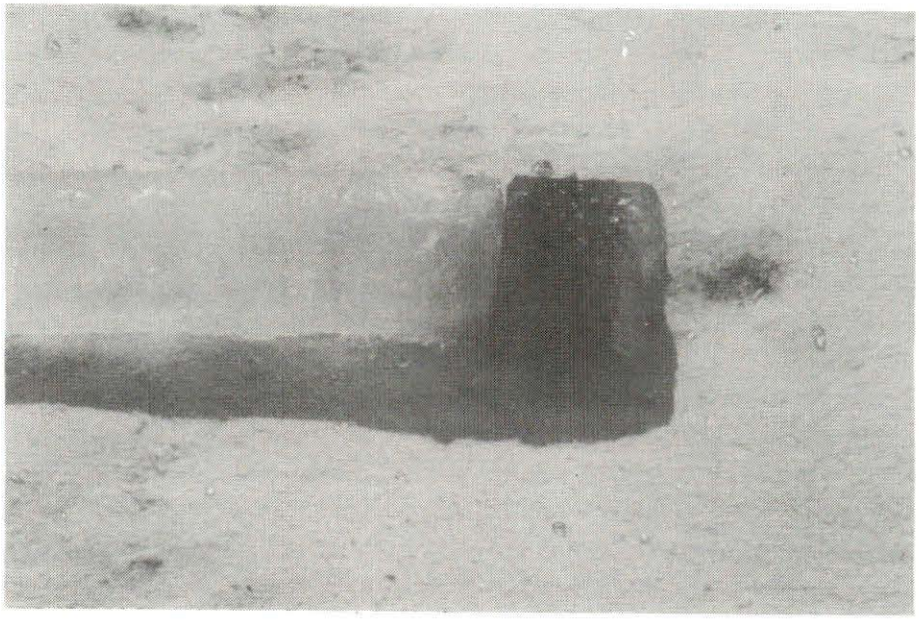

Plate 6 - 7 Detail of top core section from NW1 open water spill, taken May 15/75. Dark area is the original oil spilled on water, later contained in snow ice.

During the late fall and early winter, the ice grew at an average rate of about one centimetre per day. During this period, very little difference could be detected between the various test sites. Although the thickness of the ice was increasing, the initial thermal regime at the ice-oil interface was very similar. In all cases, the oil saturated the loose skeletal layer, and penetrated several centimetres further up open brine channels. On the average, between 4 to 6 cm of ice was contaminated. Once the oil was incorporated, a further depression in temperature had no apparent effect. A typical winter core is shown in Figure 6-2. The extent of penetration can be seen in Plate 6-8. The small dark bars near the top of the photograph are plugs of oil in brine channels. The small drops of oil below the interface, were initially suspended in the water column, and settled after the formation of the lower ice sheet.

By about mid February, the sheet began to warm and the effect was immediately detectable in the oil. With the increase in temperature, isolated pockets of brine which formerly blocked brine channels began to melt and open short passages through the ice. The high salinity layer, immediately above the oil, was likely a significant factor in accelerating this process. The oil began to migrate upward as the channels cleared. By February 22, oil in the NW2 test site had penetrated some brine channels over 16 cm (Figure 6-3). The brine channels increased in size and became better defined (Plate 6-10). Initial movement appeared to be confined principally to the high salinity zone. A core recovered from the NW4 test area on March 1 (Figure 6-4), displayed similar characteristics. The average diameter of major brine channels was about 0.1 cm. Typical oiled and unoiled channels are shown in Plate 6-12. Although the lower section of the core, in the area of the original skeletal layer, appears to be heavily oiled, the concentration of oil did not exceed four per cent by volume. The oil was confined to brine channels and the interstices between platelets (Plate 6-13).

During the initial stages of the migration, the location, or depth of the oil in the ice did not appear to influence its behavior. The early discharges, which were close to the surface, exhibited similar characteristics to the oil lenses near the bottom of the sheet. This is likely due to two offsetting factors. While temperature increases with depth, the level of absorbed solar radiation decreases. On the average, the radiation level is about six times greater at the 30 cm depth than at 60 cm depth. Since oil is an effective barrier to radiation, it is not unreasonable to assume that all radiation reaching the level of a lens will be absorbed by the oil. This could cause preferential localized warming of the lenses near the surface, and thereby enhance movement in a depressed temperature field. No differences were detected between the Norman Wells and Swan Hills crudes.

During March and April the brine channel network became more pronounced, and the oil slowly progressed upward through the ice. By early May oil had reached the surface in most test areas. A typical core recovered from the NW6 site is shown in Figure 6-6 and Plate 6-15. The oiled brine channels extended from the initial level of the lens to within 10 to 15 cm of the surface. The average diameter of the channels had increased to about 0.4 cm, and they tended to be interconnected by smaller feeder

Figure 6 - 2 ICE CORE REPORT

Discharge No: NW 2 Date Core: Jan 5
Type Crude: Norman Wells Ice Thickness: 84 cm
Date Discharge: Oct 24 Snow Depth: 13 cm
Air Temp: −36 °C

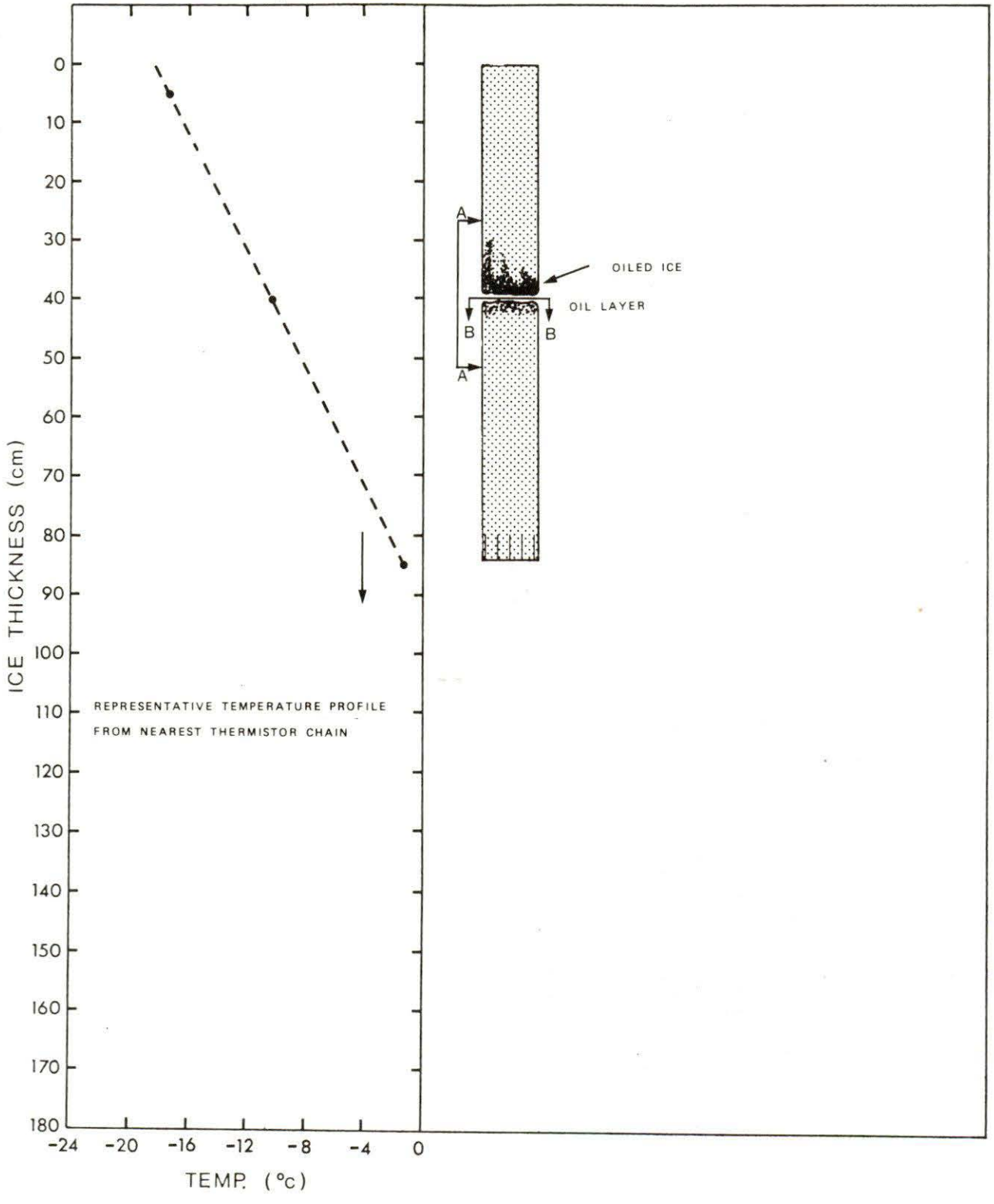

Plate 6 - 8

See section A-A, Figure 6-2
NW2 core, taken Jan 5/75.
Note fairly complete oil penetration of the skeletal layer.
Many very fine oil drops were included in the ice below the oil lens.

Plate 6 - 9

See section B-B, Figure 6-2
End view of top oil-ice interface shows rough texture and degree of oil penetration into the skeletal layer.
Clean patches could be due to freezing of brine which drained from above, after discharge.

Figure 6 - 3 **ICE CORE REPORT**

Discharge No: NW 2
Type Crude: Norman Wells
Date Discharge: Oct 24

Date Core: Feb 22
Ice Thickness: 128 cm
Snow Depth: 10 cm
Air Temp: -23 °C

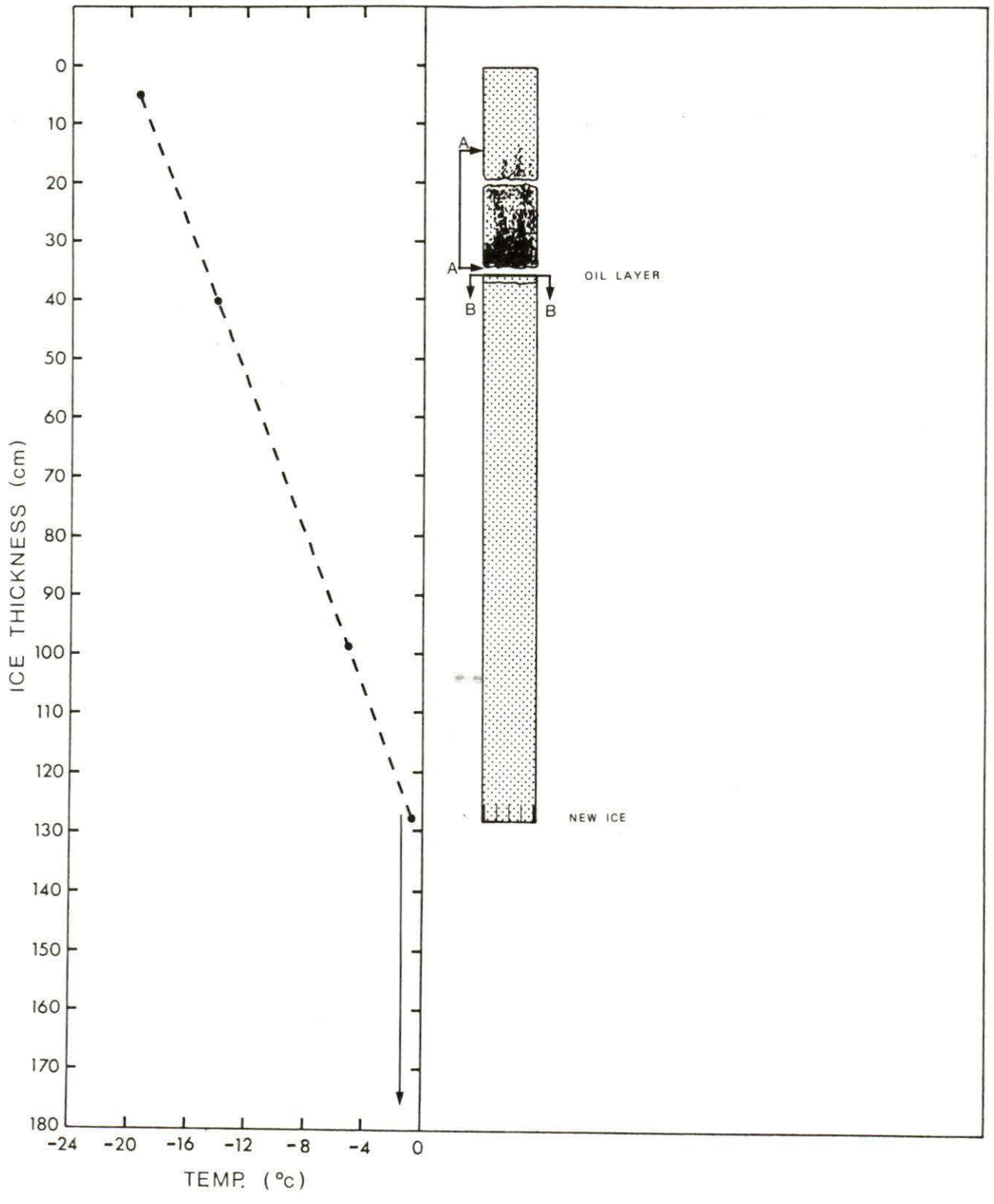

Plate 6 - 10

See section A-A, Figure 6-3
Distinct brine channels 12cm above the oil lens are oiled.
Note the extremely irregular surface of the top oil-ice interface (picture bottom)

Plate 6 - 11

See section B-B, Figure 6-3
End view of bottom oil interface shows very smooth surface. Oiled brine channels penetrated only a few mm.

Figure 6 - 4 ICE CORE REPORT

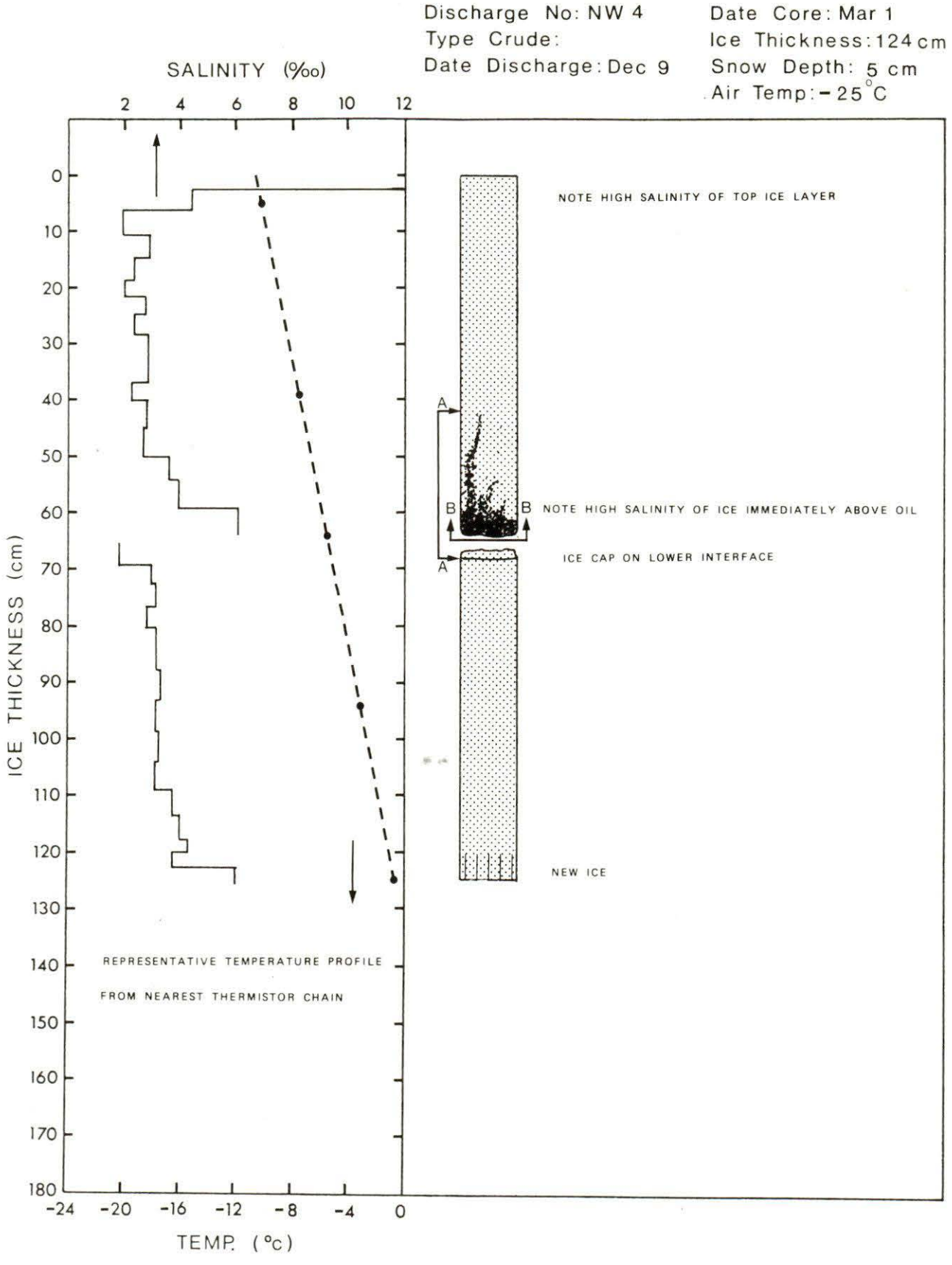

Plate 6 - 12

See section A-A, Figure 6-4
Most of the oil had migrated less than 12cm by March.
Compare to Plate 6-8.

Plate 6 - 13

See section B-B, Figure 6-4
End view of top oil -ice interface.
Selective oil penetration between platelets delineates crystal structure at this interface. Compare to plate 6-11.

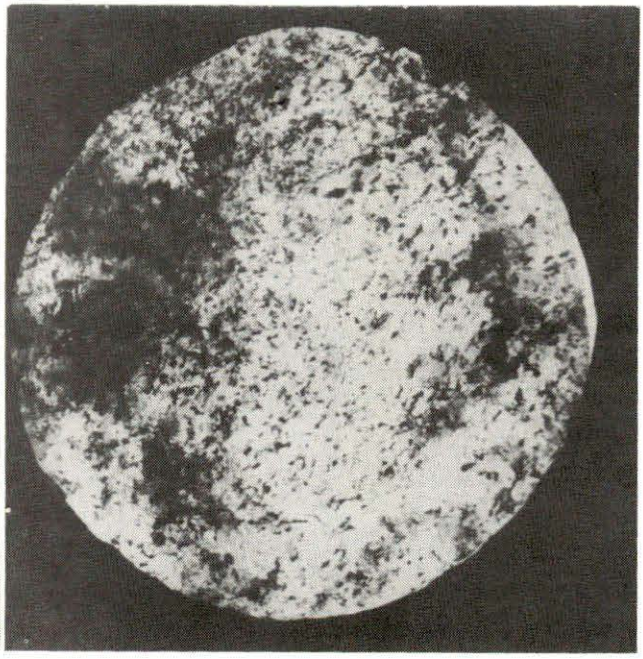

Figure 6 - 5 ICE CORE REPORT

Discharge No: NW 2
Type Crude:
Date Discharge: Oct 24

Date Core: Mar 26
Ice Thickness: 130 cm
Snow Depth: 20 cm
Air Temp: −18 °C

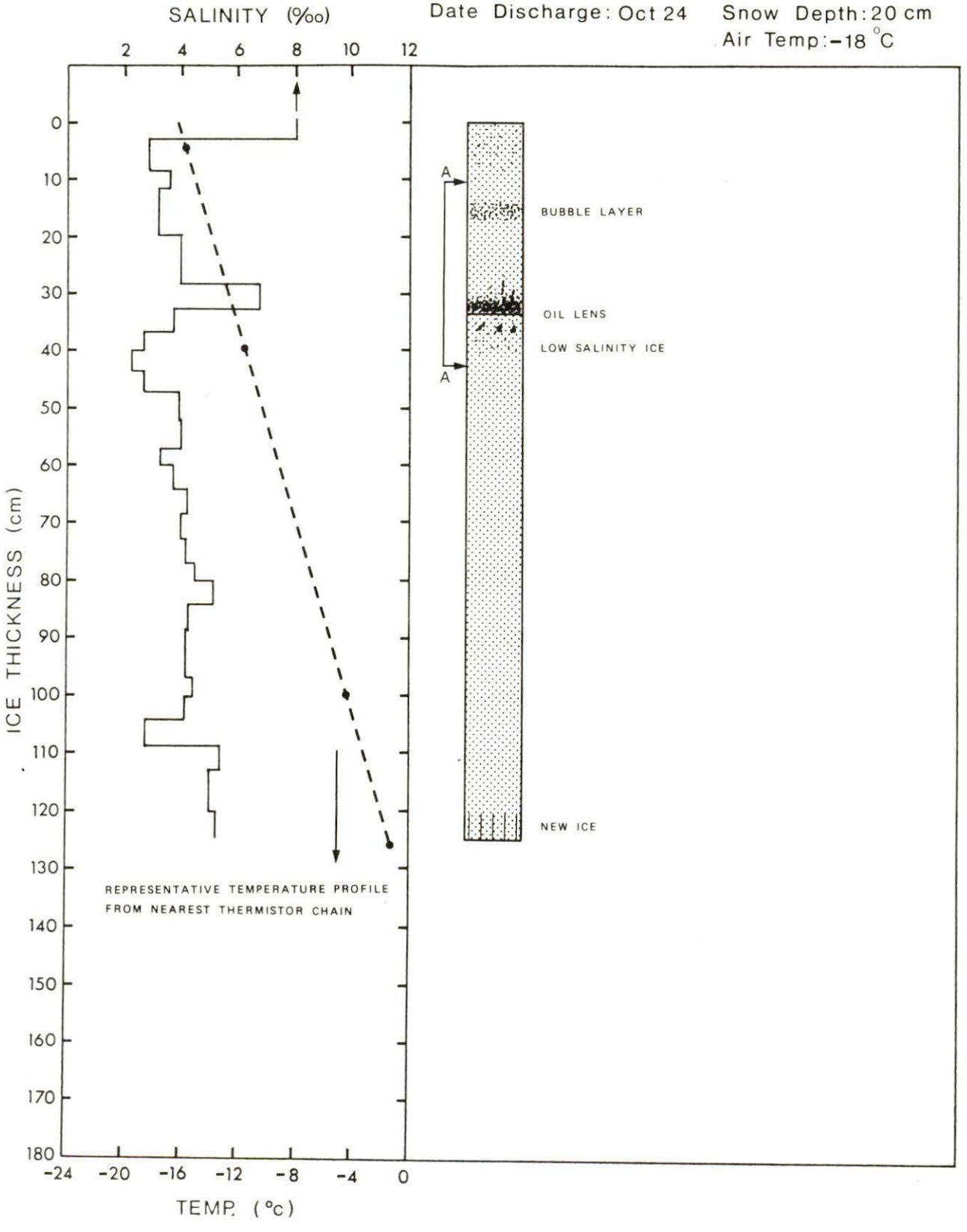

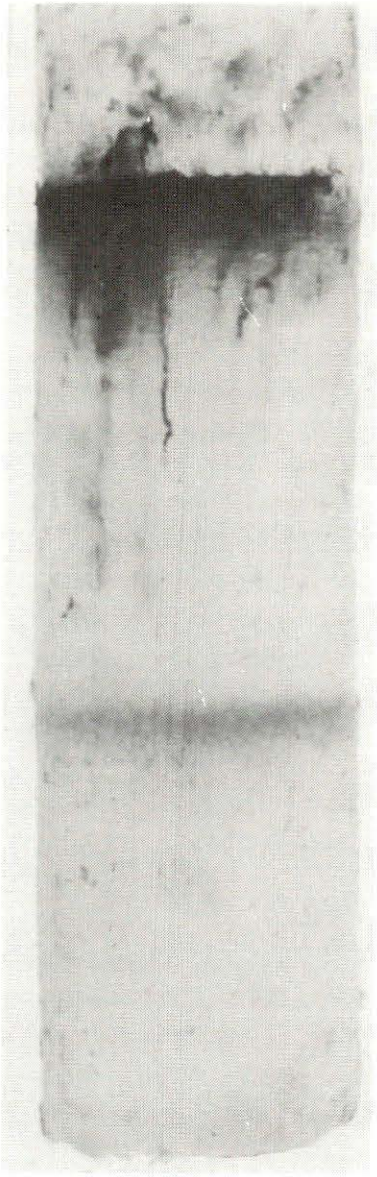

Plate 6 - 14

See section A-A, Figure 6-5
Note the layer of bubbly ice at 15cm depth.
This oil lens did not extend through the entire cross section.
A single oiled brine channel stands out clearly.

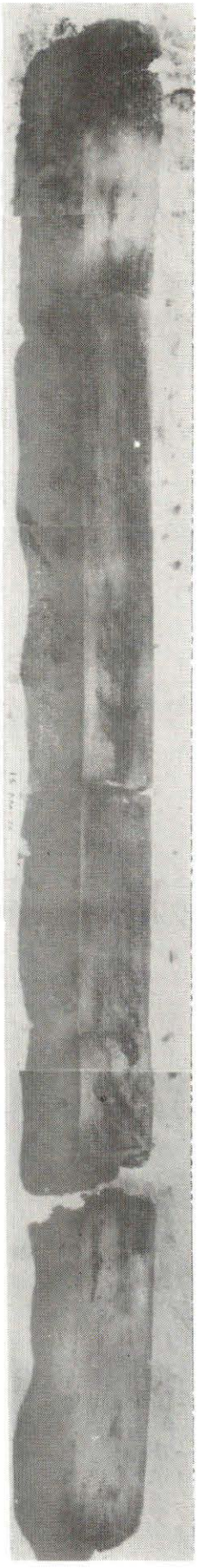

Plate 6 - 15

NW6 core taken May 15
See figure 6-6
Oiled brine channels extended almost to the ice surface, stopped by a 7cm layer of frazil ice. Note the intricate network of brine feeder channels at $\approx 45°$ angle. The top of the core was oil soaked recrystalized snow.

Figure 6 - 6 ICE CORE REPORT

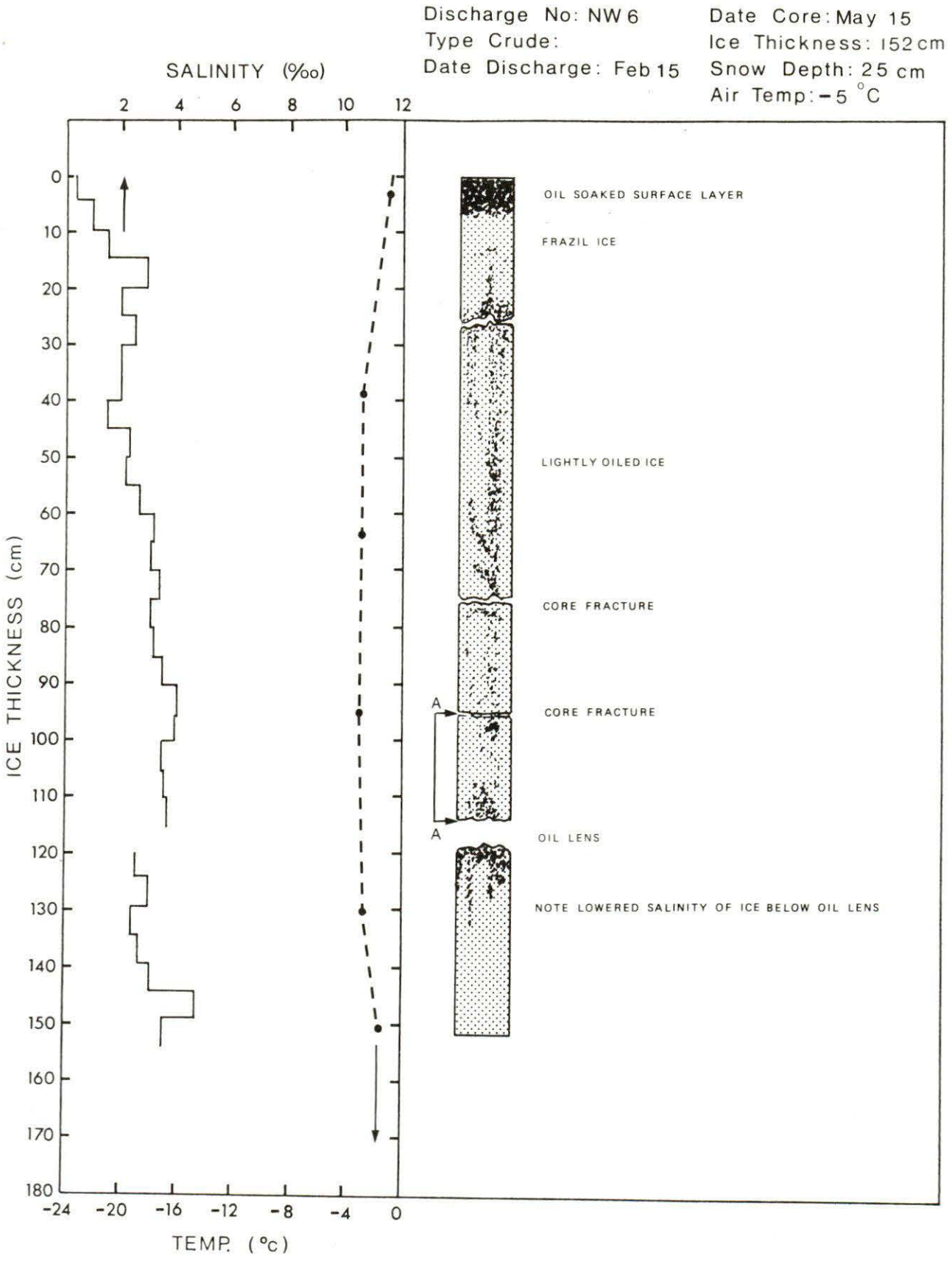

Plate 6 - 16

See section A-A, Figure 6-6
Detail of oil filled brine channels.

Figure 6-7 ICE CORE REPORT

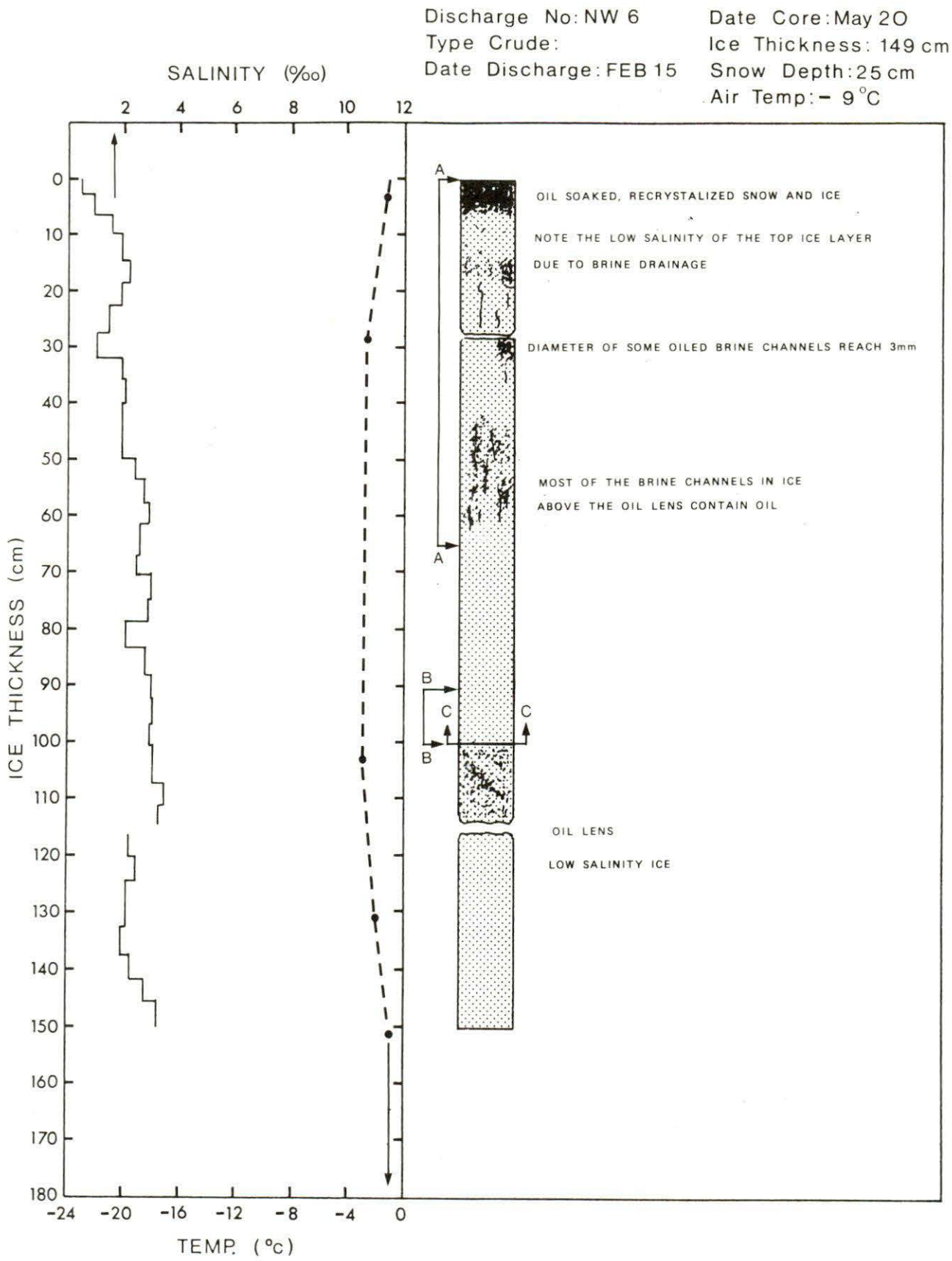

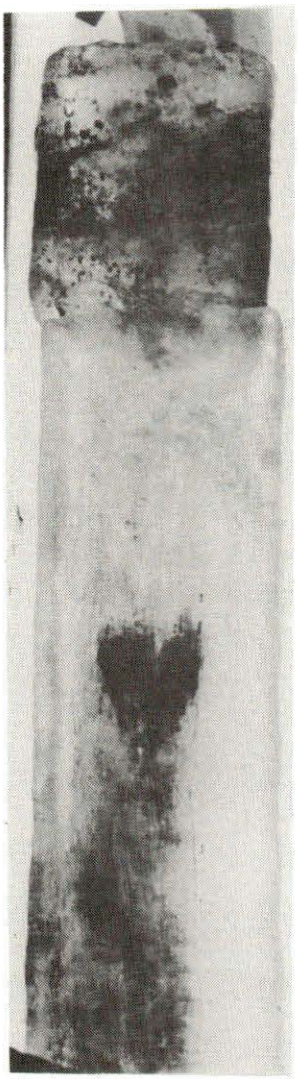

Plate 6 - 17 Detail of top core section from SH2, May 16/75.
Oiled brine channels stopped at columnar frazil ice interface.
The top cm of clear ice was probably refrozen fresh meltwater.
Upper band of oil drops was caused by lateral surface drainage from other areas.

Plate 6 - 19 Vertical thick section of a typical core in late May showing the extent of oil penetration ≈ 20cm above the lens.

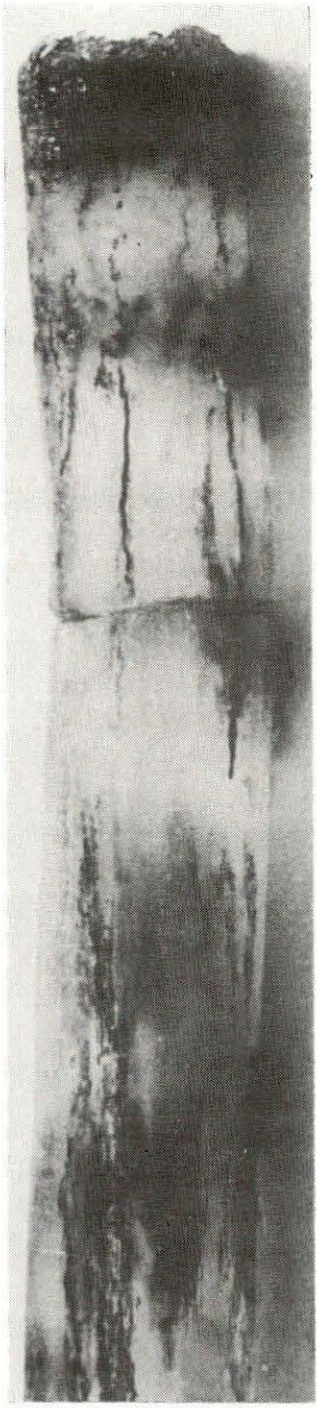

Plate 6 - 18 Detail of top section of core taken following the NW8 test, on May 20. The oiled brine channels extended to the ice surface.

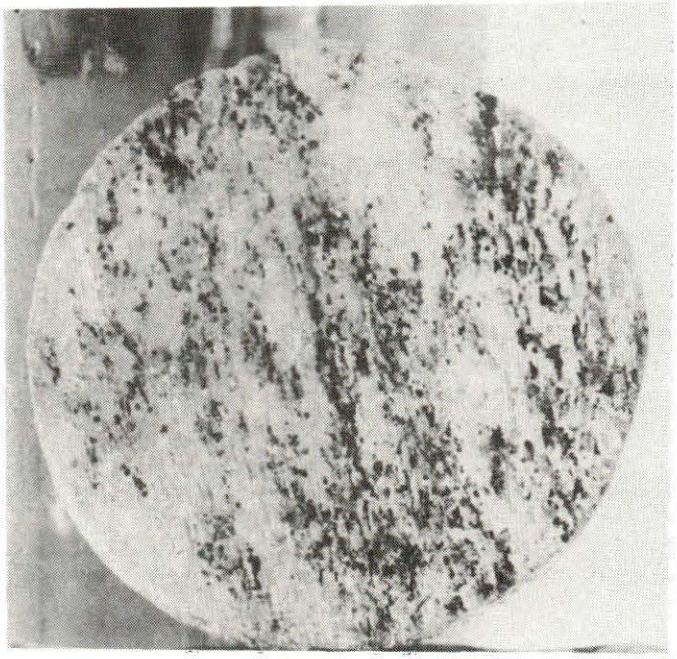

Plate 6 - 20 Horizontal cross section through above core at the same depth.

channels (Plate 6-16). At the surface there was normally a band of clear frazil ice. This layer did not have an established brine network, and was subject to repeated refreezing, in response to diurnal fluxes (Plate 6-17).

The rate of migration was controlled primarily by the condition of the ice. On May 15, 0.4 m^3 of Norman Wells crude oil was released under 195 cm of ice. The air temperature varied from -1.5 to -3.0°C, while the internal temperature of the ice was about -4.0°C. Special care was taken to ensure that the snow cover was not disturbed prior to the test. Within one hour traces of oil were detectable on the surface of the ice. Initially small pools of oil formed around isolated brine channels, which penetrated the surface layer. The average spacing between pools was about 20 to 30 cm. The pools quickly spread, covering the entire surface with oil. Upon coring in the area, the brine channels were found to be completely filled with oil (Plate 6-18), and the conditions identical to the other test areas, where the oil had been incorporated in the ice for a number of months. Similar results were observed in a test conducted for Panarctic Oils on May 5.

As the ice continued to deteriorate, the oil progressively saturated the interstices between platelets (Plates 6-19 and 6-20). The average concentration of oil increased to about 4.5 per cent. The maximum concentration recorded in a 4 cm section of core was 7 percent. Although the oil continued to flow up through the ice during the entire melt phase, all the oil was not released until the surface melt actually reached the initial level of the oil lens.

6.4 Effects of Surfaced Oil

Oil was first detected on the surface of the snow in the SH2 test area on May 9. Initially, the snow appeared to be slightly discoloured. Within 24 hours, the oil had formed a pool about 1.5 m in diameter. By May 12, approximately 10 percent of the entire test area was covered by either surfaced oil or darkened snow. For the preceding eight days the air temperature was above freezing, and a record high of 12°C was recorded on May 5. Between May 9 and May 12, the average albedo to the test site dropped from 0.7 to 0.6.

A total of 7.5 cm of snow fell between May 13 and May 21 and there was an accompanying drop in temperature. The snow completely covered the test area, and the surface appeared similar to that prior to May 9. On May 24, oil was again detected on the surface. Conditions quickly deteriorated. The average albedo dropped from 0.76 to 0.27 by June 4. Within five days a number of well defined melt pools had developed. These pools progressively grew in area and depth, until about June 4, when they became interconnected and a common water level was achieved. At this point over 45 percent of the total surface area was covered by oiled melt pools. The pools ranged in depth from several centimetres to a maximum of 50 cm. Although the snow was very wet, melt pools had not developed in the uncontaminated snow outside the test area. The rate of change in surface conditions for the first seven days of June is shown in Figure 6-8.

Figure 6-8 OILED AREA COVERAGE VS TIME

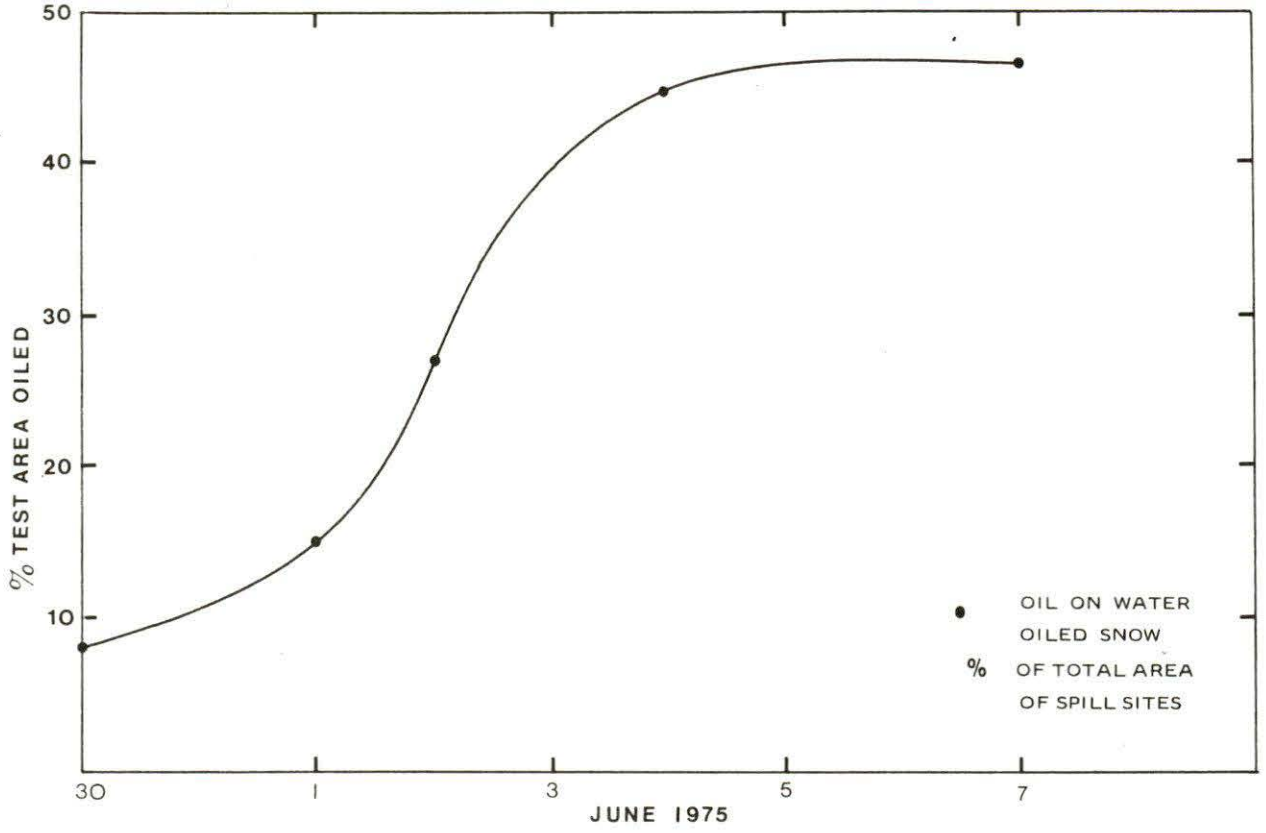

While the melt pools expanded, oil continued to migrate up through the ice. Between May 29 and June 7, the average oil film thickness on pools increased from 0.1 to 1.0 cm. A detailed mass balance is presented in Section 10.2. Much thicker films were produced if the oil was herded to one side of a pool by winds. In strong winds, some of the oil was carried up onto the surrounding snow. This resulted in rapid melting in the splash zone and a further expansion of the melt pool, beyond the boundary originally defined by the oil lens in the ice sheet. Horizontal seepage at the snow-ice interface also contributed to the expansion of pools into areas of clean ice. Some typical surface details are shown in Plates 6-21 to 6-24.

Oil-in-water emulsions were common with winds over about 25 km h^{-1}. The emulsions tended to be unstable, and as a rule broke down within 24 hours of the wind subsiding. Chunks of emulsified oil, which were deposited on the snow, above the water line, did not break down as readily. The composition of the emulsions varied, depending on conditions, but typically contained about 40 percent oil. Emulsions formed from Swan Hills crude appeared much more viscous than those from Norman Wells, but this could not be quantified. The degree of emulsification depended on the thickness and condition of the oil, the shape and orientation of the melt pool, and the wind speed. On one occasion between 30 and 50 percent of the oil in a melt pool in the SW2 test area was emulsified.

On June 4, an old core hole in the NW4 test area opened, creating a drain,

Plate 6 - 21 June 4/75.
Note control thermistor chain No.2 in foreground, skirt flotation collar and deep melt pools in SH2 test area.

Plate 6 - 22 Typical thin oil film on melt pool. A light wind was heading the oil from left to right.

Plate 6 - 23 Aerial view of typical melt pool, June 4/75.
Oiled ice is marked by dark areas visible through the water.
A thicker oil film is positioned in the upper left.

Plate 6 - 24 Close-up of oiled ice visible through a melt pool on June 4.
Round oil patches had just floated out of an open brine channel
(Lacework pattern on photo)

and water from surrounding melt pools started to flow towards the hole. A considerable vortex was established, as both water and oil were flushed down the hole. The action tended to be cyclic, roughly corresponding to the rise and fall of the tide. Within two days, the hole increased in diameter from 8 to 60 cm. On June 6, a concrete collar was placed around the hole, to permit selective drainage, and prevent the loss of oil due to the vortex action. The video system was used to examine the underside of the ice. All the oil appeared to be deposited on the bottom of the ice within two metres of the hole. Emulsified oil rose to the surface, when a core was cut near the drain hole. By June 7, several similar holes had opened, draining a substantial portion of the test area. Between June 4 and June 7, the portion of the area covered by oiled melt pools decreased from 45 to 31 percent. Sixteen percent of the area was covered by oiled snow that was left by the receding pools. The change in surface conditions from June 1 to June 7 is shown in Figures 6-9 to 6-12. These figures were prepared from aerial photographs.

Throughout the melt period, incoming shortwave radiation and net radiation were monitored continuously. Albedo measurements were made every second day at a total of 14 stations. Twelve of these stations were located within the test area, while the two controls were at undisturbed sites (Appendix 27D). Care was taken in selecting the sites to ensure the full spectrum of conditions was covered. In most cases, a simple arithmetic mean of the twelve values was a reasonable approximation of the average albedo for the entire test area.

To minimize surface disturbance, the albedometer which consisted of upward and downward facing solarimeters, was mounted on a cantilever, which could be extended up to 3 m into the test area. The maximum error of the system was ± 10 percent of the measured value (Appendix 27A). Although the albedo of most surfaces is not sensitive to zenith angle, measurements were always taken at approximately 1930 G.M.T. Each site was photographed at the same time, to permit the correlation of surface conditions with albedo. Representative albedos for typical conditions are shown in Table 6-3.

TABLE 6-3

MEASURED ALBEDOS - BALAENA BAY

Fresh snow	0.85
Wet snow	0.65
Oil on snow	0.70 to 0.30
Thin Oil Film on Water	0.10
Thick Oil Film on Water	0.06 to 0.10
Water	0.08 to 0.15

The measured change in albedo for the period May 9 to June 6 is shown in Figure 6-13. Values from all twelve stations were used in determining the average albedo for the test area. The heavily oiled curve, was based on observations in the SH2 test area, and is a reasonable approximation

Figure 6 - 9 TEST SITE APPEARANCE - JUNE 1

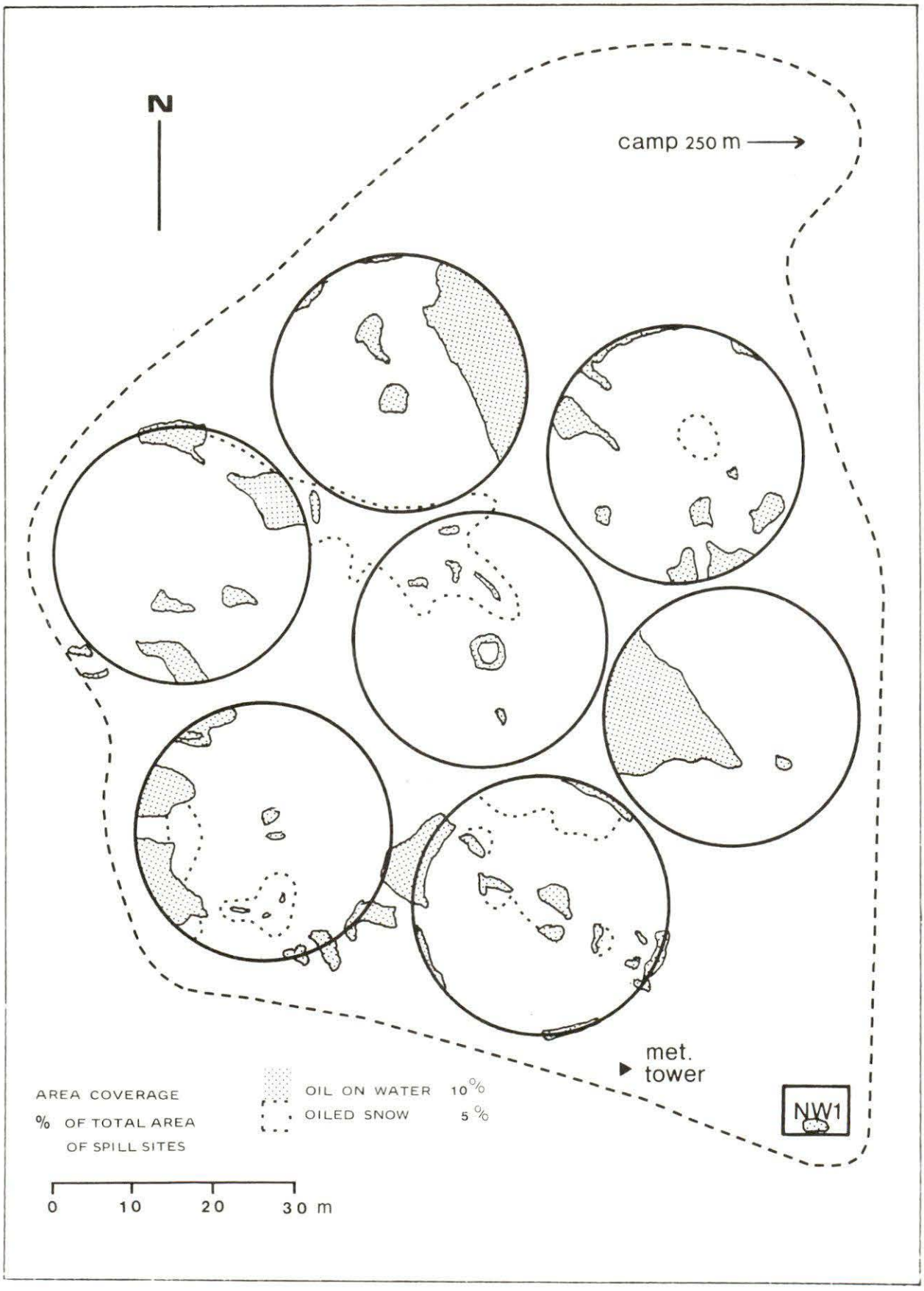

Figure 6-10 TEST SITE APPEARANCE - JUNE 2

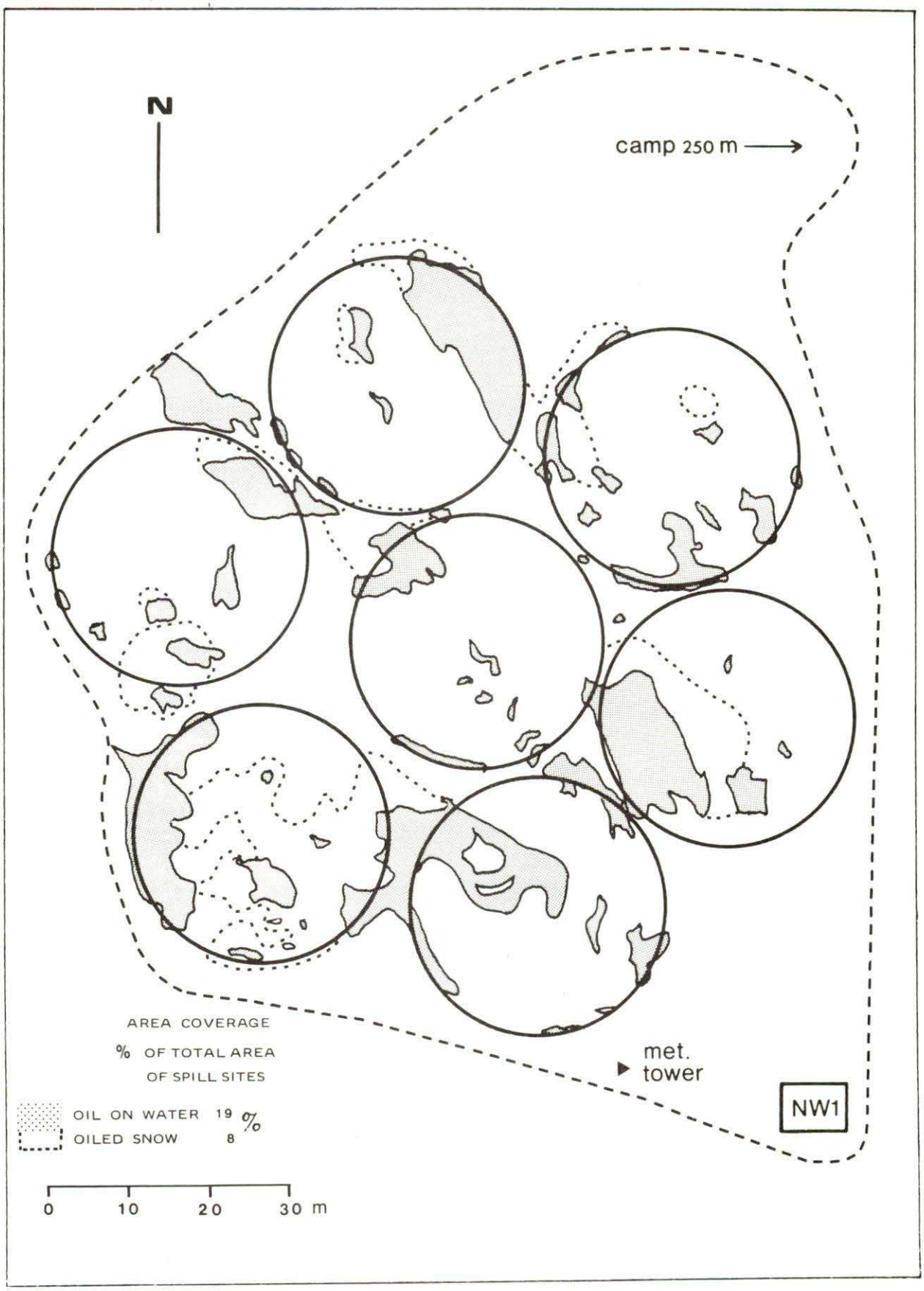

Figure 6-11 TEST SITE APPEARANCE - JUNE 4

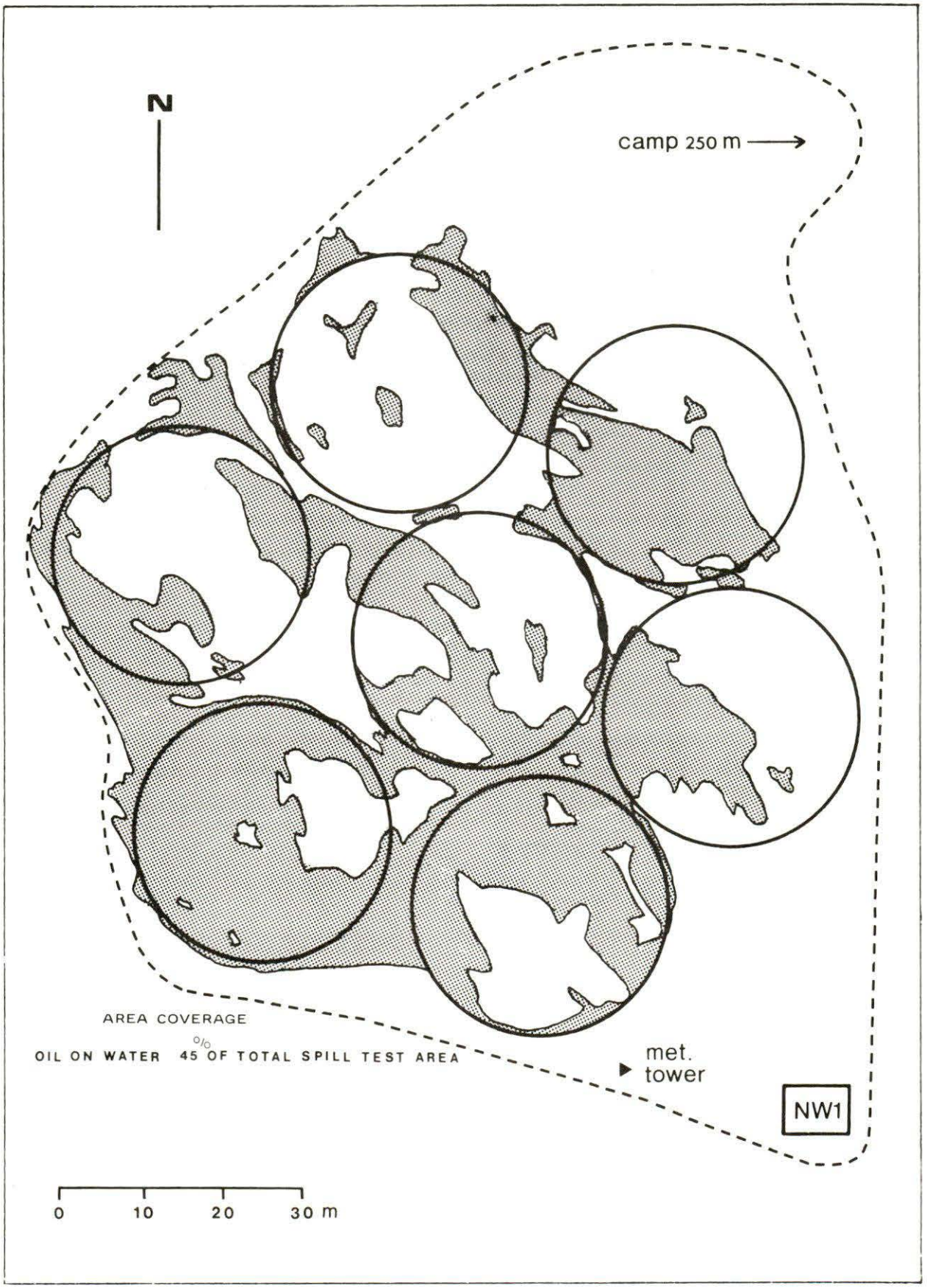

Figure 6-12 TEST SITE APPEARANCE - JUNE 7

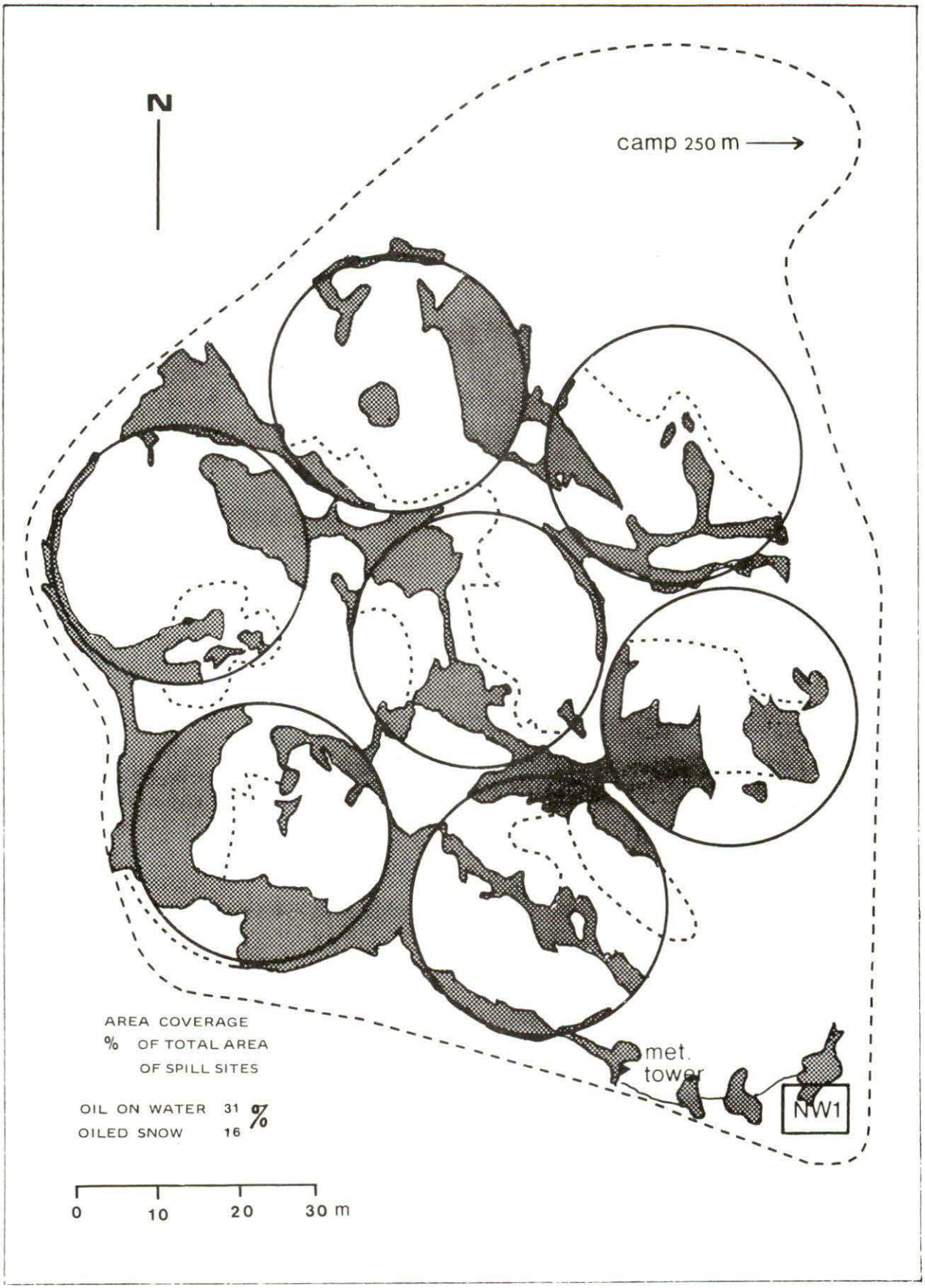

of the extreme low. The control curve is representative of the uncontaminated area. The rapid rise in all three curves about the middle of May corresponds with a series of snowfalls (for detailed weather summaries, see Appendix 27D). Of particular importance is the progressive divergence between the average albedo of the test site and the control areas after May 25.

Figure 6-13 ALBEDO MAY 5 TO JUNE 6, 1975

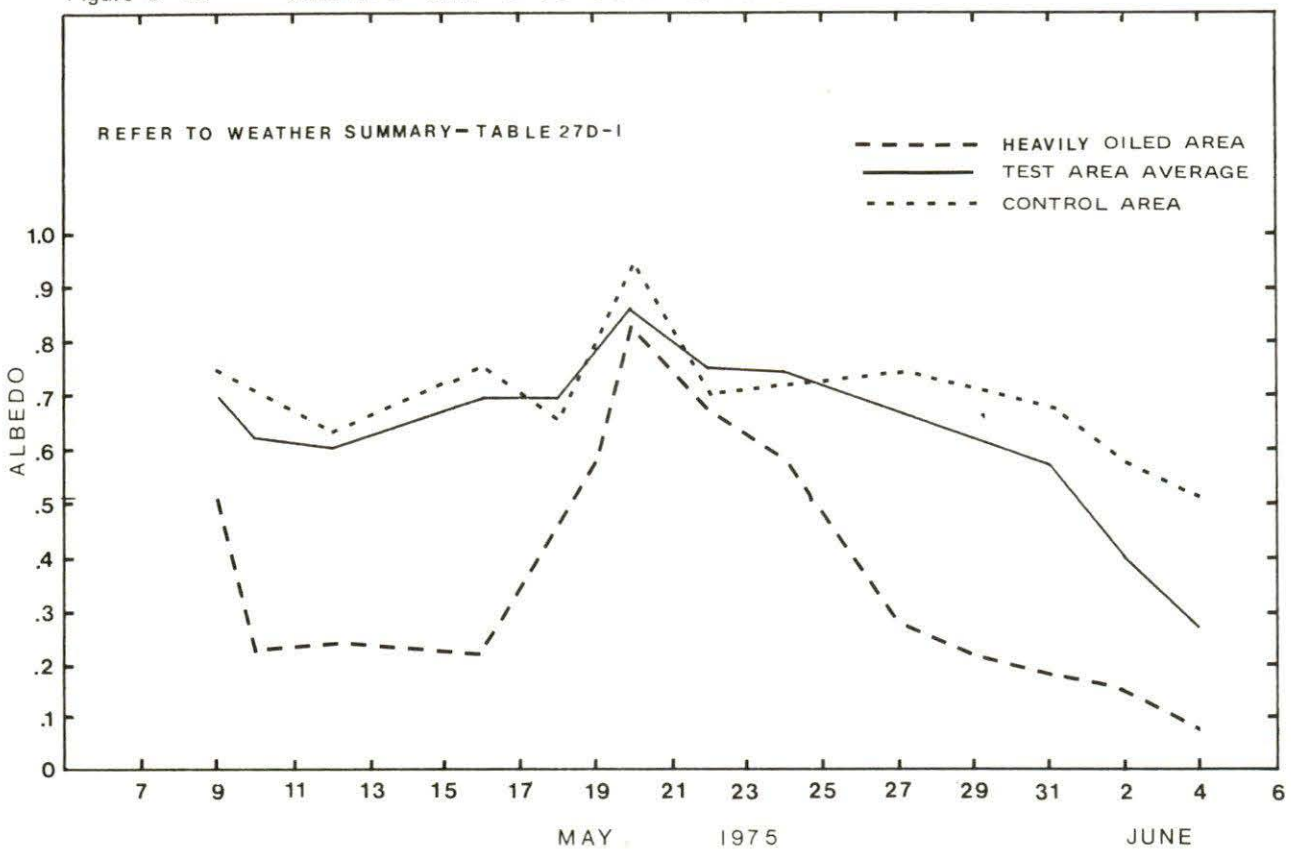

By June 4, the average albedo of the test area had dropped from 0.7 to 0.25, while the albedo of the control areas had only fallen to 0.5. Since a substantial portion of the test area was uncontaminated, the actual albedo of oiled areas was considerably less than the average for the site. The albedo of the heavily oiled SH2 location was only 0.09. From May 8 to June 6, the total daily incoming short wave radiation at ground level varied from 320 to 780 cal cm^{-2}, depending on atmospheric conditions (Figure 6-14). The average level for the period was 554 cal $cm^{-2}day^{-1}$.

In the ten day period preceding June 6, 1730 cal cm^{-2} were absorbed in the control areas, and an average of 2510 cal cm^{-2} in the test area. A total of 3690 cal cm^{-2}, or sufficient energy to melt over 40 cm of ice, were absorbed in one heavily oiled area. The depth of an adjacent melt pool was 50 cm. The effect of the increased absorption was very pronounced. The location of melt pools closely corresponded to the initial

disposition of oil lenses under the ice.

Figure 6-14 INCIDENT SOLAR RADIATION

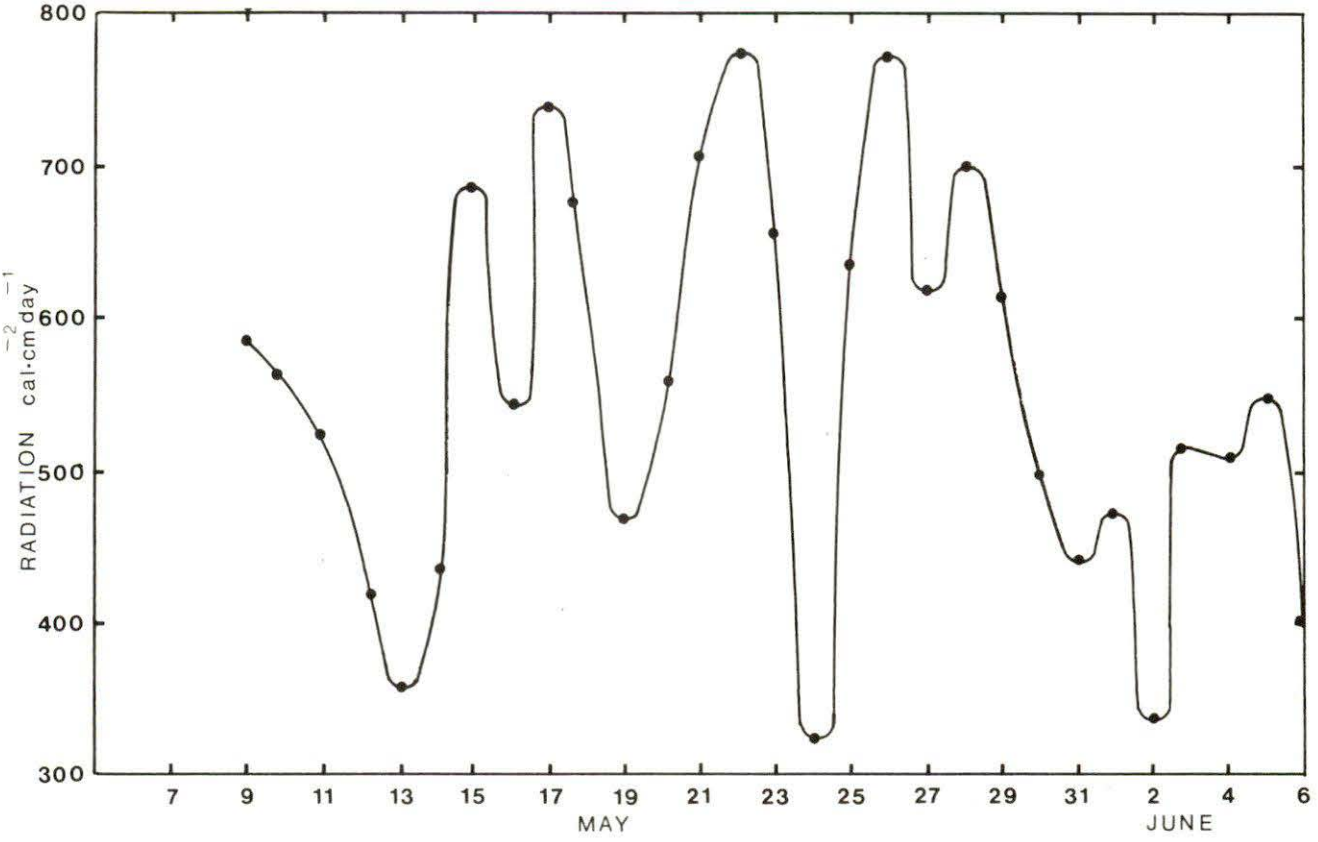

Although the albedo of a thick oil film on water and a clear melt pool are about the same, the thermal regime can be quite different. Because the oil serves as an effective barrier to radiation, most of the energy is absorbed by the oil. However, the radiation passes through a clear melt pool and is absorbed by the ice. A typical temperature profile through an oiled melt pool is shown in Figure 6-15. The average spread in temperature between the oil and the underlying water was between 8 and 10°C.

Figure 6-15 TEMPERATURES IN AN OILED MELT POOL

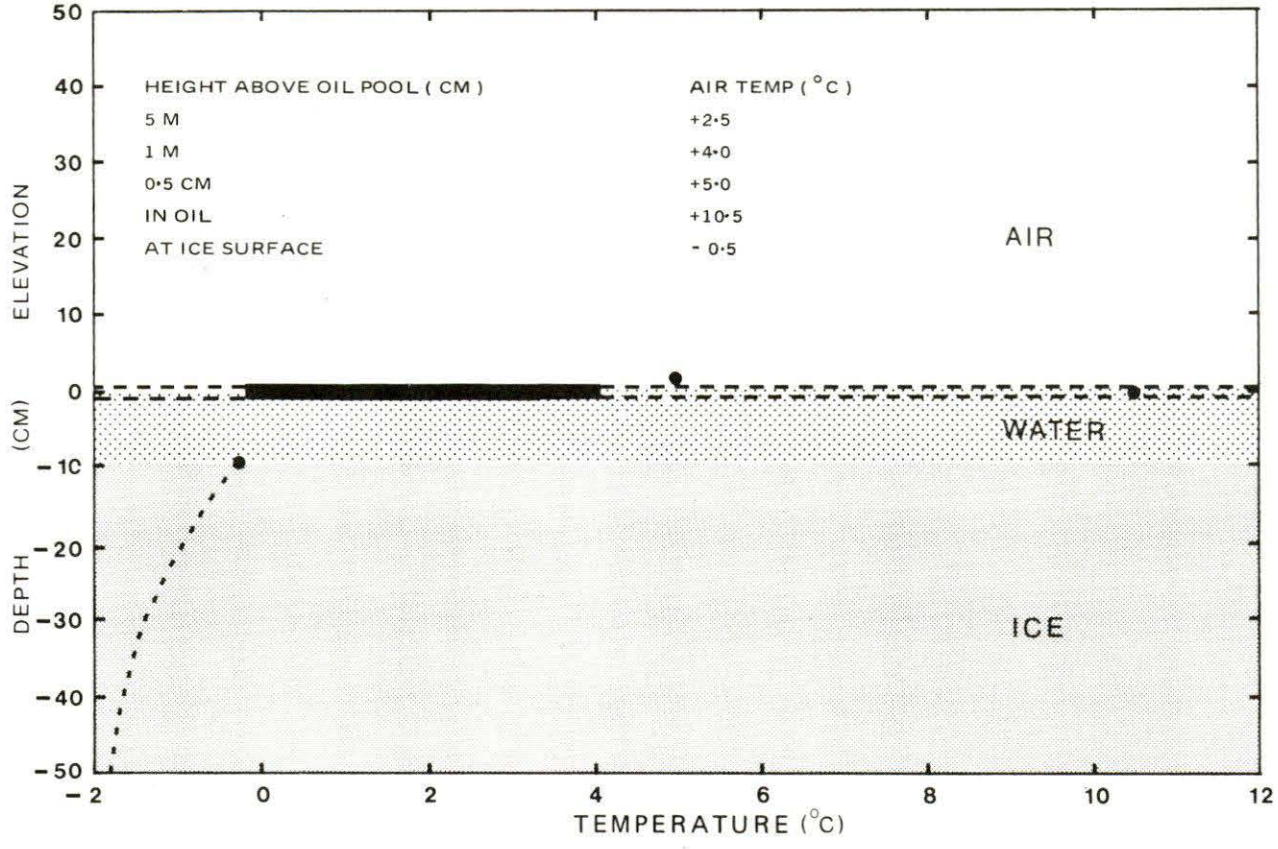

7.0 THERMAL ASPECTS OF OIL-ICE INTERACTION

7.1 Principal Components of the Energy Balance

The energy balance of an ice sheet is expressed approximately by the following equation:

$$G = (S + s)(1 - a) - L\uparrow + L\downarrow + Q_s + Q_l \qquad (1)$$

where: G = change in heat content of the sheet
S = direct solar radiation incident at surface
s = diffuse solar radiation incident at surface
a = albedo of surface
$L\uparrow$ = outgoing long wave or terrestrial radiation
$L\downarrow$ = incoming terrestrial or counter radiation
Q_s = net sensible heat flux
Q_l = net latent heat flux

There are two components to consider in determining the change in heat content of the ice. The sensible heat, which is reflected by a change in thermal regime, and the latent heat, which corresponds with growth or depletion of the sheet. Both are measurable; the thermal regime by means of thermistors imbedded in the ice, and growth or depletion by monitoring ice thickness. Direct solar, or shortwave radiation incident at the surface is a function of latitude, declination of the sun, time, and atmospheric conditions. The flux can be reasonably approximated at low latitudes, where the sun is high for a substantial portion of the time, and there is historic data on the optical air mass, or molecular density along the path of the radiation through the atmosphere. As a rule, this approach is unsatisfactory at high latitudes during the winter. The level of diffuse radiation is primarily a function of atmospheric conditions. The total of both direct and diffuse solar radiation at ground level can be measured by means of several types of pyranometers, which are typically sensitive over the spectral range of 300 to 3500 nm.

The albedo, or ratio of reflected to incident short wave radiation is a critical parameter, as it can vary from 0.95 to 0.05 depending on the nature and colour of the surface. The albedo of new snow is about 0.9, oiled snow 0.4, and a solid oil lens or open water about 0.1. The ratio can be determined by measuring the upward and downward components with a pyranometer. Since the albedo of most surfaces is independent of zenith angle, continuous monitoring is not necessary. The disposition of absorbed short wave radiation varies greatly. For example, only two percent penetrates over 10 cm in wet snow, while 20 percent reaches the same level in dry snow and 56 percent in clear ice or pure water. The penetration in water is strongly wavelength dependent. Although it is possible for some of the radiation to pass right through the ice sheet, suitable conditions rarely develop.

The earth's surface is commonly assumed to emit and absorb energy as a gray body in the infrared region, and as such obeys the Stefan-Boltzmann law;

$$L\uparrow = \varepsilon \delta T^4 \qquad (2)$$

where: T = surface temperature (°K)
ε = infrared emmisivity
δ = Stefan - Boltzmann constant

For most natural surfaces the infrared emissivity varies from about 0.9 to 0.95, and therefore the outgoing longwave or terrestrial flux is primarily a function of temperature. Although the atmosphere is nearly transparent to shortwave radiation, it readily absorbs terrestrial radiation. Only about nine per cent escapes directly to space. The remainder is absorbed by the atmosphere, and then reradiated partly to space and partly back to the surface (counter radiation, $L\downarrow$). Terrestrial radiation is critical in determining the absolute energy level of the ice, but is relatively unimportant in comparing the effect of oil, since the emissivity of the oil is about equal to that of ice. Even allowing that surface oil pools are up to 7°C warmer than the surrounding surface, the increased flux is less than 10 percent. Infrared radiation can be measured by means of a pyrgeometer, or by the use of a net radiometer in conjunction with a pyranometer.

Since the change in energy level due to ice growth or depletion is incorporated in G, the heat content of the sheet, the latent heat flux is principally in the form of precipitation or evaporation. For most of the winter evaporation tends to be insignificant. In considering a relatively small area, the precipitation component can be both positive or negative, depending on the nature of drifting. The sensible heat flux is extremely difficult to quantify, and is generally treated as the residual term. The flux can be in both directions to the atmosphere, and usually upward from the water column. The ocean and the atmosphere are dynamic, three dimensional systems, which are influenced largely by external forces. The nature of the exchange is very complex, and there is insufficient data on boundary effects, turbulent transfer and vertical gradients to permit a realistic assessment of the flux.

The various components of the energy balance equation, with the exception of sensible flux, were recorded in an effort to determine the effects of oil on surface heat exchange. However, a precise analysis was impossible for the melt phase, when the influence of the oil was most pronounced. Firstly, the size of oil pools was relatively small, in comparison to the total surface area, and side effects could not be isolated. Secondly, surface conditions were not static. Once the melt pools became interconnected, both oil and water moved freely over the test area. As well, there was a definite mass transfer at the melt holes. Thirdly, the combined instrument error was about equal to the net longwave component (Appendix 27A).

Once the oil surfaced, albedo was the dominant single parameter in the energy balance equation, and a relative comparison between oiled and unoiled areas was possible. Since the net short wave component was identical for both surfaces, the net longwave component varied by less than 10

percent, and the sensible and latent heat flux was about equal, a reasonable correlation could be established between cumulative absorbed solar radiation and ice depletion. The level of absorbed solar radiation varied by a factor of ten, depending on surface conditions. Although the oil spread into uncontaminated areas as the melt progressed, the surface immediately above an oil lens generally remained heavily oiled. To assess the impact of the oil, albedo measurements were made at minimum of 14 stations on a routine basis.

7.2 Theoretical Considerations

A major objective of the oil entrainment study was to investigate the effect of included oil on ice growth. Since the thermal conductivity of sea ice is between 15 and 20 times that of most oils, it was initially assumed that an entrained oil lens would reduce the overall heat transfer coefficient and retard ice growth. However, this effect was not readily detectable, due to natural variations in ice thickness.

Throughout the winter, ice thickness and snow depth were measured in both oil and unoiled areas. The range in observed ice thicknesses for all unoiled areas is shown in Figure 7-1. Line 1 denotes the smoothed minimum thicknesses and Line 2 the maximum thicknesses. The weekly observations by the Atmospheric Environment Service at Cape Parry (Gillet Bay) have been included for comparison. In general, once the ice thickness exceeded 50 cm, the variation was about equal to 20 percent of the average thickness. There was a strong correlation between snow cover and ice thickness. The drift pattern established in the fall remained intact throughout the winter. Consequently, the thin ice was consistently located beneath the drifts, and the thick ice in wind swept areas.

The relationship between ice thickness and snow cover for Cape Parry was examined to determine if the variations observed in Balaena Bay were simply a local phenomenum. Since only a single thickness was recorded for each observation, data for the period from 1970 to 1975 was used to construct a band of variations in thickness with time (Appendix 27D). Although minor deviations could be detected, the trend was identical to that observed in Balaena Bay. The thin ice consistently corresponded with thick snow cover, and the variation in ice thickness was approximately 20 per cent of the average thickness. In general, the snow cover had greater impact on ice growth than did variations in the ambient air temperature. During the winter of 1974-75, the average ice thickness was about 30 cm, or 15 per cent thinner than normal, while the mean monthly temperatures during the growth period were 1 and 8°C lower than normal, with the exception of February. The total precipitation during the same period was 2.6 cm, or about 20 percent higher than normal.

The composition of the ice was similar to other areas in the landfast zone. Between November and June a total of 19 cores were analyzed. The mean salinity was 4.56°/$_{oo}$, with a standard deviation of 0.63%. Generally salinities in the upper 5 cm of the sheet were in the order of 10 to 15°/$_{oo}$ and the skeletal layer was about 1 to 2°/$_{oo}$ above the average. Apart from the disturbance near the oil lens, salinity profiles taken in oiled ice did not differ appreciably from measurements in clean ice. Several representative profiles are shown in Figure 7-2.

Figure 7 - 1 ICE GROWTH 1974-75, BALAENA BAY AND CAPE PARRY

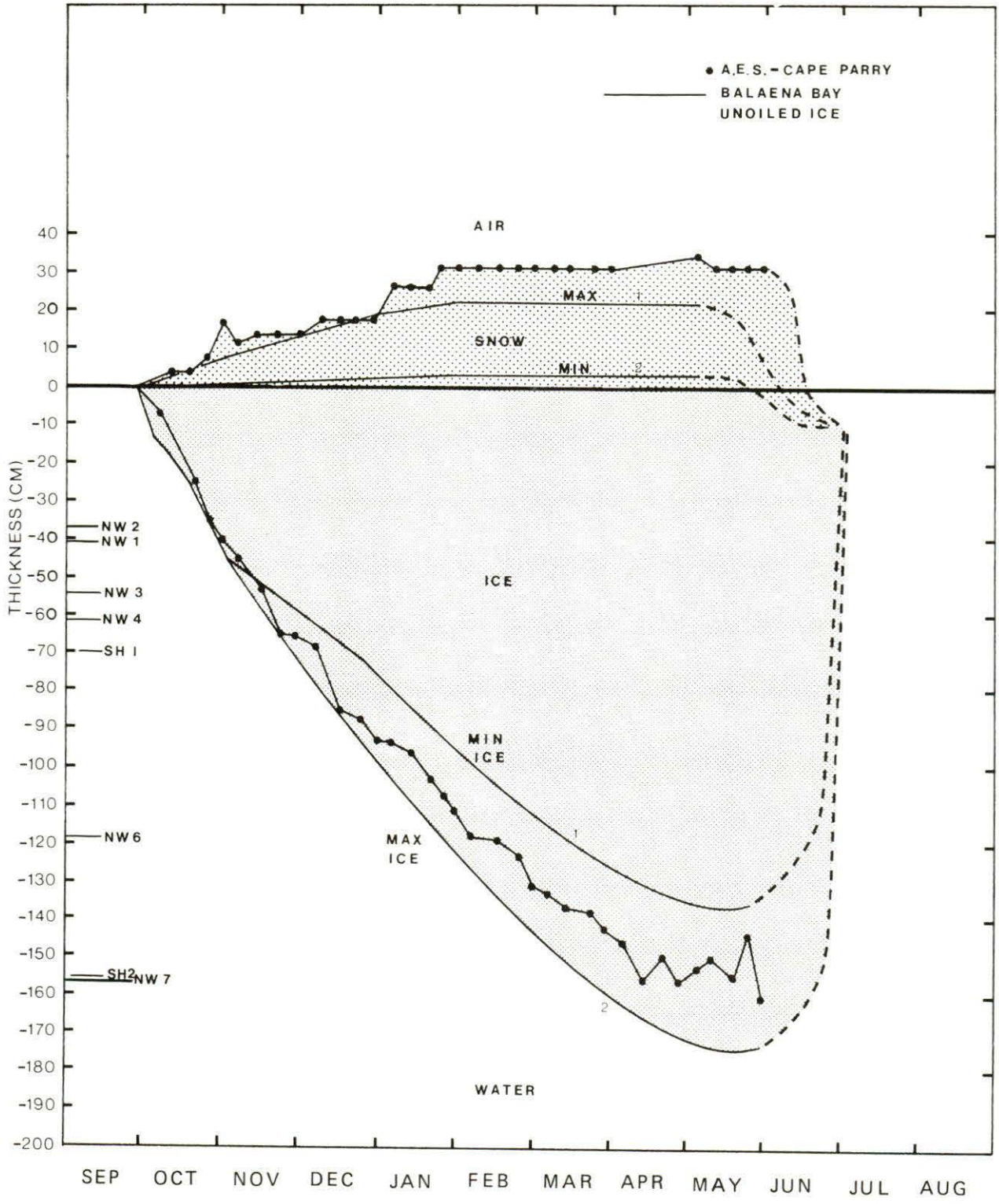

Figure 7 - 2 REPRESENTATIVE ICE SALINITY PROFILES

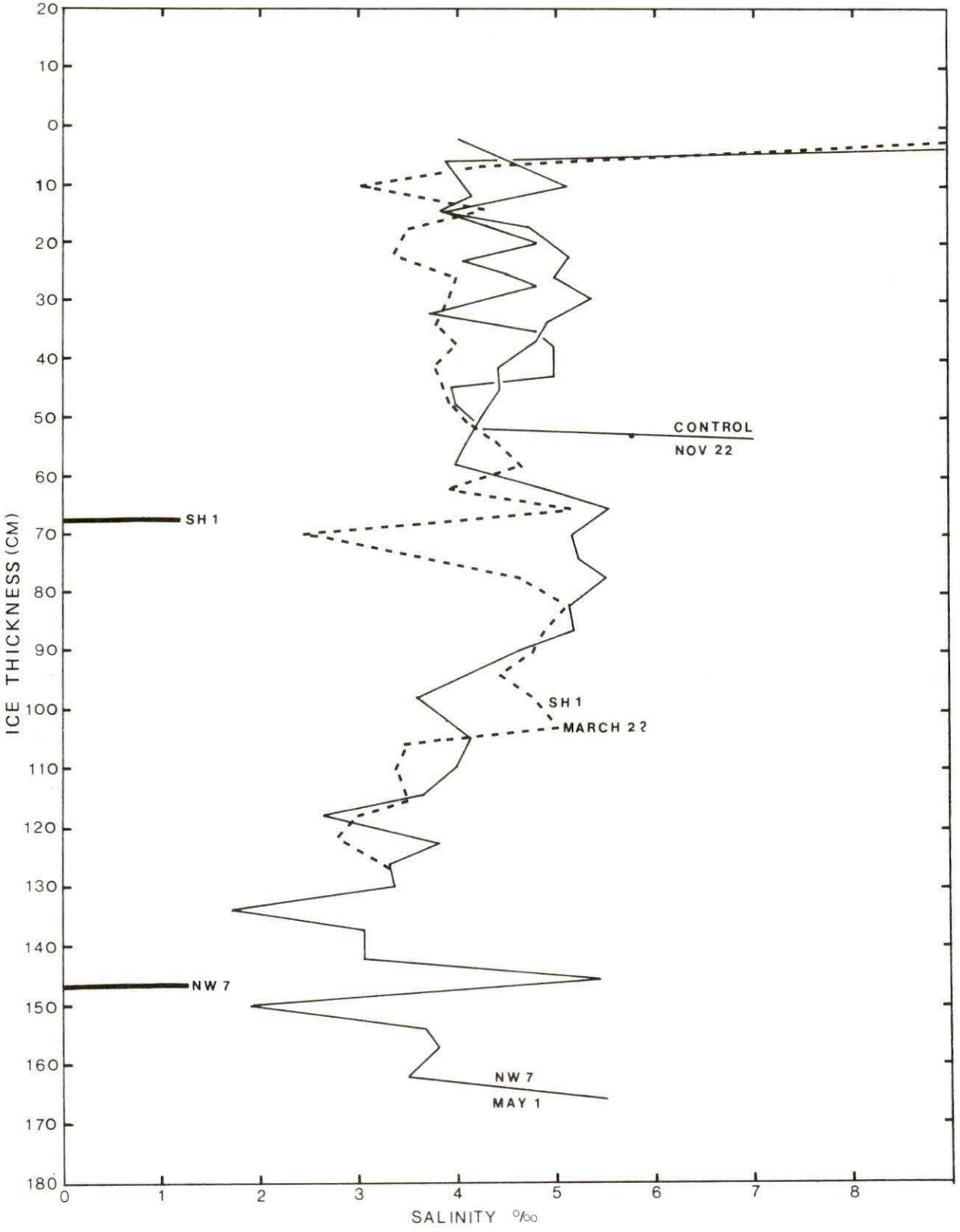

In an attempt to differentiate between the effects of snow cover and included oil on ice growth, all ice thicknesses were modified to a zero snow equivalent value. The technique developed by Leakey and modified by Burns (1974), was employed. The reduced data is presented in Figure 7-3. Although this approach effectively reduced the scatter to about 10 percent, no distinct pattern could be differentiated between oiled and unoiled areas. If the oil did increase the thermal resistance of the sheet, then contaminated areas should have appeared thinner.

Figure 7 - 3 ICE THICKNESS MEASUREMENTS IN OILED AND CLEAN AREAS NORMALIZED TO ZERO SNOW EQUIVALENT VALUES

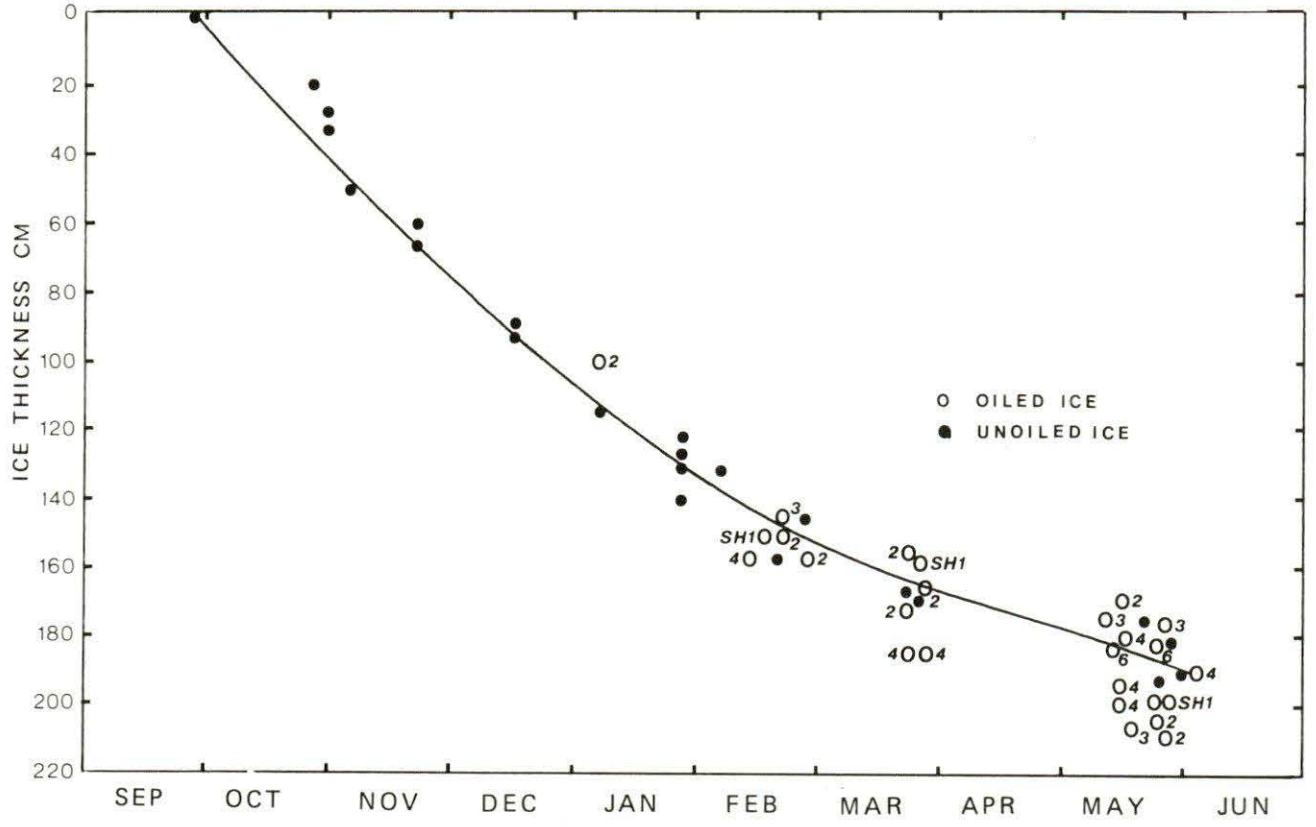

By examining the relative heat transfer coefficients for a three layer system of snow, ice and an included oil lens, some understanding can be gained of the relative effect of an oil lens on the thermal properties of the ice sheet-snow cover composite. This theoretical treatment will also aid in the subsequent interpretation of temperature profiles described in Section 7.2.4.

Although for the purposes of heat transfer calculations the oil-ice interfaces will be considered distinct and planar, in actuality, there will be a certain roughness factor at the oil-ice boundary. From observations at Balaena Bay, the upper oil-ice interface will be quite rough and indistinct in nature with the oil filling the voids for a height of 2 to 5 cm into the porous skeletal layer. The much increased surface contact area due to the mixing of oil and ice in this layer may enhance the heat exchange from the oil to the ice. From core observations, the lower oil-ice interface is very smooth where the new ice has formed below the oil. No significant migration of oil was observed across this interface. No definite evidence of ice crystals joining their two interfaces was ever observed at Balaena Bay. Only the coefficient for conductive and convective heat transfer will be considered. All other energy fluxes, such as radiation, convective heat transfer from the ice-air and ice-water interfaces, evaporative heat losses and latent heat supply, although important components of the overall energy balance, will be assumed approximately of the same order of magnitude for both oiled and unoiled areas within the range of interface temperatures encountered during the growth season.

The mode of heat transfer through the ice and snow is primarily solid body conduction. However, in the oil lens, heat transfer by free convection may be significant. Free convection results when a normal fluid whose density varies inversely with temperature is placed between plane surfaces (in this case, ice), and cooled from above. Theoretically, in the spring when mean air temperatures rise above the water temperature and the heat flux reverses direction, there can be no free convection through the oil lens. Free convection is commonly described for specific geometries in terms of the product of two dimensionless variables, the Grashof (Gr) and Prandtl (Pr) numbers. The Nusselt modulus (Nu) is a ratio of the convective heat transfer coefficient ($\bar{h}$) to the conductive heat transfer coefficient $\frac{k_{oil}}{L_{oil}}$ where L_{oil} is the oil lens thickness.

For a fluid enclosed between two plane horizontal surfaces, of which the upper surface is at a lower temperature than the lower one, an unstable density stratification is created. This situation does not give rise to convection currents as long as the Gr Pr product is low. However, when this parameter reaches a value of around 1700, a free convection flow pattern known as Benard cell convection arises, (Ekert and Drake, 1959). This laminar flow situation has been described experimentally by the empirical expression $Nu = 0.107\ (GrPr)^{0.3}$, and is maintained up to a Gr Pr product of about 47,000. Above this value there is a transition to irregular turbulence. In forced flows, the Reynolds number is normally the criterion for transition. However, with free convection such as exists in an oil lens, the establishment of turbulent conditions is marked

by a critical value of GrPr (Rayleigh Number). For the analogous case of an oil lens in an ice sheet, irregular turbulence is considered to be fully established for a Rayleigh number of 3×10^5. Globe and Drapkin (1959), made a large number of turbulent heat transfer measurements for enclosed fluid layers over a Pr # range of 0.02 to 8750 and a Rayleigh number range 3×10^5 to 7×10^9. Their empirical correlation is $Nu = -.069(Gr)^{0.33} (Pr)^{0.407}$ (McAdams, 1954). Table 7-1 shows that the physical properties of the two crudes used in this experiment differ mainly in respect to viscosity. At a given temperature, Swan Hills crude is about 2.5 times more viscous than Norman Wells crude. For the purpose of evaluating the effect of viscosity differences on convective heat transfer through an oil lens it is sufficient to consider $Nu = f(GrPr)^{1/3}$. As GrPr is a function of u^{-1} it can be calculated that there will be about 25% less convective heat transfer across a Swan Hills oil lens, than Norman Wells. Density and viscosity dependence on temperature will effect any calculations of Nu by less than 10% over the range -15°C to 0°C. It should be emphasized that other uncertainties surrounding several of the physical properties in Table 7-1 (k_{oil}, k_{ice}, Cp_{oil}, β_{oil}) could easily effect any calculation of convective heat transfer by a similar amount. In an effort to establish a worst case situation all subsequent calculations are presented for Norman Wells crude or other oils of similar viscosity. The laminar flow region covers a Nu modulus range of 1 to 2.7 while the turbulent regime presently covered by experimental data ranges from an Nu of 6.58 at $GrPr = 3 \times 10^5$ to a Nu of 187 at $GrPr = 7 \times 10^9$ for Norman Wells crude.

As the Grashof number is a function of ΔTL^3 (where ΔT is the temperature differential across an oil lens) the Nu number for both laminar and turbulent conditions can be expressed in terms of ΔT and L_{oil}.

For a natural first-year ice sheet such as that at Balaena Bay, there are upper and lower theoretical limits that can be placed on the parameters ΔT_{oil} and L_{oil}.

The oil lens thickness is dependent on the quantity of discharge and the variation in ice thickness present at the time of discharge. As the ice grows, differences in snow cover of about 20 cm observed at Balaena Bay, result in different local growth rates. Using measured values, the spread in ice thickness between points of minimum and maximum snow cover has been plotted vs mean ice thickness (Figure 7-4a). The maximum variation in ice thickness observed at the cessation of growth was 30 to 35 cm. Using this curve as a guide it can be seen for instance, that if a discharge was made in January a maximum oil lens thickness of 20 cm could be realized. This is based on the assumption that the oil thickness cannot exceed natural ice cover variations. Sessile drop theory places the minimum oil lens thickness at about 0.8 cm. Consequently, for practical purposes, the expected oil lens thickness would range from 0.8 to 30 cm.

The temperature drop (ΔT) across an oil lens will be governed by the overall temperature gradient present in the ice sheet at any given time, the lens thickness and the Nu modulus. For simple conduction, the ratio

$$= \frac{L}{\bar{h}} \qquad (3)$$

$\bar{h}$ is related to the Nusselt modulus by the expression:

$$\bar{h} = Nu \frac{k_{oil}}{L_{oil}} \qquad (4)$$

substituting (4) in (3) gives

$$R_2 = \frac{L_{oil}}{Nu\ k_{oil}} \qquad (5)$$

Substituting (2) and (5) in (1) the total thermal resistance of an oil lens can be expressed as

$$R_{oil} = \frac{L_{oil}}{(Nu+1)k_{oil}} \qquad (6)$$

The temperature gradients across an oil lens and ice sheet will be equal when $(Nu + 1)\ k_{oil} = k_{ice}$ ie. at a Nu modulus of about 14.

As previously stated, Nu can be expressed as a function of ΔT and L_{oil}

$$Nu = f(\Delta T, L_{oil}) \qquad (7)$$

If the temperature gradient through the ice sheet (Grad) is known, the thickness of an oil lens can be expressed in terms of ΔT, Nu Grad, and the ratio $\frac{k_{ice}}{k_{oil}}$.

Figure 7-4b shows representative temperature gradients measured by control chains from November to May. The peak temperature gradient, 0.2°C cm^{-1}, occurred in January. By substituting for L_{oil} in (7), $\Delta T_{oil} = f(Nu, Grad)$ can be obtained for both laminar and turbulent regimes as follows:

$$\text{Laminar } 1<Nu<2.6 \quad \Delta T_{oil} = (0.38\ Grad\ Nu^{0.1})^{0.83} \qquad (8)$$

$$\text{Turbulent } 6.58<Nu<187 \quad \Delta T_{oil} = (0.29\ Grad\ Nu^{0.01})^{.76} \qquad (9)$$

Substituting a range of ice temperature gradients observed at Balaena Bay (0.06 to 0.2 cm^{-1}), the corresponding theoretical temperature drops that could be encountered in practice are about 0.6 to 1.5°C for the laminar case and 0.54 to 1.33°C for the turbulent case.

Using these parameters for ΔT_{oil} and L_{oil}, a plot was generated showing curves of equal Nu modulus plotted against temperature drop across an oil lens and oil lens thickness (Figure 7-5).

Figure 7-5 OIL LENS TEMPERATURE DIFFERENTIAL VS OIL LENS THICKNESS

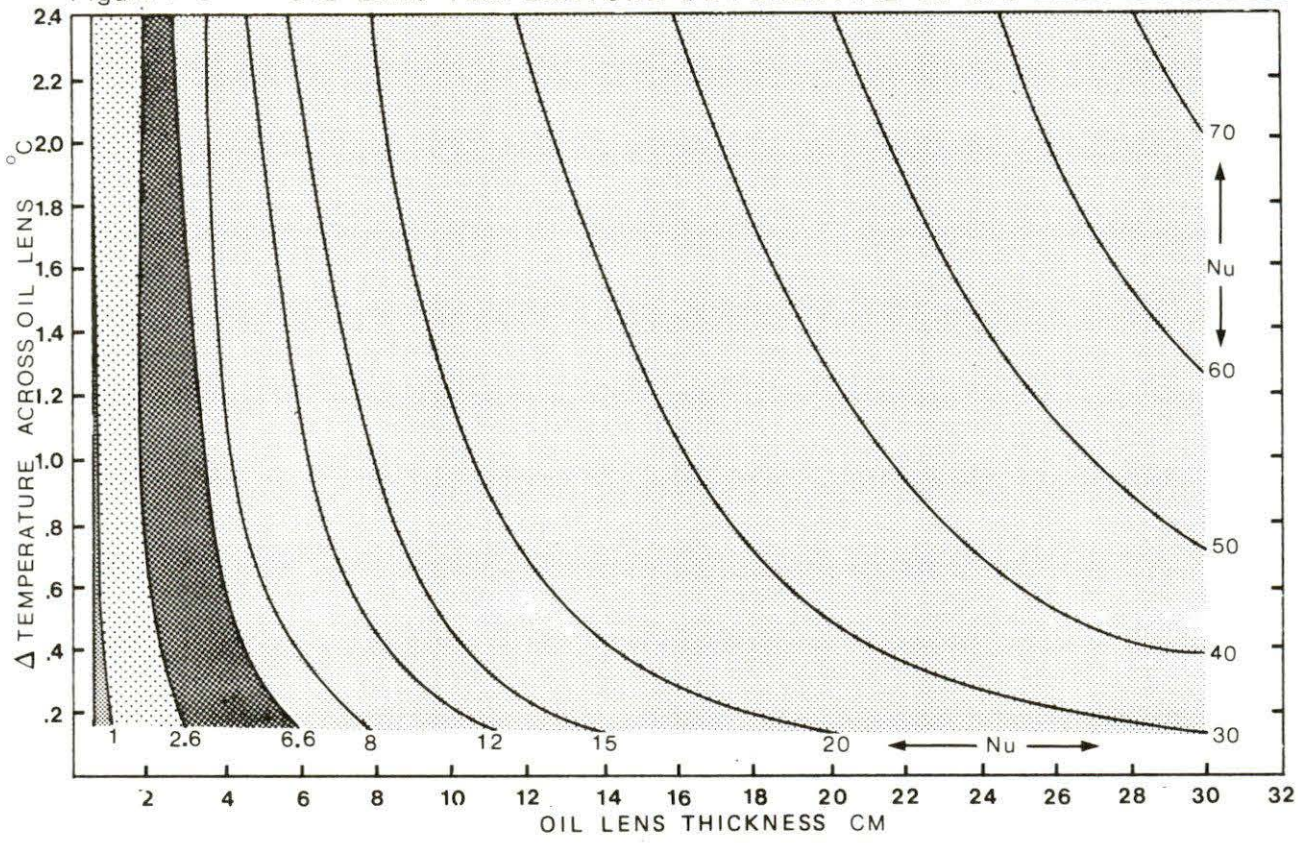

This theoretical treatment indicates that for extremely thick lenses of 25 to 30 cm, it is possible to have the situation where with Nu = 50, the temperature gradient across the oil lens is only 1/4 of the gradient through the ice sheet. This effect was never observed at Balaena Bay where none of the thermistor chains indicated an oil lens much greater than 2 cm (mean lens thickness from coring data was 2.08 cm, 20 cm max.). Therefore, it can be seen from Figure 7-5 that for most of the oil included in the ice during these tests the Nu modulus was in the range 1 to 3. The experimental temperature profiles in Figures 7-12 and 7-14, show a gradient through the oil lens of about 6 times that of ice. This agrees with the theoretical result using Nu approx = 2.2.

With an understanding of the possible heat transfer mechanisms present in an included oil lens, the overall heat transfer coefficient (U) of the oil-ice composite can be evaluated for various oil lens thicknesses. For

comparison a similar coefficient was calculated for an ice-snow composite to provide a direct measure of the relative importance of oil and snow in effecting heat flux through the ice sheet.

The heat transfer coefficient of a composite is simply the inverse of the sum of the individual thermal resistance of the different materials (see equations 2, 6).

Therefore:

$$U_{ice + snow} = \frac{1}{\frac{L_{ice}}{k_{ice}} + \frac{L_{snow}}{k_{snow}}} \qquad (10)$$

$$U_{ice + oil} = \frac{1}{\frac{L_{ice}}{(Nu+1)k_{oil}} + \frac{L_{ice}}{k_{ice}}} \qquad (11)$$

The unit thermal conductance for uncontaminated ice with no snow, ie. a one material system is referred to as U_{ice} where:

$$U_{ice} = \frac{k_{ice}}{L_{ice}}$$

Figure 7-6 shows the ratio $\frac{U_{ice + snow}}{U_{ice}}$ plotted as a function of mean ice thickness for snow depths of 4, 10 and 30 cm. Due to the insulating effect of the snow, the ratio is always less than unity. It can be seen that a 10 cm snow cover, which represented an average for the test site at Balaena Bay, would effectively reduce the overall heat transfer coefficient by an average of 50% over the growth period.

Figure 7-7 shows a similar ratio, $\frac{U_{ice + oil}}{U_{ice}}$ for discrete oil lens thicknesses from 0.75 to 30 cm. The corresponding Nusselt modulus indicating the degree of convective heat transfer present, and a representative value of ΔT_{oil} are tabulated for each curve. A reasonable constraint introduced to enhance the comparative nature of the graph is that the thickness of the composite $L_{oil} + L_{ice}$ used to calculate $U_{ice + oil}$ is equal to the clean ice thickness used to calculate the base value of U_{ice}. This seems acceptable because in any discharge the oil would seek out the points of

Figure 7 - 6 EFFECT OF SNOW ON THE OVERALL HEAT TRANSFER COEFFICIENT OF THE ICE SHEET

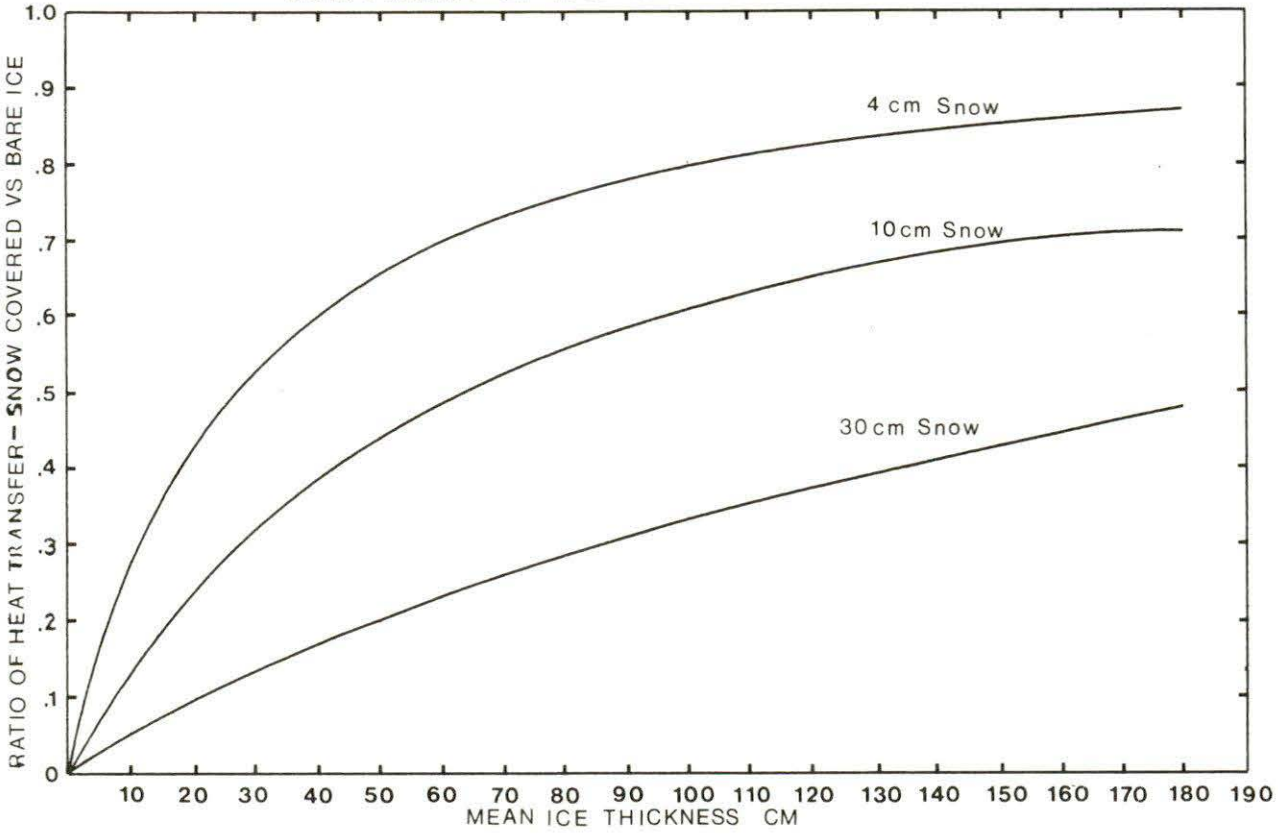

Figure 7 - 7 EFFECT OF OIL ON THE OVERALL HEAT TRANSFER COEFFICIENT

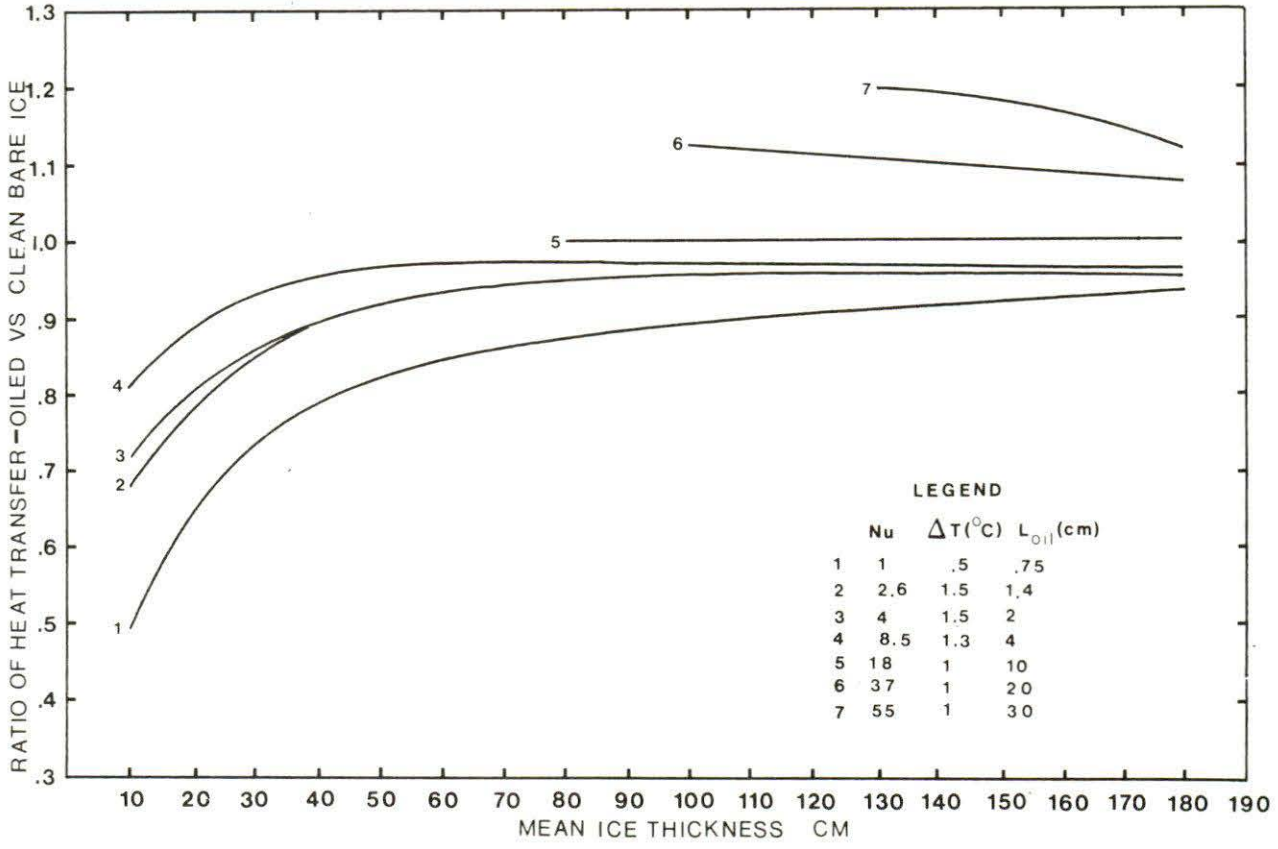

minimum ice thickness. This distinction only becomes important in the calculations where L_{oil} is an appreciable part of L_{ice} (ie. for 10 to 30 cm lenses). The curves in Figure 7-7 show that a maximum decrease in ice growth (or heat flux) will be caused by the thinnest (0.75 cm) lens where there is no convective heat transfer present. Even this "worst case" over most of the growth period of the ice sheet causes less than a 15% reduction in heat flux over the non-oiled case. This appears insignificant when compared to the 50% variation in heat flux due to changes in snow cover alone. For a lens of 2 to 5 cm corresponding to that commonly observed at Balaena Bay, the heat flux is reduced by only about 7% at an ice thickness of 50 cm. Curves 7-7 show that to get any real increase in heat flux due to large Nu numbers the oil lens must be 10 to 20 cm thick. Even then, the magnitude of the increase is generally less than 10%. A 30 cm lens would occur so near the end of the growth process that the absolute increase in heat flux due to the oil would be minimal. This theoretical treatment of heat transfer in the snow, ice, oil composite appears to confirm the field observation that compared to the natural effect of snow cover, an included oil lens causes an insignificant change in heat flux through the ice sheet during the growth process.

The insulating effect of an included oil lens diminishes as the lens thickness and associated Nu modulus increases, until with very thick lenses in the order of 25 cm it is possible to actually enhance ice growth by a small amount.

This theoretical treatment applies only to included oil lenses with ice above and below the oil. The significant thermal effect of an oil lens prior to formation of new ice below the oil (7 to 10 days following discharge) has been discussed in Section 6.2. Modifications to the ice temperature profiles during and after this inclusion period are discussed in subsequent sections.

In summary, snow cover has a profound effect on ice growth. Once the snow stabilizes, a strong correlation exists between the depth of cover and ice thickness. The oil, in seeking the highest possible level, tends to accumulate in domes or thin sections of ice, where the natural thermal resistance is high. The thermal effect of a typical oil lens is equivalent to between 5 and 8 cm of ice. This represents less than 20 percent of the natural variation in ice thickness late in the season. Convective heat transfer increases as the thickness of the oil increases. Under certain conditions, a very thick oil lens could actually enhance ice growth. In general, the oil has relatively insignificant effect on ice growth.

It should be noted that the values quoted herein for such parameters as Nu moduli are based on reasonable assumptions and a knowledge of the particular materials, but in the absence of substantiating experimental data, must be treated as approximate only.

7.3 Observed Effects of Oil on Ice Growth

The following analysis is based primarily on an interpretation of temperature profiles. A total of 30 eleven point thermistor chains were embedded in the various test areas, and three control chains were placed in undisturbed ice. The design of the chains and the spacing of probes are detailed in Section 5.3.3. For simplicity, all chains are designated first by the test number, then the chain number, and finally the probe number, if relevant. For example, NW3-5-8 indicates the eighth probe from the top on the number 5 chain in the Norman Wells 3 test area. Similarly, the control chains have been designated C1, C2 and C3. The profiles are viewed in chronological sequence, starting with the NW3 discharge in November 1974, and progressing to the NW7 and SH2 discharges in April 1975. The schedule of discharges is shown in Table 5-2. During this period over 400,000 ice temperatures were recorded, however, only representative trends are considered herein. Typical thermistor chains from the late fall, depth of winter, and early spring periods are compared with control chains.

In comparing temperature profiles over a long period, diurnal effects and rapid changes in the ambient air temperature must be taken into account. The resulting departure from linearity tends to be transient, and not truly representative of the long term trend. A typical example is the C1 profile on January 29, shown in Figure 7-8. In the preceding three days, the air temperature dropped 7.8°C. The transient effects are far more difficult to isolate in oiled areas, where the added thermal resistance of the oil causes a realignment of gradients. In most cases, adjacent control chains have been included with the profiles through oiled areas, as an aid to separating oil induced effects from external influences. Although the magnitude and response time for a given disturbance will vary with snow cover and depth in the ice, the controls provide a general indication of the prevailing trend.

As might be expected, the diurnal fluctuation is relatively insignificant during the depth of winter, and increases in the spring, as the level of solar radiation increases. Table 7-2 shows the observed variation in temperature over a 24 hour period for a typical control chain on April 12. The absolute change in air temperature was 9.6°C, while the variation at the 5 cm level in the ice was 2.1°C. The corresponding values for the same chain on December 10 were 1.9°C and 0.25°C respectively (Table 7-3).

Variations in the water temperature were examined to determine whether the vertical gradient cycled in a predictable manner. In general, the water was warmest immediately below the ice, and dropped about 0.3°C within 20 to 60 cm. The water temperature ranged from -0.9 to -1.6°C, and varied by as much as 0.2°C in a 24 hour period. It was impossible to trace the long term trends at a given depth, since as the ice thickened, the position of the thermistors changed relative to the bottom of the ice. The mean monthly water temperatures as well as the standard deviation for given depth groupings are presented in Table 7-4.

TABLE 7-2

CONTROL CHAIN 1, APRIL 12-13 1800-1500

DEPTH (cm)	TEMPERATURES (°C) 1800 h	2200 h	0200 h	0600 h	1500 h	1700 h	ABSOLUTE CHANGE(°C)
+100 Air	-11.53	-14.82	-18.16	-21.17	-16.59	-16.7	9.64
+8.2 Snow	- 9.22	- 8.99	-10.95	-12.24	-13.33	-11.79	
+4.1 Snow	- 8.95	-10.37	-10.34	-11.16	-11.77	-10.87	
-5.1 Ice	- 9.32	- 8.53	- 9.47	- 9.56	- 8.70	-10.67	2.14
-10.1 Ice	- 8.98	- 9.82	- 9.46	- 9.48	- 9.77	- 9.00	0.84
-20.0 Ice	- 9.27	- 8.86	- 9.30	- 9.23	- 8.79	- 8.79	0.44
-40.0 Ice	- 8.43	- 8.52	- 8.79	- 8.73	- 7.96	- 8.06	0.83
-59.2 Ice	- 8.69	- 7.45	- 8.09	- 8.02	- 7.53	- 7.16	1.53
-99.2 Ice	- 3.80	- 4.51	- 5.90	- 5.84	- 3.66	- 4.46	2.24
-139.2 Ice	- 2.85	- 2.87	- 2.49	- 2.49	- 2.84	- 2.77	0.38
-179.8 Water	- 1.13	- 0.78	- 1.15	- 1.20	- 1.18	- 0.83	0.42

Clear sky, approximately 16.5 hr daylight
Air temperature range (1m) - 11.53 to - 21.17°C
Snow depth 12cm
Water temperature -0.78 to -1.20°C
Ice depth 150cm
Absolute thermistor error $\pm$ 0.01°C at 0°C
$\pm$ 0.03°C at -20°C, -40°C
add $\pm$ 0.02°C up to 20°C on either side of a known point
Repeatability error involved in comparing 1 probe over short time period - negligible.

TABLE 7-3

CONTROL CHAIN 1, DEC. 10

DEPTH	0100 h	0600 h	1000 h	1300 h	2000 h	ABSOLUTE CHANGE(°C)
+100 Air	-29.60	-30.02	-29.93	-30.00	-31.49	1.89
+8.2 Snow	-25.29	-25.16	-24.72	-24.55	-26.99	
+4.1 Snow	-20.23	-20.36	-20.12	-20.02	-21.11	0.34
-5.1 Ice	-12.34	-12.39	-12.41	-12.42	-12.59	0.25
-10.1 Ice	-11.53	-11.59	-11.64	-11.64	-11.78	0.25
-20.0 Ice	- 9.71	- 9.82	- 9.88	- 9.90	-10.02	0.31
-40.0 Ice	- 6.21	- 6.29	- 6.26	- 6.40	- 6.50	0.29
-59.2 Ice	- 2.67	- 2.71	- 2.73	- 2.76	- 2.81	0.14
-99.2 Water	- 1.12	- 1.12	- 1.11	- 1.10	- 1.10	0.02
-139.2 Water	- 1.54	- 1.53	- 1.52	- 1.52	- 1.50	0.04
-179.8 Water	- 1.38	- 1.38	- 1.37	- 1.37	- 1.35	0.03

Clear sky, 0 hr sunlight

Ice depth, 68cm.

TABLE 7-4

MEAN MONTHLY WATER TEMPERATURE AND STANDARD DEVIATION (°C)

DEPTH BELOW ICE SHEET (cm)	NOV	DEC	JAN	FEB	MARCH	APRIL	MAY
20-30		-1.11		-1.32		-1.22	-1.46
		(0.08)		(0.17)		(0.16)	(0.11)
40-65	-1.25	-1.54	-1.54	-1.56	-1.27		
	(0.12)	(0.10)	(0.10)	(0.13)	(0.17)		
80-105	-1.51	-1.36	-1.57				
	(0.09)	(0.12)	(0.10)				

Selected profiles from control chain C1 for the period November 15 to May 22 are shown in Figures 7-8 and 7-9. Throughout the winter this chain was reasonably representative of the thermal regime in uncontaminated ice. To minimize diurnal effects, all profiles were taken at 1800. Figure 7-8 demonstrates the progressive cooling of the sheet, which continued until early February. The gradients tend to be stable and relatively linear. Figure 7-9 shows the general warming trend. By the end of April, the internal temperature of the ice was lower than the air temperature. The ice continued to grow, however, until about the middle of May. The ice thickness was approximated by extrapolating the thermal gradient near the bottom of the sheet to intersect the observed water temperature. Due to the fragile and indistinct nature of the skeletal layer, resolution was limited to about ± 2 cm. The problem was particularly acute late in the spring, when the gradient through the ice was close to vertical.

7.3.1 Late Fall

The NW3 discharge on November 14 was the first fully instrumented test. The average ice thickness at the time was 55 cm, and the growth rate was approximately 0.7 cm per day. Profiles from the three active thermistor chains in the test area both at the time of the discharge and 23 days after are shown in Figure 7-10. Controls C1 and C2 have also been included, as they represent the extreme profiles on November 14. The snow cover at C1 was 12 cm, as compared to 30 cm at C2. This is reflected in a general depression of the

temperature of the ice from between 1.5 and 2.0°C, and an increase in thickness of about 20 cm. The change in these two profiles in the subsequent 23 days clearly demonstrates the relative significance of natural variations. By December 7, the ice thickness at C1 increased approximately 20 cm, while the growth at C2 was less than 10 cm. As well, the difference in internal temperature had narrowed to 0.5°C at the 45 cm level.

The three test profiles were initially very similar. The ice temperature at a given level varied less than 0.7°C, and the ice thickness was within 5 cm. Although located in thinner ice, the NW3-5 chain was not oiled, and behaved in a similar manner to the control chains. The NW3-2 and NW3-3 chains were oiled, and exhibited a distinct plateau, or displacement of the profile through the oil on December 7. In both cases, the temperature immediately above the oil was about 0.5°C lower than C1 at the same depth, 1.3°C lower than C2 and 2.8°C lower than NW3-5. However, less than 10 cm of new ice had formed beneath the oil at NW3-3 and only 4 cm at NW3-2. The average growth at the two control chains during the same period was 15 cm. The variation in profiles displayed by the two oiled chains could have been due to differences in snow cover, thickness of the oil or size of pools.

The short term effects of the oil on the temperature gradient can be seen by comparing the profiles from NW3-2 immediately prior to, during and after the discharge (Figure 7-11). From the profile taken one hour prior to discharge, the interface was between 53 and 54.5 cm. Introduction of the oil, which was at about 0°C, caused a transient peak to occur when the oil struck the thermistor immediately below the ice. Simultaneously, the water temperature rose 0.1°C, likely as a result of upwelling. One hour later, the water temperature returned to its pre-spill value and the ice temperatures were depressed at the growing interface by 0.2°C. Temperature depressions of up to 0.05°C were felt up to a depth of 45 cm. One day after the discharge, the profile clearly displayed the effect of the oil lens on temperature gradients. The oil lens appeared to be about 2 cm thick judging by the points of slope change. The ratio in temperature gradients between the oil lens and the ice immediately above the oil was 12, which compares with the theoretical ratio in thermal conductivities between ice and oil of 15. This would indicate that very little convective heat transfer was taking place at this time. In 24 hours the temperature of the ice-oil interface had been lowered by 0.9°C due to the presence of an oil lens. Heat flux through the ice sheet is proportional to the temperature gradient $\Delta T/L_{ice}$. The introduction of an oil lens had the immediate effect of reducing local heat flux by a factor of 2.5.

This lower temperature gradient between 35 and 55 cm was a transient effect as can be observed by plotting the profile at 7, 14 and 21 days following discharge (Figure 7-12). After 21 days, the profile had smoothed out again with only a local perturbation through the oil lens. By extrapolating the profile above the oil lens to inter-

Figure 7 - 8 CONTROL ICE TEMPERATURE PROFILES

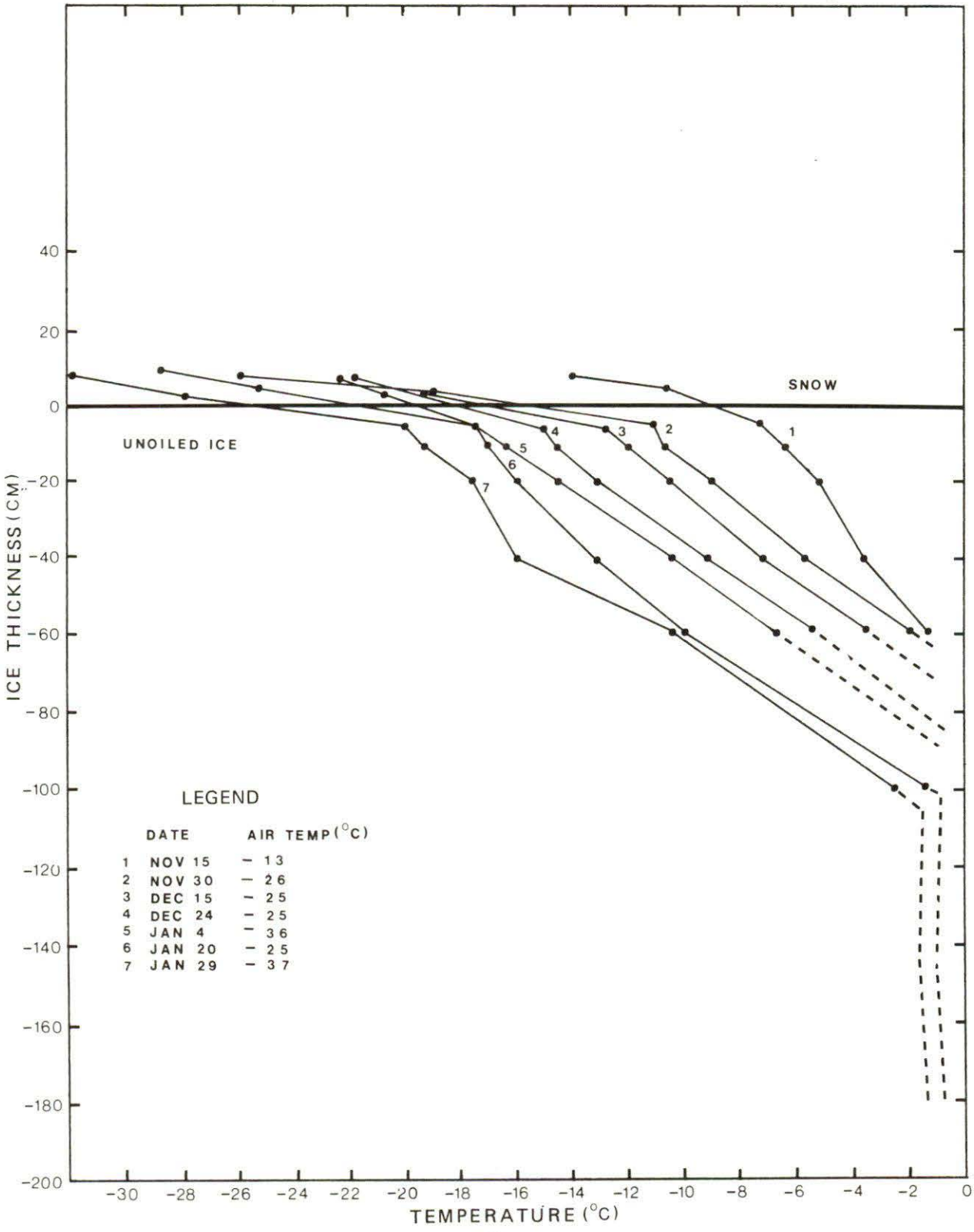

Figure 7 - 9 CONTROL ICE TEMPERATURE PROFILES

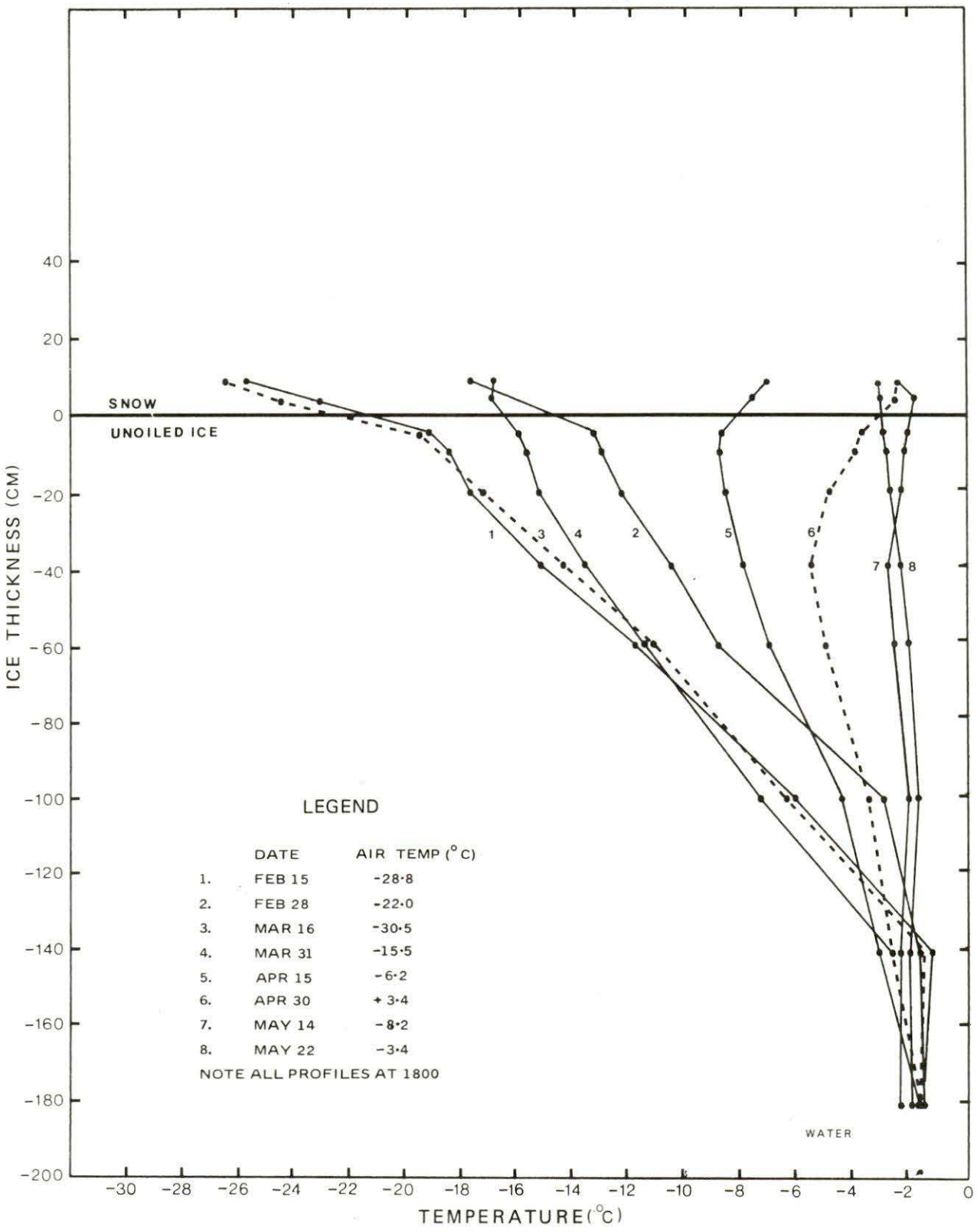

Figure 7 - 10 CONTROL AND NW3 TEMPERATURE PROFILES

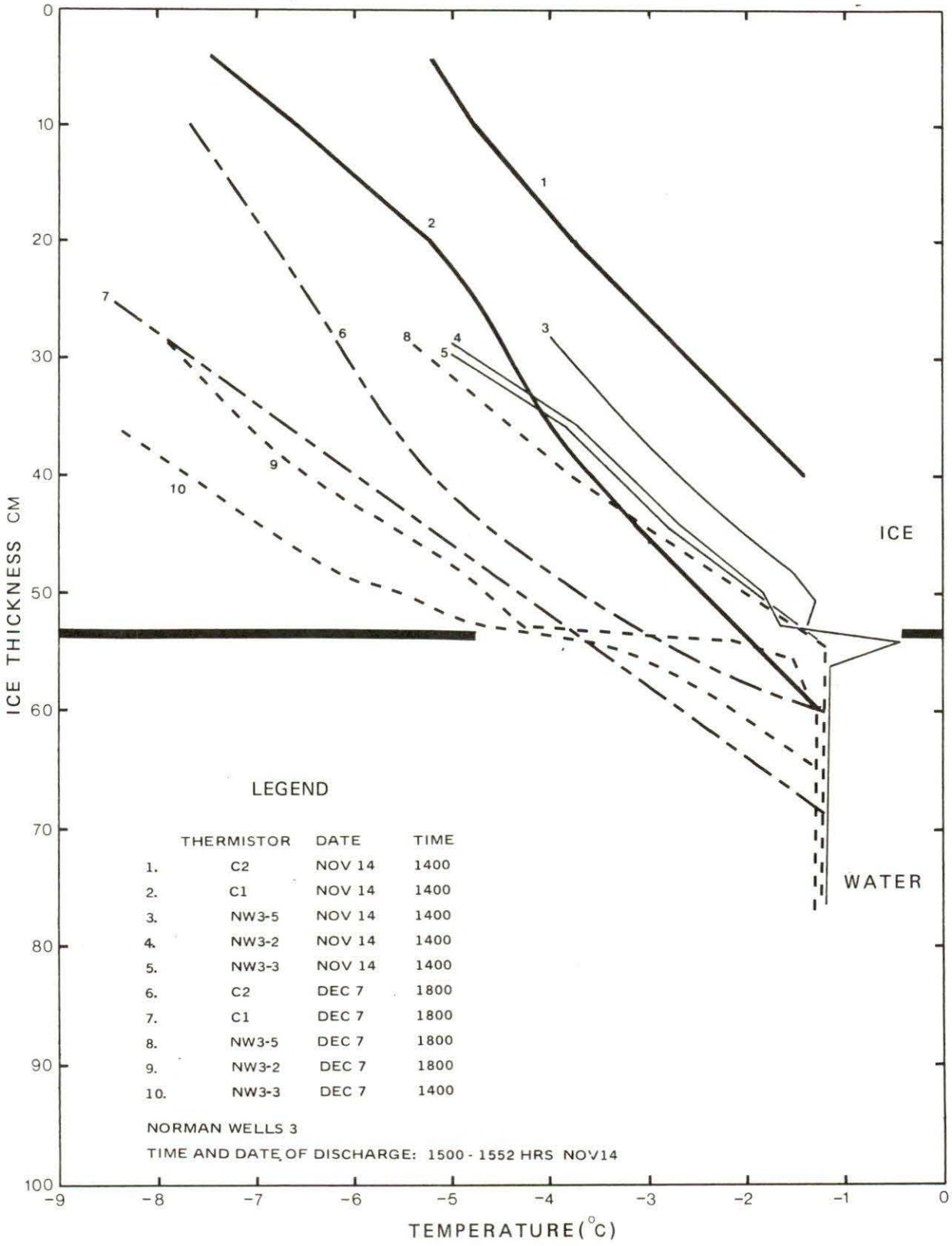

Figure 7 - 11 NW3 PROFILES - WEEKLY NOV. 14 TO DEC. 5

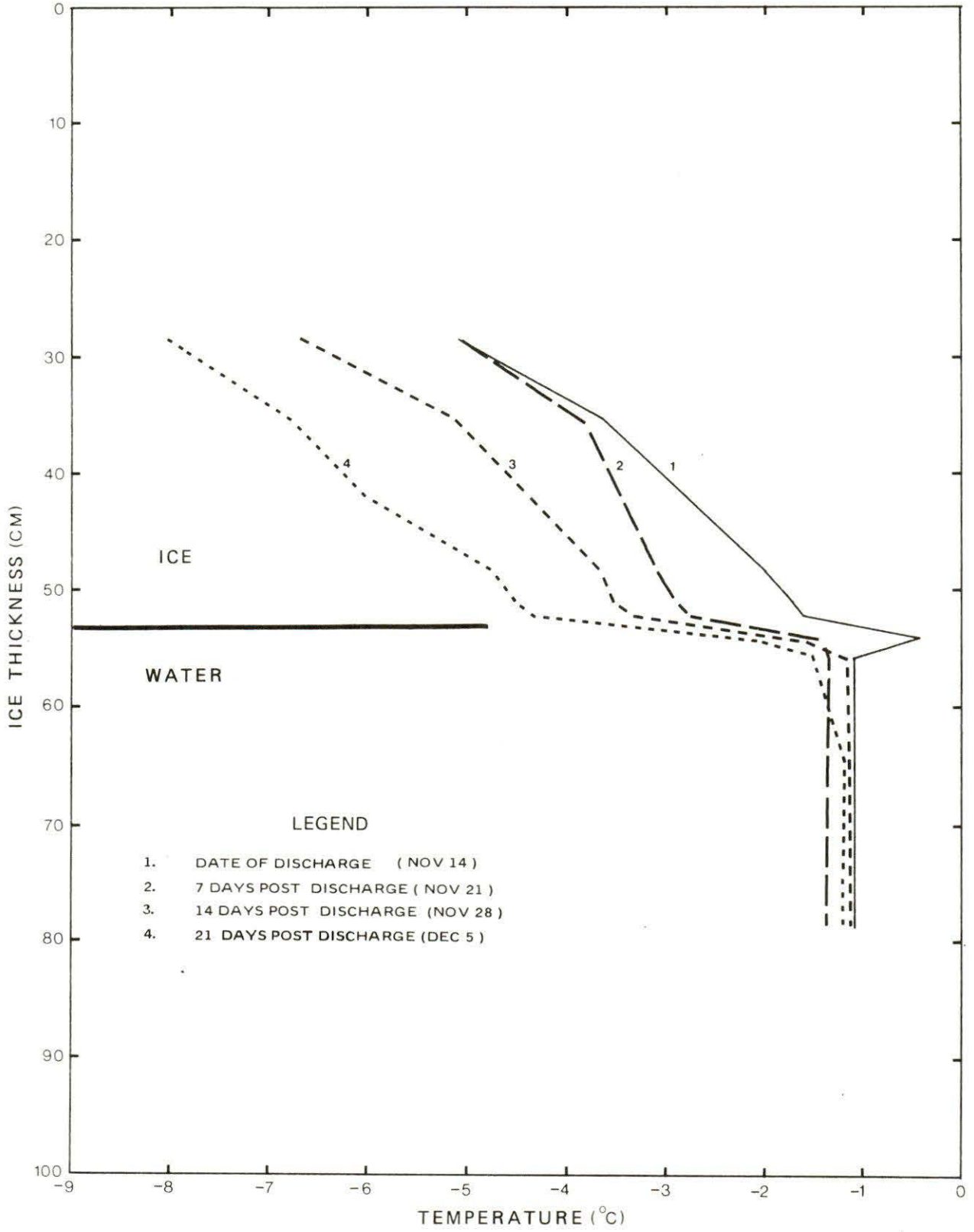

Figure 7 - 12

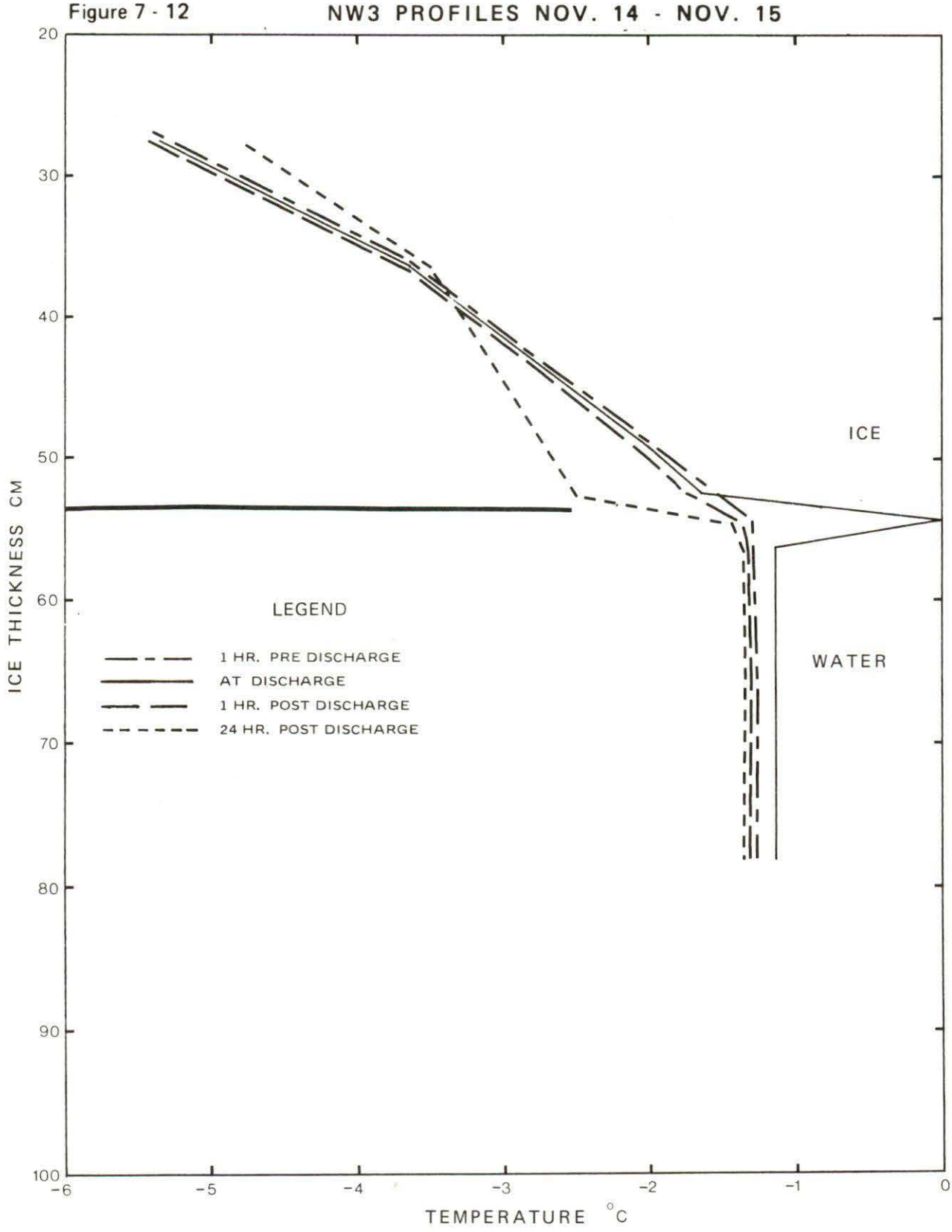
NW3 PROFILES NOV. 14 - NOV. 15
ICE THICKNESS CM
20
30
40
50
60
70
80
90
100
-6
-5
-4
-3
-2
-1
0
TEMPERATURE °C
ICE
WATER
LEGEND
1 HR. PRE DISCHARGE
AT DISCHARGE
1 HR. POST DISCHARGE
24 HR. POST DISCHARGE

cept the water temperature, it appears that the lens caused an effective 3 to 5 cm reduction in growth in the first three weeks. Unoiled ice around NW3-3 had grown about 15 cm. Therefore, the oil lens appeared to cause a 20 to 30% reduction in heat flux. The theoretical curves produced earlier describing the effect of an oil lens under steady state conditions (Figure 7-7) would predict a reduction from 10 to 20% at an ice thickness of 55 cm.

7.3.2 Depth of Winter

Temperature profiles associated with the double discharges, SH1 on December 7 and NW4 on December 9, display short and long term responses similar to NW3 (Figures 7-13, 14).

Considering SH1-3 one hour prior to discharge, the ice-water interface is seen to fall on the dense array of probes at 68.5 cm (Figure 7-13). Snow depth around the chain on December 7 was 12 cm. One day after the test, the temperature in the lower 10 cm of the sheet had been depressed by about 0.9°C while the upper 58 cm had experienced a temperature rise of up to 1.2°C at a depth of 20 cm. It is doubtful if the increase reflected by the probe at the 4 cm level was due to the oil, but rather fluctuations in the ambient air temperature.

By December 18, the temperature gradient was almost parallel to that prior to discharge. The presence of the oil lens was indicated by a sharp temperature drop of up to 1.1°C between 66.5 and 68.5 cm. By December 18, there was definite evidence that a new ice interface had formed below the oil lens. Allowing for 1 to 1.5 cm of oil, a new ice-water interface position of 71.5 cm on December 18 would indicate that less than 2 cm of ice had formed in the preceding 11 days, yielding an average growth rate of approximately 0.16 cm per day. By December 21, the ice had grown to 72.5 cm. In the period December 7 to December 21, control profiles with similar snow cover indicated a growth of about 10 cm. A profile from C1 on January 29 has been included to demonstrate that the oil lens did not have a significant effect on either the thermal regime or ice thickness after seven weeks.

Norman Wells 4 discharge took place at 1900 hours December 9. Considering the NW4-4 chain over the same time period as SH1-3, no substantial difference between the two types of oil can be seen (Figure 7-14). Detailed temperature trends through the lens are not available on NW4-4 as the ice on discharge day had not yet grown to include the dense array of probes. Consequently, the localized steepening of the temperature gradient seen on SH1-3 is not seen on NW4. Ice thickness at spill time was 63 cm. The plot on December 10 shows the characteristic clockwise rotation of the profile to warmer temperatures above and cooler below the 40 cm level. This trend continued until December 18. Then, between December 18 and December 24, the temperature gradient rapidly smoothed out and returned closely to its pre-spill shape. As with SH1-3, the recovery of the temperature profile about ten days following the spill coin-

Figure 7 - 13 CONTROL AND SH1 TEMPERATURE PROFILES

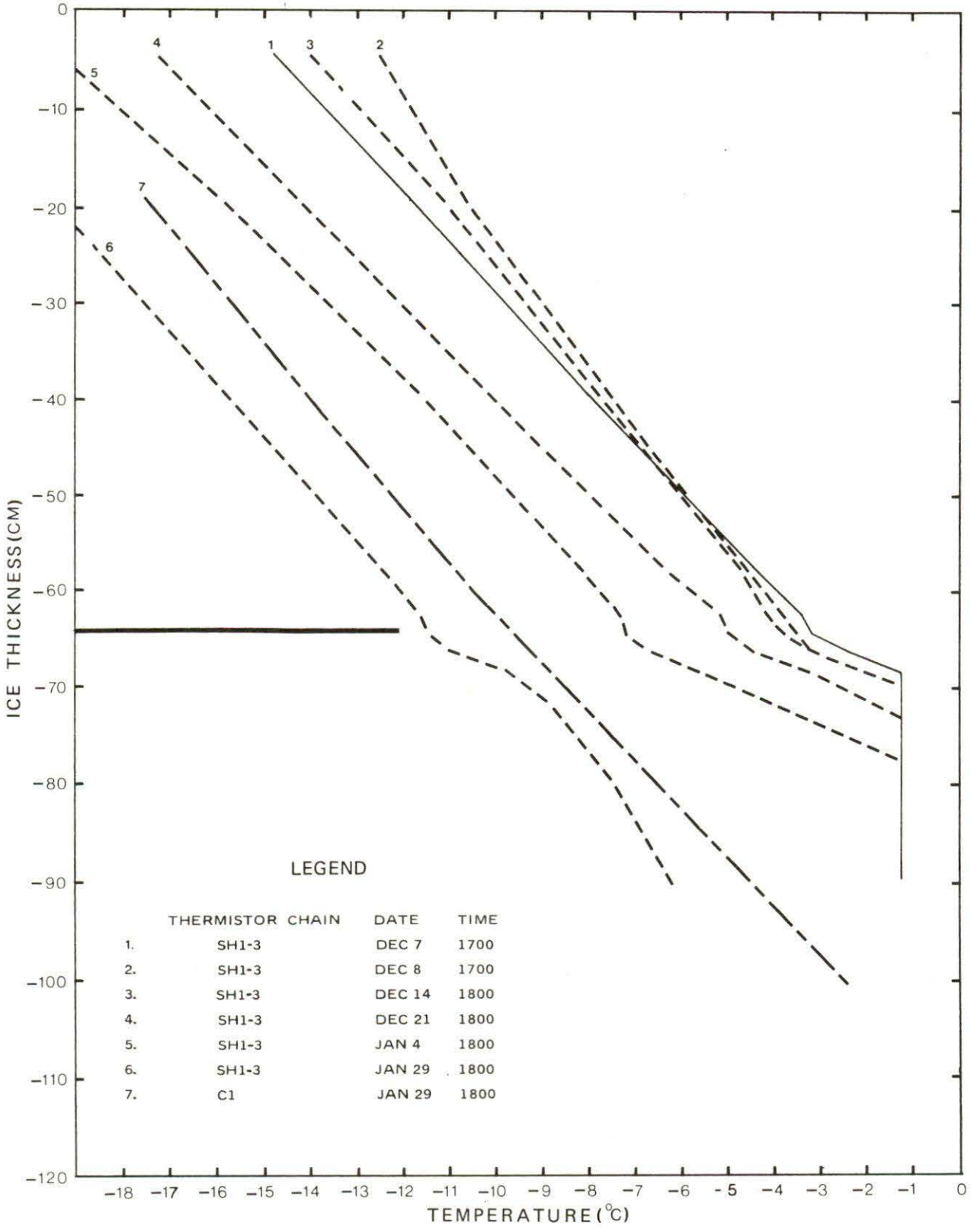

Figure 7 - 14 CONTROL AND NW4 TEMPERATURE PROFILES

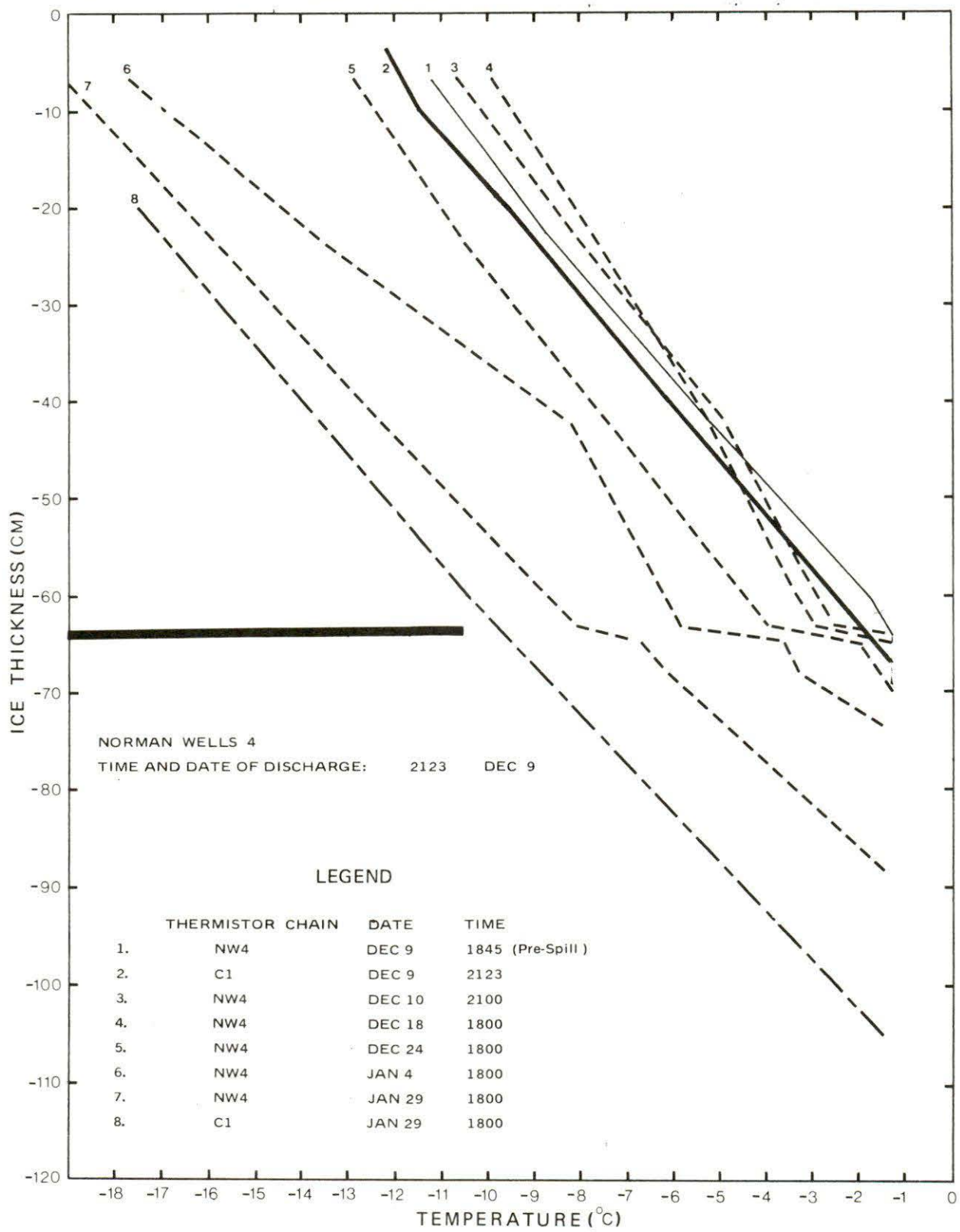

cided with the formation of a new ice interface below the oil lens. Between December 21 and 24, the temperature of the probe immediately below the oil lens fell from -1.5°C to 2.1°C, indicating that about 1 cm of new ice had formed.

The immediate reduction in heat flux throughout the sheet following the introduction of oil is clearly demonstrated by the reduced gradient in the ice. The increased thermal resistance of the oil, and the enhanced heat exchange at the relatively smooth oil-water interface, tend to retard ice growth. Once a layer of ice has formed beneath the oil, the temperature profile quickly assumes its initial gradient.

On the basis of the SH1-3 and the NW4-4 chains, there would appear to be only minor differences between the Norman Wells and Swan Hills crudes. However, a detailed comparison is difficult because of the limited number of chains actually in contact with oil. As well, variations in oil lens thickness and snow cover severely limit the significance of apparent deviations.

The oil lens thicknesses derived from thermistor plots are not precise. However, to core beside a chain would alter or destroy a lens. With probes spaced at 2 cm intervals, the probable error in estimating the thickness of a lens was likely within 1 cm. Laboratory and theoretical studies of the pooling characteristics of the two crudes indicate a minimum practical lens thickness of about 0.8 cm. From video observations at the time of discharge, the oil covered between 30 to 40 percent of various test areas, yielding an average oil thickness of about 3 cm. Aided by adjacent cores and diver observations, the error for most chains could be reduced to about 0.5 cm.

7.3.3 Early Spring

The two discharges, SH2 and NW7 were undertaken on April 12 and 15, at an ice thickness of approximately 150 cm. The sheet was rapidly warming, and the average ice growth subsequent to the tests was less than 15 cm. After about the middle of April, it became difficult to estimate growth from the thermistor chains, as the temperature of the ice below the 140 cm level was very close to the water temperature, and on occasion higher. Although growth was not always apparent from the chains, it was confirmed by coring. As well, the profiles became transient in nature, and no longer displayed the linear or near steady state behavior, characteristic of the late fall and winter.

Profiles from the SH2-1 and the C3 chains were very similar at 1700 hours on April 12, just prior to the discharge (Figure 7-15). The sharp temperature fluctuation of about 0.4°C immediately above the interface, was likely due to density currents in the water column. Twenty four hours after the test, C1 had uniformly warmed by about 0.3°C, while the test chain decreased approximately 0.5°C over its entire depth. By April 19, seven days after the discharge, the

control had continued to warm evenly, while SH2-1 exhibited the characteristic rotation, with a depression in temperature in the lower 30 cm of ice. The time taken to adopt this profile was considerably longer than in earlier discharges, where it was observed within 24 hours. However, the effects of the oil were still very pronounced.

Although the entire sheet was warming, the gradient had not recovered after three weeks. The temperature was depressed relative to the control, and 17 cm of new ice had formed beneath the oil. It is difficult to isolate the external factors, but the slow recovery could in part be due to upward migration of the oil. By May 11, oil was detected at the 93 cm level, or about 50 cm above the lens.

The NW7-2 chain was interesting, in that a distinct warm wave that was detected in C3 at the 60 cm level on April 15, appeared on the test chain one week later. This transient temporarily masked fluctuations due to the oil. By May 11, the shape of the profile was similar to SH2-1, but the temperatures were not as depressed. The general instability in the spring makes direct comparisons difficult, but no marked variations could be detected between the Norman Wells and Swan Hills crudes.

The compared study of oiled and unoiled temperature profiles demonstrated a number of interesting features. Firstly, the temperature gradient in the ice immediately above the oil is sharply reduced. In the case of the NW3 test, a reduction in the temperature gradient of 56 percent was observed within 24 hours after the discharge, while a reduction of 32 percent was observed in the same period after the NW4 discharge. This reduction could be due to a number of factors, including the added thermal resistance of the oil, alterations in brine drainage, and enhanced heat exchange at the oil-water interface. Until suitable conditions develop for the formation of a new sheet below the oil, the heat of fusion, which is typically about 70 cal g^{-1}, is not available, causing a further depression in the temperature. Studies by the Frozen Sea Research Group indicate that the heat of formation may account for between 50 and 60 percent of the total heat input into a growing sheet.

Norman Wells and Swan Hills crudes tended to have a similar impact on the thermal regime of the ice. For the oil lens thickness of 2 to 4 cm commonly encountered in Balaena Bay, the insulating effect of the oil was partially offset by convective transfer within the lens. The net reduction in heat flux through the ice as a result of the oil was less than 10 percent. Although the convective transfer might be as much as 25 percent lower in the more viscous Swan Hills crude, the effect was insignificant in comparison to natural variations.

There was no evidence of a substantial modification in temperature profiles as the oil migrated upward through the ice. However, the brine channels represent no more than 3 to 5 percent of the ice by volume, even late in the melt phase.

Figure 7 - 15 CONTROL AND SH2 TEMPERATURE PROFILES

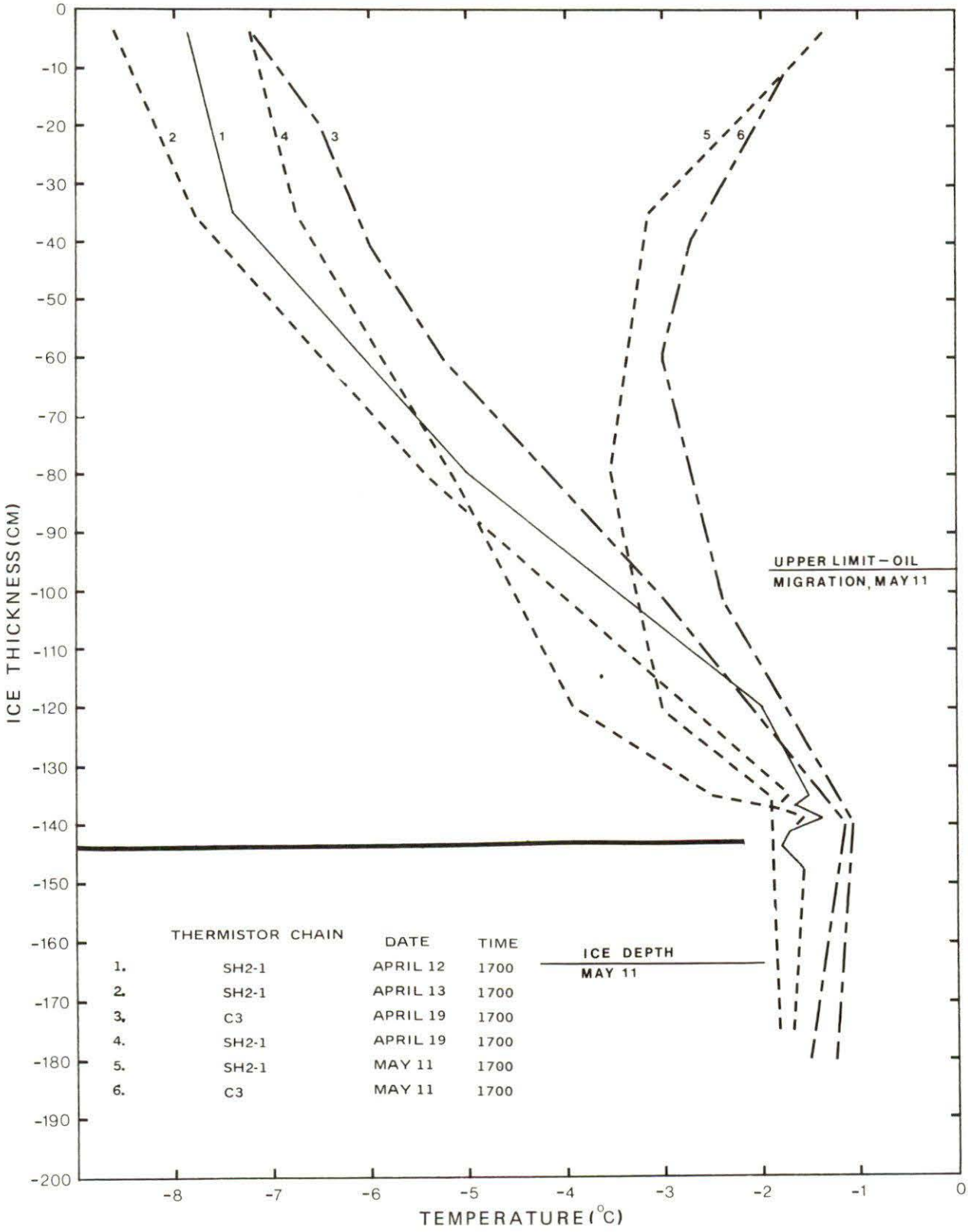

7.4 Observed Effects of Oil on Ice Depletion

Ice growth in Balaena Bay ceased by about May 20. Signs of surface melt were already evident in a number of oiled areas. The progressive change in surface conditions is detailed in Section 6.4. Consequently, only the thermal aspects, as reflected by temperature profiles, ice thickness measurements, and radiation levels, will be considered in this section.

The general trend in uncontaminated ice is best demonstrated by control chain C3. By May 4 the surface was warming faster than the ice could respond, and the profile was beginning to curve (Figure 7-16). Prior to this date the profiles had been essentially linear. The surface continued to warm until May 11, at which time the internal temperature of the ice was approximately 2°C cooler than either of the interfaces. Between May 9 and May 14 the ambient air temperature dropped from +5 to -9°C (Figure 7-17), causing a corresponding depression in the temperature in the upper levels of the ice. By May 19 the temperature profile through the ice was close to linear, and remained this way until about May 27. From May 21 onward the air temperature was progressively warming, reaching a high of 14°C by June 26. Diurnal variations of over 6°C were common during this period. On June 6, the day prior to the first full scale burn, the coolest observed temperature in the ice was -1.8°C, while the water temperature was -1.4°C, and the air temperature 2.6°C. The water temperature remained close to winter average of about -1.8°C until June 4, then began to warm at the rate of about 0.1°C per day (Figure 7-18).

By May 22 there was no significant difference between the thermal regimes of oil and unoiled ice. Representative profiles from five of the test areas and two control sites are shown in Figure 7-19. Substantial oil migration had occurred, and the brine channels were saturated with oil to within about 15 cm of the surface. The SH2 chain is the only location where an oil lens could be positively identified. There was a distinct drop of about 0.7°C across the lens. Since convective heat transfer in the oil is in part dependent on the temperature gradient, it was felt that convection would be relatively insignificant in comparison to conduction, and the insulating effect of the oil would be far more pronounced. The disturbances in the NW4 and SH1 chains at the 80 cm level were transient. The warmer temperatures exhibited by all oiled chains near the surface, was likely a direct result of increased radiation being intercepted in the upper levels of the sheet.

Once the oil began to surface it had a marked effect on ice depletion. Initially the oil appeared as a slight discolouration in the snow. Although barely detectable, it reduced the albedo by between 30 and 50 percent (Section 6.4). Since the level of absorbed solar radiation varies inversely with albedo, the contaminated areas melted much more rapidly than did the surrounding snow. As the underlying snow melted, the oil formed in small enclosed melt pools. In most areas the snow effectively contained the oil, and horizontal migration was limited to about one metre. Since the albedo of an oil lens on water is about 0.1, or less than 20 percent that of uncontaminated snow, the melt rapidly accelerated once the pools formed. Oil was splashed up on the surrounding snow by wind and wave action, and the pools grew in size, finally becoming

Figure 7 - 16

CONTROL TEMPERATURE PROFILES MAY 4 TO JUNE 5, 1975

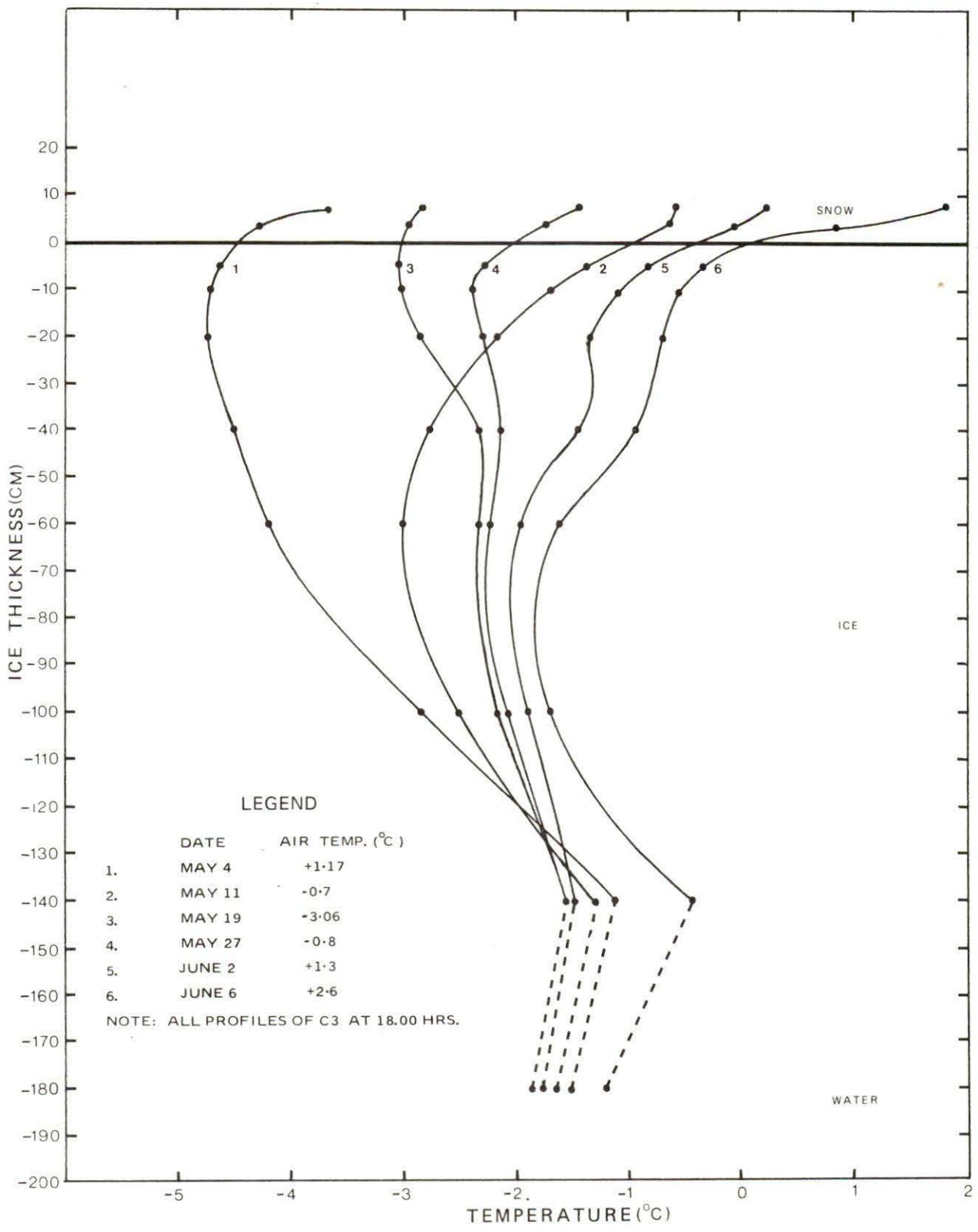

Figure 7 - 17 DAILY MEAN AIR TEMPERATURES MAY 1 TO JULY 1

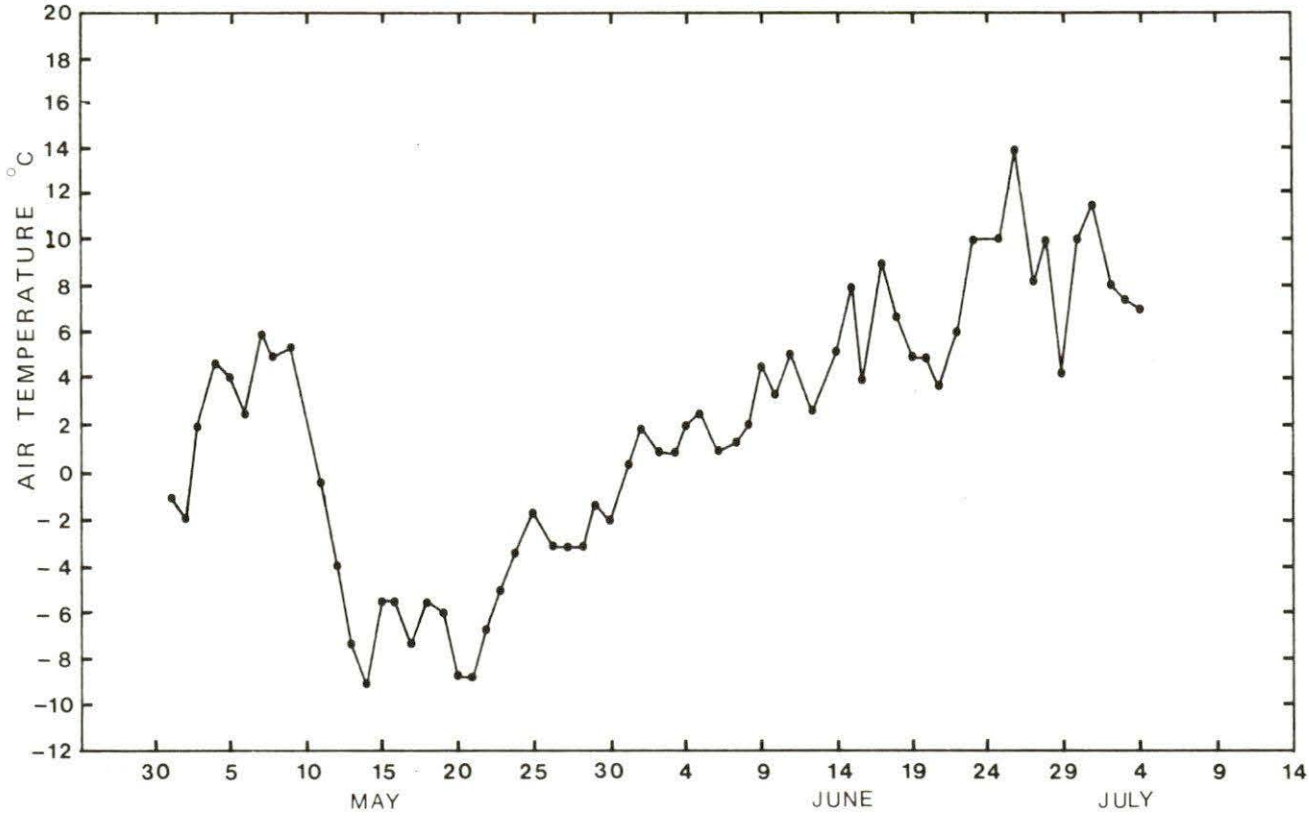

Figure 7 - 18 DAILY WATER TEMPERATURES MAY 1 TO JULY 1

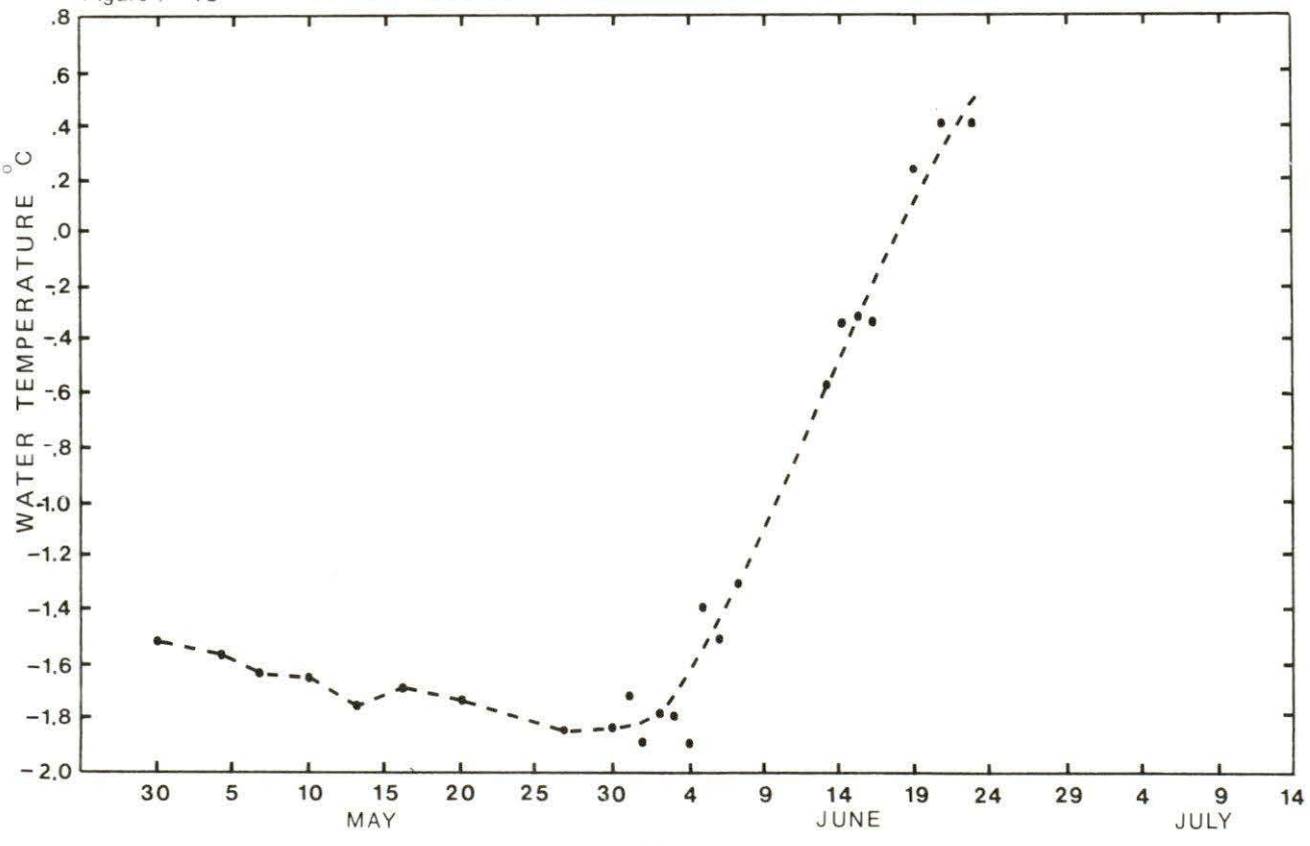

Figure 7 - 19 COMPARATIVE TEMPERATURE PROFILES MAY 22

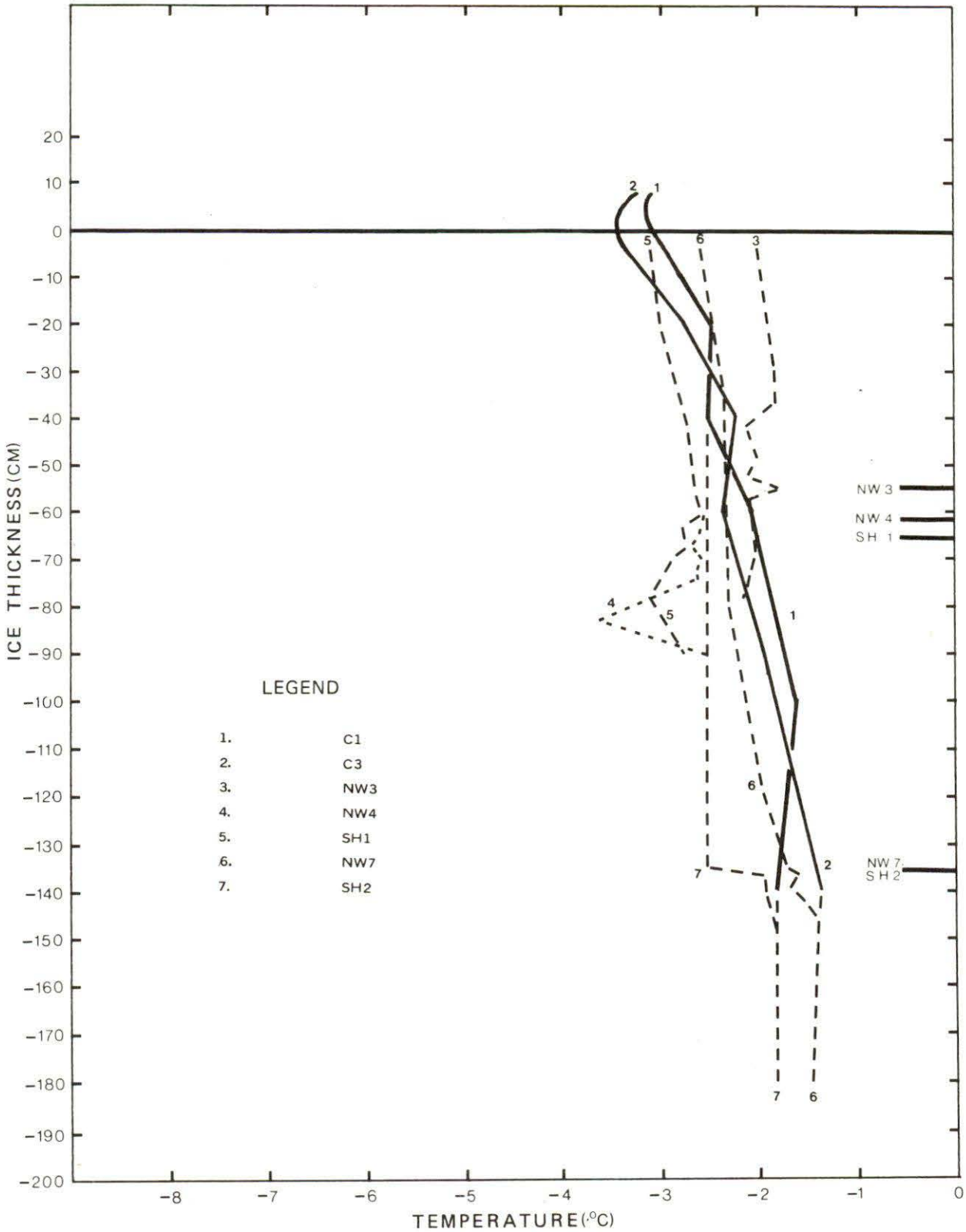

interconnected. By early June a number of melt holes had developed in the oiled areas. The significance of these holes is questionable, since they tend to form at old core holes. However, similar melt holes did not develop in the uncontaminated ice, which had also been cored. By June 27, the NW3 and NW4 test areas were essentially free of ice, and the entire test area was open by June 30. The surrounding ice sheet remained intact until July 6, when it was driven onshore by a high wind. The average ice thickness at the time was 15 cm.

The most significant factor in advancing the melt was the reduction in albedo caused by the oil. At the beginning of May there was no evidence of oil on the surface, and the average albedo was 0.78. By May 9 small oiled patches of snow were starting to appear and the average albedo of the test sites dropped to 0.70, as compared to 0.75 for the control areas. The spread continued to increase until June 6, when the average albedo of the test site was 0.15, or less than 34 percent that of the uncontaminated snow. The albedo in one of the more heavily oiled areas was 0.03. Consequently the energy input in to the oiled areas was substantially greater. The cumulative absorbed solar radiation for both the average and extreme conditions in the test area are shown in Figure 7-20. The curves are the cumulative product of the integrated direct and diffused incoming solar radiation and the average daily absorptivity. Measurements at 14 stations were used in determining the average absorptivity (1.0 - albedo) for the test area.

Between May 9 and June 6 an average of 6000 cal cm^{-2} was absorbed over the test area, while only 4800 cal cm^{-2} was absorbed at the control sites. In the same period 10,000 cal cm^{-2} was absorbed in one of the more heavily oiled areas. The limited divergence between the control and test areas until the end of May, directly reflects the percentage of the total area contaminated. On June 1, melt pools and oiled snow represented only 15 percent of the surface area (Figure 6-9). By June 6, oil was exposed over 47 percent of the site. It is unrealistic to extend the comparison beyond this date, due to fallout and other disturbances associated with the cleanup.

The distribution of absorbed solar energy within the ice sheet is considerably affected by the oil. With natural ice, approximately 40 percent of the energy penetrates to the 30 cm level (Hobbs, 1974). However, much of the energy is intercepted by the oil in the brine channels, causing a higher energy level near the surface. As well, even a very thin oil film on a melt pools serves as an effective barrier. During periods of high radiation, oil film temperatures as much as 10°C higher than the underlying water were recorded (Section 6.4). The average temperature difference was about 7°C. In accordance with the Stefan-Boltzmann Law, the longwave outgoing radiation is proportional to the fourth power of the absolute temperature, and consequently the flux from the oiled melt pools was approximately 10 percent larger than from the melting ice surface. The average emitted long-wave radiation from melting ice during the month of May is 625 cal cm^{-2} day^{-1}. On this basis, an additional 1750 cal cm^{-2} would have been radiated from the heavily oiled areas between May 9 and June 6, yielding a net gain of 3450 cal cm^{-2} relative to the control areas, or sufficient energy to

Figure 7 - 20 CUMULATIVE RADIATION MAY TO JUNE, 1975

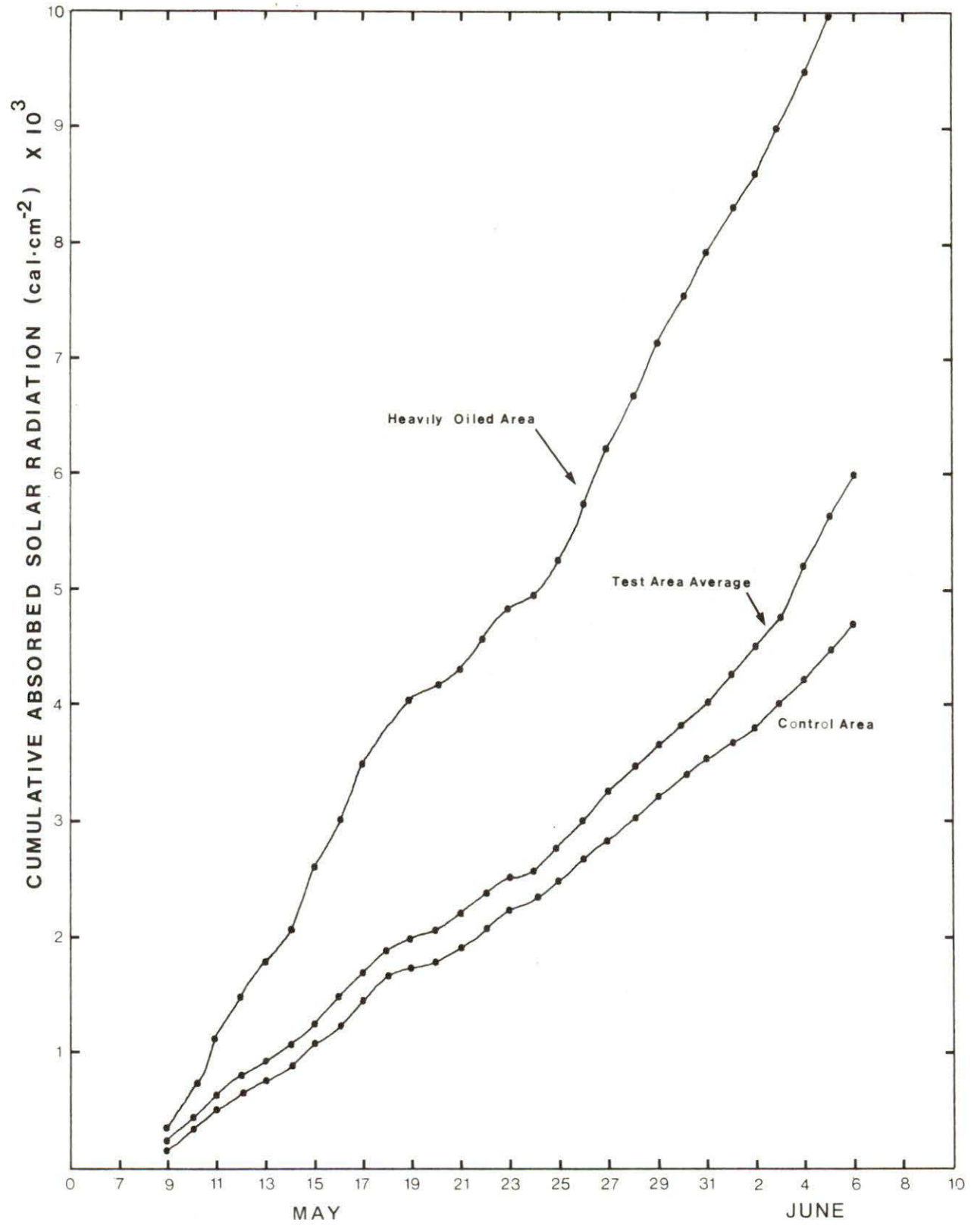

melt an additional 50 cm of ice.

On June 11, six cores were recovered from the control sites, and two from heavily oiled areas. The average thickness of the natural ice was 157.5 cm, while the average thickness of the oiled ice was 107.5 cm. The precise agreement between the observed and theoretical enhancement of ice depletion caused by the oil is somewhat coincidental, considering the broad assumptions made regarding surface heat exchange. However, it does suggest that the order of magnitude of the principal energy components is correct.

Although some general patterns would appear to exist, it is impossible to draw any firm conclusions as to the significance of the location of the oil in the ice on ice depletion. Measured ice thicknesses from the middle of May to the break-up of the sheet on July 6, are shown in Figure 7-21. Until about the end of May, the variation between oil and control areas appeared to be random. In general, the thickness of the ice varied directly with the depth of the lens. Ice thicknesses in the NW3 and NW4 test areas were consistently thinnest, and the NW7 and SH2 test areas thickest. Although oil was first detected on the surface in the SH2 test area, it was not released as rapidly as was the oil in lenses closer to the surface. By June 7, most of the oil had been released in the NW3 and NW4 test areas. Oil continued to flow from the ice in the SH2 test area until about June 20. The fact that the NW4 and SH1 tests were conducted at the same time, yet the ice was consistently thicker in the SH2 area, would suggest that the properties of the oil might have some bearing on depletion.

The clean-up activities, which commenced on June 7, disturbed the natural processes. By removing the oil, the absorptivity of the contaminated areas was substantially reduced, while traffic and fallout increased the absorptivity of the surrounding ice. If undisturbed, the oiled areas would likely have been free of ice between two and three weeks prior to the break-up of the sheet.

Figure 7 - 21

ICE DEPLETION MAY TO JULY

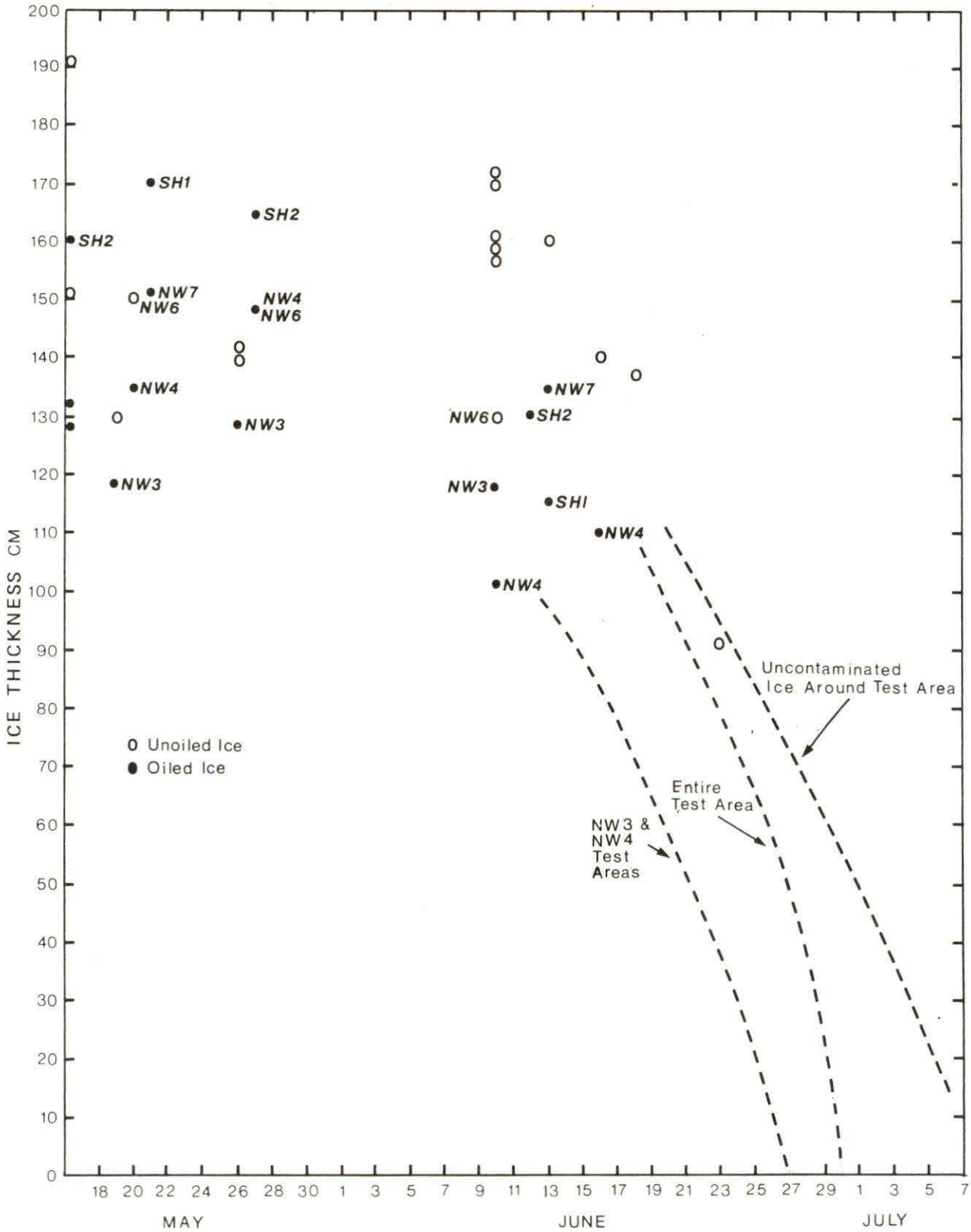

8.0 PHYSICAL AND CHEMICAL PROPERTIES OF OIL

8.1 Weathering of Oil

Due to the large number of samples involved, chromatographic analysis was found to be the best technique for assessing changes in the properties of the crudes. Through gas chromatography (GC), it is possible to separate, identify and then quantify the various components of an oil. On the basis of changes in composition, not only the extent, but also the nature of weathering can be determined. With additional tests, this information can be correlated with changes in physical properties.

The results of the gas chromatography were presented in the form of percent area covered by a specified hydrocarbon group. For this analysis the following groups were selected; C_1 to C_5, C_5 to C_6, C_6 to C_7, C_7 to C_8, C_8 to C_{10}, C_{10} to C_{12}, C_{12} to C_{16} and C_{16} to C_{24}. The chromatogram was stopped at carbon number 24. Under normal conditions, hydrocarbons above hexadecane do not evaporate significantly (Mackay 1973, Scott 1975), and therefore the C_{16} to C_{24} group was employed as a reference, to assess the relative evaporation of other components. Initially, fresh samples of both Norman Wells and Swan Hills crude oil were weathered under controlled conditions in a laboratory. This was done by placing trays of oil in a wind tunnel at a fixed temperature. Periodically, each sample was weighed in situ, and a small quantity of oil was recovered for GC analysis and the measurement of selected properties. The ratio of the area of each hydrocarbon group to the area of the C_{16} to C_{24} group was expressed as a percent (percent area ratio) and plotted against the percent evaporated by weight for the total sample (Figures B1, B2). A series of curves relating the physical properties to the percent oil evaporated was also developed (Figures B3 to B8).

The following procedure was employed in analyzing subsequent samples. A GC was run and the percent area ratio determined for each hydrocarbon group. Then, depending on the type of crude, either Figure B1 or Figure B2 was used to estimate the percent evaporated or the degree of weathering. Theoretically, each hydrocarbon group should indicate the same percent evaporated for the entire sample. In fact, this is not the case. There are normally variations of several percent between the groups, and care was necessary in interpreting the data, particularly in the early stages, when weathering was relatively small. There are two basic causes for the apparent discrepancy. Firstly, crude oil is not perfectly consistent. Variations in composition were detectable between successive drums. To minimize this effect, a composite sample was used in preparing the curves. Secondly, there are a number of limitations associated with the experimental technique.

The rate of evaporation of a complex mixture of hydrocarbons, such as a crude oil, is very difficult to quantify. The rate is dependent on the turbulence characteristics of the atmosphere, or the mass transfer coefficient, as well as the properties of the oil. The rate of evaporation of a specific compound or group of compounds depends primarily on the concentration, vapour pressure, and the activity coefficients of the hydrocarbons in the liquid phase. Generally, lower carbon number compounds

have a higher vapour pressure, and evaporate faster. Evaporation also increases with temperature, and the ratio of vapour pressures for various components does not remain constant. Thus, the nature of evaporation at 25°C may be different from that at 0°C. Scott (1975) has quantified these processes by calculating first-order evaporation rate constants and Arrhenius activation energies for the components of Arctic diesel oil. This work demonstrates the complex nature of the temperature dependence of oil evaporation. At low temperatures, there is a tendency for better fractionation during evaporation. The low carbon number compounds are lost preferentially, producing GC's as shown in Figure 8-1. However, if the oil is unmixed, some of the components which would otherwise evaporate will be shielded, and there will be a preferential retention of the lower carbon numbers (Figure 8-2).

Figure 8-1 EFFECTS OF TEMPERATURE ON WEATHERING

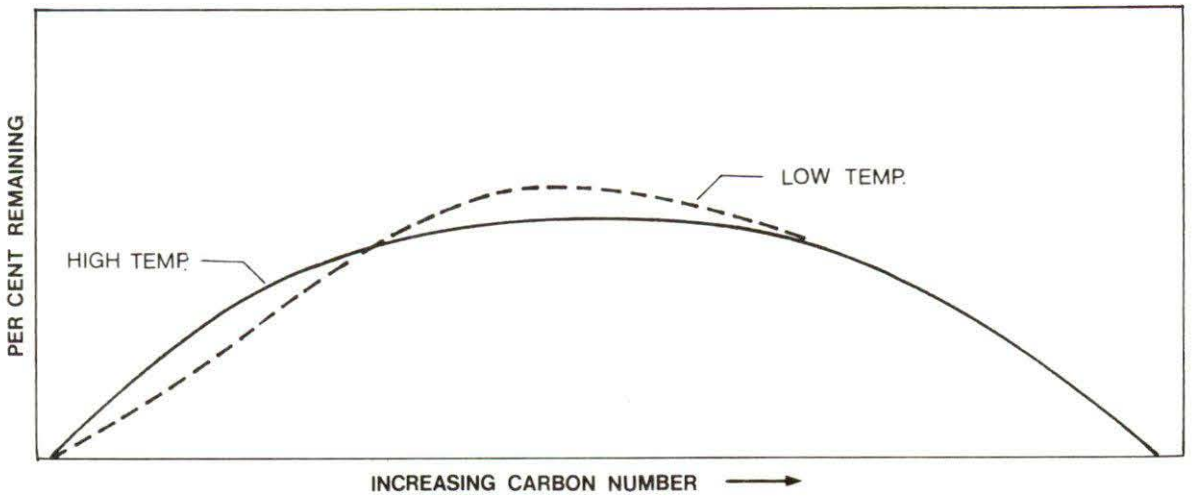

Figure 8-2 EFFECTS OF MIXING ON WEATHERING

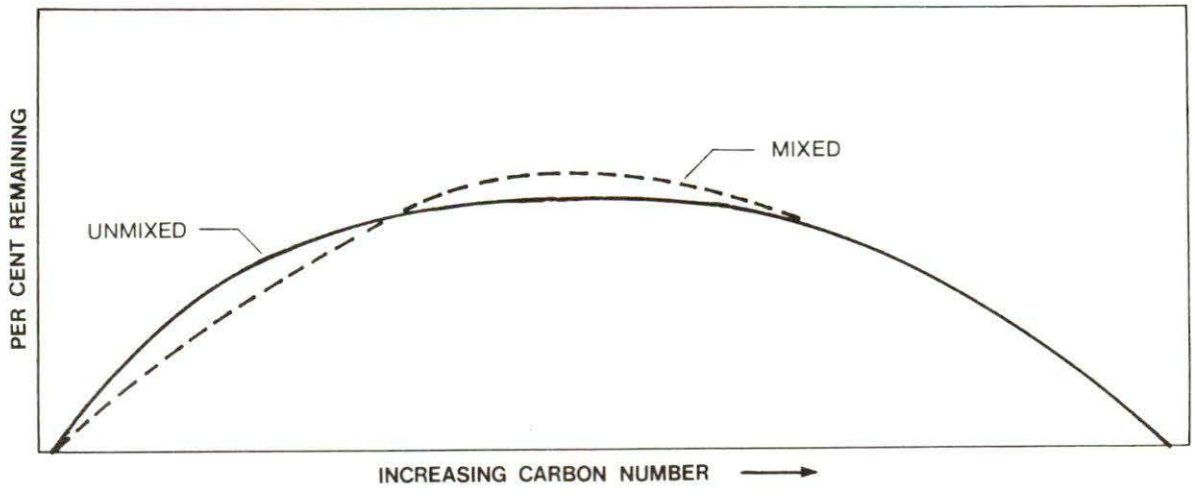

To allow for these considerations greater emphasis was placed on values for percent evaporated derived from the mid range carbon number groups that appeared consistent with each other and the aging history of the sample. The derived percent evaporated and changes in the physical properties for all samples are shown in Tables B1 to B4. Typical evaporation rates for oil samples in ice and on the surface are presented in Tables 8-1 and 8-2.

TABLE 8-1

OIL EVAPORATION IN ICE

NW2	OCT 23	NOV 15	DEC 10	JAN 21	FEB 21	MAY 9	MAY 10
Percent Evaporated	2%	3%	5%	2%	2%	5%	37% *
SH 1	DEC 7	DEC 10	DEC 30	JAN 22	FEB 18	MAY 13	JUN 3
Percent Evaporated	0%	0.5%	1%	1%	1%	1.5%	18%

* Surface sample

TABLE 8-2

OIL EVAPORATION ON SURFACE

NWC	DEC 24	JAN 11	JAN 20	JAN 24	FEB 6
Percent Evaporated	7%	20%	25%	24%	28%
SHC	DEC 24	JAN 4	JAN 20	FEB 26	
Percent Evaporated	1.5%	9%	7%	19%	

While the oil was incorporated in the ice very little evaporation occurred. This is reasonable, when it is considered that the ice is relatively solid during the depth of winter, and serves as an effective barrier to weathering. However, surface evaporation was pronounced even at sub-freezing temperatures. Within 24 hours of being exposed, the oil samples shown in Table 8-2 were covered by a layer of snow 1 to 2 cm thick. Some of the oil was absorbed by the snow. The snow remained in place for the duration of the tests. In spite of this, evaporation rates as high as 25 percent were recorded within one month. Considerably higher rates would likely occur if the oil were exposed to the atmosphere.

A comparison between derived oil properties and those measured in the

field is presented in Table B5. In general, there is close agreement. The field viscosity readings are suspect, in that the oil was thought to contain traces of ice crystals. This was indicated by the non-Newtonian behavior of the oil, and the difficulties in obtaining consistent values for the same sample. Water in oil analyses conducted at the site indicated only trace quantities of water. However, tests were not done on all samples, due to the limited sample size. A Fann type viscometer, which measures viscosities at a constant shear rate, was used in the laboratory tests, and as a rule should produce more accurate values than the Ostwald viscometer used in the field.

A number of the early gas chromatograms were examined to determine if there was significant dissolution of the oil, while in contact with the water. Three peaks, benzene, methylcyclopentane (MCP) and n-heptane were considered. The solubility of these compounds decreases from benzene to MCP to n-heptane, while the vapour pressure decreases from MCP to benzene to n-Heptane (Table 8-3). If the weathering of a crude oil were due solely to evaporation, then the relative ratios of these components in the oil would change in accordance with their vapour pressures. If for example, the peak area of these compounds from the GC, were originally 10:10:10, for MCP, benzene and n-heptane, a weathered ratio might appear as 8:9:10, indicating that relatively more MCP had evaporated than the less volatile benzene. The ratio also shows that the benzene has evaporated more than the n-heptane. Similarly, due to the difference in solubilities, the same ratio of 10:10:10 may be expected to change to 9:7:10 if there were significant dissolution occurring.

TABLE 8-3

SOLUBILITY AND VAPOUR PRESSURE OF CONTROL COMPOUNDS

COMPOUND	VAPOUR PRESSURE (Atm) at 25°C	SOLUBILITY mg. l^{-1}
Benzene C_6H_6	0.125	1780
Methlcyclopentane C_6H_{12}	0.181	42
n-Heptane C_7H_{16}	0.060	2.9

A simple method of discriminating evaporation from dissolution is thus to compare the three peak areas before and after exposure to environmental conditions, and look for evidence of evaporation or dissolution. If the peak areas of the original oil are MCP_0, B_0, and nH_0, and after weathering are MCP_1, B_1, and nH_1 for MCP, benzene and n-heptane, then if there is only evaporation, the benzene value will tend to remain roughly proportional to the mean of the other two. Expressed in symbols:

$$\frac{MCP_1 + nH_1}{B_1} = \frac{MCP_0 + nH_0}{B_0}$$

If dissolution takes place (alone or in addition to evaporation) this ratio should rise. If half the benzene dissolves, the ratio should double. Table 8-4 gives values for this ratio for some early samples. To establish a basis for comparison, ratios from samples that were not exposed to water were used to compare with later samples. The unweathered samples ranged from 4.38 to 5.41 with an average of 4.98. A ratio of 6 or higher might be expected to indicate some dissolution. The ratios of samples that had been in contact with the water did not go above 5.68. A "t" test for the null hypothesis using the unweathered samples as one group, and the other samples as the second group, gives "t" as 0.7, when the degrees of freedom equals nine. The level of significance at the 10% probability is 1.83, indicating that the null hypothesis cannot be disproven, or that the extent of dissolution is below the level of detectability in terms of oil composition.

Metal analysis performed on samples of unweathered Norman Wells and Swan Hills crudes are presented in Table B-6. Because the sulphur content of both crudes was significant, 1.76 and 2.90 percent respectively, it was decided to analyze both weathered and burned samples, to determine if the sulphur was being concentrated in the oil, or being released to the environment. The evaporated sample of Norman Wells crude had a sulphur content of 1.9 percent, while the burned sample had a sulphur content of 2.1 percent. These results indicate that the sulphur content of the oil remains relatively constant. Assuming that approximately 95 percent of the oil either evaporated or burned, then about 2000 kg of sulphur was released into the atmosphere.

8.2 Hydrocarbon Content of Water Samples

The non-biological water sampling concentrated on measuring temperature and salinity profiles and dissolved hydrocarbon content in the water column.

The hydrocarbon content was measured using pentane extraction and gas chromatography analysis. Some problems were encountered in early samples as a result of loss of pentane by evaporation during shipping. However, this was remedied by improved bottling techniques with subsequent samples.

The total amount of hydrocarbon in the pentane sample was estimated using gas chromatography, and the aqueous concentration calculated from this number. Later samples were analyzed using helium vapour phase extraction, a more sensitive and accurate technique which also enabled the identification of individual compounds. For example, if 5 ml of pentane were used to extract the hydrocarbons present in one litre of water, and a GC injection of 10 microlitres (µl) of the pentane gave a peak area corresponding to 1 microgram (µg), then by proportion, the amount of hydrocarbon in the pentane sample is 500 µg or 0.5 mg. The aqueous concentration is then calculated to be 0.50 µg l^{-1}.

An upper limit exists as to the concentration in water of a particular dissolved hydrocarbon. This limit is the saturation concentration and, for practical purposes, cannot be exceeded. In theory, this means that only so much of a particular hydrocarbon can be dissolved in a particular

TABLE 8-4

OIL SAMPLE DISSOLUTION RATIOS

SAMPLE NUMBER	SAMPLE AND DATE	PEAK AREAS BENZENE	MCP	n-HEPTANE	RATIO MCP + n-HEPTANE / BENZENE	
14	NWC Dec 8	2011	4010	4797	4.38	Original samples
17	NW2 Oct 23	1857	4410	5254	5.20	from barrels
24	NW3 Nov 14	1845	4238	5128	4.94	prior to
32	NW4 Dec 9	1691	4085	4067	5.41	discharge.
					4.98	Avg.
15	NW1 Dec 10	562	968	2217	5.67	
18	NW2 Nov 15	1860	3873	4558	4.53	
19	NW2 Dec 10	1512	3425	4328	5.13	
24	NW3 Dec 10	1304	2586	3571	4.70	
	Ice Core NW3 Dec 10					
	0 - 5cm	1481	3454	4964	5.68	
	5 - 10cm	1777	3754	5442	5.17	
	10 - 18cm	1698	3849	5258	5.36	

quantity of water, and beyond that level, that hydrocarbon will no longer dissolve. This limit of saturation value is quite small. The limit for one of the most soluble crude oil components, that of benzene, is 1,780 mg l^{-1} in distilled water, and 1,391 mg l^{-1} in sea water (Mackay, 1975). This is a very soluble component and other relatively soluble components such as toluene and xylene have solubilities of only 515 and 175 mg l^{-1} respectively. The majority of crude oil components have a solubility under 10 mg l^{-1} and can be ruled out so far as significant dissolution is concerned. A high solubility does not necessarily mean that a hydrocarbon will dissolve to the solubility limits. The rate of formation of dissolved hydrocarbons is dominated by vertical eddy diffusivity drift and it appears that in these tests the eddy diffusivity was low enough to result in dissolved concentrations about a factor of 100 below the saturation concentration.

Results of the water sampling program are shown in Table 8-5. Although the samples were recovered close to exposed oil lenses, the oil concentrations were very low. At these concentrations, even a slight contamination of the sampling apparatus could have a significant effect on the results. As well, small oil droplets were detected in the water column a number of days after a discharge. One of these droplets in a litre of water, would substantially alter the apparent hydrocarbon content. Initially, it was thought that contamination by undissolved hydrocarbon might be detected by close examination of the GC's, since undissolved crude oil retains a similar composition to the original oil, while dissolved oil reflects the solubility of the various components. This was not possible, due to the very low concentrations. However, as a result of the various sources of contamination, the measured hydrocarbon content, was likely higher than the average for the water column.

TABLE 8-5

WATER SAMPLES

SAMPLE	DATE	DISSOLVED HYDROCARBON CONCENTRATION (mg. l^{-1})
NW2, S. Corner	Dec 23	0.5
NW2, E. Corner	Jan 20	Not detectable
NW3, test + 20hr	Nov 15	1.3
NW3, NW edge	Jan 21	Not detectable
NW4, test + 10hr	Dec 9	4.6
NW4, S. Corner	Dec 23	0.2
NW4, E. Side	Jan 21	0.2
NW6	Feb 15	.006
NW7	Apr 15	.0107
SH1, pre spill	Dec 7	4.4
SH1, test + 3 days	Dec 10	Not detectable
SH1, S. Corner	Dec 23	1.3
SH1, E. Side	Jan 21	0.32
SH1		0.054
SH1	Feb 23	4.38
Surface water at tidal crack	Jun 4	0.119
Outside SH2	Jun 6	0.110
Control from Bay 200m from site	Jun 11	0.038
2m below ice in centre of test area	Jun 16	0.14

9.0 OFFSHORE INVESTIGATION

9.1 Site Survey and Selection

The principal objectives of the offshore studies were to investigate the spreading of crude oil under sea ice in the presence of a current, and the interaction of oil with a pressure ridge keel. Initially, a series of tests using up to 1000 gallons of oil had been planned, but in response to concerns expressed by local residents, only two discharges were conducted.

On the basis of work undertaken by the Frozen Sea Research Group, a current in the order of 12 to 15 cm s^{-1} had been specified. On March 27, a series of current measurements were made in the Cape Parry area to establish the best location for the tests. Currents were examined along lines running both east and west from the Cape to a distance of about 30 miles (Figure 2-2). The currents were relatively stable, and ranged from a low of 2.4 cm s^{-1} to a high of 5.0 cm s^{-1}. In an attempt to locate higher velocities, a line was then examined north of the Cape. A current of about 10 cm s^{-1}, flowing to the northwest, was found 28 km north of the Cape. Readings taken on several occasions over a 10 day period to confirm the current's stability in both magnitude and direction gave an average reading of 9.75 cm s^{-1} ± 3%.

To minimize the possibility of the tests having an impact on waterfowl, which might subsequently nest at Cape Parry, a site was finally selected at 33 km on a bearing 018 degrees true from the PIN MAIN radar. Here the ice sheet was stable, and neither open water nor recently refrozen leads could be located between the site and the Cape or along the probable route of the oil. The smooth sheet selected was approximately four miles long in the east-west direction by one mile wide, and was bounded by small pressure ridges. The ice had an average thickness of 1.1 m. The water depth was in excess of 100 m, and the salinity constant at 31°/$_{oo}$ to a depth of 12 m. Due to the configuration of the pressure ridges it was possible to conduct both tests from a single dive hole, simply by moving the position of the discharge. Figure 9-1 shows the general layout of the test area.

9.2 Oil Discharges

Both discharges were conducted by hand pumping the oil at ambient air temperature (-16°C) into a 10 cm diameter aluminum sleeve, which extended approximately 5 cm below the ice sheet. The discharge rate was about 0.016 m^3 min^{-1} (3.5 gal min^{-1}). The entire operation was monitored on the surface by means of an underwater video system, and a diver with a closed circuit breathing system was employed for still photography.

Prior to the first discharge, the diver examined the underside of the ice and reported it to be perfectly flat. Several attempts were made to assess roughness, but the variations were less than 2 to 3 mm. Discharge No. 1, which consisted of 180 gallons of Norman Wells crude took place between 1410 and 1453 hours on April 8. Although some oil initially spread several metres upstream of the sleeve, most of the spill moved

Figure 9 - 1 OFFSHORE TEST SITE - GENERAL LAYOUT

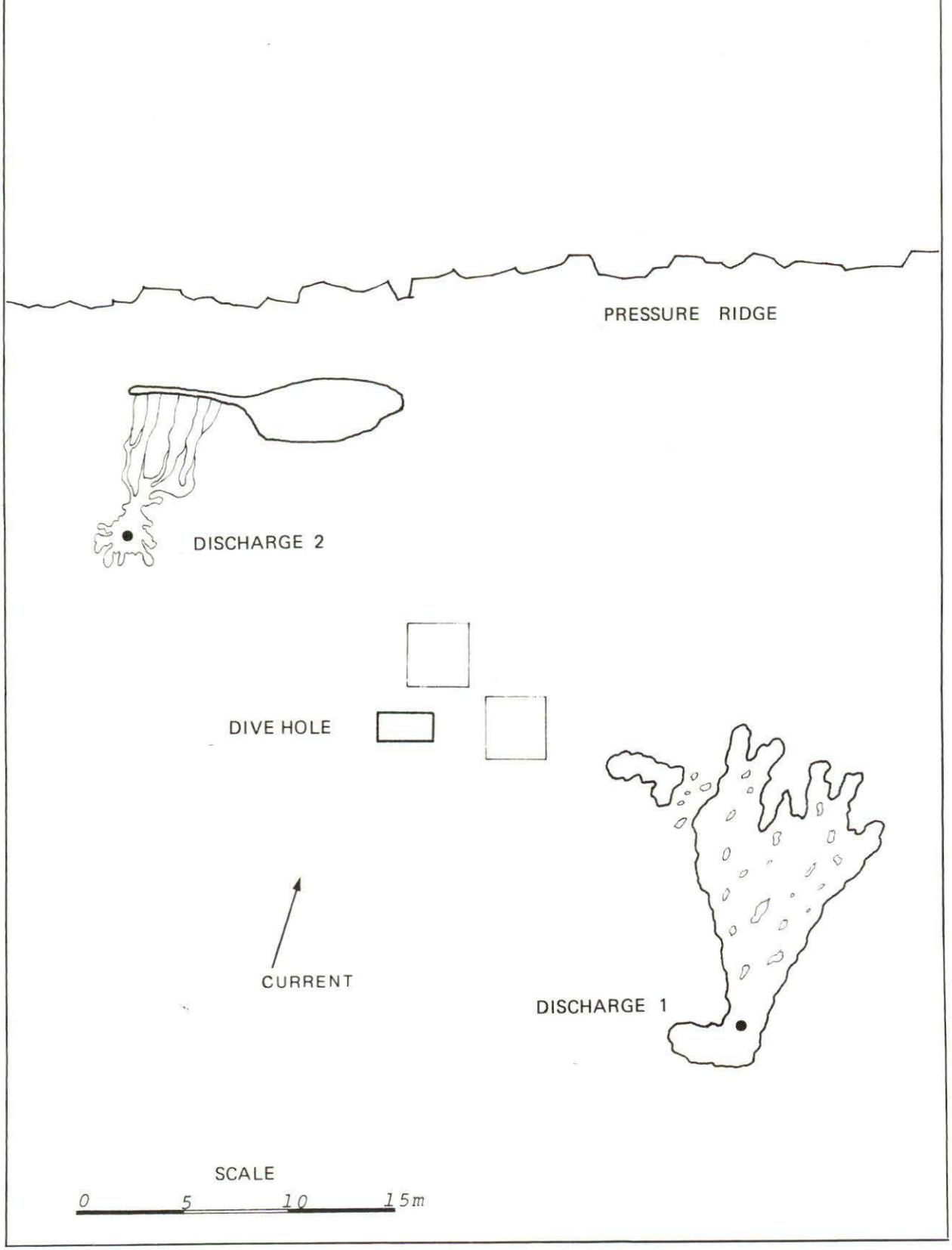

Figure 9 - 2 PLAN - OFFSHORE DISCHARGE 1

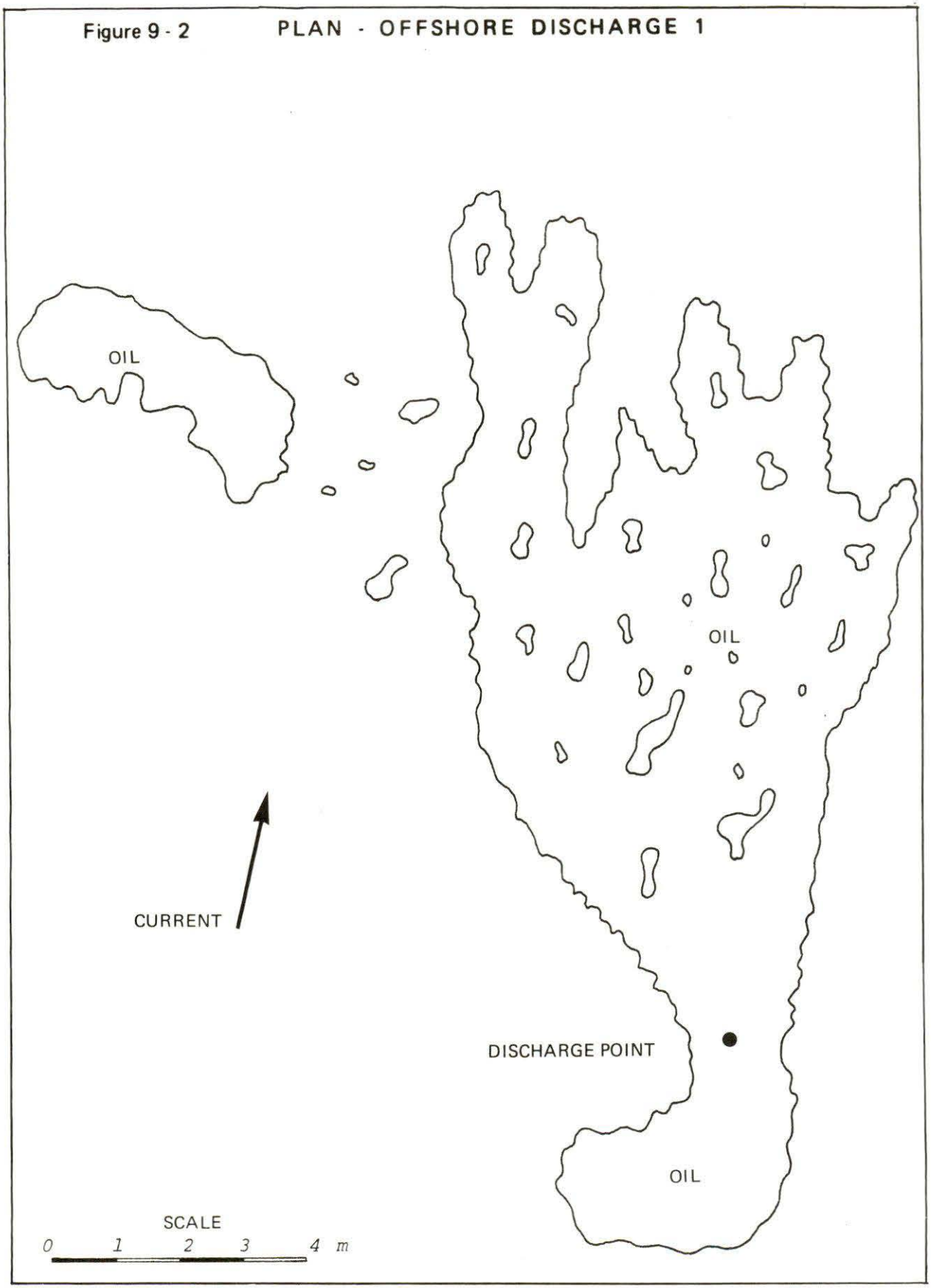

in the general direction of the current. The oil did not flow as large sessile drops, but rather as an assortment of complex shapes, ranging from patches several square metres in area to drops less than one cm across. Movement was primarily in the form of advancement of the leading edge of the main pool of oil, and closely resembled the static tests conducted in Balaena Bay. A number of fingers would extend from the pool, finally join, then grow in width to cover the encompassed patch of ice (Plate 9-1). What appeared to be slush balls were generated in the irregularities along the edge of the pool, and particularly in the voids cut off by fingers. These transparent balls ranged from 10 to 30 cm across and contained small droplets of oil. It is only possible to hypothesize as to the cause of these balls, but it is likely due in part to the cold relative temperature of the oil, and friction along the skeletal layer. A similar, but not identical phenomenon has been observed in Balaena Bay, where the oil is heated close to the ambient water temperature.

On completion of the pumping, spreading appeared to stop, although the diver felt he could detect a slight creep along the edges. The oil assumed an irregular, finger-like shape, measuring about 14 m long in the direction of the current and 7 m wide (Plate 9-1). Clear patches of ice, up to 0.5 m long and oriented in the direction of the current, were scattered through the lens. Several large patches of oil had separated from the main pool. The path taken by the oil was marked by small beads of oil along the ice. For a distance of about 7 m around the main lens, small droplets of oil could be detected on the ice. Well after completion of pumping, very small droplets, less than 0.1 cm in diameter, were suspended in the water column. The average thickness of the lens was 0.60 ± 0.10 cm.

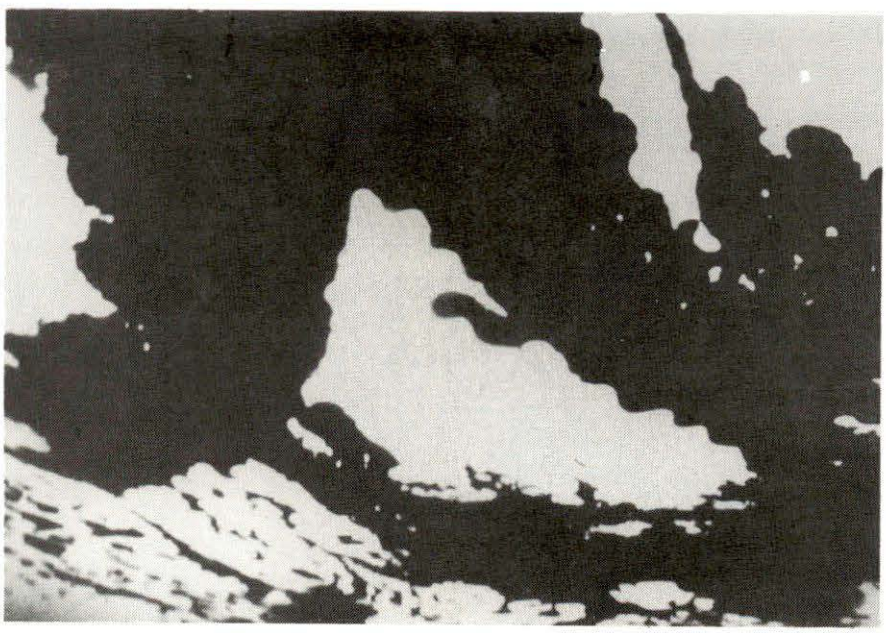

Plate 9 - 1 Typical pattern of oil discharge No. 1 after completion of pumping — April 8, 1975

The second discharge was conducted approximately 10 m up current from a small first year pressure ridge. The ridge was quite irregular, and had a keel depth of no more than one to two metres. Unlike the first discharge, the surrounding ice sheet was rough. A series of depressions or 'troughs', up to 0.5 m deep and 8 m wide, were detected running parallel to the pressure ridge. The troughs were roughly 5 m from the ridge, and may have been a direct result of the flow pattern under the keel. This roughness influenced both the movement and final disposition of the oil.

As the oil was released, it flowed in the direction of the current and towards the pressure ridge (Figure 9-3). Within several metres of the discharge point, flow became unstable and long fingers or 'rivulets' broke from the main body of oil (Plate 6-2). The rivulets, which resembled elongated sessile drops, were about 2 to 5 cm in width, and varied in length. The velocity of the rivulets was between 5 and 7 cm s^{-1}, or about one-half that of the current. Although flow in the rivulets appeared to be unstable, they tended to continuously follow the same course, suggesting that minor depressions in the ice sheet were influencing both the direction of flow and stability. Ice crystals which had been broken from the skeletal layer, were observed floating near the rivulets, which might indicate that the oil was cutting a path, but the diver could not detect any variation. Small flecks and streaks remained after passage of the oil, but in general the ice was clean.

Upon reaching the trough, the oil flowed parallel to the pressure ridge, and gathered in a pool (Plate 9-2). After completion of pumping the pool measured about 6 m by 3 m and the maximum depth of oil was 10 cm. Once the oil reached the pool, it stabilized, and did not appear to be affected by the current. The edges of the pool had the characteristic sessile drop shape, and slowly creeped outward as the pool filled. A maximum oil depth of 11.4 cm was measured at the west end of the collector arm, which extended from the pool (Figure 9-3). As the rivulets approached the arm there was a definite increase in velocity. Since the oil in both the pool and the arm did not appear to be influenced by the current, the change in velocity was likely due to gravitational forces. Unlike drops coalescing, the rivulets immediately entered the main body of oil without hesitation (Plate 9-3). There was a progressive decrease in the size of the rivulets between the discharge point and the arm.

9.3 Subsequent Site Inspections

On May 8, the site was overflown and no trace of oil could be detected. On May 28, a patch of oiled snow, measuring approximately 8 m by 5 m, was clearly visible from the air near discharge No. 1. Oil was located under the snow, above the pool from the second discharge. Three cores were taken from the first discharge and two from the second. The cores very closely resembled those from the spring discharges in Balaena Bay. The ice had grown to a depth approximately 12 cm below the lens, thereby incorporating the oil in the ice. One core recovered just beyond the main pool from discharge No. 1 contained droplets similar to those observed during the test. There were no apparent variations resulting from the current.

During an inspection on May 30, three cores were taken across the second discharge area. One core hole penetrated an oil lens 10 cm thick. Subsequent analysis indicated an oil concentration in the ice above the lens of 3.3%. The decreasing lens thickness progressing back toward the ridge delineated the trough observed by the divers, and confirmed their estimates of lens thickness at the time of discharge. This also confirmed the fact that no substantial change in lens thickness occurred between the day of discharge and the formation of new ice below the oil.

On June 8, at 0200, a burn was conducted at the offshore site. Essentially, all the oil appeared to have surfaced at that time, and the site condition before and after burning followed descriptions of the Balaena Bay test site. This was the last observation of the offshore site. The ice in that area broke up and moved away in late June.

9.4 Conclusions

The offshore study was hampered to some extent by the relatively small quantity of oil finally permitted, and the reduction in tests. It is impossible, with the limited data, to draw any firm conclusions as to the influence of current. The oil performed in a similar fashion during static tests in Balaena Bay. For example, rivulets were generated when the oil was released beneath a dome in the ice, while a pool was created if the release was below a depression. However, there were some notable differences offshore:

1. With both discharges, the direction of fingers tended to be oriented in the direction of the current. The direction was random with static tests. As well, the fingers were far more elongated.

2. In both cases, the mass of oil moved down current from the discharge point. The probability that the first discharge hit on the up-current side of a depression, and the second discharge on the down-current side of a dome is remote.

3. Although there were gravitational forces present in the second offshore discharge, current did appear to have a definite influence on the movement of the oil at the offshore site. In static tests at Balaena Bay, even with an exit velocity 20 times greater, and with the oil striking a well defined dome on the undersurface, rivulet velocity was much less than that observed offshore in the presence of a current.

4. The tests provided some indication of the importance of surface roughness and under-ice topography. The numerous clear patches in discharge No. 1, are indicative of small irregularities on the ice (Plate 9-1). Since the average oil thickness was about 1.75 cm, and the maximum stable thickness was about 0.8 cm, the clear areas had to be a minimum of about 1.0 cm thicker than the surrounding ice. This roughness would have a considerable influence on the boundary condition for both the oil and the current. The large area coverage of the oil would suggest that

the sheet was relatively smooth. It is more difficult to interpret the behavior of the oil and the current for the second discharge. The fact that the trough existed gives some indication of the influence of the pressure ridge keel on current flow. However, the oil stabilized once it reached the main pool, suggesting that gravitational forces were dominant.

5. The pressure ridge keel, although small, presented a minimum barrier of about 75 cm over the entire length examined. Even in the presence of a considerably higher current, the trough and keel combined would hold back an enormous volume of oil.

6. Once encapsulated in the ice, the oil performed in an identical fashion to that observed on static tests with much larger volumes. Other work indicated that this process of being included in the ice sheet with a fresh interface below the oil took less than one week.

10.0 CLEAN-UP

The initial terms of reference specified that in situ burning was to be the prime recovery technique. However, in January 1975, the decision was made to extend the tests as long as possible, which necessitated a re-evaluation of the clean-up procedures. To obtain the desired level of recovery with in situ burning, it was considered essential that the clean-up be completed prior to break-up of the ice sheet. The longer the test period was extended, the greater the chance of the sheet failing. Consequently, provision was made for an open water clean-up. Although in situ burning ultimately proved successful, most of mechanical techniques were tested, in anticipation of their possible use.

10.1 Mechanical Equipment

Following is a summary of the containment and recovery equipment which was stockpiled at the site, the proposed application, and the features or limitations as determined from the test program.

a) Oil Boom:

Three hundred and fifty feet of 40 inch inshore-offshore oil boom was available to close off the mouth of the large bay (Figure 4-2). The boom would have been installed had oil been detected outside the test cove. Two hundred feet of 18 inch inshore boom was available for herding slicks. At no time was there sufficient water in the melt pools to permit the use of this boom. By late June the boom could have been installed in several of the larger melt holes, but by this time virtually all the oil had been recovered.

b) Skimmers:

With several minor exceptions, there was insufficient water or oil in the melt pools to utilize skimmers properly. The skimmers could have been used in melt holes, had there been a requirement. However, this would have been a very time consuming and costly procedure, due to the large number of isolated holes, and the problems associated with handling and separating the oil.

c) Pumps:

A light weight, electric, centrifugal pump with a modified intake was tested over a three month period. It proved effective in skimming oil lenses over approximately 5 cm. An oil in water emulsion was produced with thin films. The emulsions tended to be unstable, and normally broke down in a matter of minutes. At subfreezing temperatures, ice build-up in the lines was a problem. With some relatively minor modifications this could be resolved. A two inch diameter centrifugal pump was routinely used to transfer both pure and recovered oil. At -40°C, it was possible to pump Swan Hills crude, which has a pour point of -4°C.

d) Sorbents:

Vegetable fibre, synthetic hydrocarbon polyner and plastic filament

sorbents in a variety of standard forms were tested. In all cases, they fell far short of the stated performance. In general, the products did not have sufficient strength to permit normal handling, once oiled. Delamination was a major problem, particularly with the vegetable fibre sorbent. Even using a special wringer, which could be adjusted to each manufacturers specifications, it was impossible to get more than two or three applications out of the sheet or roll material. The rolls had to be cut into short lengths simply to draw them across the water to the wringer. Due to the difficulties in handling, it was not cost effective to wring the material. Limited use was made of the vegetable fibre and polymer sorbents in the pillow and boom form. The plastic filament was totally ineffective with either of the crude oils. In general, sorbents would appear to have very limited application in large spills, with the possible exception of "polishing".

e) Beehive Burner:

A conical shaped, light weight concrete, floating burner was supplied by Gulf Oil Canada Limited. The design was similar to a unit developed for burning sumps. Due to the limited depth of water in the melt pools, it was impossible to properly test the device. However, it is doubtful if it would have a general application in large spills, since its maximum rate of consumption is about 10 gallons per hour.

Arrangements had been made to obtain a broad range of open water clean-up equipment from the Delta Environmental Protection Unit, if required. As well, various methods for on site incineration were investigated in detail. Although technically feasible, the transport of the large compressors presented special problems. In general, open water clean-up techniques would have had very limited impact even in the relatively sheltered environment in Balaena Bay. Moreover, the cost of the clean-up would have been substantially higher.

10.2 In Situ Burning

On June 5, several melt holes broke through the ice in critical locations. The total area of oiled melt pools decreased from 45 percent to less than 30 percent of the area of the test site. Much of the oil was being swept down through the holes by the tidal flush, and being reincorporated in the ice. Consequently, the decision was made to conduct the first burn June 7.

The condition of the site immediately prior to the burn is shown in Plate 10-1. A detailed mapping was prepared from aerial photographs (Figure 6-12). Thirty-one percent of the surface was covered by oiled melt pools and 16 percent by oiled snow. The film thickness in the individual pool was measured. Approximately 22 m^3 (4800 gallons) of oil was available for burning. This represented 41 percent of the total oil discharged, and about 50 percent of the oil remaining, when evaporative losses were taken into account. The maximum film thickness observed was 15 cm.

Most of the major pools were interconnected. The black 'Fabrene' in the

retaining skirts had enhanced local melting, and the oil tended to spread around the edges. In several locations, the oil and tidal flush had cut trenches over 30 cm deep between pools. The uncontaminated snow was very wet, and effectively contained the oil. With the exception of one small crack, which extended to the north-west, all the oil was contained within the snow berm (Figure 6-12). In the preceding two weeks, several small gaps had developed in the berm, which were quickly repaired. In general, the snow berm was a very effective barrier.

Although several small burning tests had been conducted, there was some concern that the removal of light ends by evaporation would limit the effectiveness of burning. Consequently, six drums of gasoline were poured into the larger melt pools. This ultimately proved unnecessary. Even by mid July, the oil could be ignited simply by pouring a small quantity of gasoline or naptha on several squares of paper towel. On thin films, a piece of sorbent made a better burning platform.

At the time of burn on June 7, the winds were blowing at about 5 mph from the east. A deep pool in the centre of the NW4 skirt was ignited first. The flames rapidly spread to the NW3 and NW7 test areas. Within a matter of minutes, the flames were reaching over 15 m into the air. The thick black plume rose 500 m before spreading below a cloud layer (Plate 10-2). Secondary fires were started in the SH2, NW6 and SH1 test areas. Within 20 minutes about 80 percent of the site was in flames. After about 30 minutes the fires tended to die down. When reignited, they would only support combustion for several minutes. Fed by natural drainage from other areas, pools in the NW4 and NW7 test areas continued to burn for over 12 hours. Approximately 20 m^3 (4400 gallons) of oil was removed, for an effectiveness of about 90 percent.

The heat produced by the first burn was sufficiently intense to cause oil entrained in the surrounding snow to flow into the burning pools. Some of the pools were slightly enlarged, although the burn did not melt as much snow as was expected. In most areas, the snow remained between 30 and 40 cm higher than the level of the pools. The snow dyke remained intact. A distinct cracking sound could be heard during the burn, suggesting the water was boiling, and possibly the oil was atomizing. Substantial combustion was occurring well above the pools. The melt pools which initially had very thick films were surprisingly clean, with only a thin film of oil and residue on the downwind sides (Plate 10-3). Globes and small pools of residue, varying in consistency from a grease to a heavy tar were deposited on the surrounding snow (Plate 10-4). Solid films, similar to a thick polyethylene sheet were located in several pools. They had sufficient strength that they could be lifted off the water by one corner. The burn was not as complete in the small isolated pools, which had thin films. The remaining oil was quite heavy but still fluid, and of an average thickness of about 0.5 cm. A number of samples of residues, of various consistencies were analyzed (Tables B3 and B4). In all cases the specific gravity was less than one.

No evidence of fallout could be located within several miles of the site. This was primarily due to the atmospheric conditions at the time. In mid April, a test burn was conducted with 0.2 m^3 of oil. The wind was

Plate 10 - 1 Aerial view of test site and camp on June 7 prior to the first burning operation.

Plate 10 - 2 Smoke plume from the burn on June 7 rising to a cloud base at 500m.

Plate 10 - 3 Oil residue on ice and snow following the first burning operation on June 7.

Plate 10 - 4 Example of tarry residue remaining in isolated patches, June 7.

blowing at between 25 and 35 mph, and the plume spread out along the ice. The snow was noticeably discoloured. Within one week all the snow had melted as a result of the dusting.

Oil continued to flow from the brine channels and surrounding snow. A well defined drainage pattern naturally developed, and most of the oil gathered in pools in the NW4 and NW7 test areas. A second burn was conducted on June 8. Although almost equally violent, it was of much shorter duration. No more than 4 m^3 (900 gallons) of oil was removed. It was impossible to ignite some of the smaller pools.

A third burn was undertaken on June 13. By this time the flow of oil from the brine channels had slowed considerably. Approximately 5 m^3 (1100 gallons) of oil was available for burning, of which no more than 50 percent was removed. The flame did not spread, and it was necessary to ignite each pool. Most of the water had drained from the ice, and the residue was deposited on the sides and bottoms of the melt pools (Plates 10-5 and 10-6). The residue tended to be very viscous and would not readily support combustion.

On June 16, it was estimated that between 2 and 6 m^3 of oil and residue remained on the ice. The flow of oil from the ice had almost completely stopped, as the melt had reached the initial level of the lenses in most areas. A number of small burns were conducted on June 17. The remaining clean-up effort was devoted to the manual removal of residue with shovels and sorbents.

Typical surface conditions are shown in Plate 10-7. The tarry residue was hosed, scraped and shovelled into oil drums or pits cut into the ice, where it was burned with gasoline. Sorbents were used to herd small pieces of floating residue to the sides of pools, and to recover very thin films and sheens. The operation was extremely labour intensive. A two man crew could recover only one 45 gallon drum (0.2 m^3) of residue in a ten hour day. By June 25, the large number of open areas and thin spots made working on the ice very hazardous. By June 27, all the accessible residue had been removed, and activities on the ice were terminated.

The entire test area was free of ice by June 30. The tidal crack was very pronounced, but the sheet was essentially intact. The average ice thickness was between 20 and 30 cm. Very little oil was evident on the water. On July 7, the ice was broken by a 15 to 20 mph wind from the west, and driven on shore close to the camp. Most of the ice grounded, and loose residue was swept up on the beach. As the ice rotted in the shallow water, the remaining oil and residue were swept on shore.

Although the contamination was concentrated in a small inlet just to the south of the camp, traces of oil could be detected along 900 m of shoreline (Figure 11-1). The residue tended to form in tarry clumps or balls on the beach (Plate 10-9). The clumps, which varied in size from about 2 to 15 cm, were sufficiently firm that they could be picked up with a shovel. Approximately 0.6 m^3 (130 gallons) of residue was recovered in this manner. Upon completion of the clean-up, the only evidence of oil

Plate 10 - 5 Patch of oiled snow following the third burn on June 13/75.

Plate 10 - 6 General view of surface conditions following the third burn. Note the dried melt pools.

Plate 10 - 7 Ice surface conditions on June 20, about halfway through manual residue clean-up operations.

Plate 10 - 8 Close up of beach showing patches of heavily weathered residue before clean-up.

Plate 10 - 9 View from the time lapse camera position showing the test area as open water on July 7. Low hills in background are on the South shore of Baleana Bay 0·5 KM away.

Plate 10-10 Visual appearance of test cove and beach on August 26, 1975.

was a thin film on the shingles in the tidal zone. This was estimated to represent no more than about 1.0 m^3 or 1.8 percent of the total oil discharged. When inspected on August 28, 1975, there was very little evidence of oil along the beach.

10.3 Effectiveness

In situ burning proved to be extremely effective with both Norman Wells and Swan Hills crudes. Oil exposed on the surface for up to six weeks could be ignited as long as the film thickness was over approximately 0.5 cm. All but the heavily burned residues could be ignited with the addition of fresh oil, from the ice. In an attempt to determine the natural drainage patterns, the snow cover was not altered. However, a number of strategically placed trenches would have substantially reduced the area of surface contamination. The efficiency of burns would have been higher, due to the thicker oil films and the residue would have been more concentrated.

A precise mass balance was impossible, due to the difficulties in accurately determining rates of evaporation for the weathered and burned components. The prevailing wind speed, temperature and pool size were applied to a correlation developed by Matsuga and MacKay (1975) to estimate the total evaporation to June 7. As well, wind set-up and edge effects made the accurate measurement of film thicknesses extremely difficult. In both cases the probable error was in the range of 10 to 20 percent.

Following is a summary of the dominant terms in the balance:

Evaporation to June 1	10 m^3
Burn No. 1, June 7	20 m^3
Burn No. 2, June 8	4 m^3
Burn No. 3, June 13	2 m^3
Burn No. 4, June 17	1 m^3
Residue removed from ice	5 m^3
Residue removed from shore	0.6 m^3
Oil on beach	1 m^3
TOTAL	43.6 m^3

A total of 54 m^3 (11,900 gallons) of oil was discharged, leaving 10.4 m^3 (2300 gallons) unaccounted for. Since all samples of residue had a specific gravity of less than one, and there was no evidence of sinking, it is doubtful if much oil was lost to the water. The apparent discrepancy likely resulted from the failure to include evaporation between June 7 and July 7, and the difficulties in accurately estimating weathering and film thicknesses. The fact that less than three percent of the oil reached the beach, and oil slicks were not detected in the bay, would indicate that the bulk of the oil either evaporated or was burned.

In conclusion, in situ burning was both effective and efficient. With ideal surface conditions and the proper timing over 80 percent of the oil could be burned with relatively little effort. However, the removal and disposal of the residue is very time consuming and labour intensive. It should be noted that the work was undertaken in a small sheltered cove, primarily because the sheet rotted in place. Under more typical offshore conditions, the sheet would have failed several weeks earlier, greatly reducing the effectiveness of the clean-up.

11.0 ENVIRONMENTAL IMPACT OF TESTS

A biological study of the test site was conducted over the period August 1974 to August 1975. Sampling and analytical procedures have been outlined in Section 5.4.4.

Detailed species lists, and analysis results are provided in Appendix 27E.

11.1 General Description of Test Cove

Most of the land surrounding the East arm of Balaena Bay, where the oil spill sites are located, is relatively low with rounded hills and occasional steep cliffs near the shores. The ground consists mainly of clastic till with frequent boulders scattered due to the movement of glaciers. The underlying rock is limestone.

The shoreline of the bay in the vicinity of the spill sites consists of shingle beaches (55%), steep, low cliffs (20%), and narrow strips of salt marshes (25%) at the bottom of secondary bays (Fig. 11-1). Rocks and shingles cover the immediate subtidal area down to 2 to 4m, except in the smaller bays where muddy bottoms predominate with only scattered shingle and boulders. At depths greater than 3 to 4m, the bottom becomes smooth and muddy with randomly distributed rocks. The tidal action in the bay is relatively small, and results in rapid currents only at the narrow mouth of the bay (Station 1, Inset 1, Fig. 11-1). Even greater currents occur in the narrow, very shallow passage connecting the head of the bay with a further inland extension (Station 4, Inset 1, Fig. 11-1). The measured differences between high and low tides in September 1974 and July 1975 ranged from 30 to 42cm. The East arm of Balaena Bay is relatively shallow; most of the depths soundings made were 6 to 8m, and the greatest depth obtained was only about 16m.

11.2 Biological Components of the Bay and Surrounding Terrestrial Environment

Although the opportunities to observe the birds and mammals in the Balaena Bay area were rather limited, a considerable number of species were recorded (Tables E1 and E2). Eider ducks, loons and sea gulls were particularly common among the sea birds, and ringed seals were frequently observed in the bay. The terrestrial plant species (Table E3) are those of a typical high tundra ecosystem with very few low-growing shrubs (Salix spp) and sparse plant cover. Lichens represent a high proportion of the total plant community.

Salt marshes, although not very extensive in depth, constitute a significant portion (approx. 25%) of the shoreline in the vicinity of the oil spill area. The vertical zonation and species composition of the salt marsh regions studied are presented in Figure E-1. The dominant plant species was the grass *Puccinellia phryganodes*. A surprising find was the moss *Bryum marrattii* which exhibited a very definite zonation in the salt marsh where it was covered by seawater during most normal high tides. Only one moss species, *Bryum nitidulum*, has previously been observed at

Figure 11 - 1 **BIOLOGICAL SAMPLING SITES - BALAENA BAY**

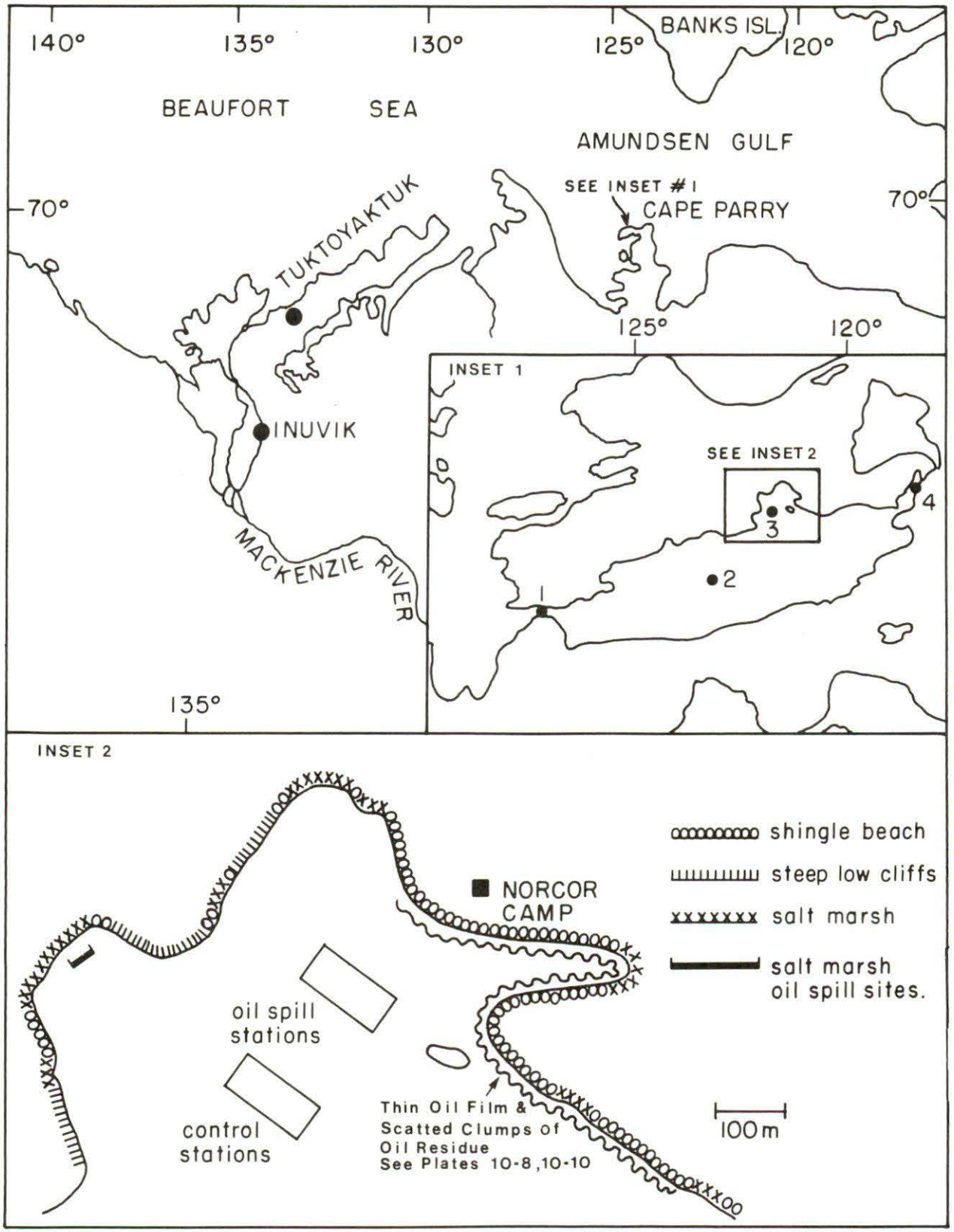

this level in a salt marsh (Walton, 1922). Since colonies of nitrogen-fixing blue-green algae were abundant along the seaward edges of the salt marshes at Balaena Bay, these communities probably play an important role in introducing reduced nitrogen into the general ecosystem.

Most of the shore in the vicinity of the oil spill sites consists of shingle beaches, and to a lesser extent of low limestone cliffs. Partly because of the crumbly consistency of the rocky shores, and the ice-scouring activities in this region, practically no macro-algae were found growing on this substratum. However, numerous rapidly growing microalgae and fiamentous brown and green seaweeds were found on shingles extending from high tide to about the 2m depth (Table E4). The maritime lichen *Caloplacca elegans*, and the black marine lichen *Verrucaria maura* were found in the splash zone. The only large seaweeds found along the shingle shores were algae torn loose from the sublittoral zone by wave action (mainly *Fucus distichus* and *Chaetomorpha* spp. with associated pennate diatoms). *Fucus distichus* was the dominant seaweed below the ice-scouring zone, and the macro-algae in this area were generally covered with heavy layers of pennate diatoms, which due to their high growth capacity probably account for a considerable portion of the total primary productivity in the area. The relatively high light transparency (attenuation coefficient, k=0.16, corresponding to a depth of 29m [euphotic zone] for the 1% surface light level) would allow rapid net photosynthesis to take place by plants in the benthic environment, which seldom extended beyond a depth of 8m.

On the bottom of the narrow inlet of the bay (Station 1, Inset 1, Figure 11-1), where there are rapid tidal currents and abundant rocky substratum with almost no silt cover, large kelps, *Laminaria* spp., as well as dense beds of *Fucus*, were observed.

Lists of phytoplankton and zooplankton species are presented in Tables E5 and E6. The zooplankton species are typical for arctic surface waters as observed by Grainger (1965). The presence of low-salinity surface water due to melting of ice (Table E7) was probably the main reason for the presence of numerous brackish-water rotifers and euryhaline algae such as *Dinobryon* sp. and green flagellates (mainly *Pyramimonas* spp.) (Bursa, 1961 a,b, 1963). When Balaena Bay was first studied by us in August 1974, the surface temperature at the entrance of the bay (Station 1, Inset 1, Fig. 11-1, and Table E6) was +0.1°C and the phytoplankton appeared to be at its peak of development (5.2×10^5 cells per litre). The dominant phytoplankton species were the diatoms *Thalassiosira nordenskioldii* and *Nitzschia seriata*, and the chrysophyte *Dinobryon* sp. A large number of young stages of copepods and rotifers were abundant. The station near the oil spill site (Station 3, Inset 1, Fig. 11-1 and Table E6) surface temperature 5.5°C was found in a much more advanced stage of development of the typical single-peak phytoplankton production of arctic marine environments. The population was already reduced due to grazing, and many species appeared chlorotic presumably due to nutrient deficiencies. The zooplankton population was well developed, and consisted largely of adult copepods, advanced copepodite stages and rotifers.

Among benthic invertebrates in the spill area, polychaetes were most numerous, particularly *Pectinaria* spp. (Table E8). The bivalve *Mytilus edulis* was very abundant in the benthic environment below 3m where it was attached to *Fucus* or to rocks. The bivalves *Mya arenaria, Cyprina islandica* and a *Macoma* sp. were abundant in muddy and silty environments. Small invertebrates such as tartigrades, protozoans and nematodes were frequently observed in mud samples, or among algae covering rocks and shingles. No large invertebrates were observed in the upper 2m shingle zone, probably due to the abrasive action of waves and ice on this unstable substratum. Sea urchins (*Strongylocentrodes drobachiensis*) and large sea anemones (unidentified) were observed at high densities in the benthic environment immediately below the dense *Fucus* zone, and more scattered populations extended to greater depths.

Little information is available about fish populations in the bay. Only the four-horned sculpin *Myzocephalus quadriconris* was observed frequently by divers in the oil spill area. However, the frequent presence of ringed seals indicated the presence of significant numbers of fish in Balaena Bay.

11.3 Results from Quantitative Biological Studies in Control and Oil Spill Areas to Test Potential Damage of the Oil Spills to Marine Organisms

No significant differences were observed between the abundance of zooplankton (Table E9) or phytoplankton (Table E10) components from control and oil spill sites. Measurements of primary productivity at these locations also revealed no significant differences (Table E11), as was expected following the disappearance of the ice cover and removal of most of the weathered oil by burning. The primary productivity values, estimated to be about 1.5 g.°C m^{-2} day^{-1}, compare favourably with the maximum values of about 0.4 g.°C m^{-2} day^{-1} obtained by Welch and Kalff (1975) for Frobisher Bay, indicating that this is a relatively productive marine environment during at least part of the ice-free season.

Phytoplankton samples were taken from different water depths under control and oil sites on June 4, when the phytoplankton population was still quite low and consisted mainly of naked dinoflagellates, cryptomonads and pennate diatoms, showed significant reductions in cell numbers presumably due to the presence of crude oil (Table E12). Similar samplings made during the productive season in July, 1975 in open water showed no significant differences between oiled and control sites (Table E13) as was expected.

Although the weathered crude oil from the 1974-75 under-ice spills was quite effectively cleaned up by burning and other measures, certain portions of the nearby shore environment were unavoidably polluted to different extents for several weeks. Tests of photosynthetic capacities of salt marsh plants and algae from rocky and muddy shore areas were carried out in locations of different degrees of oil pollution as compared with control areas (Table E14). The degree of beach contamination present from July to August varied from scattered clumps of heavily weathered residue to a very thin film in the tidal zone, serving

to coat the shore area (Plates 10-8, 10-9). The clumps were all subsequently buried, and the thin film had completely disappeared by the last site visit made August 26, 1975 (Plate 11-1).

As expected in areas contaminated with heavy residues (less than 0.5% of the shoreline affected) photosynthetic capacity was reduced by almost 90%. Chlorophyll contents were much less affected. Some short term effects may be observed in rapid erosion of the limestone shingles and in the salt marsh areas. However, in view of the nature of plants colonizing the affected areas, (mainly annuals growing from spores), recovery will probably be quite rapid.

Controlled spills of 40 to 50 l with fresh and weathered Norman Wells crude oil were made on uncontaminated salt marsh areas as indicated in Fig. 11-1 (Inset 2). Percent cover of the major species in these sites are given in Table E2. Observations of the spill sites 6 weeks later show that the vegetation was extensively killed by both fresh and weathered crude oil, except for the crucifer *Cochlearia officinalis* (scurvey weed) which appears to be surprisingly resistant to the very high level of crude oil applied (20 litres m^{-2}). Only marsh plants above the water line at the time of oiling were affected by the spill.

Toxicity experiments with fresh and weathered crude oil (collected from the under-ice oil spills before removal of the oil by burning) were carried out with freshly collected phyto and zooplankton populations from Balaena Bay (Tables E16 and E17). For the experiments, glass cylinders were used to contain the plankton samples. The cylinders each contained 1.5 l of seawater with plankton. Total height of the water column was 25cm. Sufficient oil was added to the water surface to form a 2 cm thick layer, and the cylinders were closed tightly with rubber stoppers to prevent the escape of volatile components. The cylinders including controls were kept at ambient temperatures (1 to 8°C) in a tent at Balaena Bay.

Zooplankton populations were obtained by net tows, and the animals added to each cylinder as described in the heading for Table E16. The comb jelly *Pleurobrachia pileus* was extremely resistant to the presence of both fresh and weathered crude oil, while young stages of the jelly fish *Cyanea capillata* were quite sensitive. Copepods were not immediately affected, but with time stayed away from the water column near the oil surface, probably in response to the diffusion of toxic water soluble components into the water column. After 36 h, large numbers of copepods were killed, and the approximate 25% remaining live copepods stayed close to the bottom. In the control column, approximately 70% remained alive after 36 h, and most of the copepods were distributed throughout the water column.

After 36 h, the oil at the surface was removed completely, and the zooplankton removed from the seawater by straining through a No. 20 nylon net. Freshly collected zooplankton was then added to the seawater in the cylinders that had originally contained fresh, weathered or no crude oil. The seawater of both the crude and weathered crude oil cylinders was extremely toxic to the young jellyfish stages of *Cyanea*

capillata. They ceased to move within 30 seconds of being transferred to the filtered media, and the tentacles contracted after 2-3 minutes. The medusae stopped swimming after about 5 minutes, while the comb jellies appeared almost unaffected during the next 24 h. The amphipods also appeared nearly normal for this period of time in the weathered crude oil cylinders, but slowed down considerably in the fresh crude oil cylinder soon after the transfer, and were dead after about 24 h. The copepods stayed in the lower half of both the fresh crude and weathered crude cylinders, while a fairly even distribution throughout the water column was observed in the control cylinder. After 24 h of transfer of copepods to the oiled seawater columns, about 80% were dead in the fresh crude oil and 60% in the weathered crude oil cylinders. All of the live copepods in these cylinders were found in the bottom 5-10 cm at this time. It is obvious that toxic components from the original crude and weathered crude oils added to the surface had diffused into the seawater during the initial 36 h period of the experiment.

In the phytoplankton toxicity experiments, 1.5 litres of surface water containing Balaena Bay plankton in normal concentrations were used in the same experimental containers as for the zooplankton experiments. Twenty-four hours after adding the crude oil (2 cm layer) and weathered crude oil to the cylinders, the oil was removed and 50 ml samples taken from control, crude and weathered crude oil cylinders for photosynthesis experiments. The samples were suspended at 1 m depth in the bay for 6 h with $NaH^{14}CO_3$, and rates of photosynthesis determined in the same way as for primary productivity determinations. Table E17 shows an almost complete depression of photosynthesis by fresh crude oil, while weathered crude oil depressed photosynthesis by over 80%. Since no crude oil was present during the photosynthesis experiment, toxic water soluble components of crude and weathered crude oil which had penetrated into the water column during the preceding 24 h period must have been responsible for the inhibition of photosynthesis. It should be noted that this was an extreme case of toxic effects of the crude oil, since the water column was only 25 cm deep and there was no movement of water under the oil layer as would be the case in an open ocean system.

11.4 Results from Laboratory Oil Toxicity Experiments on Cold Water Phytoplankton

Two types of crude oil, Norman Wells and Atkinson Point, were used in these experiments. The growth of a phytoplankton culture obtained from Balaena Bay in mid December, 1974 (mainly pennate diatoms) was comparatively unaffected by 30% aqueous crude oil extracts of the two crude oils (Table E18). *Thalassiosira nordenskioldii*, an important component of the summer phytoplankton bloom in Balaena Bay (Table E6) was inhibited considerably by both crude oils at the 30% and 100% levels. On the whole, Norman Wells crude oil was more inhibitory to growth of the algae tested than Atkinson Point crude oil.

Rates of photosynthesis in short term experiments were relatively less affected, than growth rates by the presence of aqueous components of the two crude oils (Table E19). Inhibitions by 100% extracts of the two oils for the different species and cultures ranged from 19 to 91%, while the

30% levels caused a maximum inhibition of only 52%.

11.5 Conclusions

Balaena Bay is relatively rich in both plant and animal life, excepting the almost barren ice scoured zone along the upper 2 m of the benthic zone along the shores. Primary productivity rates during the summer plankton bloom are also quite high, and the relatively abundant sea birds and seals in this area reflect the productivity of the bay. The rocky shores are very unproductive due to the combination of ice scouring and the easily eroded limestone rocks and cliffs. The relatively small salt marshes found in this area form an exception being densely covered with higher plants and algae, including nitrogen-fixing blue greens. The terrestrial flora is relatively impoverished as is typical for most high arctic regions.

Laboratory and field toxicity experiments demonstrated the damaging effects of fresh crude oil on physiological and behavioral activities of phytoplankton and zooplankton from Balaena Bay. Weathered crude oil was also toxic, probably due to small losses of low molecular weight toxic components while the oil was trapped in or under the ice at low temperatures. However, in most cases little practical effect was noted on phytoplankton, and no effect on zooplankton and benthic organisms due to the winter oil spills. To a large extent, this must be due to the very effective clean up of the weathered crude oil before ice break-up. Only in very limited areas, where concentrated amounts of crude oil were observed to coat the vegetation on intertidal shingles or salt marshes, were considerable decreases in chlorophyll contents and photosynthetic capacities observed. The rocky shores are normally populated with rapidly growing small or microscopic algae, which often overwinter as resistant spores. Thus, it may be expected that even a heavy contamination by crude oil in these areas would eventually be followed by at least partial recovery after a few years in response to general weathering and microbial degradation of the oil. Also, removal of weathered oil by erosion. Salt marshes in this area would likely be more permanently damaged, but only long term studies can prove or disprove these predictions.

By July 25, when all shoreline clean-up was complete the only visual evidence remaining of the tests was a very thin sheen of oil deposited in the tidal zone. The total quantity of oil represented by this thin film was no more than 10 barrels. A further site visit was made on August 26, 1975. By this time, there was no evidence of an oil sheen or emulsified oil anywhere on the shoreline in the vicinity of the tests. Plate 11-1, shows the visual appearance of the test cove and beach on August 26, 1975.

12.0 CONCLUSIONS

Following is a summary of the principal conclusions. The findings have been subdivided by topic. Where appropriate, relevant sections of the report have been indicated in brackets.

1. The Plume

When crude oil is released in the water column, it rises towards the surface in conical shaped plumes. Flow tends to be unstable and the oil breaks into particles of about 1 cm in diameter or less, within a short distance of the orifice. Work by Topham (1975) indicates that much smaller particles would result from a combined oil and gas released. Small particles remain suspended in the water column and could be transported considerable distances by currents. Dissolution was insignificant with the two crudes used in the tests (6.1).

2. Area of Contamination

On striking the underside of the ice sheet, the oil radiates outward progressively filling depressions in the underside of the sheet. Since most crudes naturally form sessile drops at an ice-water interface, the minimum film thickness is about 0.8 cm. Spherical drops of a lesser diameter can exist, but these normally only occur near the periphery of the contaminated area, where the probability of collision with other drops is small. The maximum film thickness is controlled by the depth of depressions or variations in ice thickness, which are typically about 15 to 20 per cent of the mean thickness, once the sheet exceeds 50 cm in thickness (6.1). Assuming sinusoidal relief, the average depth of oil for a large discharge would be in the range of 7 to 10 percent of the mean ice thickness. The addition of gas would substantially enlarge the area of contamination. The gas, being lighter, will preferentially displace the oil, causing it to flow towards the periphery. For solid ice cover, the total volume of oil and gas should be used in determining the areal extent of contamination. In most cases leads, cracks and ridges are likely to limit spreading. It is doubtful if advection currents of the magnitude normally encountered in the Beaufort Sea, will have a significant effect on the movement of oil under the ice sheet (9.2).

3. Incorporation

Due to the added thermal resistance of the oil, a lip of ice forms around each lens or pool within a matter of hours of the oil coming in contact with the sheet (6.2). The lip effectively prevents further horizontal movement. The time required for a new sheet of ice to form beneath the oil is primarily a function of the thickness of the oil and the thermal gradient. During the late fall, when the gradient is steep and the lenses relatively thin, new ice was detected within about five days. This period increased to approximately seven days for a typical lens during the depth of winter, and over ten days in the spring. Once entrapped, the oil is stabilized. Weathering and degradation are minimal (8.1).

4. Migration

Throughout the winter the oil only penetrates between 5 and 10 cm into the loose skeletal layer on the bottom of the sheet. As the sheet begins to warm in the spring, activity intensifies in the brine channels and the oil begins to migrate upwards. Initially the movement is slow; typically in the range of 15 to 20 cm during the months of February and March. The rate of migration increases with the level of solar radiation and the ambient air temperature. Oil released in late April under 150 cm of ice was detected on the surface within one hour. However, all the oil is not released until the melt actually reaches the level of the lens (6.3). The maximum concentration of oil in the ice, even late in the season, is about 5 percent by volume.

5. Effect of Oil on Ice Growth

Although the thermal conductivity of most crude oils is about one fifteenth that of natural sea ice, the insulating effect is partially offset by free convection, once the lens is encapsulated. Convective heat transfer increases as the thickness of the oil increases, and under certain conditions a lens can actually enhance rather than retard ice growth (7.2). In general, the effect of the oil tends to be relatively insignificant in comparison to natural variations. The thermal resistance of the average oil lens at Balaena Bay was equivalent to between 5 and 8 cm of ice, or less than 20 percent of the natural variation in ice thickness late in the season.

6. Effect of Oil on Ice Depletion

On reaching the surface of the ice, the oil saturates the snow cover, and substantially reduces the albedo. This causes an increase in the level of absorbed solar radiation, which accelerates the process. Oiled melt pools quickly develop. The albedo of an oil film on water is about one quarter that of oiled snow, and consequently the melt is further accelerated. Oil is splashed on the surrounding snow by wind and wave action, and pools gradually enlarge until interconnected. New oil is continually being released until the melt reaches the initial level of the oil lens (6.4). Once the melt holes develop and surface drainage patterns are established, the sheet rapidly deteriorates. Depending on the nature and location of the sheet, oiled areas are likely to be free of ice between one and three weeks in advance of the gross failure of the sheet.

7. Clean-Up

In situ burning is both the most efficient and effective method of removing oil from solid ice cover. Even after exposure on the surface for up to six weeks, both Norman Wells and Swan Hills crude could be ignited by sprinkling gasoline or naptha on a piece of paper towel floating on the surface. A minimum thickness of approximately 0.5 cm was required to sustain combustion. With a high wind, the oil would be herded to one side of the pools, and much thinner films could be burned. The effectiveness of burning is primarily dependent on the condition and thickness of the oil on the pools (10.2). On the first burn at Balaena Bay,

approximately 90 percent of the oil in the melt pools was removed. This decreased to 50 percent on the fourth burn, while the average was about 80 percent. The removal of the residue is both time consuming and labour intensive. On the average, only 0.07 m^3 (15 gallons) of residue was recovered per man-day.

Caution should be exercised in extending these findings to offshore areas. Balaena Bay was selected for the tests because it was sheltered and the ice rotted in place. As a result, the maximum time was available for clean-up operations. A single crack connecting the test area with the tidal crack system would have greatly reduced the effectiveness of the clean-up, and caused a much larger section of shoreline to be contaminated. As well, the oil was injected inside containment skirts, and the precise position of each pool was known in advance. The film thickness was measured daily, and samples recovered to determine the timing of burns. Care was taken to prevent fallout on the surrounding ice; which would have accelerated the melt. Since offshore conditions vary greatly, it is difficult to project the likely effectiveness of in situ burning in combating a major spill. However, even with reasonable care and unlimited resources, it is doubtful if more than 70 percent of the oil could be burned in fast or stationary ice, and possibly 30 to 40 percent in the moving pack.

8. Impact

Even while the oil was being discharged, only trace quantities of dissolved hydrocarbons could be detected in the water column. In the presence of strong currents, the small particles of oil, which remain suspended in the water, could be swept out of the area and have far reaching effects. This was not detected in Balaena Bay, but the discharges were relatively shallow and the currents feeble. Once the oil is incorporated in the ice, there is little opportunity for direct contact. Although the tests had no significant effect on primary productivity, this might have been due in part to the small area of contamination. Even in the centre of the test area, less than 35 percent of the ice was oiled. The greatest impact was observed along the shoreline. The photosynthetic capacity was reduced by almost 90 percent in several heavily oiled areas (11.3).

There were no observations of wildlife coming in contact with the oil in Balaena Bay. The high level of activity likely served as a deterrent. Only two oiled ducks were observed at the offshore site, but the location was selected because it was beyond the normal feeding grounds. It was impossible to determine if waterfowl can differentiate between oiled and clean melt pools. If they cannot, the kill from a major spill could be very large, since the melt pools develop several weeks earlier in the oiled areas. The locations for the tests and the experimental techniques were selected to minimize impact. Consequently, the findings cannot be directly extended to most offshore areas.

4. Migration

Throughout the winter the oil only penetrates between 5 and 10 cm into the loose skeletal layer on the bottom of the sheet. As the sheet begins to warm in the spring, activity intensifies in the brine channels and the oil begins to migrate upwards. Initially the movement is slow; typically in the range of 15 to 20 cm during the months of February and March. The rate of migration increases with the level of solar radiation and the ambient air temperature. Oil released in late April under 150 cm of ice was detected on the surface within one hour. However, all the oil is not released until the melt actually reaches the level of the lens (6.3). The maximum concentration of oil in the ice, even late in the season, is about 5 percent by volume.

5. Effect of Oil on Ice Growth

Although the thermal conductivity of most crude oils is about one fifteenth that of natural sea ice, the insulating effect is partially offset by free convection, once the lens is encapsulated. Convective heat transfer increases as the thickness of the oil increases, and under certain conditions a lens can actually enhance rather than retard ice growth (7.2). In general, the effect of the oil tends to be relatively insignificant in comparison to natural variations. The thermal resistance of the average oil lens at Balaena Bay was equivalent to between 5 and 8 cm of ice, or less than 20 percent of the natural variation in ice thickness late in the season.

6. Effect of Oil on Ice Depletion

On reaching the surface of the ice, the oil saturates the snow cover, and substantially reduces the albedo. This causes an increase in the level of absorbed solar radiation, which accelerates the process. Oiled melt pools quickly develop. The albedo of an oil film on water is about one quarter that of oiled snow, and consequently the melt is further accelerated. Oil is splashed on the surrounding snow by wind and wave action, and pools gradually enlarge until interconnected. New oil is continually being released until the melt reaches the initial level of the oil lens (6.4). Once the melt holes develop and surface drainage patterns are established, the sheet rapidly deteriorates. Depending on the nature and location of the sheet, oiled areas are likely to be free of ice between one and three weeks in advance of the gross failure of the sheet.

7. Clean-Up

In situ burning is both the most efficient and effective method of removing oil from solid ice cover. Even after exposure on the surface for up to six weeks, both Norman Wells and Swan Hills crude could be ignited by sprinkling gasoline or naptha on a piece of paper towel floating on the surface. A minimum thickness of approximately 0.5 cm was required to sustain combustion. With a high wind, the oil would be herded to one side of the pools, and much thinner films could be burned. The effectiveness of burning is primarily dependent on the condition and thickness of the oil on the pools (10.2). On the first burn at Balaena Bay,

approximately 90 percent of the oil in the melt pools was removed. This decreased to 50 percent on the fourth burn, while the average was about 80 percent. The removal of the residue is both time consuming and labour intensive. On the average, only 0.07 m^3 (15 gallons) of residue was recovered per man-day.

Caution should be exercised in extending these findings to offshore areas. Balaena Bay was selected for the tests because it was sheltered and the ice rotted in place. As a result, the maximum time was available for clean-up operations. A single crack connecting the test area with the tidal crack system would have greatly reduced the effectiveness of the clean-up, and caused a much larger section of shoreline to be contaminated. As well, the oil was injected inside containment skirts, and the precise position of each pool was known in advance. The film thickness was measured daily, and samples recovered to determine the timing of burns. Care was taken to prevent fallout on the surrounding ice; which would have accelerated the melt. Since offshore conditions vary greatly, it is difficult to project the likely effectiveness of in situ burning in combating a major spill. However, even with reasonable care and unlimited resources, it is doubtful if more than 70 percent of the oil could be burned in fast or stationary ice, and possibly 30 to 40 percent in the moving pack.

8. Impact

Even while the oil was being discharged, only trace quantities of dissolved hydrocarbons could be detected in the water column. In the presence of strong currents, the small particles of oil, which remain suspended in the water, could be swept out of the area and have far reaching effects. This was not detected in Balaena Bay, but the discharges were relatively shallow and the currents feeble. Once the oil is incorporated in the ice, there is little opportunity for direct contact. Although the tests had no significant effect on primary productivity, this might have been due in part to the small area of contamination. Even in the centre of the test area, less than 35 percent of the ice was oiled. The greatest impact was observed along the shoreline. The photosynthetic capacity was reduced by almost 90 percent in several heavily oiled areas (11.3).

There were no observations of wildlife coming in contact with the oil in Balaena Bay. The high level of activity likely served as a deterrent. Only two oiled ducks were observed at the offshore site, but the location was selected because it was beyond the normal feeding grounds. It was impossible to determine if waterfowl can differentiate between oiled and clean melt pools. If they cannot, the kill from a major spill could be very large, since the melt pools develop several weeks earlier in the oiled areas. The locations for the tests and the experimental techniques were selected to minimize impact. Consequently, the findings cannot be directly extended to most offshore areas.

13.0 RECOMMENDATIONS

This study, as a first step, focused on the behavior of oil in stationary first-year ice. As such, it has direct application to the fast ice zone. Although minor gaps exist, there is sufficient information to develop effective countermeasures, and to assess the probable impact of a major spill. However, offshore drilling and related activities are proposed for the seasonal and permanent and polar pack zones, where conditions are very dynamic and there is a large proportion of multi-year ice. Considerable work is required simply to delineate conditions in the two zones, let alone develop effective response procedures.

Information on the composition, characteristics and movements of ice in both zones is very sparse. Without data on the roughness of the underside of the pack, it is impossible to assess the probable depth and size of pools, and the areal extent of contamination. As well, reliable statistics are required on the frequency, orientation, size and dynamics of leads to properly evaluate the significance of "lead matrix pumping", and the spread of oil between floes. Detailed information on ice movement and associated parameters required for modelling is vital for predicting the ultimate disposition of the oil.

Studies of the entrainment and migration of oil in second and multi-year ice are of prime importance. Brine channels, by means of which the oil reaches the surface in first year ice, do not exist in older ice. Consequently, barring cracks, "worm" holes and other flaws, the oil could remain entrapped until the surface melt actually reaches the level of the oil. Surface contamination, even in limited quantities, and the interception of solar radiation by oil within the sheet, will likely shorten the natural depletion rate, which is commonly estimated to be between four and seven years. However, at this stage, it is impossible to predict when the oil will surface. Since the ice is continuously moving, it is also impossible to predict where the oil will surface. If the oil is released after one year, clean-up activities from a blow-out in MacKenzie Bay, might extend as far as Barrow, Alaska, while if it takes two years, the oiled ice could be as far as Vamkarem, U.S.S.R.

Because the pack is continuously converging and diverging, the width of the contaminated band will progressively increase with distance from the discharge point. After several years, oiled floes could be spread over a very large area. Since there will be insufficient time to mobilize a large clean-up force after the oil surfaces, some method of detecting the oil while it is still entrapped in the ice is required. A number of techniques have been proposed, but none have been tested.

Further work is also required on the effects of an oil slick on sea ice formation, particularly under dynamic conditions. As well, long term studies of weathering and degradation are needed to assess the fate and impact of oil which is not recovered.

BIBLIOGRAPHY

ANISIMOV, M.I., 1961: An Approximate Evaluation of Formulas on Thermal Conductivity of Snow. Translated by I. Donehov, Foreign Area Section, Office of Climatology, Moscow.

ARNON, D. 1949: Copper Enzymes in Isolated Chloroplasts. Plant Physiology 24: 1-15.

AYERS, R.C., JOHNS, H.D., and GLAESER, J.L., NOVEMBER 1974: Oil Spills in the Arctic Ocean - Extent of Spreading and Possibility of Large Scale Thermal Effects... Letter in Science Vol. 186 pp 843-4, with a reply by CAMPBELL, W.J. and MARTIN, S. on following pages.

BARRY, R.G., and CHORLEY, R.J., 1968: Atmosphere, Weather and Climate, Methuen & Co. Ltd., London

BELL, L.: Oil Under Ice Study, Resolute Bay, N.W.T. A proposal by W.A.T.E.R. Associates Ltd., Box 86, Tobermary, Ontario.

BLUMER, M., SASS, J., SOUZA, G., SANDERS, H., GRASSLE, F., AND HAMPSON, G., 1970: "The West Falmouth Oil Spill" Unpublished manuscript. Reference No. 70044, Woods Hole Oceanographic Institution, Woods Hole, Mass.

BURNS, B.M., 1974: The Climate of the Mackenzie Valley - Beaufort Sea, Vols. I & II, Environment Canada, Climatological Studies No. 24, Toronto.

BURSA, A.S. 1961a: Phytoplankton of the Calanus Expeditions in Hudson Bay, 1953 and 1954. J. Fish, Res. Bd. Canada 18: 51-83.

BURSA, A.S. 1961b: The Annual Oceanographic Cycle at Igloolik in the Canadian Arctic. II. The Phytoplankton, J. Fish. Res. Bd. Canada 18: 563-615.

BURSA, A.S. 1963: Phytoplankton in Coastal Waters of the Arctic Ocean at Point Barrow, Alaska. Arctic 16: 239-262.

CAMPBELL, W.J. and MARTIN, S., JULY 1973: Oil and Ice in the Arctic Ocean: Possible Large Scale Interactions... Vol. 181, pp. 56-58 Science.....

CHEN, E.C. and GUARNASCHELLI, FEBRUARY 1973: Changes in Surface Tension During the Initial Aging of Some Petroleum Crudes. Vol. 51 pp. 134-136, The Canadian Journal of Chemical Engineering, Ottawa

CHEN, E.C., OVERALL, J.C.K., and PHILLIPS, C.R., FEBRUARY 1974: Spreading of Crude Oil on an Ice Surface. The Canadian Journal of Chemical Engineering, Vol. 52, pp. 71-74, Ottawa.

DRAKE, R.M. and ECKERT, E.R.G., 1959: Heat and Mass Transfer, McGraw Hill Publishing Company, New York.

EIDE, L.I. and MARTIN, S. 1974: The Formation of Brine Drainage Features in Young Sea Ice, Department of Oceanography WB-10, University of Washington, Seattle.

FERTUCK, L.J., HUSBAND, W.H.W. and SPYKER, J.W., 1971: Numerical Estimation of Ice Growth as a Function of Air Temperature, Wind Speed and Snow Cover, The Engineering Journal, December.

GADE, H.G., LAKE, R.A., LEWIS, E.L. and WALKER, E.R., 1973: Oceanography of an Arctic Bay, Deep Sea Research, Vol. 21, Pergamon Press, Oxford.

GLAESER, LtJg JOHN L. and VANCE, LCOR GEORGE P., FEBRUARY 1971: A Study of the Behavior of Oil Spills in the Arctic. Project No. 714108/A/001,002, Office of Research & Development, U.S. Coast Guard, Washington, D.C.

GOLDEN, LtJg Paul C., JANUARY 1974: Oil Removal Techniques in an Arctic Environment. Vol 8, No. 8, pp 38-43 MTS Journal.

GRAINGER, E.H. 1965: Zooplankton from the Arctic Ocean and Adjacent Canadian Waters. J. Fish. Res. Bd. Canada 22: 543-564.

HOULT, D.P., O'DEA, S., PATUREAU, J.P., and WOLFE, S. 1975: Oil in the Arctic Report No. CG-D-96-75, Prepared for Department of Transportation, United States Coast Guard, Office of Research & Development, Washington, D.C.

KAUSS, P., HUTCHINSON, T.C., SOTO, C., HELLEBUST, J. and GRIFFITHS, M., 1973: The Toxicity of Crude Oil and its Components to Fresh Water Algae. Department of Botany and Institute of Environmental Sciences and Engineering, University of Toronto.

KEEVIL, B.E., and RAMSEIER, R.O., Behavior of Oil Spilled Under Floating Ice, Department of the Environment, Inland Waters Directorate, Ottawa.

KREITH, F. 1969: Principles of Heat Transfer, International Text Book Company, Scranton.

LAKE, R.A., and LEWIS, E.L., 1970: Salt Rejection by Sea Ice During Growth, Journal of Geophysical Research, Vol. 75, No. 3.

LEINONEN, P.J. and MACKAY, D., FEBRUARY 1975: A Mathematical Model of the Evaporation and Dissolution of Oil on Land, on Ice and Under Ice, paper presented at the 11th Annual Symposium on Water Research to be published in the proceedings.

LEWIS, E.L., JULY 1975: Oil in Sea Ice. Third International Conference on Port and Ocean Engineering, University of Alaska, Fairbanks.

MACKAY, D., and MATSUGU, R.D., AUGUST 1973: Evaporation Rates of Liquid Hydrocarbon Spills on Land and Water. Vol. 51, The Canadian Journal of Chemical Engineering, Ottawa.

MACKAY, D. and SHUI, W.Y., The Aqueous Solubility and Air-Water Exchange Characteristics of Hydrocarbons Under Environmental Conditions. Department of Chemical Engineering and Applied Chemistry and Institute for Environmental Studies, University of Toronto.

MACKAY, D., SHUI, W.Y., and WOLKOFF, A.W., 1975: Gas Chromatographic Determination of Low Concentrations of Hydrocarbons in Water by Vapour Phase Extraction. Special Technical Publication 573, American Society for Testing and Materials, Philadelphia.

MACKAY, D., MEDIR, M. and THORNTON, D.E., 1975: Spreading Behavior of Oil Under Ice. Unpublished manuscript.

MACKAY, D., LEINONEN, P.J., OVERALL, J.C.K., and WOOD, B.R., MARCH 1975: The Behavior of Crude Oil Spilled on Snow. Journal of the Arctic Institute of North America, Vol. 28, No. 1, Montreal.

MCADAMS, W.H., 1954: Heat Transmission, McGraw Hill Publishing Co., New York.

MCMINN, LtJg T.J., SEPTEMBER 1972: Crude Oil Behavior on Arctic Winter Ice. Project 734108, Environmental and Transportation Technology Division, Office of Research & Development, U.S. Coast Guard, Washington, D.C.

MILLER, A., 1966: Meteorology, Charles E. Merrill Publishing Co., Columbus

NORCOR ENGINEERING AND RESEARCH LIMITED, 1974: Investigation of Oil Spill, Riviere St. Paul, Quebec, internal document for Gulf Oil Canada Limited.

NORCOR ENGINEERING AND RESEARCH LIMITED, 1975: Investigation of Techniques for the Recovery of Crude Oil from Under Solid Ice Cover, internal document for Panarctic Oils Limited.

NORCOR ENGINEERING AND RESEARCH LIMITED, 1975: Remote Sensing of Crude Oil in Arctic Sea Ice, Centre of Spill Technology, Department of the Environment.

RAMSEIER, R.O., GANTCHEFF, G.S., and COLBY, L. 1973: Oil Spill at Deception Bay, Hudson Strait. Scientific Series No. 29, Inland Waters Directorate, Water Resources Branch, Ottawa.

RAMSEIER, R.O.: An Overview of Potential Oil Pollution in the High Arctic, Inland Waters Directorate, Department of the Environment, Ottawa.

REGNIER, Z.R. and SCOTT, B.F., 1975: Evaporation Rates of Oil Compounds. Vol. 9, No. 5, Water Science Section, Water Quality Research Division, Environment Canada, Ottawa.

ROSSENEGGER, L.W., 1976. The Movement of Oil Under Sea Ice. Beaufort Sea Project Technical Report #28. Dept. of the Environment, Victoria, B.C. (In Press.)

SCOTT, B.F., and CHATTERJEE, R.M., 1975: Behavior of Oil under Canadian Climatic Conditions. Scientific Series No. 50, Inland Waters Directorate, Water Quality Branch, Ottawa.

SCOTT, B.F., 1975: Investigation of the Weathering of a Selected Crude oil in a Cold Environment. Special Technical Publication 573, Copyright ASTM Philadelphia.

SELLERS, W.D., 1965: Physical Climatology. The University of Chicago Press, Chicago.

TOPHAM, D.R., 1976. Hydrodynamics of an Oilwell Blowout. Beaufort Sea Project Technical Report #33. Dept. of the Environment, Victoria, B.C.

WALTON, J. 1922: A Spitsbergen Salt Marsh: With observations on the geological phenomena attendant on the emergence of land from the sea. J. Ecol. 10: 109-121.

WALKER, E.R., 1976. Oil, Ice and Climate in the Beaufort Sea. Beaufort Sea Project Technical Report #35. Dept. of the Environment, Victoria, B.C.

WEEKS, W.F.: Understanding the Variations of the Physical Properties of Sea Ice. Snow and Ice Branch, U.S. Army Cold Regions Research and Engineering Laboratory, Hanover, N. H.

WELCH, H.E. and KALFF, J., 1975: Marine Productivity at Resolute Bay, N.W.T. in "Circumpolar Conference on Northern Ecology". September 15-18, 1975, Ottawa. National Research Council (In press).

WELLER, G., 1967: Heat-Energy Transfer Through a Four-Layer System: Air, Snow, Sea Ice, Sea Water. Journal of Geophysical Research, Vol. 73, No. 4, February 15, 1967.

WILLIAMS, G.P. and GOLD, L.W., 1958: Snow Density and Climate, Research Paper No. 60, Division of Building Research, National Research Council, Ottawa.

APPENDICES

APPENDIX A

EQUIPMENT SPECIFICATIONS

MEASUREMENT ACCURACY

FIGURE A-1 THERMISTOR CHAIN CONSTRUCTION

APPENDIX 27A

EQUIPMENT SPECIFICATIONS

I Sampling and Analytical Instruments

a) Multimeter: manufactured by HEWLETT PACKARD
Display Model # 34740A
Multimeter Model # 34702A
Battery Pack Model # 34720A

Accuracy at 23°C ± (.01% of reading + .005% of range)

Temperature Coefficient ± (.0035% of reading + .001% of range) /°C

b) Salinity Meter: manufactured by YELLOW SPRINGS INSTRUMENT CO.
Model 33

Accuracy: Salinity: Above 4°C ± .9°/$_{oo}$ at 40°/$_{oo}$
± .7°/$_{oo}$ at 20°/$_{oo}$
Below 4°C ± 1.1°/$_{oo}$ at 40°/$_{oo}$
± 0.9°/$_{oo}$ at 20°/$_{oo}$

II Radiation Instruments

a) Solarimeter: manufactured by KIPP AND ZONEN
Model CM6

Effective wave length band measured: 300 nm to 2.5 nm

Sensitivity: 1 g cal cm^{-2} min^{-1} has potential of 8.4 mv

Accuracy: within 1%; temperature coeff. 0.15% per °C

b) Albedometer: manufactured by KIPP AND ZONEN
Model CM7

Effective wave length band measured: 300 nm to 2.5 nm

Sensitivity: 1 g cal cm^{-2} min^{-1} has potential of 8.0 mv

c) Net Radiometer: (Fritschen Type)
manufactured by MICROMET INSTRUMENTS
Model MNR

Effective for all wave length bands

Sensitivity: 1 g cal cm^{-2} min^{-1} develops potential of 3.05 mv

III Surface Weather and Ice Temperatures

a) Anemometer: manufactured by TEXAS ELECTRONICS INC.
Model #446

b) Barometer: recording type manufactured by TAYLOR INSTRUMENTS

c) Telethermometer: manufactured by YELLOW SPRINGS INSTRUMENT CO.
Model #47
Absolute accuracy: ± 1% of scale range
Sensitivity and readability: ± 0.4% of scale range

d) Thermistor Beads: manufactured by YELLOW SPRINGS INSTRUMENT CO.
Part # 44005X
Time Constant (time for a thermistor to indicate 63% of a newly impressed temperature) = 1 sec.
Dissipation Constant (power required to raise a thermistor 1°C above surrounding temperature) = 8 mw/°C
An error of 10^{-5} °C was introduced by electrical heating of the bead
Accuracy: ± 0.01°C at 0°C
± 0.03°C at -20 and -40°C
add ± 0.02°C up to 20°C on either side of a known point
(calibrated at 0°C, -20°C, -40°C)
Repeatability error - negligible

IV Recording Instruments

a) Scroll-Chart Recorder: manufactured by RUSTRAK INSTRUMENTS and modified by TEXAS ELECTRONICS INC.
Model # 446

b) Two-Pen Recorder: manufactured by FISCHER SCIENTIFIC INSTRUMENTS LTD.
Model # 5000

c) Underwater Television Camera: manufactured by HYDRO PRODUCTS
Model TC-125

d) Colour Videocorder: manufactured by SONY CORPORATION
Colour Videocorder Model AV-8400
AC Adaptor Model AC-1000

e) Datalogger with Scanner, Integrator, and Output Mechanisms:
manufactured by VIDAR DATA ACQUISITION SYSTEMS
Model 5400 DAS

which included the following components:

100 channel scanner
Digital Volemeter: Non-linearity: ± .015% full scale
Resolution: ± .01% full scale
Time Stability: ± .01% per month
Ohms Converter: ± .026% for worst case
Digital Printer
Tape Punch
10 Integrators

APPENDIX 27A

MEASUREMENT ACCURACY

Solar Radiation - combined error of Instrument Calibration, Vidar DVM, and Integrator < 8% of reading.

Albedo - combined error of Instrument Calibration and HP multimeter
< ± 10% of Albedo Value (Albedo > 0.2)
< ± 13% of Albedo Value (Albedo < 0.2)

Net Radiation - combined error of Instrument, VIDAR DVM and Integrator Drift. Difficult to quantify, owing to unstable integrator drift of approx. 80 $\mu V\ h^{-1}$ approaching the magnitude of instrument output.
Generally the possible error exceeded ± 50%. For this reason, Radiometer values were discounted in the analysis.

Air Temperature - $\leq$ ± 0.5°C at 5 m
$\leq$ ± 0.05°C at 1 m

Water Temperature - $\leq$ ± 0.02°C

Ice Temperature - $\leq$ ± 0.04°C

Figure A - 1 THERMISTOR CHAIN CONSTRUCTION

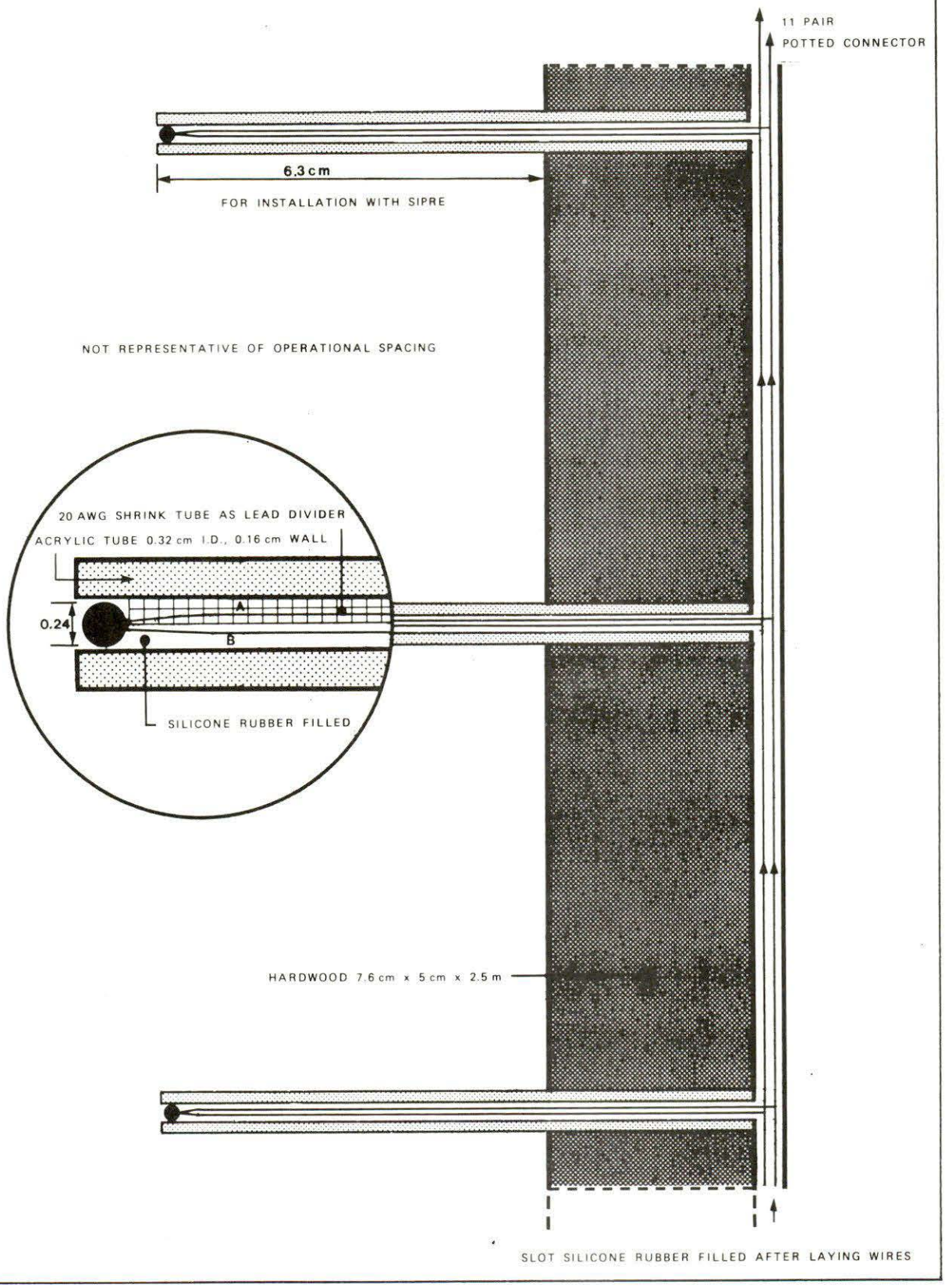

APPENDIX B

Figure B - 1 NORMAN WELLS CRUDE OIL COMPOSITION VS PER CENT EVAPORATION AT 25 C

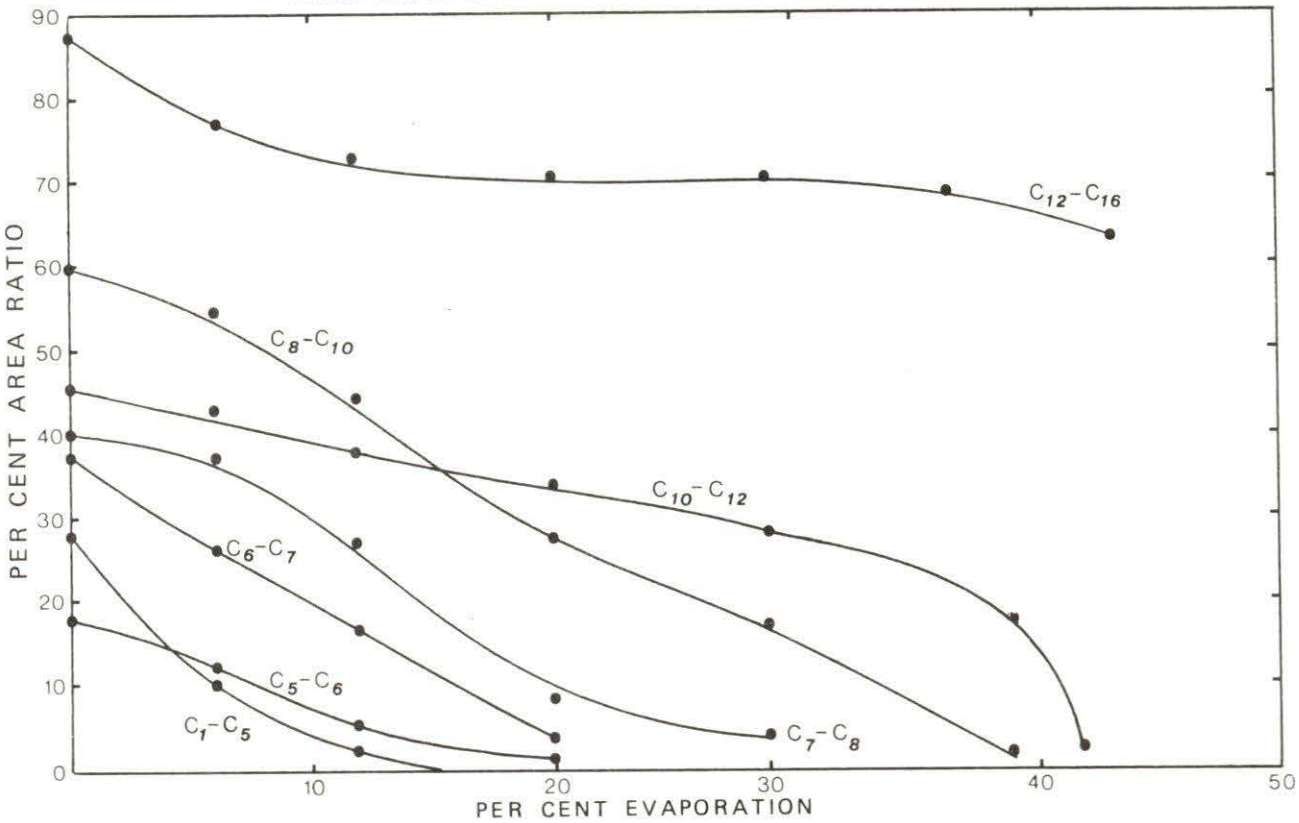

Figure B - 2 SWAN HILLS CRUDE COMPOSITION VS PER CENT EVAPORATION

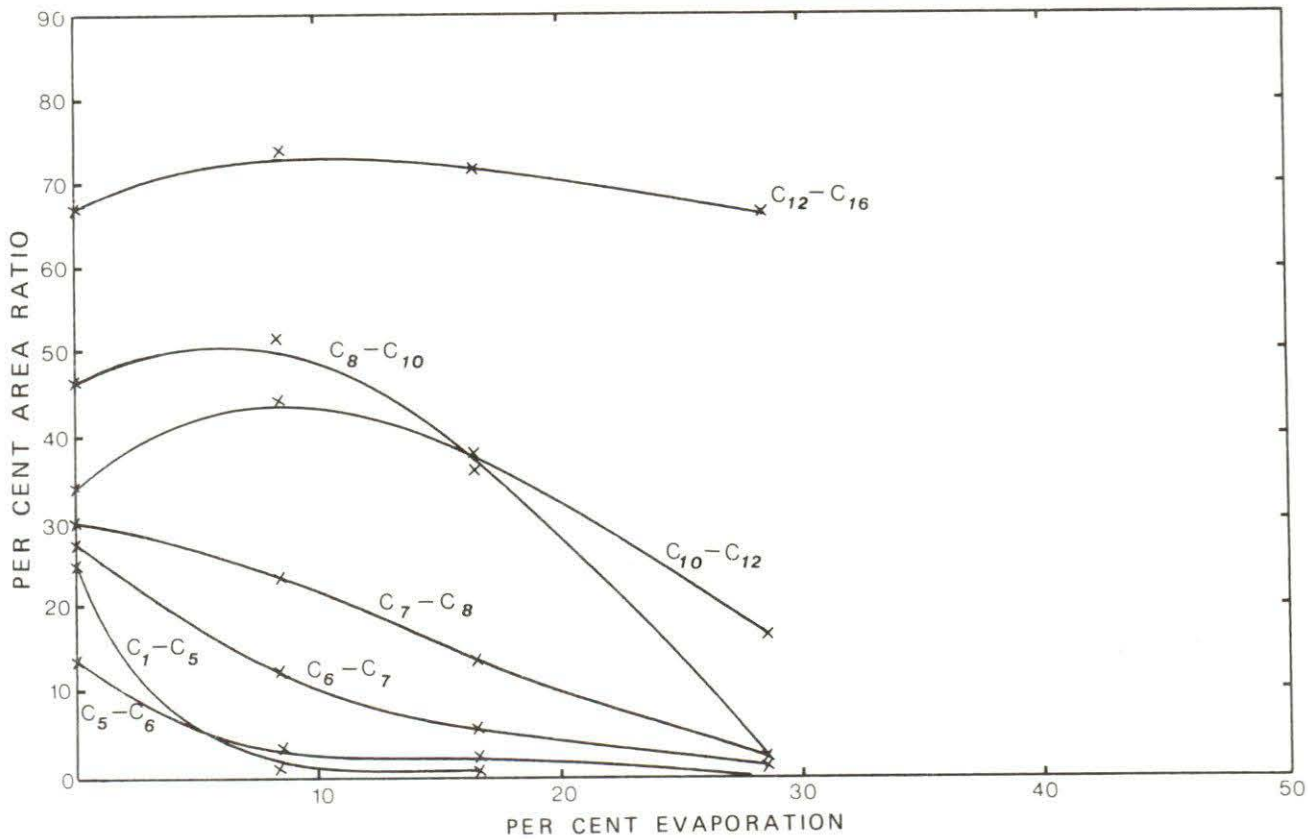

Figure B - 3

VISCOSITY OF NORMAN WELLS CRUDE OIL

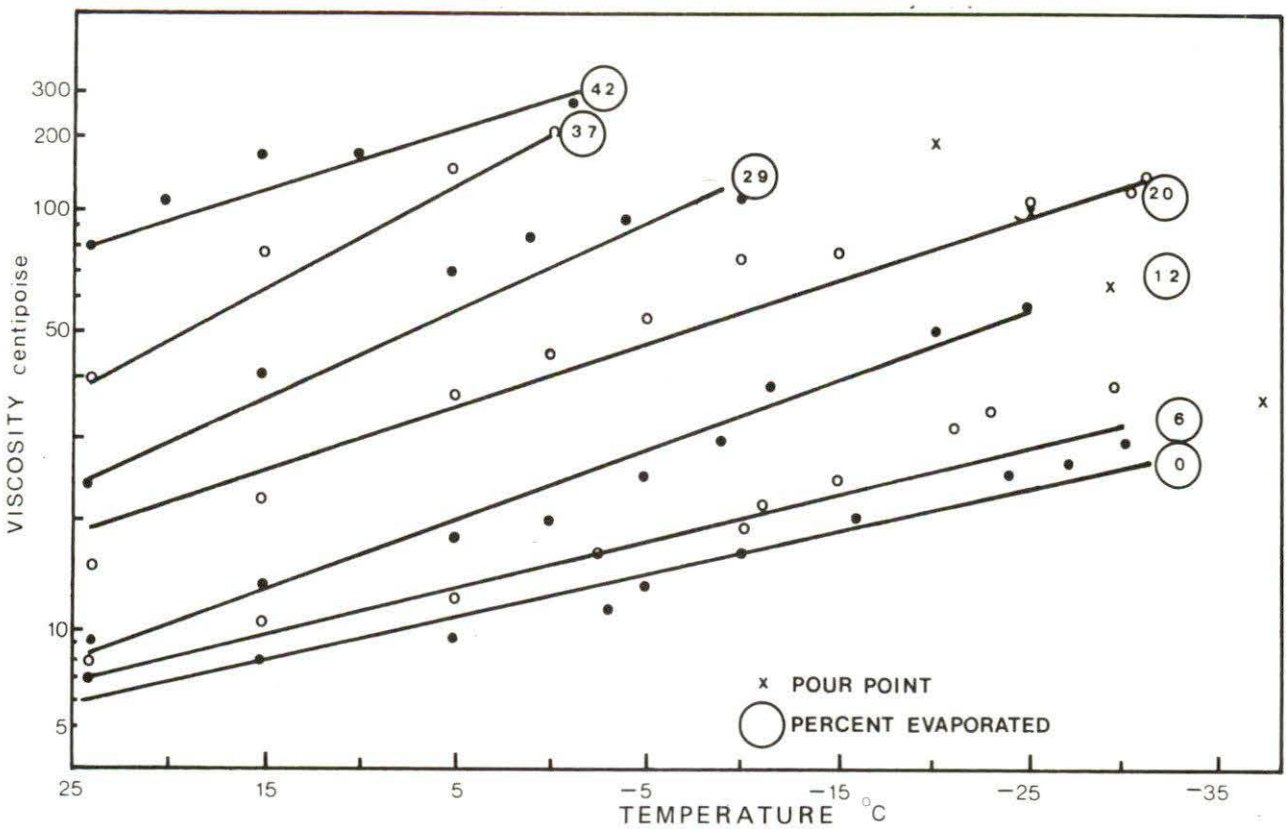

Figure B - 4

DENSITY OF NORMAN WELLS CRUDE OIL

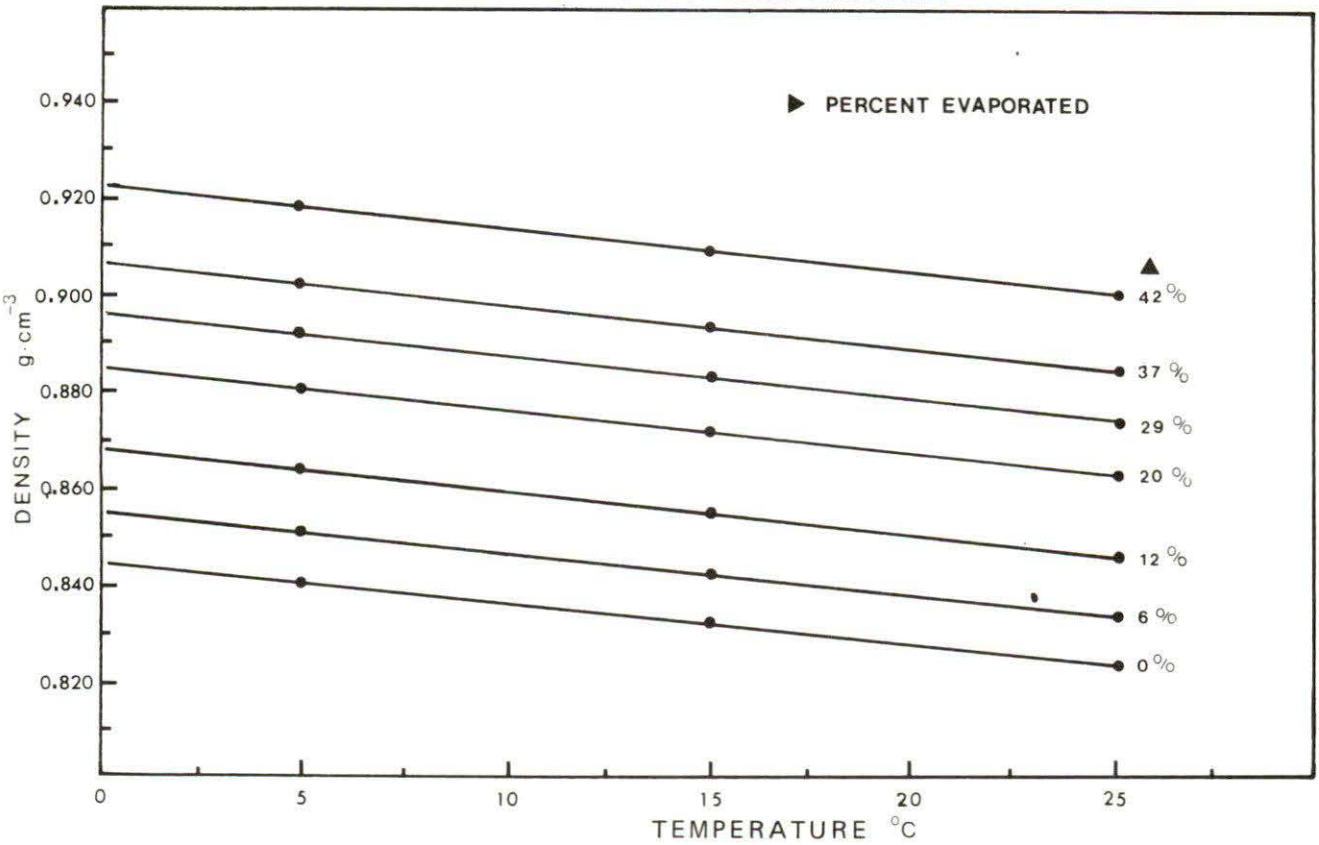

Figure B - 5

VISCOSITY OF SWAN HILLS CRUDE OIL

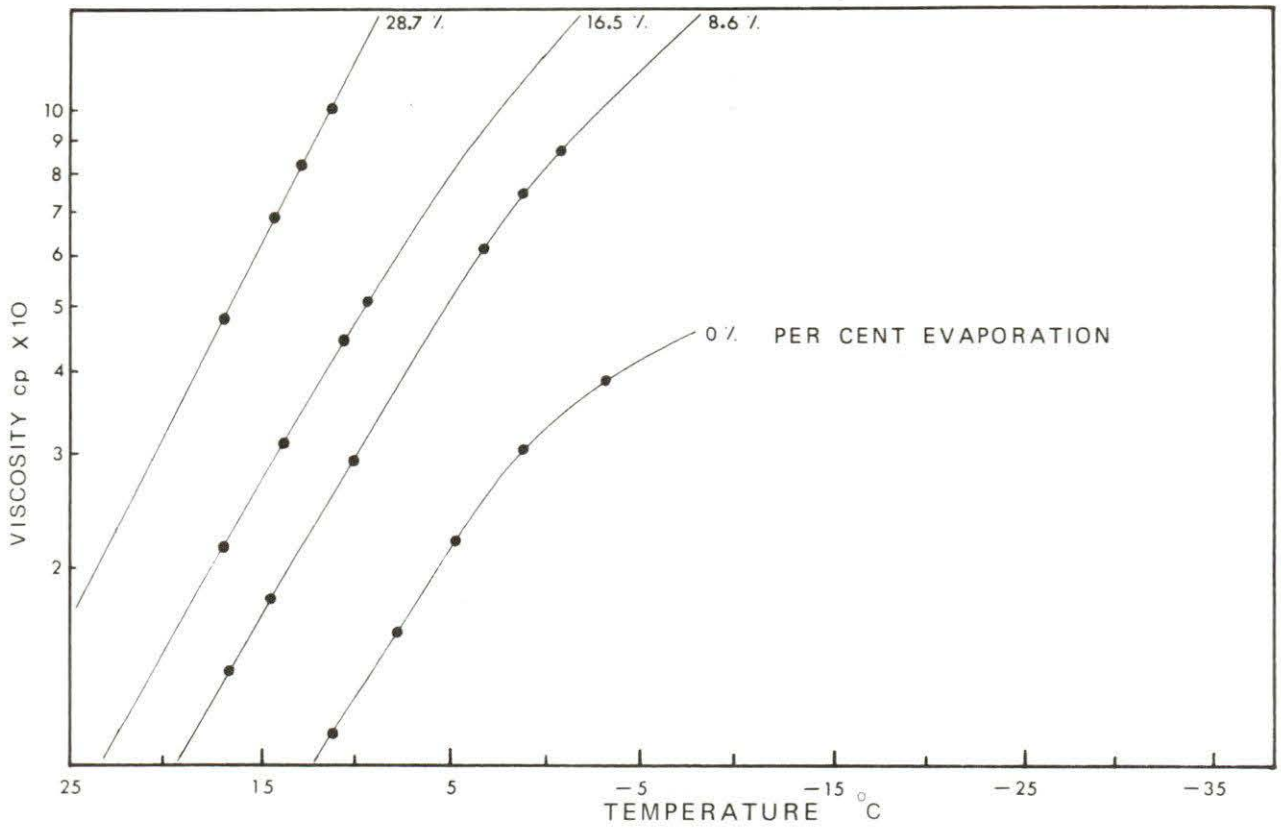

Figure B - 6

DENSITY OF SWAN HILLS CRUDE OIL

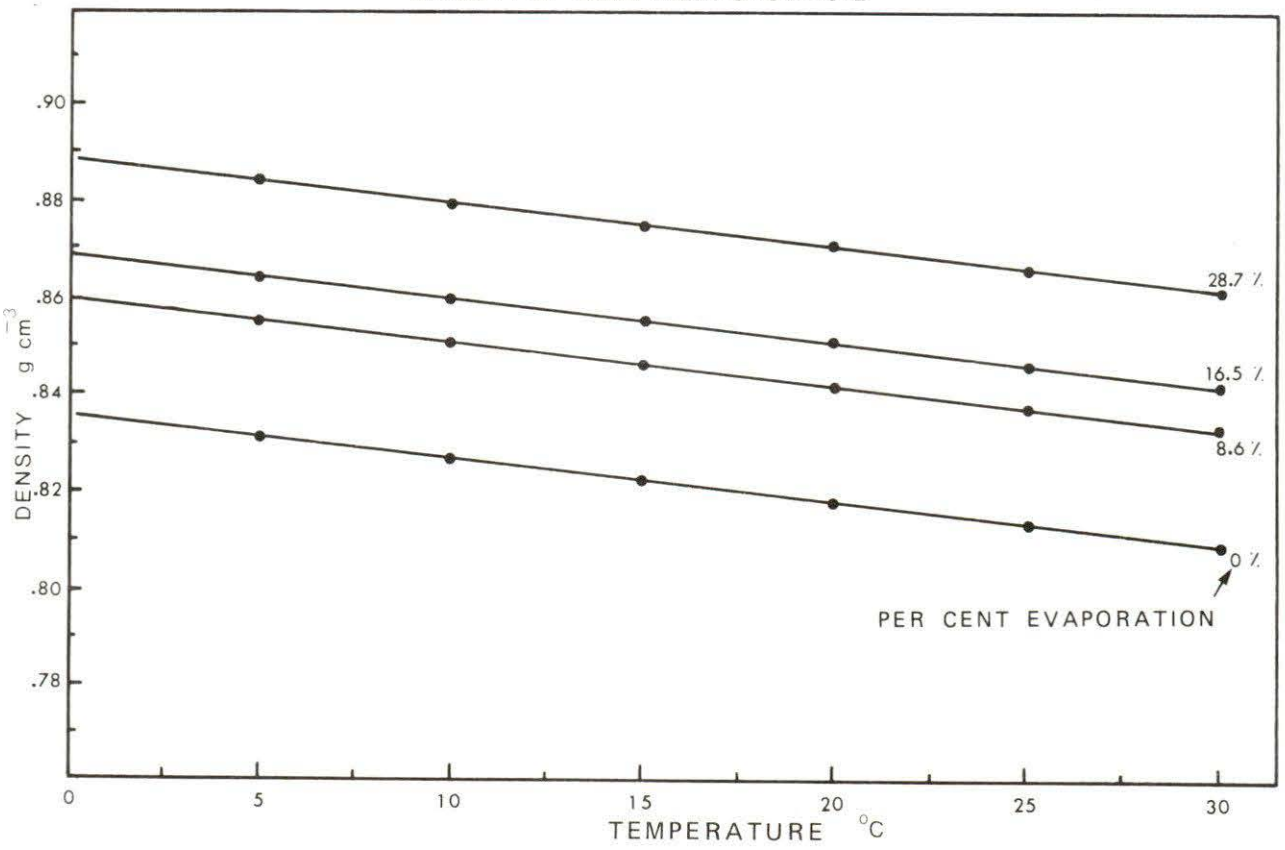

Figure B - 7 CRUDE OIL SOLUBILITY VS PER CENT EVAPORATION AT 25 C

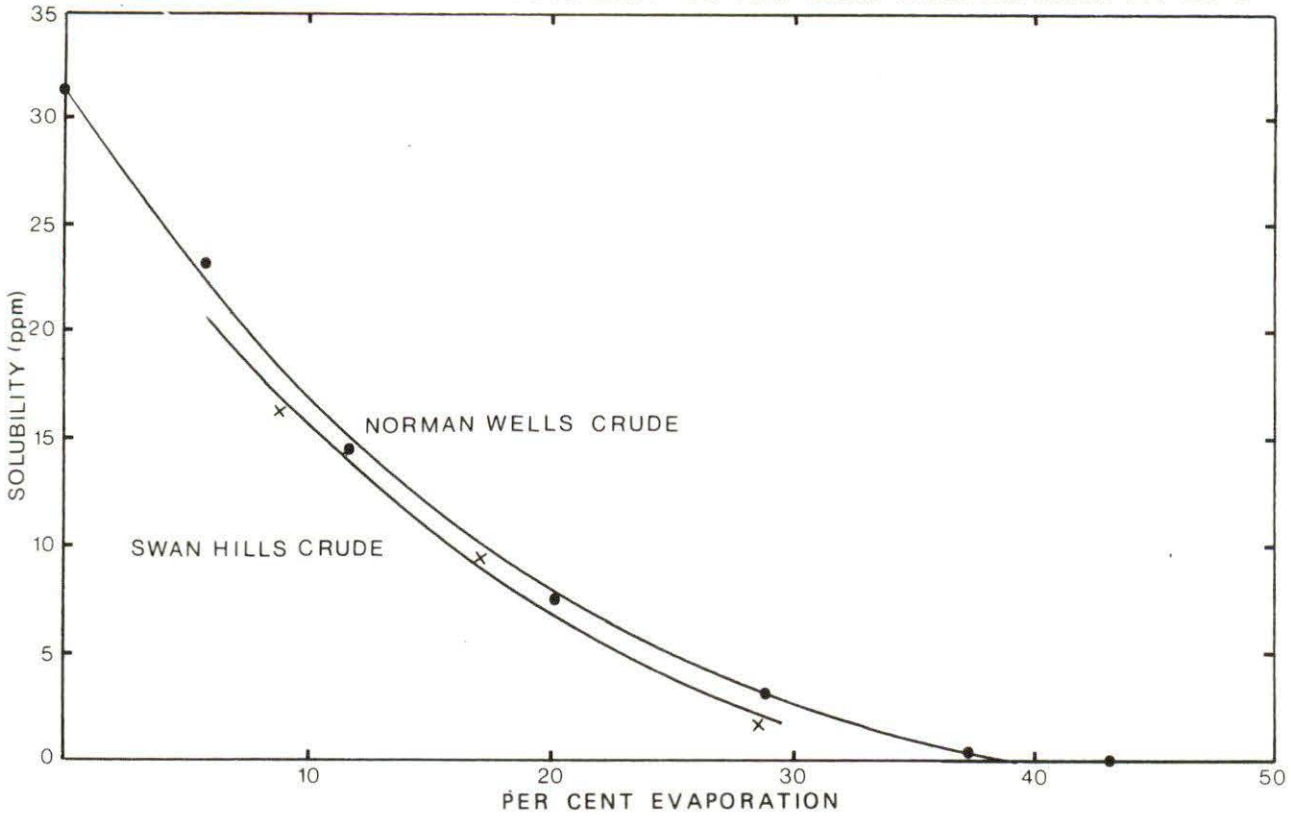

Figure B-8 CRUDE OIL POUR POINTS VS PER CENT EVAPORATION AT 25 C

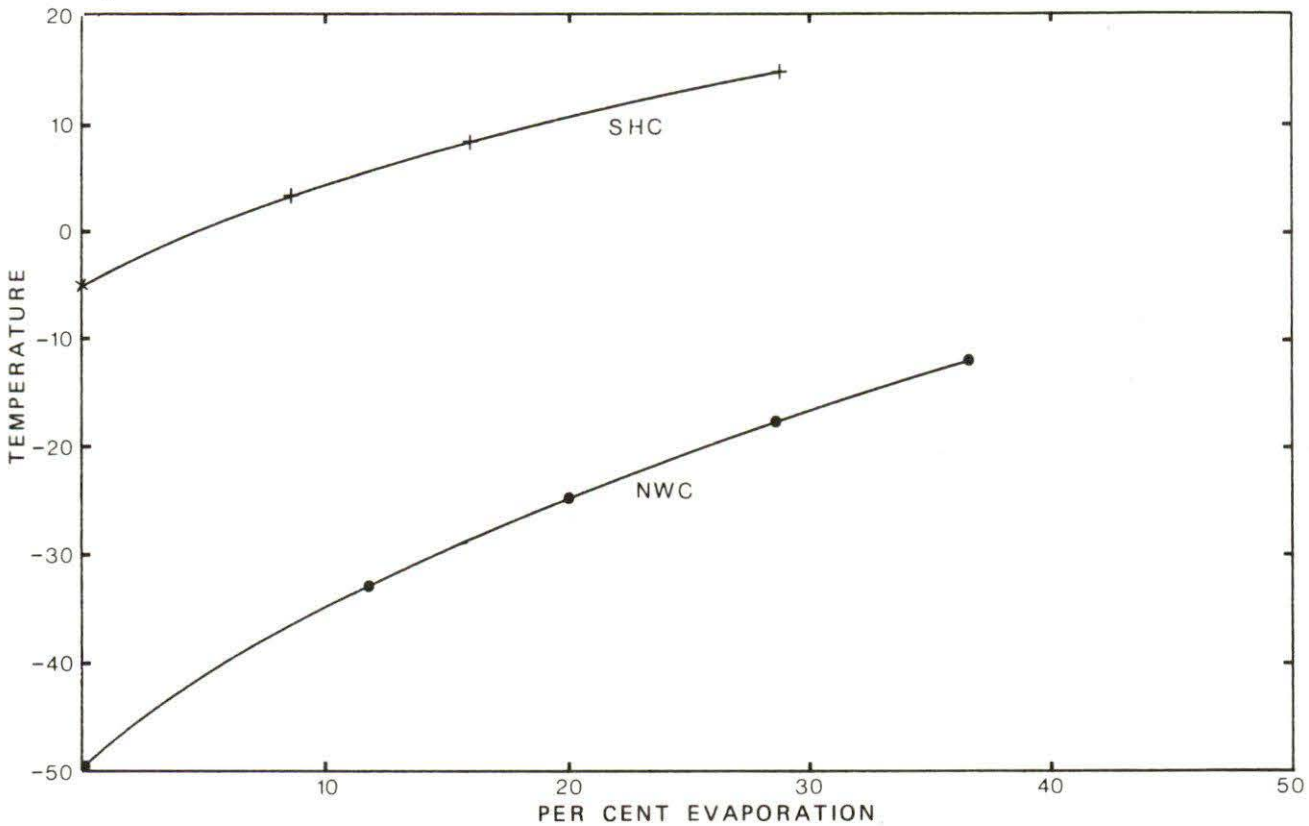

TABLE B-1

PERCENT AREA RATIO AND CORRESPONDING PERCENT EVAPORATION FOR NORMAN WELLS CRUDE

NO.	SAMPLE	C1-C5	>C5-C6	>C6-C7	>C7-C8	>C8-C10	>C10-C12	>C12-C16	>C16-C24	% EVAP
14	NWC FROM	25.2	15.7	30.0	36.6	57.5	44.5	84.6	100	3
	DRM DEC 8	0.8	2.6	3.0	5.0	3.6	0	1.2		
15	NW1	0.02	1.7	11.2	24	57	49	86	100	17
	DEC 10		1.8	15	12.6	4	-	0.8		
16	NW1	0.16	0.5	6.0	15.9	46.4	44.9	85.6	100	19
	JAN 21			19	18	12	-	1		
17	NW2 FROM	32	16.5	31.2	35.8	54	40.8	74.6	100	2
	TNK OCT 23	-	1.8	2.2	5.6	6.2	6	10		
18	NW2	25.6	15.1	29	36.0	56.6	43.8	81.4	100	3
	NOV 15	1	2.8	3.6	5	4.4	1.8	3.2		
19	NW2	19.6	12.9	26.9	33.9	54.6	42.4	78.6	100	5
	DEC 10	2.2	5	5	6.5	6	3.8	5.8		
20	NW2	28.6	16.7	32.6	38.8	60.8	47.3	82.9	100	2
	JAN 21	1	2	3.8	2.2	-	-	2		
21	NW2	26.7	16.6	32.4	38.9	60.7	46.6	83.0	100	2
	FEB 21	1	2	2	2.6	-	-	2.2		
22	NW2	14.6	12.1	21.7	33.8	54.8	42.3	76.9	100	5
	MAY 9	4.2	5.2	8	7	6	4	7.8		
23	NW2	-	-	0.18	0.75	5.4	15.7	65.4	100	37
	MAY 10					36.4	39	42		
24	NW3 TANK	21.4	14.4	28.4	33.6	52.4	40.2	77.5	100	4
	NOV 14	1.8	3	3.8	7	7.4	7.5	6		
25	NW3	8.9	9.9	22.9	33.6	59.4	46.9	87.1	100	7.5
	DEC 10	6.4	7.6	7.4	7	1	1	0.6		
26	NW3	17.2	14.1	29.4	36.3	58.4	45.4	81.3	100	3.3
	JAN 22	3	3.8	3	4.5	2.6	-	3.4		
27	NW3	22.2	15.9	31.7	38.5	60.3	46.0	82.1	100	2
	FEB 21	18	2	2	36	0	-	2.8		
28	NW3	18.9	13.9	28.6	35.9	64.8	43.6	79.9	100	4
	MAY 12	2.8	3.8	3.8	5	-	2	4		
29	NW3	-	-	-	-	0.63	12.2	40.3	100	41
	MAY 26					>40	41			
30	NW3		-	-	0.34	7.3	26.6	74.6	100	34
	JUN 6					36	31	10		
31	NW3	16.9	12.8	26.7	49.4	54.4	48.9	77.7	100	6
	JUN 10	3.7	4.2	6	-	-	-	6		
32	NW4 FROM	17.9	14.2	29.1	34.3	54.9	43.3	79.5	100	3.5
	TNK DEC 9	3	3.7	3.5	6.2	6	2	4.2		

TABLE B-1

NO.	SAMPLE	C1-C5	C5-C6	C6-C7	C7-C8	C8-C10	C10-C12	C12-C16	C16-C24	% EVAP
33	NW4	14.3	14.7	32.0	40.6	66	51.6	90.6	100	3
	FEB 5	4.2	3	2	-	-	-	-		
34	NW4	16.9	15.3	31.7	40.0	63.1	49.0	86.3	100	2.5
	FEB 21	3	2.8	2	0	-	-	0.4		
35	NW4	12.4	10.6	24.1	31.9	53.9	42.9	79.4	100	6
	MAY 13	5	7	6.6	8	6.4	2.2	5.5		
36	NW4	14.7	13.0	27.9	35.5	58.1	45.7	83.6	100	4
	MAY 27	4.2	4.4	4.0	5.8	3	-	2		
37	NW4	-	-	3.0	6.0	9.7	27.8	75.5	100	26
				2.2	26	33.4	29	9		
38	NW4	-	-	-	-	1.3	3.3	22.3	100	43
	JUN 13									
39	NW6	13.7	12.6	26.0	32.8	54.1	42.9	78.7	100	5
	FEB 15	4.6	5.0	5.2	7	6.4	2.2	5.0		
40	NW6	0.08	0.1	0.6	1.2	12.0	30.9	69.7	100	23
	MAY 10	16.5	22	?	?	31	25	26		
41	NW6	3.5	4.7	14.5	25	50	41.4	78.2	100	12
	MAY 15	11.6	10.4	12.6	12	9	6	6		
42	NW6	-	-	-	-	0.56	4.3	35.4	100	43
	JUN 12						43			
43	NW7	-	0.7	9.7	24.5	51.2	41.2	75.8	100	20
	MAY 10		20	16	12.4	8.4	6	6		
44	NW7	-	-	-	1.1	17.5	35.1	79.8	100	27
	JUN 6				?	27	19	4		
45	NW7	-	-	0.25	0.99	6.0	21.0	67.5	100	36
	JUN 11					37	36			
46	NW7	-	-	-	-	-	0.87	11.5	100	
	JUN 12									
47	NW7	-	-	-	-	.006	2.1	37.7	100	50
	JUN 13									
48	NW3	-	-	-	-	1.4	5.7	41.1	100	42
	JUN 26									
49	SHORELINE	-	-	-	-	1.5	6.3	39.1	100	42
	JUL 7									
50	SHORELINE	-	-	-	-	0.011	1.9	27.9	100	>50
	JUL 7									
51	EVAP NWC	8.3	10.6	23.6	31	49.7	38.4	71.3	100	7
	DEC 24	7.4	7	7.0	8.6	9.0	11.2	21		
52	EVAP NWC	0.5	0.9	4.6	11.4	36.1	38	75.2	100	20
	JAN 11	16.5	20	20	21	16	12	9		
53	EVAP NWC	.06	.21	1.8	6.5	34.8	40.8	77.5	100	25
	JAN 20	17		24	26	17	7	6		
54	EVAP NWC	-	0.34	2.5	7.8	34.1	40.4	76.6	100	24
	JAN 24		21	23	24	17	8	7		
55	EVAP NWC	.17	.21	.9	3.4	30.7	43.2	81.8	100	
	FEB 6									

TABLE B-2

PERCENT AREA RATIO AND CORRESPONDING PERCENT EVAPORATION FOR SWAN HILLS CRUDE

NO.	SAMPLE	C1-C5	>C5-C6	>C6-C7	>C7-C8	>C8-C10	>C10-C12	>C12-C16	>C16-C24	% Evap
1	SHC FROM DRM DEC 7	25.8 0	14.8 0	30.8 0	35.0 0	61.6 0	42.2 0	68.1	100	0
2	SH1 FROM TNK DEC 10	21.4 0.5	13.9 0.6	30.0 0.6	33.6	51.1	37.9	68.9	100	0.5
3	SH1 DEC 30	18.3 0.6	13.8 0	30.2 -	35.8 -	56.7 -	42.9 6.5	75.7 -	100	1
4	SH1 JAN 22	20.6 0.5	15.2 0.1	33.4 -	39.3 -	61.1 --	45.9 8.5	79.4 -	100	1
5	SH1 FEB 18	21.7 0.5	15.7 1.0	34.3 -	40.3 -	62.9 -	50.8 -	77.0 -	100	1
6	SH1 MAY 13	12.2 1.6	10.4 1.2	25.9 0.8	33.2 -	53.8 -	40.6 2.6	73.4 4.5	100	1.5
7	SH1 JUN 3	1.4 8	1.3 16	5.2 17	11.1 18.6	33.1 18.4	34.7 18.8	69.9 22	100	10
8	SH1 JUN 13	0.12	0.58	2.3	3.0 28	7.4 28	15.2 29	32.5	100	28
9	SH2 MAY 10	-	0.1	0.7 26	3.6 26	26.4 21	34.7 19	72.2 18	100	26
10	SH2 MAY 27	0.9 8.5	3.1 8.4	14.7 6.6	28.5 3.8	52.7 6	54.3 -	69.9 1	100	8
11	SH2 MAY 29	-	-	-	0.2	3.7 29	20.7 27	74 -	100	28
12	SH2 MAY 29	0.45 11	0.22 22	0.97 26	1.4 29	6.1 28	24.2 25	74.5 -	100	24
13	SH2 JUN 12	-	-	-	-	0.16 30	3.5 35	31.7	100	33
56	EVAP SHC DEC 24	9.7 1.5	10.8 2	26.6 0.5	33.8 -	56.1 -	44.2 -	77.7 -	100	1.5
57	EVAP SHC JAN 4	0.6 9	3.1 8	11.9 9.4	20.9 9	50.0 10.0	44.7 -	80.9 -	100	9
58	EVAP SHC JAN 20	3.0 5.6	3.9 6	13.4 7.6	23.2 9	54.6 6	46.7 -	82.0 -	100	7
59	EVAP SHC FEB 26	0.8 8.4	1.0 1.9	0.5 26	11.4 19	41.5 15	42.3 12	76.3 -	100	19

TABLE B-3

DERIVED PROPERTIES OF THE
NORMAN WELLS CRUDE SAMPLES (AT 0°C)

SAMPLE NUMBER	SAMPLE & DATE	% EVAP.	DERIVED VISCOSITY (cp)	DERIVED DENSITY g cm^{-3}	DERIVED POUR POINT °C	DERIVED SOLUBILITY ppm
14	NWC, DEC 8	3	11	0.850	-45	26
15	NW1, DEC 10	17	28	0.880	-27	10
16	NW1, JAN 22	19	32	0.882	-25	8
17	NW2, OCT 23	2	11	0.848	-47	27.5
18	NW2, NOV 15	3	11	0.850	-45	26
19	NW2, DEC 10	5	12	0.853	-42	23
20	NW2, JAN 21	2	11	0.848	-47	27
21	NW2, FEB 21	2	11	0.848	-47	27
22	NW2, MAY 9	5	12	0.853	-42	23
23	NW2, MAY 10	37	180	0.407	-11	0.25
24	NW3, NOV 14	4	12	0.852	-43	25
25	NW3, DEC 10	7.5	13	0.858	-38	20
26	NW3, JAN 22	3.3	11	0.851	-44	26
27	NW3, FEB 21	2.2	11	0.849	-47	27.5
28	NW3, MAY 12	4	12	0.852	-43	25
29	NW3, MAY 26	41	220	0.920	-7	0
30	NW3, JUN 6	34	160	0.903	-13	1
31	NW3, JUN 10	6	12	0.855	-40	22
32	NW4, DEC 9	3.5	11	0.851	-44	25
33	NW4, FEB 5	3	11	0.850	-45	26
34	NW4, FEB 21	2.5	11	0.874	-46	27
35	NW4, MAY 13	6	12	0.855	-43	25
36	NW4, MAY 27	4	12	0.852	-43	25
37	NW4, JUN 6	26	50	0.892	-20	4
38	NW4, JUN 13	43	300	0.923	-5	0
39	NW6, FEB 15	5	12	0.853	-42	23
40	NW6, MAY 10	23	45	0.888	-22	6
41	NW6, MAY 15	12	18	0.869	-32	14
42	NW6, JUN 12	43	300	0.923	-5	0
43	NW7, MAY 10	20	35	0.885	-25	8
44	NW7, JUN 6	27	60	0.894	-11	3.8
45	NW7, JUN 11	36	170	0.904	-13	0
46	NW7, JUN 12	>50	>400	>0.94	>0	0
47	NW7, JUN 13	>50	>400	>0.94	>0	0
48	NW3, JUN 26	42	300	0.922	-8	0
49	RESID. JUL 7	42	300	0.922	-8	0
50	RESID. JUL 7	>50	>400	>0.94	>0	0
51	EVAP. DEC 24	7.1	13	0.858	-39	20.5
52	EVAP. JAN 11	20	35	0.885	-25	7.5
53	EVAP. JAN 20	26	55	0.892	-20	4
54	EVAP. JAN 24	24	50	0.890	-22	5
55	EVAP. FEB 6	33	90	0.901	-14	1

TABLE B-4

DERIVED PROPERTIES OF THE
SWAN HILLS CRUDE SAMPLES (AT 0°C)

SAMPLE NUMBER	SAMPLE & DATE	% EVAP.	DERIVED VISCOSITY (cp)	DERIVED DENSITY g cm^{-3}	DERIVED POUR POINT °C	DERIVED SOLUBILITY ppm
1	SHC, DEC 7	0	32	0.837	-5	29
2	SH1, DEC 10	0.5	32	0.838	-5	28
3	SH1, DEC 30	<1	33	0.838	-5	27
4	SH1, JAN 22	<1	33	0.838	-5	27
5	SH1, FEB 18	1	34	0.839	-4	27
6	SH1, MAY 13	1.5	36	0.840	-3	26
7	SH1, JUN 3	18	200	0.870	+9	8
8	SH1, JUN 13	28	400	0.888	+15	2
9	SH2, MAY 10	26	350	0.883	+13	3
10	SH2, MAY 27	8	80	0.860	+3	17
11	SH2, MAY 29	28	400	0.888	+15	2
12	SH2, MAY 29	24	300	0.880	+12	4
13	SH2, JUN 12	33	500	0.89	+17	0
56	EVAP. DEC 29	1.5	36	0.840	-3	26
57	EVAP. JAN 4	9	95	0.862	+4	16
58	EVAP. JAN 20	7	70	0.858	+2	17
59	EVAP. FEB 26	19	210	0.874	+13	8

TABLE B-5

MEASURED AND DERIVED

DENSITIES

SAMPLE NUMBER	SAMPLE & DATE	DENSITY		
		DERIVED @ 0°C	MEASURED AT TEMP.	MEASURED CORRECTED TO 0°C
16	NW1, JAN 22	0.882	0.872 @ 15 °C	0.882
	NW2, OCT 24	0.848	0.831 @ 15 °C	0.844
18	NW2, NOV 15	0.850	0.832 @ 15 °C	0.845
19	NW2, DEC 10	0.853	0.839 @ 15 °C	0.850
20	NW2, JAN 21	0.848	0.829 @ 17 °C	0.843
21	NW2, FEB 21	0.848	0.831 @ 15 °C	0.844
24	NW3, NOV 14	0.852	0.836 @ 20 °C	0.850
26	NW3, JAN 22	0.851	0.838 @ 15 °C	0.849
27	NW3, FEB 21	0.849	0.835 @ 15 °C	0.848
32	NW4, DEC 9	0.851	0.834 @ 15 °C	0.846
34	NW4, FEB 21	0.849	0.836 @ 15 °C	0.849
1	SH1, DEC 7	0.837	0.823 @ 15 °C	0.836
3	SH1, DEC 30	0.838	0.822 @ 17 °C	0.838
4	SH1, JAN 22	0.838	0.819 @ 20 °C	0.838
5	SH1, FEB 18	0.839	0.819 @ 20 °C	0.839

TABLE B-6

METAL ANALYSIS OF
UNWEATHERED CRUDE OIL SAMPLES

	NORMAN WELLS	SWAN HILLS
Sulphur	1.76%	2.90%
Aluminum (Al_2O_3)	<0.5 p.p.m.	<0.5 p.p.m.
Barium	<0.5 p.p.m.	<0.5 p.p.m.
Calcium (CaO)	<0.5 p.p.m.	5 p.p.m.
Copper	<0.5 p.p.m.	<0.5 p.p.m.
Iron (Fe)	0.3 p.p.m.	0.3 p.p.m.
Lead	0.5 p.p.m.	20 p.p.m.
Magnesium (MgO)	<0.5 p.p.m.	<0.5 p.p.m.
Nickel	1 p.p.m.	<0.5 p.p.m.
Silicon (SiO_2)	<0.5 p.p.m.	<0.5 p.p.m.
Sodium(Na_2O)	<1 p.p.m.	1 p.p.m.
Tin	<0.5 p.p.m.	<0.5 p.p.m.
Vanadium	3 p.p.m.	<0.5 p.p.m.
Zinc	-	20 p.p.m.

APPENDIX C

Table C-1 CORE LOGS

TABLE C-1

CORE LOG

DATE	LOCATION	ICE THICKNESS	SNOW THICKNESS	CORE LENGTH	OIL LENS THICKNESS	OIL LENS DEPTH	AVERAGE SALINITY°/oo
Oct 3	Bay	12.7cm					
Oct 7		15-18cm					
Oct 11		19cm	1.3cm				
Oct 17		26.5cm					
Oct 29	NW1	33cm	Tr.				
	NW2	33cm	Tr.				
	NW3	38cm	0				
	SH1	38cm	0				
Nov 3	Bay	40.5-44cm					
	NW4	46cm	7cm				
Nov 20	NW4	51cm	20cm				
Dec 17	NW3	71cm	25cm				
Dec 21	NW2	75cm					
	NW3	75cm					
Dec 23	NW2	72cm					
	NW3	77cm					
	NW4	75cm					
	SH1	79cm					
Dec 30	NW4	74cm			Tr.	67cm	
	SH1	86cm					
Jan 6	NW2	84cm	13cm			36cm	
Jan 27	NW6	96cm	19cm				
	NW6	105cm	13cm				
	NW6	93cm	23cm				
	NW6	118cm	5cm				
Feb 7	NW6	120cm					
Feb 18	SH1	108cm		107cm	1.8cm	61cm	
Feb 21	NW2	128cm	10cm	125cm		35cm	
	NW3	90.1cm	53.3cm	86cm	3 cm	59cm	
	NW4	127cm	10cm	127cm	1.3cm	60cm	
Feb 23	Control 3	112cm	20cm				4.5

TABLE C-1

CORE LOG

DATE	LOCATION	ICE THICKNESS	SNOW THICKNESS	CORE LENGTH	OIL LENS THICKNESS	OIL LENS DEPTH	AVERAGE SALINITY°/∞
Feb 23	SH1	140cm	10cm				4.8
Mar 1	NW2	133cm	10cm				4.9
	NW4	124cm	5cm				4.3
Mar 18	NW2	130cm	27cm				
	NW6	130cm	27cm	137cm		121cm	4.7
	NW6	138cm	17cm	139cm		121cm	4.4
Mar 19	NW6	143cm	20cm	127cm	3 cm	110cm	5.3
Mar 20	SH1	120cm	20cm	120cm		60cm	4.1
Mar 21	NW2	128cm	10cm				
	NW6	130cm	27cm				3.7
Mar 22	NW3	118cm	25cm	104cm			4.7
	SH1	145cm	11cm	130cm			4.6
Mar 26	NW1	139cm	15cm	136cm		129cm	5.1
	NW2	130cm	20cm	126cm		30cm	4.6
May 9	NW2			163cm		33cm	
May 11	SH2	168cm		168cm		158cm	
May 12	NW7	160cm		160cm		160cm	
	SH2	189cm					
	NW3	132cm	31cm	132cm	1 cm	20cm	
May 13	NW4	150cm	20cm		1.5cm		6.2
	SH1	168cm	18cm	168cm		68cm	
May 15	NW6		25cm				
	NW2	132cm		132cm	1.5cm	32cm	
	NW6	152cm		152cm	4 cm	114cm	3.7
	NW1					10cm	
May 16	NW8	195cm				195cm	
	SH2	160cm		160cm	3 cm	151cm	
	NW8	195cm				195cm	
May 19	NW3	118cm	31cm	113cm	1 cm	69cm	
	NW3	130cm	13cm	130cm			
May 20	NW4	36cm	18cm	136cm	3 cm	58cm	

TABLE C-1

CORE LOG

DATE	LOCATION	ICE THICKNESS	SNOW THICKNESS	CORE LENGTH	OIL LENS THICKNESS	OIL LENS DEPTH	AVERAGE SALINITY°/$_{oo}$
May 20	NW6	149cm	28cm		2 cm	115cm	4.2
May 21	SH1	171cm	8cm				
	SH1	172cm			5 cm	74cm	
	NW7	152cm	43cm		1.5cm	145cm	
May 24	NW2	169cm		169cm	1.5cm	43cm	
	NW2	169cm		169cm	1.5cm	43cm	3.75
May 26	Control	137cm	33cm				
	NW3	130cm	15cm				
	NW3	130cm	31cm		0.5cm	58.5cm	
	NW1	134cm	25cm				
	Control	142cm	18cm				
May 27	NW4	147cm	8cm		3 cm	63cm	
	SH2	164cm	1.5cm		2 cm	154cm	
May 29	Panarctic	168cm	7cm		1 cm	150cm	
	Panarctic					148cm	
Jun 10	NW4	160cm		160cm		8cm	
	NW4	102cm		102cm			
	NW6	130cm		130cm	2 cm	91cm	
	NW3	118cm		118cm	3 cm	20cm	
Jun 12	SH2	132cm		132cm	3 cm	126cm	
	NW4	94cm		94cm	1 cm	38cm	
	SH2	160cm		160cm			2.8
Jun 13	NW7	135cm		135cm	2 cm	62cm	
	SH1	116cm		116cm	1 cm	20cm	

APPENDIX D

Figure D - 1 EXTREMES OF ICE & SNOW DEPTHS, CAPE PARRY 1970–75

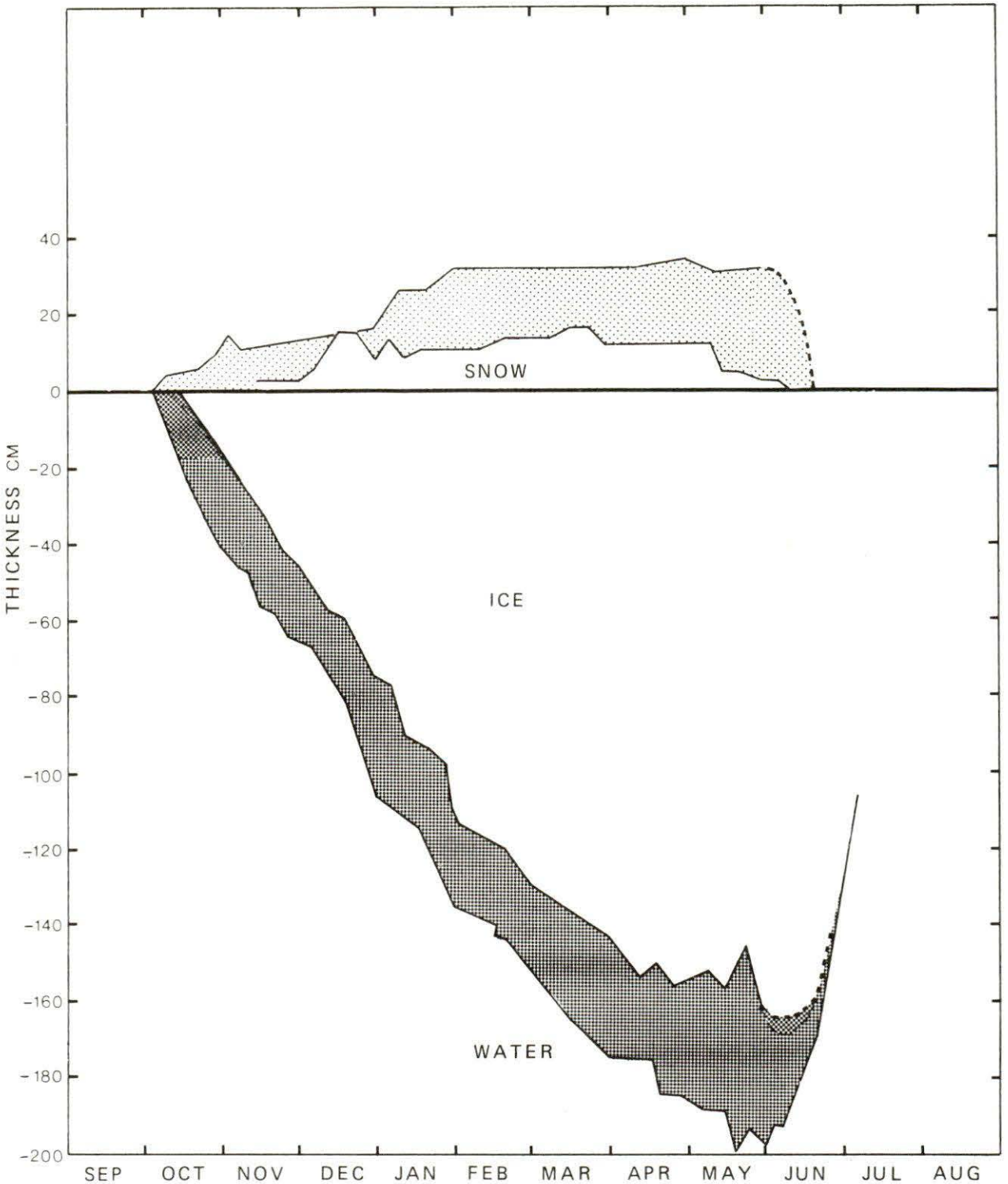

Figure D-2 MONTHLY MEAN TEMPERATURES - BALAENA BAY 1974 - 1975

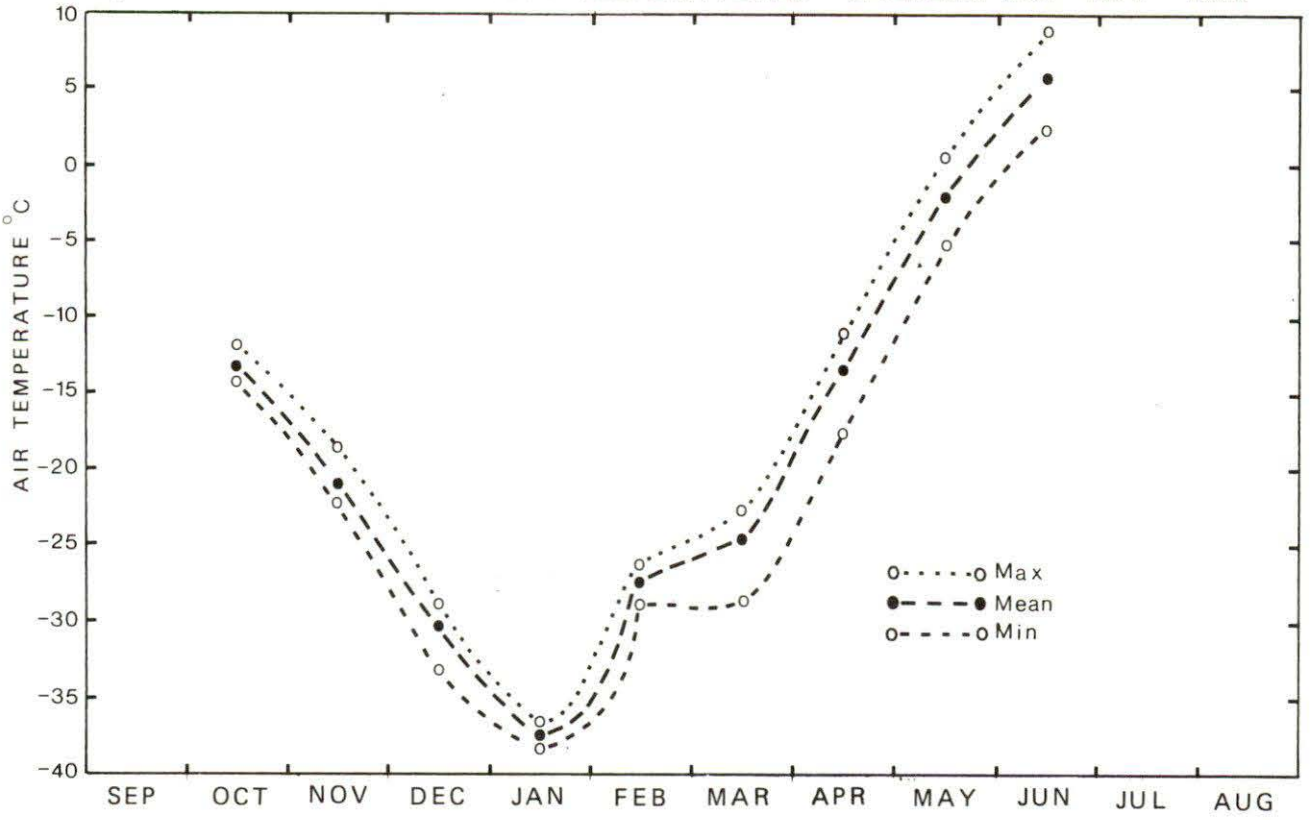

Figure D-3 MONTHLY MEAN TEMPERATURES - CAPE PARRY

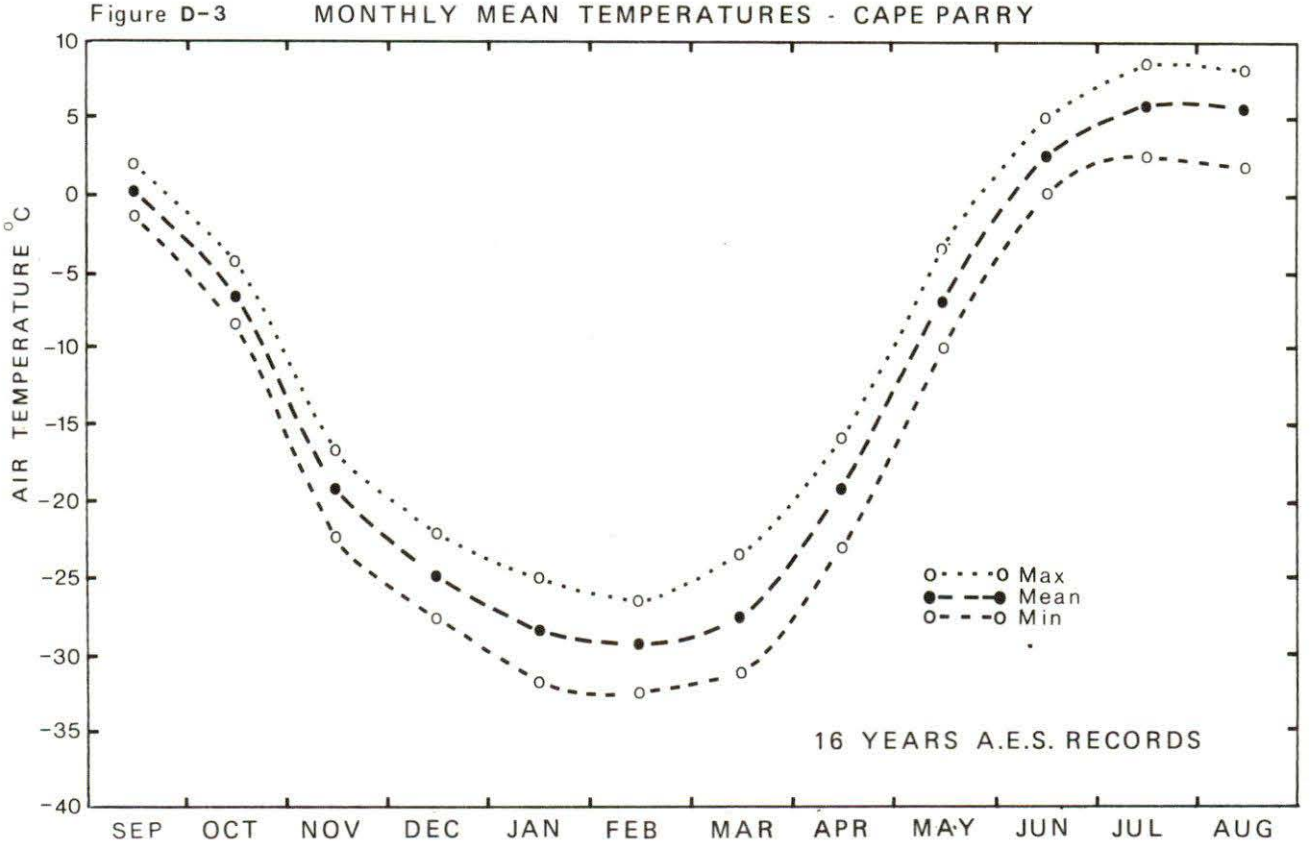

Figure D - 4 CAPE PARRY WIND REGIME

10 year normals

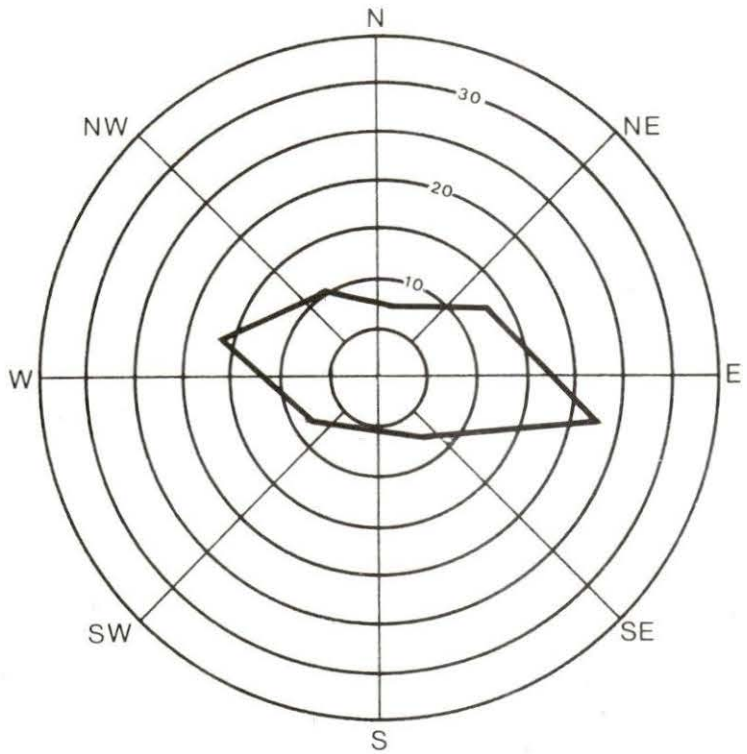

PERCENTAGE FREQUENCY
BY DIRECTION

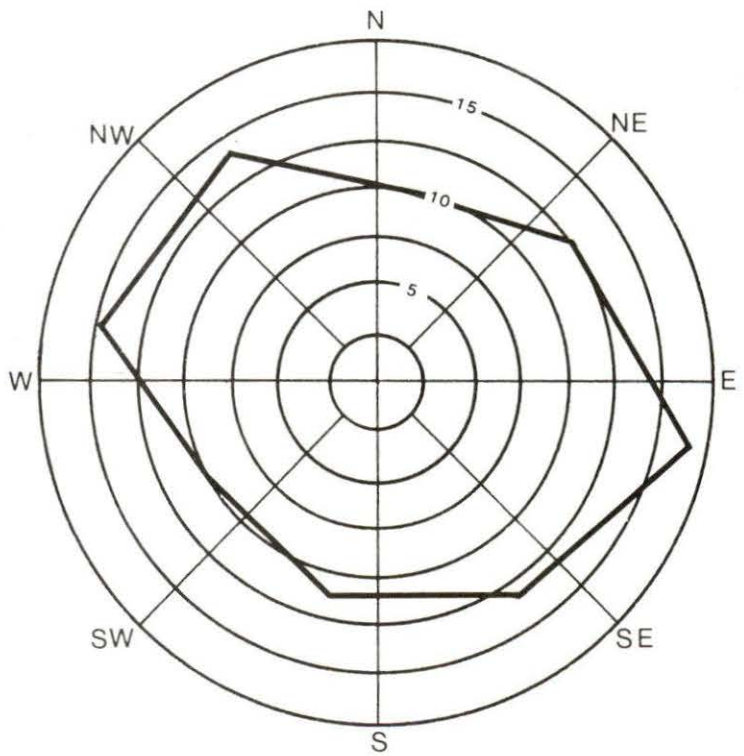

AVERAGE WIND SPEED
BY DIRECTION MPH

Figure D - 5

DURATION OF DAYLIGHT

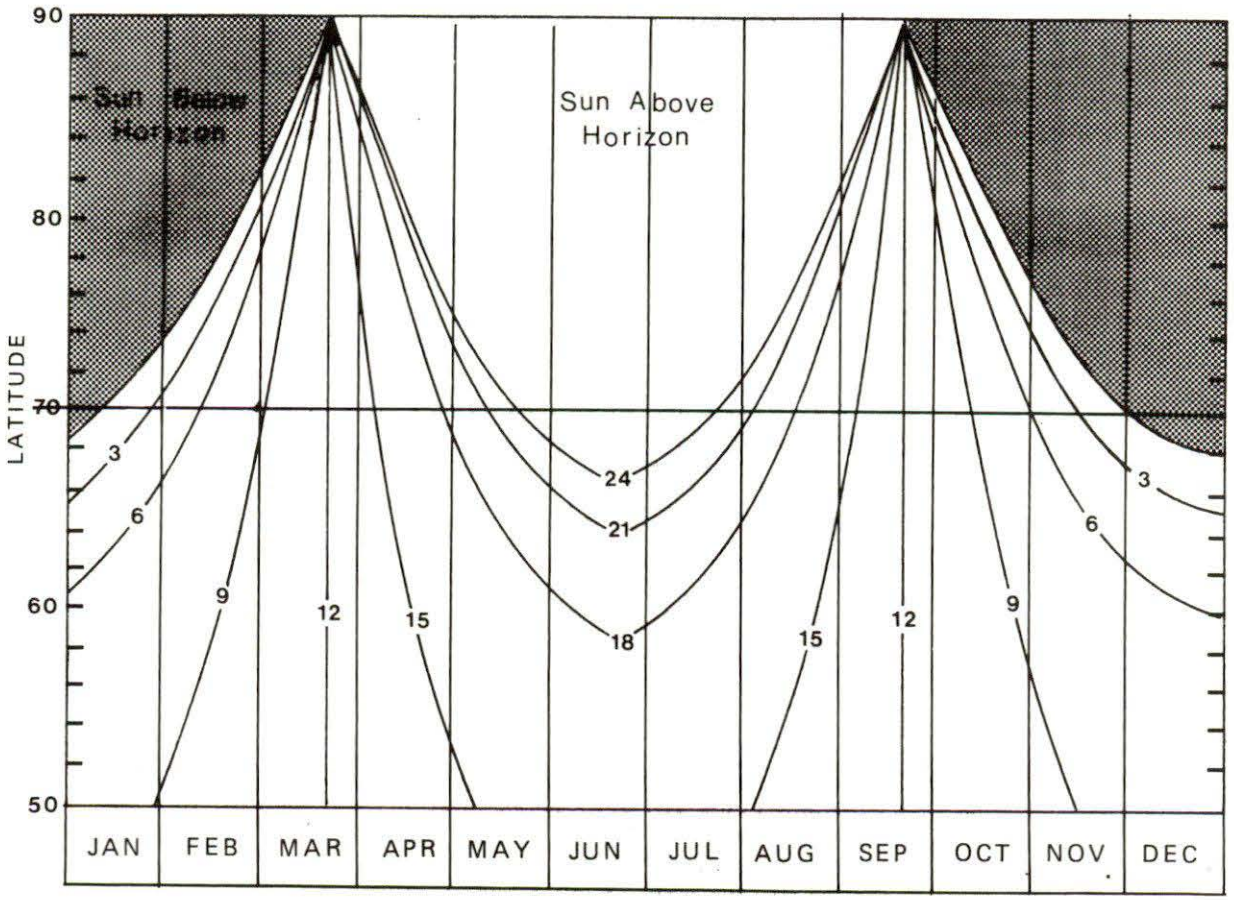

Figure D-6 ALBEDO SITES AND THERMISTOR CHAIN POSITIONS

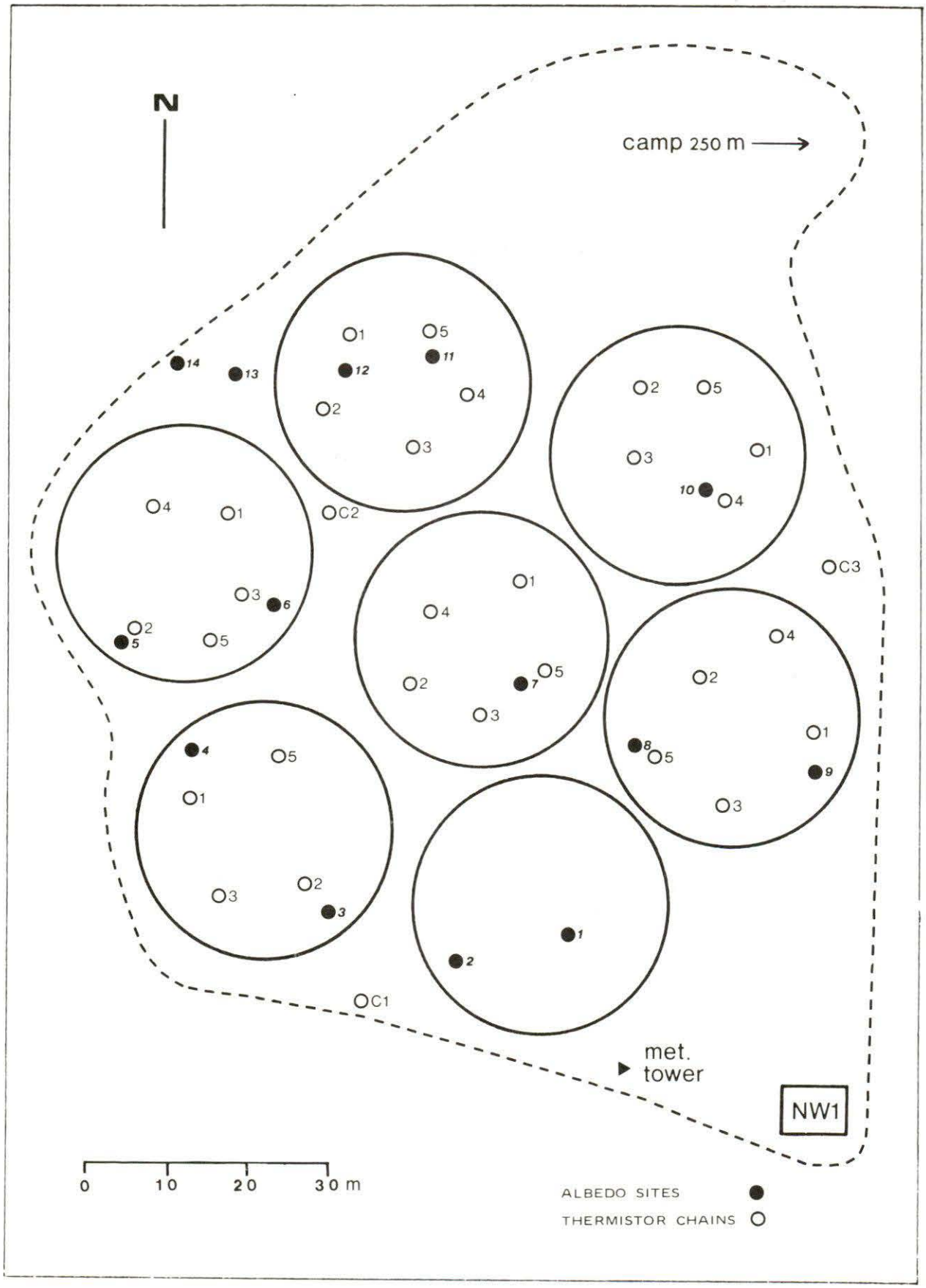

Figure D-7 TYPICAL HOURLY ALBEDO CHANGES

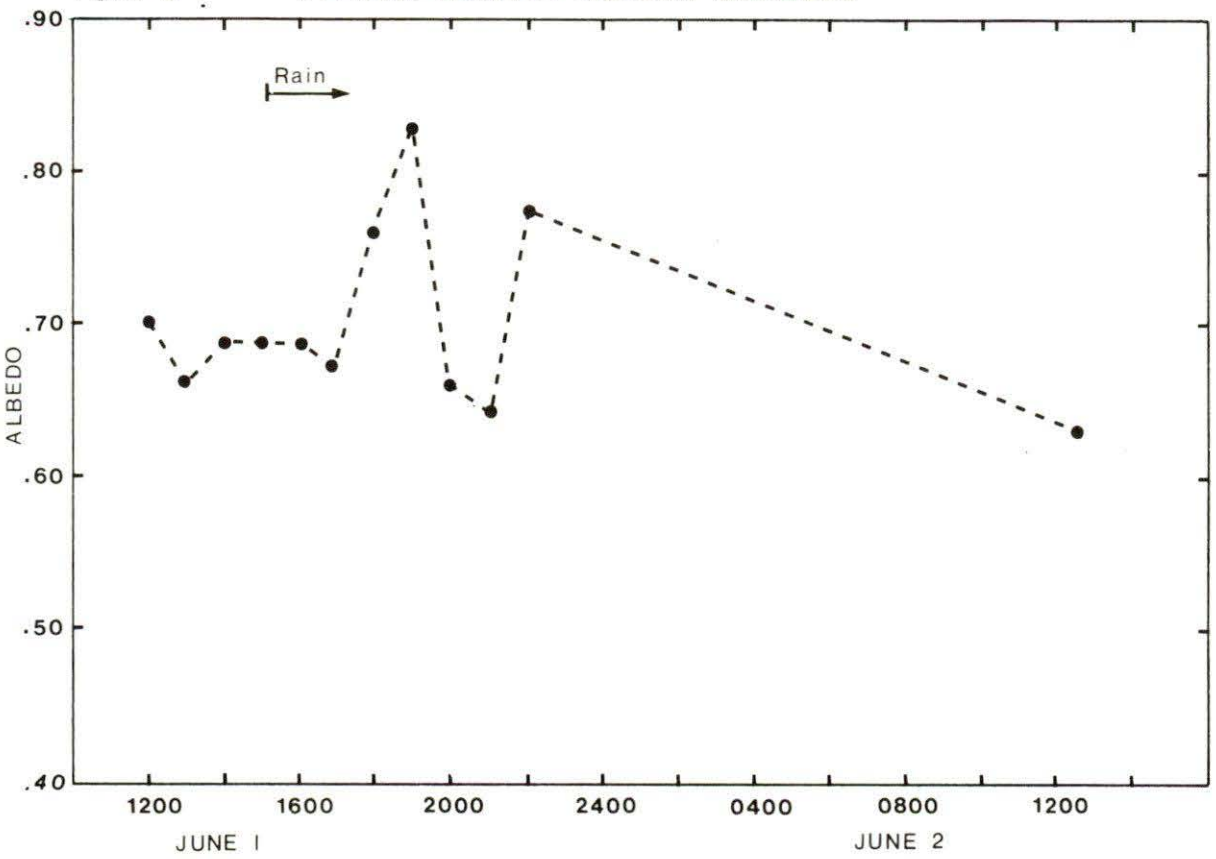

TABLE D-1

DAILY WEATHER SUMMARY FOR PERIOD OF ALBEDO MEASUREMENTS

DATE	CLOUD /10				TEMPERATURE (°C)				PRECIPITATION	CEILING (m)	SOLAR RADIATION (cal cm $^{-2}$min $^{-1}$)
	1000	1300	1900	2300	1000	1300	1900	2300			
MAY											
9	7	0	0	2	+4	+10	+7	+1	--	700 to 2000	0.91
10	3	0	10	10	-	-	-	-	--	--	0.89
11	10	10	9	10	+1	+ 4	-3	-4	Trace snow	<200	
12	10	10	10	10	-5	- 1	-5	-6	" "	<200	0.65
13	10	10	10	10	-8	- 6	-9	-7	2cm snow	<200	
14	10	10	10	10	-9	- 9	-9	-10	1.3cm snow blowing	<300	
15	9	2	0	1	-10	- 4	-2	-5	--	CAVU	
16	10	10	9	0	-5	- 2	-5	-10	Trace	<300	0.71
17	0	0	0	3	-8	- 6	-6	-10	--		
18	0	0	0	0	-8	- 1	-4	-9	--	CAVU	0.98
19	10	10	5	10	-8	- 5	-4	-9	Rain 2100, 1.3cm snow		
20	10	10	3	10	-8	- 8	-8	-10	3cm blowing snow	<300	0.78
21	8	0	0	0	-8	- 6	-9	-11	Trace		
22	0	0	0	1	-11	- 2	-5	-8	--	CAVU	1.01
23	0	2	10	10	-7	- 3	-4	-5	--		
24	10	10	10	10	-5	- 2	-2	-3	Fog,Light rain,Tr. snow	<300	0.60
25	10	5	0	0	-2	+ 1	0	-4	--		
26	3	7	7	1	-8	+ 1	-2	-3	Trace		
27	0	10	0	0	-6	- 1	-1	-4	Trace	<700	0.89
28	4	5	0	1	-6	- 2	0	-2	--	CAVU	
29	5	2	6	10	-4	0	+1	-3	--	CAVU	0.99
30	10	10	10	10	-3	- 1	-2	-2	Trace	<300	
31	10	7	7	9	-1	+ 2	+3	-1	0.8cm snow 0900-1200 2400	<1000 Variable	0.83 to 1.10
JUN											
1	9	10	9	10	+5	- 1	+1	0	Rain 1200 →	<1000	
2	10	10	10	10	+1	+ 1	+1		Rain all day	<700	0.55
3			10	10		+ 1	+2			<300	
4		10	10	10		+ 3	+2	0		<700	0.61
5	8	10	10	10	+2	+ 3	+2	+2		<700	

NOTE: All radiation measurements at approximately 1300 hrs.

APPENDIX E

TABLE E1

BIRDS OBSERVED AT BALAENA BAY IN THE VICINITY OF THE OIL SPILL SITES, JULY 17 - 22, 1975

SPECIES		COMMENTS	NESTING
Gryfalcon	*Falco rusticatus*	Pair observed nesting in nearby cliffs	Yes
Rough-legged hawk	*Buteo lagopus*	Uncommon	Yes
Common eider	*Somateria millissima*	Frequently observed	Yes
King eider	*Somateria spectabilis*	Common	N[1]
Oldsquaw	*Clangula hyemalis*	"	N
Arctic loon	*Gavia arctica*	"	N
Red-throated loon	*Gavia stellata*	Rare	-
Semipalmated sandpiper	*Ereunetes pusillus*	Common	N
Semipalmated plover	*Charadrius semipalmatus*	"	N
Pectoral sandpiper	*Erolia melanotus*	Uncommon	N
Snow bunting	*Plectrophenax nivalis*	Common	Yes
Northern phalarope	*Lobipes lobatus*	"	N
Lapland longspur	*Calicarius lapponicus*	"	N
Glaucous gull	*Larus hyperboreus*	"	N
White winged scoter	*Melanitta deglandi*	Uncommon	-
Surf scoter	*Melanitta perspicillata*	"	-
Whistling swans	*Olor columbianus*	"	-
Parasitic jaeger	*Stercorarius parasiticus*	"	-
Pomarine jaeger	*Stercorarius pomarinus*	"	-
Common raven	*Corvus corax*	Common	N

[1] Nesting inferred from behavior or presence of old nests.

TABLE E4

SEAWEEDS AND BENTHIC MICROALGAE IDENTIFIED IN BALAENA BAY NEAR SPILL SITES JULY, 1975 AND THEIR APPROXIMATE ZONATION AND RELATIVE ABUNDANCE

1. UPPER SHINGLE ZONE: (extending from high tide level to about 2m depth)

Calothrix scopulorum	(nitrogen-fixing blue-green)
Oscillatoria spp.	(blue-green filaments)
Chroococcus sp.	(coccoid blue-green)
Pennate diatom spp.	
Protoderma marinum	(dominant green forming light green covering on shaded side of shingles and cobbles)
Sphacelaria arctica	(dominant filaments - brown)
Pylaiella littoralis	(filaments - brown)
Ralfsia fungiformis	(crustose brown)

2. LOWER SHINGLE-COBBLE ZONE: (extending from 2 - 4m below tide level)

Fucus distichus spp. *evanescens*	(dominant brown macroalga forming main *Fucus* belt)
Chaetomorpha linum	(fine filamentous green)
C. melagonium	(coarse filamentous green)
Tube-forming *Navicula*, sp.	(diatom)
Melosira sulcata	(centric diatom)
Nitzschia closterium	(pennate diatom)

In addition to the above algae, large amounts of epiphytic *Sphacelaria arctica* and smaller amounts of the other algae observed in zone 1.

3. MUD ZONE: (extending from about 4 to 8m or more, scattered cobbles and boulders with attached seaweeds)

Fucus distichus ssp. *evanescens*	(dominant brown seaweed)
Desmarestia aculeata	(sub-dominant brown)
Chaetomorpha melagonium	(dominant green)
C. linum	(also abundant green)
Sphacelaria arctica	
Laminaria saccharina	(kelp, occasional individuals)
Halosaccion ramentaceum	(red tubular seaweed)
Polysiphonia arctica	(branched red seaweed)

Pennate diatoms occur abundantly as epiphytes on seaweeds and on surface of mud layer.

TABLE E5

ZOOPLANKTON SPECIES IDENTIFIED FROM HORIZONTAL AND VERTICAL ZOOPLANKTON TOWS AT 3 STATIONS IN BALAENA BAY, AUGUST 13, 1974.
(SEE INSET 1, FIG. 11-1 FOR STATION LOCATIONS)

(+ + + + = dominant; + + = common; + = present)

SPECIES	STATIONS		
	1 (mouth of Bay)	2 (mid-Bay)	3 (near oil spill site)
Medusae			
Sarsia princeps		+	+
Cyanea capillata (jelly fish)		+	+
Unidentified spp.	+	+	+
Ctenophora			
Pleurobrachia pileus		+	+
Rotifera			
Unidentified spp.	+	+ +	+ +
Copepoda			
Calanus glacialis	+	+	
Pseudocalanus minutus	+ +	+ +	+ +
Microcalanus pygmaeus	+	+	+
Eurytemora herdmani	+ +	+ +	+ +
Limnocalanus grimaldi	+ + + +	+ + + +	+ + + +
Acartia spp.	+ +	+ +	+ +
Oithona similis	+	+	+
Unidentified spp.	+	+	+
Nauplii	+ + + +	+ +	+ +

TABLE E6

PHYTOPLANKTON SPECIES IDENTIFIED FROM HORIZONTAL PHYTOPLANKTON NET SAMPLES (1-2m IN DEPTH), AND TOTAL CELL NUMBERS FROM WATER SAMPLES TAKEN AT 4m DEPTH AT 3 STATIONS IN BALAENA BAY, 13 AUG. 1974.
(SEE INSET 1, FIG. 11-1 FOR STATION LOCATIONS.)

(+ + + + = dominant; + + = common; + = present)

SPECIES	STATIONS		
	1 (mouth of Bay)	2 (mid-Bay)	3 (near oil spill site)
Thalassiosira nordenskioldii	+ + + +	+ + + +	+ + + +
Nitzschia seriata	+ + + +	+ + + +	+ + + +
Dinobryon sp. (chrysophyte)	+ + + +	+ +	+ + + +
Chaetoceros decipiens	+ +	+ +	+ +
C. breve	+ +	+ +	+ +
C. lorenzianus	+ +	+ +	+ +
Thalassiosira gravida	+ +	+ +	+ +
Leptocylindrus danicus	+ +	+ +	+ +
Nitzschia delicatissima	+ +	+ +	+ +
Acnanthes taeniata	+	+ +	+ +
Skeletonema costatum	+	+	+
Coscinodiscus oculus-iridis	+	+	+
C. centralis	+	+	
Porosira glacialis		+	+
Rhizozolenia sp.	+		+
Chaetoceros diadema	+		+
C. gracilis	+	+	+
C. Socialis	+	+	+
C. mitra	+	+	+
Fragillaria oceanica	+	+	+
Thalassiothrix nitzschioides	+	+	+
Ceratium arcticum (dinoflagellate)	+	+	+
Peridinium pellucidum	+	+	+
Total cell number (cells l^{-1} x 10^{-5})	5.2	2.4	2.1

TABLE E7

CHEMICAL AND PHYSICAL PARAMETERS OF WATER IN BALAENA BAY AT CONTROL AND OIL SPILL SITES, JULY 19, 1975.
(FOR STATION LOCATIONS SEE INSET 2, FIG. 11-1)

(N.B. VALUES FOR CONTROL AND OILED STATIONS WERE ALMOST IDENTICAL).

PHYSICAL AND CHEMICAL PROPERTIES	DEPTH			
	SURFACE	1m	4m	8m
Temperature (°C)	6.2	6.5	6.4	3.8
Salinity (°/$_{\infty}$)	13	14	30	32
pH	7.7	7.8	8.2	8.2
CO_2 conc. (mMole l^{-1})	0.92	0.96	1.72	1.87

TABLE E8

BENTHIC INVERTEBRATE SPECIES IDENTIFIED FROM DREDGE AND EDMAN SAMPLES FROM 4-8m AT CONTROL AND OIL SPILL SITES, JULY 17-22, 1975. (SEE INSET 2, FIG. 11-1 FOR SAMPLING LOCATIONS.)

(+ + + + = dominant; + + = abundant; + = present)

SPECIES	STATIONS	
	CONTROL SITE	OIL SPILL SITE
Polychaeta		
Pectinaria granulata	+ +	+ +
Pectinaria	+ + + +	+ + + +
Spirorbis borealis (on *Fucus*)	+ +	+ +
Amphitrite	+	+
Unidentified spp.	+ +	+ +
Pelecypoda		
Macoma	+ +	+ +
Mya arenaria[1]	+ +	+ +
Cyprina islandica	+	+
Mytilus edulis[1] (on seaweeds & rocks)	+ +	+ +
Unidentified sp. " " " "	+ +	+ +
Echinoidea		
Strongylocentrodes drobachiensis[1]	+ +	+ +
Holothuroidea		
Cucumaria sp. 1	+ +	+ +
Cucumaria sp. 2	+	+
Decapoda		
Hyas coarcticus	+ +	+ +
Amphipoda		
Unidentified sp.	+ +	+ +
Cnidaria		
Large unidentified sea anemone[1]	+	+
Hydrozoans epiphytic on seaweeds	+	

[1] More common in shallower benthos (2-4m).

TABLE E9

QUANTITATIVE DETERMINATION OF ZOOPLANKTON ORGANISMS FROM VERTICAL ZOOPLANKTON HAULS AT OIL SPILL AND CONTROL SITES IN BALAENA BAY JULY 20, 1975.

ORGANISM	NO. OF INDIVIDUALS m^{-3}			
	Control		Oil Site	
	1	2	1	2
Copepods	1,600	780	1,300	2,690
Copepod nauplii	2,100	1,700	780	1,900
Medusai	32	31	6	41
Echinopluteus larvae	1,100	920	310	1,500

TABLE E10

PLANKTON ORGANISMS IN MIDWATER SAMPLES UNDER CONTROL AND OIL SPILL SITES AT BALAENA BAY, FEB. 7, 1975

	Cells $l^{-1} \times 10^{-3}$			
	CONTROL		OILED	
	1	2	1	2
Dinoflagellates	8.1	6.2	6.0	5.2
Cryptomonads	0.5	0.7	0.4	1.4
Pennate diatoms	1.1	1.2	1.3	0.8
Chrysophyte flagellates	0.7	0.2	1.2	1.6
Total phytoplankton	10.4	8.3	8.9	9.0
Tintinnids (protozoans)	0.3	0.5	0.2	0.4

TABLE E11

PRIMARY PRODUCTIVITY AT CONTROL AND OIL SPILL STATIONS IN BALAENA BAY, JULY 19-20, 1975.

(SAMPLES WERE INCUBATED *IN SITU* FOR 24 H)

	PRIMARY PRODUCTIVITY (mg^{0} C m^{-3} day^{-1})			
	CONTROL STATIONS		OIL SPILL STATIONS	
SAMPLING DEPTHS	1	2	1	2
(m)				
1	114	73	105	61
4	216	230	283	226
8	156	182	223	143
Average Total productivity (mg^{0} C m^{-2} day^{-1})	1,470		1,560	

TABLE E12

ABUNDANCE AND DEPTH DISTRIBUTION OF PHYTOPLANKTON AT CONTROL AND OILED SITES ON JULY 18, 1975

	SAMPLING LOCATION AND DEPTH (m)											
	Control 1			Control 2			Oiled 1			Oiled 2		
Types of algae	1	4	8	1	4	8	1	4	8	1	4	8
Diatoms:												
Centric	5	51	16	2	29	53	20	82	47	3	58	67
Pennate	382	80	5,633	9	163	3,711	137	186	3,931	49	81	2,172
Total	387	111	5,649	11	192	3,764	157	268	3,978	52	139	2,239
Dinoflagellates:												
Armoured	8	1	7	8	3	1	10	6	4	9	5	7
Naked	170	68	19	28	62	70	55	28	12	19	65	5
Total	178	69	26	36	65	71	65	34	16	28	70	12
Other flagellates:												
Total	142	39	12	136	76	17	681	45	5	210	101	14
Total phytoplankton:	707	219	5,687	183	333	3,852	903	347	3,999	290	300	2,265

TABLE E13

ABUNDANCE AND DEPTH DISTRIBUTION OF PHYTOPLANKTON AT CONTROL AND OILED SITES ON JUNE 4, 1975

	SAMPLING LOCATION AND DEPTH (m)									
	CONTROL					OILED				
TYPES OF ALGAE	2.4	3.5	4.5	5.0	6.5	2.4	3.5	4.5	5.0	6.5
Diatoms:										
Centric	8	0	4	0	8	0	1	2	2	16
Pennate	89	64	55	54	70	20	40	35	54	55
Total	97	64	59	54	78	20	41	37	56	71
Dinoflagellates:										
Armoured	1	1	0	0	0	1	0	0	2	0
Naked	48	82	41	67	75	23	33	39	70	27
Total	49	83	41	67	75	24	33	39	72	27
Other flagellates:										
Total	108	255	156	303	165	34	24	30	74	25
Total Phytoplankton	254	402	256	424	318	78	98	106	202	123

TABLE E14

PHOTOSYNTHETIC CAPACITY AND CHLOROPHYLL CONTENT OF VEGETATION IN SALT MARSH AND ON ROCK AND MUD ENVIRONMENTS FROM CRUDE OIL-POLLUTED SHORE AREAS AS COMPARED WITH THOSE FROM UNCONTAMINATED CONTROL AREAS IN BALAENA BAY, JULY 19-20, 1975

SAMPLING AREAS	DEGREE OF LOCAL OIL CONTAMINATION	CRUDE OIL RESIDUES (mg/cm^2)	PERCENT PHOTOSYNTHETIC CAPACITY	PERCENT CHLOROPHYLL CONTENT
Salt marsh	Control	3.1	100	100
	Medium	32	25	66
	Heavy	145	13	11
Rock algae	Control	2.2	100	100
	Medium	32	31	67
	Heavy	156	10	24
Mud algae	Control	1.2	100	100
	Medium	45	23	82
	Heavy	128	2	18

TABLE E15

COVER ESTIMATES FOR CONTROL AND OIL SPILL SITES IN SALT MARSH. PLOT 1 WAS OILED JULY 21, 1975 WITH WEATHERED NORMAN WELLS CRUDE OIL (20 ℓ m^{-2}), AND PLOT 2 WITH FRESH NORMAN WELLS CRUDE OIL (20 ℓ m^{-2}). PLOTS 3 AND 4 ARE CONTROL SITES (SEE INSET 2, FIG. 11-1, FOR LOCATION OF SPILLS.)

Plot[1]	PERCENT COVER			
	1	2	3	4
Species				
Puccinellia phryganoides	90	65	75	90
Wilhelmsia physodes	80	80	80	80
Bryum marratii	8	8	4	4
Puccinellia andersonii	0	0	1	1
Cochlearia officinalis	1	1	1	1
Carex spp.[2]	5	35	30	5

[1] Estimated areas of plots: 1(2.5m^2); 2(2.0m^2); 3(2.0m^2); 4(2.0m^2).

[2] Mainly *Carex subspathacea*.

TABLE E16

RESULTS OF EXPERIMENTS ON TOXICITY OF CRUDE AND WEATHERED CRUDE OIL ON MARINE ZOOPLANKTON SPECIES FROM BALAENA BAY, JULY 19-21, 1975
EXPERIMENTAL DESIGN AND PROCEDURE EXPLAINED IN TEXT.
(3 COMB JELLIES, 3 MEDUSAE, 1 YOUNG JELLYFISH, 2 AMPHIPODS AND CA.500 COPEPODS PER CYLINDER)

SPECIES	EFFECTS OBSERVED*		
	IMMEDIATE	12 H	36 H
Pleurobrachia pileus	Attracted to oil surface; normal swimming movements	Occasionally touching oil surface; normal behavior	Less active but still normal
Medusae (unidentified)	Stayed near bottom; bells pulsating	Near bottom; slow movements	Dead
Cyanea capillata (jellyfish)	Stayed near bottom; swimming	Slow movements near bottom	Dead
Amphipods (unidentified)	Normal activity migrating up and down	Normal activity	Slower movements
Copepods (several species)	Copepods active, frequently touching oil layer	Copepods still active but avoiding upper 5 cm. water layer	Many dead copepods on oil surface. About 25% still alive in bottom 5cm layer

* Somewhat more rapidly damaging effects noted with fresh, compared with weathered crude oil.

TABLE E17

EFFECTS OF CRUDE AND WEATHERED CRUDE OIL ON RATES OF PHOTOSYNTHESIS OF PHYTOPLANKTON SAMPLES FROM BALAENA BAY, JULY 19, 1975

(RESULTS REPRESENT AVERAGE VALUES FROM DUPLICATE EXPERIMENTS)

SAMPLE	RATE OF PHOTOSYNTHESIS (% OF CONTROL)
Control (no oil added)	100
+ Fresh crude oil	2
+ Weathered crude oil	17

TABLE E18

EFFECT OF DIFFERENT CONCENTRATIONS OF AQUEOUS CRUDE OIL EXTRACTS ON GROWTH OF BOREAL AND ARCTIC PHYTOPLANKTON IN OPEN AND CLOSED SYSTEMS

SPECIES	ORIGIN AND CONC. OF AQUEOUS CRUDE OIL EXTRACT	GROWTH (% OF CONTROL)					
		4 DAYS		11 DAYS		19 DAYS	
		OPEN	CLOSED	OPEN	CLOSED	OPEN	CLOSED
Chaetoceros septentrionalis	Atkinson Point:						
	30%	110	76	115	92	-	-
	100%	55	74	105	86	-	-
	Norman Wells:						
	30%	50	42	75	86	-	-
	100%	16	18	14	12	-	-
Thalassiosira nordenskioldii	Atkinson Point:						
	30%	64	24	76	55	25	18
	100%	26	6	20	8	20	9
	Norman Wells:						
	30%	-	-	36	18	33	8
	100%	-	-	14	9	8	5
Balaena Bay mixed Culture (*Amphiprora* and *Navicula* spp. dominant)	Atkinson Point:						
	30%	-	-	186	102	76	97
	100%	-	-	146	87	44	52
	Norman Wells:						
	30%	100	58	88	95	-	-
	100%	48	26	75	44	-	-
Phaeodactylum tricornutum	Atkinson Point:						
	30%	98	68	97	91	-	-
	100%	54	42	78	72	-	-
	Norman Wells:						
	30%	74	37	84	90	-	-
	100%	13	5	43	6	-	-

TABLE E19

EFFECT OF DIFFERENT CONCENTRATIONS OF AQUEOUS CRUDE OIL EXTRACTS ON PHOTOSYNTHETIC RATES OF BOREAL AND ARCTIC PHYTOPLANKTON

SPECIES	ORIGIN AND CONC. OF AQUEOUS CRUDE OIL EXTRACT	PHOTOSYNTHETIC RATE (% OF CONTROL) i)	ii)
Chaetoceros septentrionalis	Atkinson Point:		
	30%	93	73
	100%	73	26
	Norman Wells:		
	30%	85	64
	100%	9	14
Thalassiosira nordenskioldii	Atkinson Point:		
	30%	77	82
	100%	52	47
	Norman Wells:		
	30%	91	87
	100%	52	44
Balaena Bay mixed culture (*Amphiprora* and *Navicula* spp. dominant)	Atkinson Point:		
	30%	48	74
	100%	32	48
	Norman Wells:		
	30%	76	72
	100%	42	19
Phaeodactilum tricornutum	Atkinson Point:		
	30%	93	98
	100%	81	70
	Norman Wells:		
	30%	88	86
	100%	12	16

FIGURE E1

DIAGRAM OF ARCTIC SALT MARSH SHOWING VEGETATIONAL ZONES IN RELATION TO LEVELS OF HIGH AND LOW TIDE

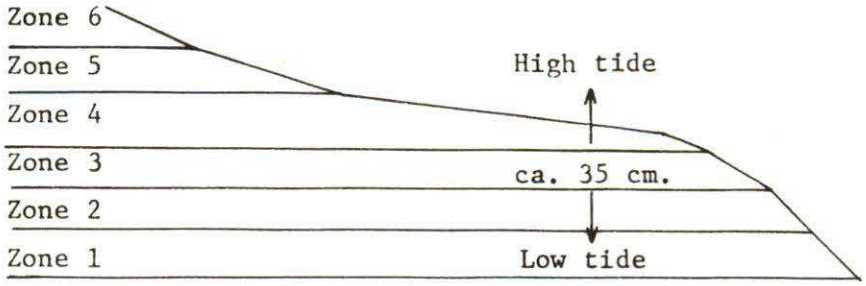

ZONE 1: Often bare mud or turf where marsh is eroding, or where silt deposits. Pennate diatoms observed, and frequent colonies of nitrogen-fixing blue-greens (*Rivularia* sp.) in some areas.

ZONE 2: Dark bluish-green thick mat of algae dominated by the xanthophyte, *Vaucheria* sp., and blue-green *Oscillatoria* spp. Several species of pennate diatoms and the blue-green nitrogen-fixing alga *Anabaena* sp., were also present. Nematodes and protozoans were observed in the algal and soil layer in zones 2-4.

In wet depressions and tidal ponds in salt marshes: Dominant: *Chaetomorpha linum*. Subdominant: *Enteromorpha* sp., *Rhizoclonium* sp., and *Ulothrix* sp.. Bottom mud densely covered by pennate diatom species and blue-greens.

ZONE 3: This zone is dominated in most locations by the moss *Bryum marratti*. Overlapping to some degree are the grass *Puccinellia phyganodes* and the dicot *Wilhelmsia physodes*. The soil layer is covered by the same matforming algae as in Zone 2, where the moss layer is sparse or absent.

ZONE 4: *Puccinellia phryganodes* is dominant, and *Wilhelmsia physodes* subdominant. Also occuring is the scurvy-weed *Cochlearia officinalis*. The soil is covered by mats of the same algae as observed in Zone 2. The green alga *Enteromorpha* sp.

ZONE 5: *Puccinellia phryganodes* and *Wilhelmsia physodes* are co-dominant. The sedges *Carex subspathacea* and *C. ursina*, *Puccinellia andersonii* and *Cochlearia officinalis* occur in low numbers.

ZONE 6: *Elymus arenarius*, *Puccinellia andersonii*, *Carex rotundata*, *C. subspathacea*, *C. ursina*, *Cochlearia officinalis*, *Salex glauca*, *Draba nivalis*, *Oxytropis nigresence*, *Hedysarum mackenzii*, *Dryas integrifolia*, *Eriophorum angustifolium*, *Umbellicaria decussata*. On rocks and

shingles: the lichens *Caloplaca elegans, Centatia nivalis, C. cucullata, Thamnolia* sp.